

**NON VIRAL GENE DELIVERY IN CANCER
CELLS USING POLYSACCHARIDES MODIFIED
WITH POLYETHYLENEIMINE AND VINYL
MONOMERS**

M.CAROLINE DIANA SHERLY

PhD THESIS

2019



**SREE CHITRA TIRUNAL INSTITUTE
FOR
MEDICAL SCIENCES AND TECHNOLOGY, TRIVANDRUM
Thiruvananthapuram**

**NON VIRAL GENE DELIVERY IN CANCER
CELLS USING POLYSACCHARIDES MODIFIED
WITH POLYETHYLENEIMINE AND VINYL
MONOMERS**

A THESIS PRESENTED BY

M.CAROLINE DIANA SHERLY

TO

**SREE CHITRA TIRUNAL INSTITUTE FOR
MEDICAL SCIENCES AND TECHNOLOGY, TRIVANDRUM
THIRUVANANTHAPURAM**

**IN PARTIAL FULFILMENT OF THE REQUIREMENTS
FOR THE AWARD OF
DOCTOR OF PHILOSOPHY**

2019

CERTIFICATE

I, ***M.CAROLINE DIANA SHERLY***, hereby certify that I had personally carried out the work depicted in the thesis entitled, “***Non viral gene delivery in cancer cells using polysaccharides modified with polyethyleneimine and vinyl monomers.***”

No part of the thesis has been submitted for the award of any other degree or diploma prior to this date.

M. Caroline Diana Sherly

31-05-2019

The thesis entitled

**“Non viral gene delivery in cancer cells using
polysaccharides modified with polyethyleneimine and vinyl
monomers.”**

Submitted by

M. Caroline Diana Sherly

for the degree of

Doctor of Philosophy

of

SREE CHITRA TIRUNAL INSTITUTE

FOR

MEDICAL SCIENCES AND TECHNOLOGY, TRIVANDRUM

Thiruvananthapuram

Is evaluated and approved by

Dr. Rekha MR

Examiner

The thesis entitled

**“Non viral gene delivery in cancer cells using
polysaccharides modified with polyethyleneimine and vinyl
monomers”**

Submitted by

M. Caroline Diana Sherly

for the degree of

Doctor of Philosophy

of

SREE CHITRA TIRUNAL INSTITUTE

FOR

MEDICAL SCIENCES AND TECHNOLOGY, TRIVANDRUM

Thiruvananthapuram

Is evaluated and approved by

Dr. Rekha M.R.

Examiner

ACKNOWLEDGEMENT

First and foremost, I owe my heartfelt thanks to The Almighty for giving me strength and courage to complete my thesis.

I take this opportunity to extend my sincere gratitude and appreciation to all those who made this Ph.D thesis possible.

I express my sincere gratitude and indebtedness to my research guide, Dr Rekha M.R, for introducing me to this exciting field of nanoscience and for her dedicated help, advice, inspiration, encouragement and continuous support, throughout my Ph.D.

I am thankful to the to the former and present Director of SCTIMST and the Head, BMT Wing for giving me the opportunity and facilities to do my research in my area of interest in this prestigious institution.

I am extremely thankful to the former and present Dean, Associative Dean, Registrar, Deputy Registrar and all members of the academic division and Director's office for their help and support.

I owe my sincere gratitude to my Doctoral Advisory Committee members Dr. T.V. Kumary, Dr.P. Ramesh for the valuable suggestions and critical comments in each stage of my work.

I am grateful to Council of Scientific and Industrial Research (CSIR), India for the research fellowship.

My special words of thanks should also go to Dr. Chandra P. Sharma, former guide for his support and assistance during initial periods of work.

I am grateful to Dr. HK Varma, Dr. Manoj, Dr.Suresh Babu, Mr. Adarsh, Bioceramics laboratory for helping me in Fourier Transform Infra Red spectroscopy

I warmly thank Dr. Lissy Krishnan, Dr. Anugya Bhatt, Mr. Renjith Kartha, Ms.Priyanka, Mr. Anil Kumar, Ms.Renu Ramesh, Ms.Subha and all staffs of Thrombosis Research unit for providing me FACS, microplate reader and gel doc facilities

I express my gratitude to Dr. Roy Joseph, Mr. Willi Paul, for providing me facilities in Central Analytical Facility

I am sincerely grateful to Dr. Anoopkumar Thekkuveetil, Mr.Binoy, Laboratory of Molecular medicine for their assistance to isolate plasmid DNA required for my study.

I wish to thank Dr. Jayasree, Dr.Lekshmi, Ms. Hema, Ms.Reshmi, Ms.Parvathy, Ms.Marina, Mr.Jibin, Mr.Jayaram, Biophotonics Laboratory for their help in fluorescence microscopy and in vivo image analyser.

I express my gratitude to Dr. Hari Krishnan, Mr. Manoj, Mr.Sunil, Mr.Anoop Ms.Jolly, all staffs of DLAS for helping me in animal studies.

I am thankful to Dr. Maya Nandhakumar, Mr. Pradeep, Ms. Amalu, Ms. Keerthi, Division of Microbial Technology for micro plate reader facility.

My heartfelt gratitude to Dr. Anil Kumar PR, Ms. Deepa, Mr. Vinodh, all staffs of Division of Tissue Culture for all their support and assistance

I am thankful to Dr. Sreenivasan, Dr. Radha, Mr. Hari, Laboratory of Polymer Analysis for helping in chemical characterisation

Also I wish to acknowledge Dr. Anil Kumar TV, Dr.Sabareeshwaran, Ms. Sulekha Baby, Mr.Joseph, Dr. Geetha, Dr. Akhila and all staffs and students of Division of Pathology for providing me deep freezer facility

My heartfelt thanks to all my labmates- Ms. Jasmine, Ms. Rajalekshmi, Ms.Priya, Ms. Annie, Ms.Hanna, Ms. Mitha, Dr. Thasneem, Dr. Susan, Dr. Radhika, Ms. Rajasree, Ms. Linsha for their wonderful friendship and support

A special mention of thanks to all my friends especially Ms.Dhanya, Ms. Bridget, Dr. Remya, Ms. Niji, Ms. Sakhi and all students in the SCTIMST campus for their friendship, care and love.

Finally and most importantly I would like to thank my husband, daughter and my family members for their unceasing love, patience, support and care that extended over this entire tenure.

TABLE OF CONTENTS

	Page
Declaration by the Student	i
Certificate of Guide	ii
Approval of Thesis	iii
Acknowledgements	iv
Table of Contents	vii
List of Figures	
List of Tables	
Abbreviations	
Synopsis	
1. Introduction	1
1.1 Cancer	2
1.2 Conventional cancer treatment methods	3
1.2.1. Surgery	4
1.2.2 Chemotherapy	5
1.2.3 Radiation therapy	6
1.2.4 Hormonal therapy	6
1.2.5 Immunotherapy	7
1.2.6 Targeted therapy	7
1.3 Cancer and gene therapy	8
1.4 Gene delivery vectors	9
1.5 Strategies to overcome the barriers of gene therapy	11
1.5.1 Formulation and design of vector	11
1.5.2 Extracellular barriers	13
1.5.3 Plasma membrane	14

1.5.4 Endosomal escape	15
1.5.5 Cytoplasmic trafficking	17
1.5.6 Nuclear import	19
1.6 Aims	20
1.7 Hypothesis	21
1.8 Objectives	21
2.Review of literature	23
2.1 Pullulan and dextran as vector backbone in gene delivery	23
2.1.1 Pullulan	23
2.1.2 Dextran	28
2.2 Polyethyleneimine (PEI) and gene delivery	32
2.3 Significance of vinyl monomers	40
2.4 Role of p53 gene in cancer	43
3.Materials and methods	47
3.1 Cationisation of polysaccharides- pullulan & dextran	47
3.1.1 Materials	47
3.1.2 Synthesis	48
3.1.3 Fourier transform infrared spectroscopy (FTIR)	48
3.1.4 Proton nuclear magnetic resonance spectroscopy (¹ H NMR)	48
3.1.5 Determination of free amino groups	49
3.1.6 Buffering capacity	49
3.1.7 Preparation of polymer/ctDNA nanoplexes	50
3.1.8 Size and zeta potential	50
3.1.9 DNA binding ability and effect of plasma on nanoplex stability	50
3.1.10 Nanoplex stability in the presence of digestive enzyme, DNase	51
3.1.11 Polymer interactions with plasma proteins	51

3.1.12 Cell culture studies	52
3.1.13 Cell viability	52
3.1.14 Cellular uptake of polyplexes	53
3.1.15 Polymer trafficking studies	54
3.1.16 Gene transfection	54
3.1.17 Annexin V staining	55
3.2 Synthesis and characterisation of ethylene glycol dimethacrylate (EGDMA) cross linked CPs	56
3.2.1 Materials	56
3.2.2 Synthesis	56
3.2.3 Fourier transform infrared spectroscopy (FTIR)	57
3.2.4 Proton nuclear magnetic Resonance (^1H NMR)	57
3.2.5 Determination of free amino groups	57
3.2.6 Buffering capacity	57
3.2.7 Polymer/ctDNA polyplexes preparation	58
3.2.8 Size and zeta potential	58
3.2.9 DNA binding ability and effect of plasma on nanoplex stability	59
3.2.10 Polymer interactions with plasma proteins	59
3.2.11 Cell culture studies	59
3.2.12 Cell viability	60
3.2.13 Cellular uptake of polyplexes	61
3.2.14 Gene transfection	61
3.3 Synthesis and characterisation of [2-(Acryloyloxy) ethyl] trimethylammonium chloride (AOETMAC) grafted CPs	62
3.3.1 Materials	62
3.3.2 Synthesis	63
3.3.3 Fourier transform infrared spectroscopy (FTIR)	63

3.3.4 Proton nuclear magnetic resonance (^1H NMR)	63
3.3.5 Determination of free amino groups	63
3.3.6 Buffering capacity	64
3.3.7 Polymer/ctDNA polyplexes preparation	64
3.3.8 Size and zeta potential	64
3.3.9 DNA binding ability and effect of plasma on nanoplex stability	65
3.3.10 Polymer interactions with plasma proteins	65
3.3.11 Cell culture studies	66
3.3.12 Cell viability	66
3.3.13 Cellular uptake of polyplexes	67
3.3.14 Gene transfection	68
3.4 Synthesis and characterisation of vinyl imidazole (VI) grafted CPs	
3.4.1 Materials	
3.4.2 Synthesis	
3.4.3 Fourier transform infrared spectroscopy (FTIR)	
3.4.4 Proton nuclear magnetic resonance (^1H NMR)	
3.4.5 Buffering capacity	
3.4.6 Preparation of polymer/DNA polyplexes	
3.4.7 Size and zeta potential	
3.4.8 DNA binding ability and effect of plasma on nanoplex Stability	
3.4.9 Nanoplex stability in the presence of digestive enzyme, DNase	
3.4.10 Polymer interactions with plasma proteins	
3.4.11 Cell culture studies	
3.4.12 Cell viability	
3.4.13 Cellular uptake of polyplexes	
3.4.14 Cellular uptake in the presence of endocytotic inhibitors	

3.4.15 Gene transfection	
3.5 Synthesis and characterisation of 2-Diethyl amino ethyl methacrylate (DEAEM) grafted CPs	
3.5.1 Materials	
3.5.2 Synthesis	
3.5.3 Fourier transform infrared spectroscopy (FTIR)	
3.5.4 Proton nuclear magnetic resonance (^1H NMR)	
3.5.5 Determination of free amino groups	
3.5.6 Buffering capacity	
3.5.7 Polymer/ctDNA polyplexes preparation	
3.5.8 Size and zeta potential	
3.5.9 DNA binding ability and effect of plasma on nanoplex Stability	
3.5.10 Nanoplex stability in the presence of digestive enzyme, DNase	
3.5.11 Polymer interactions with plasma proteins	
3.5.12 Cell culture studies	
3.5.13 Cell viability	
3.5.14 Cellular uptake of polyplexes	
3.5.15 Cellular uptake in the presence of endocytotic inhibitors	
3.5.16 Intra cellular trafficking of polymer	
3.5.17 Gene transfection	
3.5.18 Annexin V staining	
3.5.19 Immunostaining	
3.5.20 Biodistribution studies	
4. RESULTS	
4.1 Cationisation of polysaccharides – Pullulan & Dextran	
4.1.1 Synthesis	

4.1.2 Fourier transform infrared spectroscopy (FTIR)	
4.1.3 Proton nuclear magnetic spectroscopy(¹ H NMR)	
4.1.4 Copper sulphate assay	
4.1.5 Buffering capacity	
4.1.6 Size and zeta potential	
4.1.7 DNA binding ability and effect of plasma on nanoplex Stability	
4.1.8 Nanoplex stability in the presence of digestive enzyme, DNase	
4.1.9 Polymer interactions with plasma proteins	
4.1.10 Cell viability	
4.1.11 Cellular uptake of polyplexes	
4.1.12 Polymer trafficking studies	
4.1.13 Gene transfection	
4.1.14 Annexin V staining	
4.2 Synthesis and characterization of EGDMA modified CPs	
4.2.1 Synthesis	
4.2.2 Fourier transform infrared spectroscopy (FTIR)	
4.2.3 Proton nuclear magnetic spectroscopy(¹ H NMR)	
4.2.4 Copper sulphate assay	
4.2.5 Buffering Capacity	
4.2.6 Size and zeta potential	
4.2.7 DNA binding ability and effect of plasma on nanoplex stability	
4.2.8 Polymer interactions with plasma proteins	
4.2.9 Cell viability	
4.2.10 Cellular uptake of polyplexes	
4.2.11 Gene Transfection	
4.3 Synthesis and characterization of AOETMAC modified CPs	

4.3.1 Synthesis	
4.3.2 Fourier transform infrared spectroscopy (FTIR)	
4.3.3 Proton nuclear magnetic spectroscopy	
4.3.4 Copper sulphate assay	
4.3.5 Buffering Capacity	
4.3.6 Size and zeta potential	
4.3.7 DNA binding ability and effect of plasma on nanoplex stability	
4.3.8 Polymer interactions with plasma proteins	
4.3.9 Cell viability	
4.3.10 Cellular uptake of polyplexes	
4.3.11 Gene transfection	
4.4 Synthesis and characterisation of vinyl imidazole grafted cationised polysaccharides	
4.4.1 Synthesis	
4.4.2 Fourier transform infrared spectroscopy (FTIR)	
4.4.3 Proton nuclear magnetic resonance spectroscopy (^1H NMR)	
4.4.4 Buffering capacity	
4.4.5 Particle size and zeta potential	
4.4.6 DNA binding ability and effect of plasma on nanoplex stability	
4.4.7 Nanoplex stability in the presence of digestive enzyme, DNase	
4.4.8 Polymer interactions with plasma proteins	
4.4.9 Cytotoxicity studies –MTT assay	
4.4.10 Cellular uptake of polyplexes	
4.4.11 Cellular uptake in the presence of endocytic inhibitors	
4.4.12 Gene transfection	

4.5 Synthesis and characterisation of 2- diethyl amino ethyl methacrylate grafted cationised polysaccharides	
4.5.1 Synthesis	
4.5.2 Fourier transform infrared spectroscopy (FTIR)	
4.5.3 Proton nuclear magnetic spectroscopy	
4.5.4 Copper sulphate assay	
4.5.5 Buffering capacity	
4.5.6 Size and zeta potential	
4.5.7 DNA binding ability and effect of plasma on nanoplex stability	
4.5.8 Nanoplex stability in the presence of digestive enzyme, DNase	
4.5.9 Polymer interactions with plasma proteins	
4.5.10 Cell viability	
4.5.11 Cellular uptake of polyplexes	
4.5.12 Cellular uptake in the presence of endocytic inhibitors	
4.5.13 Polymer trafficking studies	
4.5.14 Gene transfection	
4.5.15 Annexin V staining	
4.5.16 Immunostaining	
4.5.17 Biodistribution studies	
5. Discussion	
5.1 Cationisation of polysaccharides – Pullulan & Dextran	
5.2 Ethylene glycol dimethacrylate cross linked cationised polysaccharide for gene delivery	
5.3 [2- (acryloyloxy) ethyl] trimethylammonium chloride (AOETMAC) grafted cationised polysaccharides for gene delivery	
5.4 Vinyl imidazole grafted cationised polysaccharides for gene	

Delivery	
5.5 Diethyl amino ethyl methacrylate (DEAEM) modified cationised polysaccharide for gene delivery	
6. Summary and Conclusion	
7. References	
8. List of publications and conferences	

List of Figures

Figure 1: FTIR spectra for evaluation of functional groups in PEI, native polysaccharides and their cationised derivatives- (A) dextran (B) pullulan (C) PEI (D) dextran PEI, DP (E) pullulan PEI, PP

Figure 2: Proton NMR spectra of polysaccharides, PEI and CPs.

Figure 3: Buffering capacities of cationic polymers and saline over the pH range 10 to 4 which was determined by acid base titration.

Figure 4(A): Hydrodynamic sizes of the polyplexes that prepared by complexing cationic polymers (DP, PP & PEI) with ctDNA at different weight ratios.

Figure 4(B): Zeta potential measurements of polyplexes prepared at different weight ratios by complexing different volumes of 1mg/ml cationic polymer solutions with fixed amount of ctDNA

Figure 5: Stability of the nanoplexes and the ability of cationic polymers to retard the movement of DNA under electric field were assessed by agarose gel electrophoresis.

Figure 6: Nanoplexes of CPs were prepared with ctDNA at different weight ratios (0.5:1 to 5:1) and treated with 4 μ l DNase (569 U/mL).

Figure 7: Interaction of cationic polymers with plasma proteins was evaluated by polyacrylamide gel electrophoresis following incubation of plasma with the respective polymers

Figure 8: Cytocompatibility of cationic polymers evaluated by MTT assay in three different cell lines – (A) C6, (B) HeLa and (C) L929 cell lines at four different polymer concentrations (25, 50, 75 and 100 µg/ml).

Figure 9 : Cellular uptake studies of cationic polymers in C6 glioma and HeLa cell lines.

Figure 10: Polymer trafficking studies in C6 cells.

Figure 11: Assessment of transfection efficiency of CPs and PEI using p53 plasmid. A, B, C and D, E, F are C6 cells and HeLa cells that are transfected with polyplexes of DP, PP and PEI respectively.

Figure 12: Flow cytometric data of HeLa cells transfected with polyplexes of cationic polymers prepared with p53 plasmid.

Figure 13: FTIR spectrum of pullulan PEI ethylene glycol dimethacrylate (PPE)

Figure 14: Proton NMR spectra of PPE in deuterated water.

Figure 15: Buffering capacities of EGDMA derivatives of PP over the pH range 10 to 4 by acid base titration.

Figure 16(A): Hydrodynamic diameter of PPE polyplexes prepared with ctDNA at different weight ratios.

Figure 16(B): Zeta potential measurements of PPE polyplexes prepared with ctDNA at six different weight ratios.

Figure 17: Stability of PPE polyplexes to retain ctDNA under electric field was assessed by gel retardation assay.

Figure 18: Plasma protein interactions of PPE derivatives was studied by performing poly acrylamide gel electrophoresis

Figure 19: Cytocompatibility of PPE derivatives was evaluated by MTT assay in (A) C6, (B) HeLa and (C) L929 cells.

Figure 20: Cellular uptake of PPE polyplexes prepared at 5:1 ratio with YOYO I tagged ctDNA that emits green fluorescence.

Figure 21: Transfection efficiency of PPE I derivatives were assessed by using p53 plasmid whose expression induces apoptosis in cancer cells.

Figure 22: Flow cytometric quantification of cell death that occurred in C6 cells after transfecting with polyplexes of PPE I (A), PPE II (B) that prepared with p53 plasmid at the weight ratio 5:1. Dead cells were stained with propidium iodide.

Figure 23: FTIR spectrum of AOETMAC derivatives (A) DPA (B) PPA.

Figure 24: ¹H NMR spectra of AOETMAC derivatives- (A) DPA (B) PPA

Figure 25: Buffering capacities of AOETMAC derivatives of CPs over the pH range 10-4 by acid-base titration

Figure 26(A): Hydrodynamic size of nanoplexes of AOETMAC derivatives prepared with ctDNA at different weight ratios.

Figure 26(B): Zeta potential measurements of AOETMAC derivatives nanoplexes prepared with ctDNA.

Figure 27: Nanoplex stability of AOETMAC derivatives assessed by agarose gel electrophoresis.

Figure 28: Nanoplex stability of AOETMAC derivatives assessed in the presence of plasma proteins by agarose gel electrophoresis.

Figure 29: Interactions of AOETMAC derivatives with plasma proteins studied by performing polyacrylamide gel electrophoresis.

Figure 30: Cytocompatibility of AOETMAC derivatives in three different cell lines- (A) C6 (B) HeLa (C) L929 at four different polymer concentrations i.e. 25, 50, 75 and 100 μ g/ml.

Figure 31: Cellular uptake of nanoplexes of AOETMAC derivatives prepared with YOYO I tagged ctDNA (green fluorescence) at the optimised weight ratio i.e. 5:1 in C6 cells.

Figure 32: Cellular uptake of AOETMAC derivatives in HeLa cells.

Figure 33: Live dead assay in C6 cells transfected with polyplexes of PPA II prepared with p53 plasmid at the weight ratio 5:1.

Figure 34: FTIR spectra of VI derivatives. (A) DPI (B) PPI

Figure 35: ^1H NMR spectrum of (A) Dextran PEI Imidazole (DPI), (B) Pullulan PEI Imidazole (PPI) in D_2O .

Figure 36: Buffering capacity of VI derivatives over the pH range 10-4 determined via acid-base titration by sequential addition of 0.01N HCl (50 μL).

Figure 37(A): Hydrodynamic size of polyplexes prepared from DPI and PPI derivatives by complexing with ctDNA at six different weight ratios (0.5:1 to 5:1).

Figure 37(B): Zeta potential measurements of nanoplexes prepared by complexing VI derivatives with ctDNA at six different polymer to DNA weight ratios.

Figure 38: Nanoplex stability of VI derivatives analysed by performing agarose gel electrophoresis.

Figure 39: Stability of the nanoplexes of VI derivatives prepared with ctDNA in the presence of plasma proteins.

Figure 40: Nanoplex stability of VI derivatives prepared with ctDNA at six different weight ratios (0.5 to 5) was analysed in the presence of the digestive enzyme, DNase.

Figure 41: Decondensation of nanoplexes of VI derivatives in the presence of anionic polysaccharide, heparin.

Figure 42: Plasma protein interactions with VI derivatives. (A) Pullulan derivatives (B) Dextran derivatives

Figure 43: MTT assay was used to analyse the percentage Cell viability of three cell lines- C6 (A), HeLa (B) and L929 (C) by incubating with VI derivatives at four different polymer concentrations.

Figure 44: Cellular internalization of nanoplexes in C6 cells. Nanoplexes of VI derivatives were prepared with YOYO I tagged ct DNA (green) at the weight ratio, 5:1.

Figure 45: Cellular internalization of nanoplexes of VI derivatives prepared at the weight ratio, 5:1 with YOYO I tagged ct DNA (green).

Figure 46: Live/dead assay in C6 cells transfected with nanoplexes of VI derivatives prepared with p53 plasmid at the weight ratio 5:1 (polymer to DNA).

Figure 47: Live/dead assay in HeLa cells transfected with nanoplexes of VI derivatives.

Figure 48: Flow cytometric quantification of cell death in C6 (A-C) and HeLa (D-F) cells by transfecting with polyplexes of PPI I, PPI II and PPI III that prepared with p53 plasmid at the weight ratio 5:1 by propidium iodide staining.

Figure 49: FTIR spectra of 2-diethyl amino ethyl methacrylate (DEAEM) derivatives- (A) dextran PEI diethyl amino ethyl methacrylate (DPD), (B) pullulan PEI diethyl amino ethyl methacrylate (PPD)

Figure 50: ^1H NMR spectra DEAEM derivatives. (A) DPD (B) PPD. H-1 is the protons associated with methyl group of DEAEM molecules.

Figure 51: Buffering capacities of DEAEM derivatives over the pH range 10 to 4 determined by the acid base titration.

Figure 52(A): Hydrodynamic sizes of the polyplexes formed by the DEAEM derivatives with ctDNA at different weight ratios polymer to DNA weight ratios.

Figure 52(B): Zeta potential measurements of nanoplexes of DEAEM derivatives prepared with ctDNA at different weight ratios.

Figure 53: DEAEM derivatives ability to retard the movement of DNA under electric field was assessed by agarose gel electrophoresis.

Figure 54: (A-D) are DNase treated nanoplexes of DPD I, DPD II, PPD I and PPDI derivatives respectively. (E-F) are heparin treated nanoplexes of DPD I, DPD II, PPD I and PPDI derivatives respectively.

Figure 55: Interactions of plasma proteins with DEAEM derivatives were analysed by polyacrylamide gel electrophoresis after incubating the respective polymers with plasma.

Figure 56: MTT assay to determine cytocompatibility of DEAEM derivatives at four different polymer concentrations (25, 50, 75 and 100 µg/ml) in the cell lines – (A) C6, (B) HeLa and (C) L929.

Figure 57: Cellular uptake of polyplexes of DEAEM derivatives prepared with YOYO I tagged ctDNA (green) at the weight ratio 5:1 in C6, HeLa and L929 cell lines.

Figure 58: Flow cytometric quantification of cellular uptake of nanoplexes of DEAEM derivatives prepared with YOYO I tagged ctDNA at the weight ratio 5:1.

Figure 59: Confocal microscopic images of trafficking DEAEM derivatives in C6, HeLa and L929 cells.

Figure 60: Transfection efficiency of DEAEM derivatives assessed by using p53 plasmid in C6, HeLa and L929 cells. Dead cells are stained red with ethidium bromide while live cells are stained green with calcein AM.

Figure 61: Flow cytometric quantification of cell death by propidium iodide staining. (A-D) and (E-H) are C6 and HeLa cells transfected with polyplexes of DEAEM derivatives that are prepared with p53 plasmid at the weight ratio 5:1.

Figure 62: (A -D) Live dead assay in C6 cells treated with DEAEM derivatives DPD I, DPD II, PPD I and PPD II respectively.

Figure 63: Live dead assay in C6 (A-D) and HeLa cells (E-H) transfected with polyplexes of DEAEM derivatives and their parent chains (DP and PP) prepared with ctDNA. A,B,C, D are C6 cells that transfected with nanoplexes of DP, DPD II, PP, PPD II while E,F,G,H are that in HeLa cells respectively.

Figure 64: Flow cytometric data of HeLa cells transfected with polyplexes of DEAEM derivatives that are prepared with p53 plasmid

Figure 65: Immunostaining of C6 cells that transfected with polyplexes of DPD II, PPD II and PEI prepared with p53 plasmid. Nanoplexes were prepared at the weight ratio, 5:1 for DEAEM derivatives and 2:1 for PEI.

Figure 66: Biodistribution of DEAEM derivatives in BALB/c mice at 4 different time periods.

List of Tables

1. Percentage reduction in amino groups present in the CPs after AOETMAC grafting.
2. Cellular internalisation of nanoplexes of PPI derivatives prepared with YOYO I tagged ctDNA were quantified in C6 and HeLa cell lines by flow cytometric analysis.
3. Flow cytometric data of cellular uptake of nanoplexes of PPI II prepared with ctDNA at the 5:1 weight ratio in the presence of various endocytotic inhibitors.
4. Transfection efficiency of PPI derivatives was analysed in C6 and HeLa cells by using p53 plasmid whose expression triggers apoptosis in these cell lines. Dead cells are quantified using flow cytometer by staining with propidium iodide.
5. Flow cytometric quantification of cellular uptake of nanoplexes of DEAEM derivatives in C6 cells in the presence of various endocytic inhibitors.

6. Table 6: Live, apoptotic (early and late), necrotic cells in C6 that occurred by the transfection with polyplexes of DEAEM derivatives analysed by annexin V staining. Nanoplexes are prepared with p53 plasmid at the weight ratio, 5:1.

List of schemes

1. Schematic representation of synthesis of cationised polysaccharides (CPs) by CDI chemistry- (A) Dextran PEI, (B) Pullulan PEI.
2. Schematic presentation of synthesis of PPE. Pullulan PEI (PP) was crosslinked with EGDMA using ceric ammonium nitrate (CAN) as the catalyst.
3. Schematic representation of the synthesis of AOETMAC derivatives by Michael addition reaction -(A) Dextran PEI acryloyloxy ethyl trimethyl ammonium chloride (DPA), (B) Pullulan PEI acryloyloxy ethyl trimethyl ammonium chloride (PPA).
4. Schematic representation of synthesis of (A) DPI and (B) PPI by free radical addition reaction using CAN as the initiator.
5. Schematic representation of synthesis of 2-diethyl amino ethyl methacrylate (DEAEM) derivatives- (A) dextran PEI diethyl amino ethyl methacrylate (DPD), (B) pullulan PEI diethyl amino ethyl methacrylate (PPD)

Abbreviations

Abs	Absorbance
AOETMAC	[2-(Acryloyloxy) ethyl] trimethyl ammonium chloride
EGDMA	Ethylene glycol dimethacrylate
DEAEM	2-Diethyl amino ethyl methacrylate
VI	Vinyl imidazole
CPs	Cationised polysaccharides
DP	Dextran PEI
PP	Pullulan PEI
PPA	Pullulan PEI [Acryloyloxy) ethyl] trimethyl ammonium chloride
DPA	Dextran PEI [Acryloyloxy) ethyl] trimethyl ammonium chloride
PPD	Pullulan PEI Diethyl amino ethyl methacrylate
DPD	Dextran PEI Diethyl amino ethyl methacrylate
PPE	Pullulan PEI Ethylene glycol dimethacrylate
PPI	Pullulan PEI Vinyl imidazole
DPI	Dextran PEI Vinyl imidazole
CPP	Cell penetrating peptides
ctDNA	calf thymus Deoxyribonucleic acid
DLS	Dynamic light scattering
DMEM	Dulbecco's modified Eagle's medium
EDTA	Ethylene diamine tetra acetic acid
EPR	Enhanced permeability and retention effect
FBS	Foetal bovine serum

FTIR	Fourier transform infrared spectroscopy
kDa	kilo Dalton
MEM	Minimal essential medium
MTT	3-(4, 5-Dimethylthiazol-2-yl)-2, 5-diphenyltetrazolium bromide
mV	milli Volt
Mw	Molecular weight
nm	nano meter
NMR	Nuclear magnetic spectroscopy
PBS	Phosphate buffered saline
pDNA	plasmid DNA
PEG	Polyethylene glycol
PEI	Polyethyleneimine
ppm	parts per million
RES	Reticulo endothelial system

SYNOPSIS

Cancer is a collective term used to refer a group of related diseases characterised by abnormal or uncontrolled cell growth and it is the second leading cause of death worldwide. Extensive knowledge gathered about cancer cell biology over the past decades, has helped in designing various new therapeutic approaches to fight against this disease. However, the heterogeneous nature of these diseases offers them resistance to most of these therapeutic strategies. Conventional treatment methods include surgery, radiation therapy, chemotherapy, immunotherapy and hormonal therapy. The limitations associated with these therapies, emphasizes the need for more powerful modality for the treatment of this deadly disease.

Gene therapy is one such modality which has the potential to create the revolution in the field of medicine from treatment mode to that of prevention level. Here, the nucleic acids are used as the pharmaceutical agent. Over the past two decades, different approaches have evolved in the field of cancer gene therapy. Despite its fabulous application, the growth of gene therapy as a treatment modality is still at the stage of its infancy due to the lack of proper gene delivery vector. Gene delivery vectors are widely classified into two – viral and non viral vectors. Viral vectors are found to possess higher gene transfection efficiency when compared to that of non viral vectors. However, the adverse health effects associated with these vectors and also their cost of production limits their application in the field of gene delivery. Hence, this study

primarily focused on non viral vectors especially the polymeric systems for gene delivery.

Non toxic and non immunogenic nature of polymers as compared with that of viral counter parts and also the simple protocol for their production makes them attractive in the field of gene delivery. Among the various polymers used for gene delivery, PEI is considered as one of the golden standards as it transfects a wide variety of cells with reproducible results. However, the inherent cytotoxicity associated with PEI owing to their higher charge density and also unwanted interactions with blood components limit their application as the gene delivery vector. PEI can be made into an effective gene delivery vector if we can reduce its cytotoxicity without affecting its transfection efficiency. As an attempt to address these issues, in this study, PEI was modified with non-ionic polysaccharides and with selected vinyl monomers to impart specific functions. Pullulan and dextran were selected as vector backbones as they are inexpensive, renewable, biodegradable and biocompatible polysaccharides. Moreover, their modifications also prevent unwanted interactions with blood components. Therapeutic gene, the p53 gene was selected as it gets mutated in 50% of human cancers. Also, the expression of this gene induces apoptosis in tumour cells by initiating the intrinsic pathway, while causes reversible growth arrest in normal cells.

The present study design has two parts- phase I deals with synthesis and characterisation of cationised polysaccharides while phase II comprises of the derivation of these cationised polysaccharides (CP) with vinyl monomers and their characterisation. Vinyl monomers selected for this study include ethylene glycol dimethacrylate (EGDMA), 2-

(acryloyloxy ethyl) trimethyl ammonium chloride (AOETMAC), vinyl imidazole (VI) and 2-diethyl amino ethyl methacrylate (DEAEM). Chemical modifications of these derivatives were confirmed by FTIR and NMR spectroscopy. The buffering capacity of these grafted polymers was analysed over the pH range 10–4 by acid-base titration.

Polyplexes of these grafted polymers were prepared by vortexing with ctDNA at six different weight ratios (0.5:1, 1:1, 2:1, 3:1, 4:1, 5:1). Size and zeta potential of these polyplexes were determined using Malvern Zetasizer. Polyplex stability was evaluated by performing agarose gel electrophoresis. Interaction of cationic polymers with plasma proteins was determined by performing native polyacrylamide gel electrophoresis (Native PAGE). Cytocompatibility of these cationic polymers and also their nanoplexes, prepared with ctDNA at their optimised weight ratio were analysed by carrying out MTT assay in C6, HeLa and L929 cells. Cellular internalisation was studied in two different cancer cell lines - C6 and HeLa by preparing nanoplexes of these grafted polymers with fluorescently (YOYO iodide) tagged ctDNA. Transfection efficiency of these grafted polymers was assessed in cancer cell lines - C6 and HeLa using p53 plasmid whose expression leads to apoptosis in these cells. Biodistribution of the selected polymer was also analysed in BALB/c mice over a period of 24 h.

Polysaccharides were cationised with PEI using CDI (1, 1'-carbonyldiimidazole) chemistry. The polysaccharide to PEI weight ratio is optimised as 2.5:1 because at this weight ratio, there is a balance between cytotoxicity and transfection efficiency. Chemical structures of these cationised polysaccharides (CPs) were confirmed by FTIR

and NMR spectroscopy. CPs exhibit the appreciable level of buffering capacity over the endosomal pH range i.e., 7-5 and form stable, nanosized positively charged polyplexes with ctDNA. However, they exhibit interactions with plasma proteins and also become toxic at higher polymer concentrations in C6 and L929 cells. Good cellular uptake and transfection efficiency were observed for these CPs in both C6 and HeLa cell lines. CPs synthesised at this weight ratio, 2.5:1 (polysaccharide: PEI) were further derivatized with vinyl monomers in order to provide specific functions.

Ethylene glycol dimethacrylate (EGDMA) monomers were selected in order to improve cytocompatibility of CPs and also to avoid unwanted interactions with plasma proteins. EGDMA crosslinked pullulan PEI (PP) was synthesised at two different weight ratios (10:0.01 and 10:0.15) by free radical addition reaction using ceric ammonium nitrate as the initiator. Similarly, dextran PEI (DP) derivatives were synthesised but it was found to be insoluble due to extensive crosslinking. Even though, no new bands appeared in the FTIR spectrum owing to EGDMA crosslinking, NMR spectra confirm the cross linking of this vinyl monomer to PP. These derivatives exhibit good buffering capacity over the pH range 7-5. They form stable, nanosized complexes with higher positive zeta potential and narrow PDI at the weight ratio of 5:1, which was optimised for further cell studies. This modification greatly improves the cytocompatibility. However, the cellular uptake and transfection efficiency get affected by the crosslinking of PP with this vinyl monomer in HeLa cells.

2-Acryloyloxy trimethyl ammonium chloride (AOETMAC) monomers avoid interactions with plasma proteins and hence modification with this molecule improves the half life of cationic polymers in the systemic circulation. AOETMAC grafted CPs were synthesized at 3 different weight ratios (10:0.01, 10:0.015 and 10:0.0025) through Michael addition reaction. Here also, no new bands appeared in the FTIR spectra owing to the grafting of this vinyl monomer, however, this chemical modification was confirmed by the NMR spectra. These derivatives exhibit excellent buffering capacity over the pH range 7-5. They form nanosized complexes with ctDNA, however, their zeta potential remains nearer to zero even for the polyplexes that prepared at higher weight ratio ie., 5:1. The polyplexes formed from these derivatives were also not stable. However, this modification greatly improves the cytocompatibility of these cationic polymers and also exhibit good cellular internalization in C6 cells. However, the transfection studies with p53 plasmid reveal that they are poor transfection agents. The polyplexes of these derivatives exhibit poor cellular uptake and transfection efficiency in the HeLa cells.

Vinyl imidazole (VI) moieties assist the polymeric vectors in their endosomal escape and also inhibit Ras protein which plays an important role in cancer cell proliferation. CPs were grafted with VI at three different weight ratios (10:0.005, 10:0.01 and 10:0.02) to synthesize six polymer derivatives. Chemical modification was confirmed by the FTIR and NMR spectra. These derivatives exhibit good buffering capacity over the pH range 7-5. These derivatives form stable, smaller sized, positively charged polyplexes with ctDNA at their optimized weight ratio, 5:1. This modification improves the

cytocompatibility of CPs to the greater extent. They also exhibit excellent cellular uptake and transfection efficiency in both C6 and HeLa cell lines. However, the poor reproducibility and also the instability over longer periods of storage, limit the application of VI derivatives as gene delivery vectors.

2-Diethyl amino ethyl methacrylate (DEAEM) monomers possess the ability to transiently disrupt the cellular membrane and thereby assist the modified polymers in their cellular entry. Moreover, grafting with this monomer helps to buffer the acidic pH prevailing within the endosomes. DEAEM grafted CPs were synthesized by Michael addition reaction at two different weight ratios (10:0.01 and 10:0.005). No new bands appear in the FTIR spectra corresponding to their grafting. However, in NMR spectra, the appearance of chemical shift over 1 ppm corresponds to the resonance of protons in methyl group of DEAEM confirms the grafting of this vinyl monomer to these CPs. These derivatives form nanosized, positively charged stable polyplexes with ctDNA at their optimized weight ratio 5:1 and also exhibit good buffering capacity over the pH range, 7-5. Their derivatization greatly improves the cytocompatibility of CPs. Moreover, they also show excellent cellular internalization and transfection efficiency in both C6 & HeLa cell lines. Biodistribution studies carried out in BALB/c mice revealed the accumulation of these polymer derivatives in liver tissue. These derivatives also exhibit good renal clearance in these animal models.

In this present study, all these vinyl monomer modifications improved the cytocompatibility of the CPs. Among pullulan and dextran derivatives, former exhibit

better cytocompatibility and transfection efficiency. Among VI monomers, EGDMA and AOETMAC reduce interaction with plasma proteins at the same time their cellular uptake also gets reduced in HeLa cells. Of the 4 derivatives prepared, DEAEM was found to be better gene delivery vector since they transfect the cells more efficiently with reproducible results.

1. Introduction

Gene therapy has the potential to revolutionize the field of medicine from the practice of treatment to that of prevention level. It is the application of genetic principles at the molecular level to correct the malfunctioned genes to cure both genetic and acquired diseases. Over the past few decades, researchers revealed the involvement of genes in the development of various diseases (Jackson *et al*, 2018). Hence by gene therapy, it is possible to cure these diseases at their root cause i.e. by tackling the defective genes. Despite its fabulous application, the translation of this approach from the conceptual level to reality is limited due to the lack of proper gene delivery vector. An ideal gene delivery vector is the one that should protect the nucleic acid all the way inside the human body till they reach their final destination (nucleus/cytosol/mitochondria of targeted cells) and after their unloading, these vectors should be released back from the cell without any detrimental effects. So far no such ideal gene delivery vector is discovered or designed. Most of the clinical trials in gene therapy were carried out using viral vectors but still, their efficacy is limited by their immunogenic nature. Currently, non viral vectors emerges as an attractive alternative to the viral vectors as they exhibit better safety profile, simple and cost effective manufacturing process involved in their production (Li *et al*, 2018; Bottai *et al*, 2017; Lam & Dean, 2010). During the time period, 2004 to 2013, there was significant increase in the use of non viral vectors in the clinical trials (Ramamoorth & Narvekar, 2015). Hence in this study, we focused on non-viral systems especially on polymeric vectors due to their ease of synthesis, cost-effectiveness and less toxic nature compared to that of viral counterparts. Efficacy of

these polymeric vectors was analysed in cancer cell lines using p53 plasmid whose expression leads to apoptosis in these cells. p53 gene was selected as it is one of the most commonly mutated tumour suppressor genes in various cancer conditions.

1.1 Cancer

Cancer is a cluster of diseases occur as a result of uncontrolled cell growth and it is the second leading cause of death worldwide. According to World Health Organisation (WHO) report, in 2015 there were about 8.8 million cancer deaths and the situation is quite alarming that one in every six deaths is due to cancer. In India, as stated by the Indian Council of Medical Research (ICMR), over 7.36 lakhs people were expected to succumb to cancer in 2016 and it was also estimated that the figure may shoot up to 8.8 lakhs by 2020. One-third of cancer deaths occur due to unhealthy food habits, obesity, lack of physical exercise, tobacco and alcohol use.

Cancer is reported from very olden times and its occurrence was mentioned in ancient Egyptian manuscripts that date back to 3000BC, though the term ‘cancer’ was not used. The first description about cancer was written in Edwin Smith Papyrus, an ancient Egyptian textbook on trauma surgery, in which about 8 cases of tumours or ulcers of the breast were reported to be removed by cauterization using the tool called the fire drill. It was also mentioned that the disease was incurable. Hippocrates (460-370 BC), “the Father of Medicine” described this non-ulcer forming and ulcer-forming tumours using the terms *carcinosis* and *carcinoma* owing to their crab-like morphology. Later Roman physician, Celsus (28-50 BC) translated this Greek word to Latin and coined the term *cancer* meaning crab.

Cancer cells are transformed normal cells that lack control over cell growth and division thereby disrupting body homeostasis. Normal cell growth and division are tightly regulated processes. Transformation of normal cells into cancer is a multistep process that involves the accumulation of genetic defects over a period of time leading to the development of lump of mass called tumour or neoplasm. These tumours are either benign or malignant. Benign tumours are non-cancerous and are confined to the particular area while malignant tumours are life-threatening ones which can grow and spread to other parts of the body via metastasis. Malignant neoplasm is the medical term used to refer cancer.

1.2 Conventional cancer treatment methods

The advent of modern technologies and also growth in knowledge about cancer biology has made significant progress in early detection, treatment and prevention of cancer in the recent years. Occurrence of intratumour heterogeneity was one of the key factors that contribute to the therapeutic failure and drug resistance of these cancer cells. Intratumour heterogeneity is the occurrence of different types of cells having different genotype and phenotype within the tumour mass. The magnitude of this heterogeneity is so high that no two identical cells exist either within a single tumour or between different tumours. The reason behind this massive inter and intratumour heterogeneity is due to the occurrence of about 10,000-20,000 mutations in the genome of each cancer cell which results in the generation of over $10^{68,000}$ different cells (Sverdlov, 2011, 2016).

Basic understanding about molecular biology behind the cancer cell and also the pathways involved in the transformation of normal cells into malignant neoplasm

helps to design the more effective cancer treatment methodology. Conventional cancer treatment methods include surgery, radiation therapy, chemotherapy, hormonal therapy, immunotherapy and targeted therapy. These treatment methods are either given as alone or in combination based on the patient performance status, location, and grade of the tumour as well as the stage of the disease.

1.2.1 Surgery

Surgery is one of the oldest methods for the cancer treatment. It is also used to diagnose, prevent and grade the different stages of cancer. This modality is more effective in the treatment of localised tumours. After the invention of anaesthesia in 1846, surgeons like Bilioth, Handley and Halsted, the pioneers in the cancer surgery, used to treat cancer by removing the entire tumour mass along with the underlying lymph nodes. Pagat, another English surgeon through his famous “seed and soil” hypothesis, explained the phenomenon of metastasis of cancer tissue. The advent of imaging techniques transformed the most exploratory open surgeries to miniature level endoscopy that helps the recovery of the patients easier. Recently less invasive cryosurgery (liquid nitrogen to freeze and kill tumour tissue) and surgery using laser to remove tumour tissue were also explored for the treatment of this deadly disease. The major disadvantage of this treatment method is that it is applicable only to localised solid tumours and also, as it is technically impossible to remove each and every cancer cell, there is a greater chance of the resurgence of the disease.

1.2.2 Chemotherapy

In chemotherapy, chemical agents (drugs) are used to kill cancer cells. Most of these drugs are either given as pills or by intravenously even though the other ways such as subcutaneous, intramuscular, intrapleural, intraperitoneal, intra-arterial, intraventricular/intrathecal are also possible. Chemotherapeutic drugs are cytotoxic in nature and are designed to kill the rapidly dividing cancer cells. Unfortunately, these drugs are not capable to distinguish between actively dividing normal cells from cancer cells. As a result, the actively dividing normal cells of the body, like hair follicle cells, bone marrow cells and also the cells that line the stomach also get affected by these chemotherapeutic drugs. Hence the major drawback of this therapy includes hair loss (alopecia), myelosuppression (destruction of blood cells), and mucositis (inflammation in the lining of the stomach) causing stomach upset. Most of these drugs exhibit narrow therapeutic indices that mean the dose at which these drugs are effective against a tumour is close to the level at which these drugs exhibit unacceptable toxic side effects. Hence for more effective treatment, combinations of different drugs at various dosages over a period of time are recommended in order to the balance between the benefits and adverse effects of these drugs (Petrovski A, 2001). Based on the mode of action and also on the stage of cell- life cycle that gets interrupted, these chemotherapeutic drugs are classified into five categories – alkylating agents, topoisomerase inhibitors, anthracycline antibiotics, plant alkaloids, antimetabolites and other antitumour agents. Doxorubicin, Paclitaxel, Chlorambucil, 5-flourouracil are the some of the most commonly used antitumor drugs. Mode of action of these drugs is either by damaging the DNA which halts the cell replication

or by inhibiting the synthesis of new DNA strands by blocking the formation of nucleotides. Some of the drugs also interfere with the cell division by disrupting spindle fibre formation.

1.2.3 Radiation therapy

In radiation therapy, the ionizing radiation is used to shrivel or kill the cancer cells. It is also called X-ray therapy, radiotherapy, or irradiation. Radiation therapy is done either by giving external beam directly to the affected tissues (EBRT) or by administering internally via brachytherapy. Radiation therapy prevents growth and division of cancer cells by causing damage to their DNA. Although normal cells also get affected by this therapy, most of them recover from the radiation effects and function properly. Hence radiation is given in many fractions so that the normal cells get time to recover from the damage caused by each fraction of radiation.

1.2.4 Hormonal therapy

Certain tumours like breast and prostate cancers are sensitive to hormones. In hormonal therapy, the endocrine system was manoeuvred through the administration of hormones or drugs in order to inhibit the production and activity of specific hormones. This is because hormones, particularly steroid hormones play an important role in the regulation of gene expression in certain cancers and hence by altering the levels or activity of such hormones, the growth of the cancer cell can be ceased or even causes their cell death. For example, breast and ovarian cancers require estrogen for their growth. Hence by using aromatase inhibitors or Tamoxifen,

the selective estrogen receptor modulator (SERM), the growth of these tumours can be hampered.

1.2.5 Immunotherapy

In immunotherapy, therapeutics is designed either to stimulate or boost the immune response against cancer cells. Cancer cells possess tumour-associated antigens (TAA) on their cell surface which are often proteins or other macromolecules that can be recognised by the immune system. Based on the mode of action, immunotherapies are classified into three categories viz active, passive and hybrid (active and passive). If the tumour cells are directly attacked by targeting TAAs then it is called active immunotherapy while in passive immunotherapy the existing antitumour responses are enhanced by the use of monoclonal antibodies, lymphocytes and cytokines.

1.2.6 Targeted therapy

Targeted therapy impedes the growth and spread of cancer by the administering drugs or other substances which interfere with specific molecules called molecular targets that are involved in growth, progression and spread of cancer. Unlike chemotherapeutic agents which are cytotoxic and interfere with all dividing cells, these drugs act only on specific molecules and are often cytostatic in nature. “Molecularly targeted therapies/drugs”, “precision medicines” are the other names used to refer targeted therapies. In most of the cases, these targeted therapies are either small molecules or monoclonal antibodies. The major limitations of this

therapy include the occurrence of resistant cancer cells to the particular target and also difficulty in developing therapeutic molecules for the identified cancer targets.

1.3 Cancer and gene therapy

Potential of gene therapy as treatment modality was first explored in rare fatal monogenetic disorders like SCID. However, advances in science and technology over the past decades widened the application of gene therapy to various chronic and acquired diseases such as cancer, neurodegenerative and cardiovascular diseases. About 64.41% of ongoing clinical trials in gene therapy is for cancer (Hanna *et al*, 2017).

Cancer, the collective term used to refer the cluster of diseases that arise due to the alterations occurring in the status and expression of multiple genes that confer survival advantage and immense proliferative potential to somatic or germinal cells (Sotiriou *et al*, 2004). Tumour suppressor genes, (proto) oncogenes and DNA repair genes are the three major classes of genes that frequently get altered -in the disease cancer. Resistance to the natural and inherent cell death mechanisms (apoptosis and like processes) together with the impairment of cell proliferation regulatory circuits contributes for the immense cancer cell proliferation (Nagpal *et al*, 2016).

Cancer arises due to the defects or alterations in gene regulatory circuits together with the incompetence of immune cells to recognise these abnormal cells. So gene therapy against cancer involves two different approaches, one is directly targeting the tumour cells and the other one is the indirect approach in which either immune cells are targeted to sensitize them against cancer cells or by destroying stromal cells

that support the growth and metastasis of these cells (Douglas & Curiel, 2005).

Various strategies currently explored in gene therapy to target cancer cells include

- a) inserting gene either to induce apoptosis or to sensitize cells to the chemotherapeutic drug,
- b) insertion of wild-type tumour suppressor gene like p53,
- c) blocking the expression of oncogene by antisense approach and
- d) by inducing cancer cell-specific cytotoxicity either by the insertion of suicide genes or by the use of mutant lytic virus that specifically replicate in these cells (Das *et al*, 2015).

Cancer gene therapy was also explored for the recognition and destruction of tumour cells by stimulating the immune response of the host body. Tumour tissue utilises different strategies to escape from the host immune response and these include creating immune-suppressive tumour environment, down regulating or weakening immunogenicity of target antigens. Hence, cancer gene therapy can also be used to boost the host immune system either by elevating antigenic stimulation (anti – cancer vaccination) or by eliciting cytotoxic response towards cancer cells. For example, researches redirected the immune system towards cancer cells by genetically modifying CD8+ T lymphocytes (Giacca, 2010).

1.4 Gene delivery vectors

The success of gene therapy largely relies on the choice of the vector to carry the gene of interest. The anionic nature of naked DNA limits their cellular internalisation

and also they are highly susceptible to degradation by the serum nucleases. Hence there is a need of a vehicle to carry these genes safely to their target site. Currently there are two types of vectors—viral and non viral vectors. Viruses are naturally evolved successful nucleic acid carriers. These viruses can be made into vectors to carry gene of our interest after removing disease causing genes from their genome and this process is called crippling. Owing to their higher transfection efficiency, about 78% of gene therapy clinical trials were carried out using viral vectors. However, tumorigenicity and immunogenicity associated with these vectors and also their cost of production, formulation and scalability issues limit their application as gene delivery vectors (Douglas & Curiel, 2005; Yin *et al*, 2014). Irrespective of the fact that intense efforts to overcome these issues are underway, some are hard to address and may even be insurmountable. Hence, currently considerable attention is paid towards the development of non-viral gene delivery systems to design vectors capable of delivering the gene of interest with minimum immunogenicity. These non-viral vectors use either physical forces or chemicals to transfect cells. Although these non-viral vectors are considered superior over viral vectors due to their decreased immunogenicity, their success has been limited due to poor cellular uptake and transfection efficiency (Glover *et al*, 2005; Al-Dosari & Gao, 2009; Ramamoorth & Narvekar, 2015). In the following section, various strategies are discussed to improve the gene transfection efficiency of non-viral vectors, especially cationic polymers.

1.5 Strategies to overcome the barriers of gene delivery

The success of gene delivery vectors largely relies on how efficiently these vectors overcome both extracellular and intracellular barriers to reach the target site and deliver its cargo to elicit the desired response. Viruses are naturally evolved species that have the inborn capacity to overcome all these hurdles to transfer their genetic materials. However, polymeric gene delivery systems have no such inherent mechanisms but can be tailored and fabricated to surpass these barriers by introducing specific functionalities.

Polymeric gene delivery systems have to encounter myriad of obstacles throughout their journey, commencing from the point of administration to the target site. First and foremost hurdle for these delivery systems is the stability in the complex milieu of blood plasma. Another barrier is to escape from the clearance by the reticulo endothelial systems (RES). Once the vector overcomes these extracellular barriers and reaches the target cell intracellular barriers need to be tackled. These include semi-permeable nature of plasma membrane, endosomal escape before its fusion with lysosomes, cytoplasmic trafficking towards the nucleus and finally nuclear entry. Strategies to overcome these barriers are discussed in the following sections.

1.5.1 Formulation and design of vector

The first step in the gene delivery process is the design and formulation of the vector to form stable complexes with nucleic acids. Polymeric vectors are tailored in such a way to possess specific chemical and biophysical properties that helps to overcome the barriers to gene delivery. Cationic polymers condense anionic nucleic acids

through electrostatic interactions into submicron-sized, quasi-stable structures called polyplexes (nanoplexes). The degree of complexation and/or the quantity of material being used will decide the formulation process and also the resulting structure (Bloomfield, 1997). The optimum ratio of polymer to the nucleic acid will be selected based on how effectively the former retards the mobility of later under electric field in a gel retardation assay.

Stability of these polyplexes is determined by the cationic charge density of the polymer. At-least six to eight charges per polymer chain are essential for the effective nucleic acid condensation. Formulation and designing of cationic polymer with optimum charge density is one of the rate-limiting steps for the success of gene delivery. The higher charge density of the polymer leads to the formation of more compact and stable complexes that makes vector unpacking difficult. Moreover, excess cationic charge in these nanoparticles triggers unwanted interactions with plasma proteins and other blood cells that ultimately results in rapid clearance by RES and also causes cytotoxicity. On the other hand, if the cationic charge density of the polymer is too low then it will lead to premature vector unpacking and release of nucleic acids before reaching their target site prompting degradation by nucleases. Furthermore, these nanoparticles will aggregate that makes their cellular internalisation more difficult and also elicit rapid clearance from the bloodstream by RES. All these factors collectively contribute to the lower transfection efficiency of the cationic polymer having lower charge density.

1.5.2 Extracellular barriers

Multiple factors that exist within the extracellular milieu, may pose the significant barrier for the polymeric gene delivery systems that are administered via systemic circulation. Depending on the topology, the half - life of intravenously administered naked DNA varies between 1.2 to 21 minutes. The reason behind this very short half - life of naked DNA is due to their degradation caused by endo and exonuclease activity that present in the blood plasma. So polymeric vectors intended for gene delivery should have the capability to protect the DNA from these nucleases. Interactions of cationic polymer with plasma proteins and other blood cells pose another barrier. Albumin, immunoglobulins, fibronectin, β_2 -glycoprotein, apolipoproteins, complement and C-reactive protein are some of the key plasma proteins that have been identified to interact with polymeric vectors. Most of these interactions either hinder the biological activity of the vector or confiscate it for degradation and/or removal from the circulatory system.

Majority of these undesired interactions can be addressed by modifying vector surface with hydrophilic shielding moieties such as PEG, HPMA, sugars, and proteins (Jones *et al*, 2013b). The shielding effect depends on various parameters such as molecular mass, grafting density, and method of attachment of the chosen molecule. Surface PEG coating (i.e., stealth particles) sterically hinders the interactions of blood components and degradative enzymes with the vector surface, thus, preventing opsonisation and recognition by phagocytic cells (e.g., macrophages, dendritic cells, and monocytes) and resulting in prolonged circulation in the blood.

Electrostatic interactions of cationic polymers with the negatively charged plasma membrane of blood cells (erythrocytes, leukocytes and platelets) also affect the bioavailability and efficiency of these vectors. Activation of the immune system is another important barrier that should be considered. Eventhough viral vectors are considered as major culprits in eliciting an immune response, some of the non-viral vectors also found to activate the immune system (Gottfried & Dean, 2013). For example, intravenous administration of cationic lipoplexes found to elicit an inflammatory response by triggering the release of cytokines TNF α and IFN γ into the serum (Dow *et al*, 1999). The inflammatory response is believed to be caused by the recognition of unmethylated CpG motifs present in the plasmid DNA by Toll-like receptors (Zhao *et al*, 2004; Yasuda *et al*, 2005). Hence by the removal of these unmethylated CpG motifs, the gene transfection efficiency of thesenon-viral vectors may be improvised (Hyde *et al*, 2008). Cationic polymers like PEI also found to stimulate the immune response through the activation of the complementary system and also elicit both Th1 and Th2 response (Regnström *et al*, 2003). Moreover, PEGylation, the strategy used to synthesis stealthy nanoparticles may also result in the production of anti-PEG IgM which has the potential to interfere with every subsequent administration of the vector (Ishida *et al*, 2006, 2007; Wang *et al*, 2007).

1.5.3 Plasma membrane

Once the non-viral vector reaches the target cell, then negatively charged plasma membrane poses the next significant barrier to gene delivery. Naked DNA cannot readily associate with this membrane due to their anionic nature. Cationic polymers

circumvent this problem by neutralizing the negative charge of DNA and effectively associating with the plasma membrane. Once semi-stable interactions have been established, nanoparticles are likely to redistribute over the cell surface to be taken up by a variety of uptake pathways. The most common route of nanoparticle uptake is through the receptor-mediated endocytosis and it includes a variety of entry pathways such as clathrin- and caveolae-mediated endocytosis, macropinocytosis, and both clathrin- and caveolae-independent pathways (Rehman *et al*, 2013; El-Sayed & Harashima, 2013). The uniqueness of each pathway depends on their particle size preference and also the involvement of specific proteins that mediating endocytic entry. Depending on the cell type, the particle size requirements for each uptake mechanism may vary, but for most cells it follows the order of 200 nm or less for endocytosis, 500 nm for macropinocytosis, and particles up to 10 μm size may enter the cells via phagocytosis (Jones *et al*, 2013b, 2013a).

All these approaches facilitate endocytosis or direct entry into the cytoplasm of any cell type while one of the goals of gene therapy is cell-specific targeting. In most cases, cell-specificity is achieved by specific interactions between ligands on the vector and receptors on the cell surface. For example, most of the tumour cells over express receptors for nutrients, such as folate and transferrin, this phenotype has been exploited for the development of DNA and drug delivery vehicles having either folic acid or transferrin as ligands (Zhang *et al*, 2016).

1.5.4 Endosomal escape

Most of the non-viral vectors enter the cell via endocytosis mechanism. The major endocytic pathways that are involved in the uptake of the non-viral vectors include

clathrin-mediated endocytosis, caveolae-mediated endocytosis, macropinocytosis and phagocytosis. Non-viral vectors which enter the cell via endocytosis get entrapped in the early endosomes. Here they experience a drop in pH, from neutral to slightly acidic pH 6. These early endosomes then mature into late endosomes where pH further drops to 5-6 by the action of membrane bound ATPase proton pumps. In the subsequent step, these late endosomes fuse with lysosomes which contain hydrolytic enzymes to form endolysosomal complex where the pH further drops to approximately 4.5 that facilitate substrate degradation by these enzymes.

Non viral vectors exhibit different mechanisms to escape from these endosomal compartments before their fusion with lysosomes. Polymeric vectors like polyethyleneimine (PEI), polyamido amine exploit proton sponge mechanism for their endosomal escape. According to this hypothesis, cationic polymers act as the sponge that absorbs the excess protons prevailing within the endosomal compartment due to its acidic pH. So in order to maintain acidic pH, membrane bound ATPase proton pumps translocate more protons from the cytoplasm into the endosomes. This proton influx also results in the passive intake of more chloride ions that creates osmotic gradient across the endosomal membrane. To maintain the ionic equilibrium, water molecules rush into the endosome, that result in the swelling and subsequent rupturing of endosomal membrane releasing these polyplexes into the cytosol.

Cationic lipid based gene delivery systems use 'flip flop' mechanism to escape from the endosomal compartment. Here the cationic lipids interact with anionic phospholipids of endosomal membrane causing the release of nucleic acid into the cytoplasm. Inclusion of neutral helper lipids like dioleoyl phosphatidyl ethanolamine

(DOPE) can significantly improve the transfection efficiency of these cationic liposomes since they can transit from bilayer to inverted hexagonal structures that enhance the endosomal escape. Cell-penetrating peptides (CPPs), another promising candidate for non-viral gene delivery exploit different mechanism for endosomal escape. Some of the examples of CPPs include TAT (trans-activating transcriptional activator), pep analogues, GALA (glutamic acid-alanine-leucine-alanine), MPG, CADY and LAH4 derivatives etc. These peptides are supposed to get released from endosome either through the formation of transient pores (Melikov and Chernomordik 2005) or by the membrane destabilisation (Kichler, Mason et al. 2006). Endosomal escape can also be triggered by the use of photosensitizers like TPPS₄ (*Meso*-tetra (4-sulfonatophenyl) porphine), TPPS_{2a} (meso-tetra phenyl porphyrin disulphonate), AlPcS_{2a} (Al (III) phthalocyanine chloride disulfonic acid) and dendrimer-based photosensitizer (DP) –dendrimer phthalocyanine (DPc) that primarily localized in the membrane of the endosomes and lysosomes. These photosensitizers get activated upon illumination, triggers the release of endosomal content into the cytosol by membrane destabilisation through the formation of reactive singlet oxygen (Berg, KristianSelbo et al. 1999; Endoh and Ohtsuki 2009).

1.5.5 Cytoplasmic trafficking

Once the polyplex get escape from the endosome, then its decondensation to release the gene of interest is the next important task to encounter. This is usually done by competitive binding of negatively charged mRNA and anionic proteins present in the cell cytoplasm (Vaughan & Dean, 2006; Labat-Moleur *et al*, 1996). To improve vector unpacking, polymers may also be designed in such a way to degrade in the

reductive environment prevailing within the cell cytoplasm by introducing either ester or thiol linkage (Funhoff *et al*, 2004; Luten *et al*, 2006). Once the vector gets unpacked and releases the DNA, then its mobility through the cytoplasm to reach the nucleus is the next important barrier. Nucleases present in the cytoplasm causes the degradation of free DNA. Studies carried out by Lachardeur *et al.*, revealed that half life of plasmid DNA in the cytoplasm of HeLa and COS cells is about 60 to 90 minutes (Lechardeur *et al*, 1999). This is one of the major barriers faced by the nanoplexes that dissociate before the nuclear entry. However, the DNA that released from its vector not occurs as a naked or free form in the cytoplasm rather they associates with various host cellular proteins to form protein-DNA complex. The protein corona that binds with DNA is dynamic in nature i.e. it differs with time. However, these proteins play multiple roles and assist DNA in their cytoplasmic trafficking through the cytoskeleton, protects against the degradation caused by the nucleases and also help in their nuclear entry (Bai *et al*, 2017).

The viscous nature of the cytoplasm further decelerates the mobility of these macromolecules. DNA reaches the nucleus by moving through the microtubule network using the motor protein dyenin (Vaughan & Dean, 2006; Salman *et al*, 2005; Mesika *et al*, 2005). However, the direct interaction of DNA with dyenin is not possible. So to bridge them, multiprotein complexes comprising transcription factors are required. Hence the velocity of the plasmid DNA across the cytoplasm can be enhanced by the incorporation of transcription factors binding site like CREB in the plasmid (Badding *et al*, 2012). Acetylation of microtubules also found to improve the mobility of DNA. Hence by modulating the activity of the enzyme histone

deacetylase 6 (HDAC6) which plays an important role in the microtubule acetylation, the gene transfer efficiency can be improved (Vaughan *et al*, 2008).

1.5.6 Nuclear import

Once the DNA alone or combined with vector overcomes all these above mentioned barriers and reaches the perinuclear area, then the next hurdle to be faced is their entry through the nuclear envelope. Various studies were conducted to estimate the amount of unmodified plasmid DNA that successfully transferred by non viral vectors into the nucleus of the cells using different techniques like quantitative PCR, southern blot and electron microscopy (Glover *et al*, 2010; Cohen *et al*, 2009). It was found that only 1 – 10% of plasmid DNA that are delivered to the cell found within the nucleus and it also depends on various factors like the applied dosage of DNA, cell type transfected and also the methods used for detection (Cohen *et al*, 2009; Glover *et al*, 2010). From these studies, it was clear that only a small percentage of input DNA enters the nucleus which was available for gene expression. Studies also revealed that more number of transfected DNA get into the nucleus of dividing cells as compared to that of non dividing cells. The reason behind this higher nuclear uptake of plasmid DNA in dividing cells is due to the disappearance of nuclear envelope during mitotic cell division in these cells. Nuclear transfer of plasmid DNA can be enhanced either by exploiting cells protein nuclear import machinery like nuclear localisation peptides (NLS), or by the incorporation of DNA nuclear targeting sequence (DTS). DTS is a 72bp sequence of SV40 enhancer that harbours ubiquitously expressed transcription factor binding sites which enhances nuclear import both in dividing and non dividing cells (Gottfried & Dean, 2013).

NLS peptides are either covalently or non covalently attached with DNA in order to improve their nuclear entry (Vaughan *et al*, 2006). However, the single NLS peptide fused with linear DNA that was capped with DNA hair pins at both ends found to possess higher nuclear targeting (Zanta *et al*, 1999). To link NLS peptides to DNA, peptide nucleic acids (PNAs) are also used. PNAs are analogs to the nucleic acid having polyamide backbone with repeated *N*-(2-aminoethyl) glycine units in the place of phosphodiester bond (Dean, 2000; Koppelhus & Nielsen, 2003). They bind with specific sequences of DNA with great affinity ($10^{-6} - 10^{-9}$ M) and form triplex structures (Dean, 2000). These PNAs preserve supercoiled conformation of plasmid DNA without altering its nuclear trafficking ability or transcriptional properties (Zelphati *et al*, 2000, 1999). Eight fold increase in gene expression observed when nanoplexes were prepared with PEI and plasmids that complexed with PNA-NLS peptides as compared to that of uncomplexed plasmid DNA (Brandén *et al*, 1999).

High mobility group-1 (HMG-1) proteins, nucleoplasmin, histone H1, p50 subunit of the NF- κ B transcription factor are the some of the proteins that are explored for improving gene expression of plasmid DNA by assisting in its nuclear entry (Vaughan *et al*, 2006).

1.6 Aims

Aim of this study is to develop cationic polysaccharide based gene delivery systems for efficient gene transfer in cancer cells.

1.7 Hypothesis

"Designing polymeric vector with nonionic hydrophilic polysaccharides and selected vinyl monomers having specific function improves the cytocompatibility of the PEI without compromising its transfection efficiency"

1.8 Objectives

1. Synthesis of cationic vectors by modifying cationized polysaccharides with selected vinyl monomers
2. Physiochemical characterisation of synthesised cationic vectors to ensure their ability to form stable nano-based systems with DNA
3. To assess cytocompatibility of these cationic vectors with different cell lines
4. Evaluating the cellular internalisation and transfection efficiency of these vectors in different cancer cell lines

This thesis work is an attempt to develop cost-effective, cytocompatible and efficient polymeric gene delivery systems to treat cancer and it includes the following chapters. ***Chapter 1*** provides an overview of cancer and its existing treatment modalities. This chapter also focuses on gene therapy as an emerging treatment modality to treat this deadly disease and also the hurdles faced by the gene delivery vector to accomplish this task. ***Chapter 2*** provides a detailed literature survey carried out to find the gaps and lacuna in the topic of interest. ***Chapter 3*** deals with the experimental section executed to test the hypothesis. ***Chapter 4*** delineates the results of all experiments conducted in this study. ***Chapter 5*** discusses and interprets the

results and draws the inference from the data collected. *Chapter 6* comprises the summary of the whole study. It discusses whether the objectives were addressed using this study design and also the major findings drawn at the end of the study.

2. Review of literature

2.1 Pullulan and Dextran as vector backbone in gene delivery

2.1.1 Pullulan

Pullulan is an exopolysaccharide produced by the fungus *Aureobasidium pullulans* and its production was first discovered by Bauer in 1938 (Singh *et al*, 2015). Isolation and characterisation of this polysaccharide from *A.pullulan* were done by Bernier in 1958 and the name was given by Bender, Lehmann and Wallenfels in 1959 (Bernier, 1958; Bender *et al*, 1959). Pullulan is a linear glucan having repeated units of maltotriose linked together by α (1-6) glycosidic bond. These maltotriose units comprises of three glucose residues connected by α (1-4) glycosidic linkage (Synytsya & Novak, 2014; Catley, 1971). Moreover, this polysaccharide also contains maltotetrose units to a extent of 7% (Catley *et al*, 1986). Structure of pullulan is an intermediate between amylose and dextran as there is a coexistence of both α (1-4)and α (1-6) linkages. Pullulan exhibit greater segmental mobility around the α (1-6) centred linkages and behaves as a random coil polymer in aqueous solutions (Singh *et al*, 2015; Dais *et al*, 2001).

Biocompatibility of pullulan attributes for its wider application in the field of medicine, cosmetics and food industry (Mishra *et al*, 2011). It is also used as a carrier in drug and gene delivery due to its non-immunogenic, non-toxic, non-carcinogenic, non-mutagenic and biodegradable nature (Kimoto *et al*, 1997; Akiyoshi *et al*, 1998; Na & Bae, 2002). Moreover, the hydroxyl groups present in the pyranose rings make the chemical derivatization of pullulan easier. Each repeating

unit of this polysaccharide contains 9 hydroxyl groups. Depending on the nature of the solvent and the polarity of reagents used, various derivatization reactions are possible (Shingel, 2004; Singh *et al*, 2015). Some of these include esterification, etherification, chlorination, amidification, sulfation, oxidation, co-polymerization etc(Bataille *et al*, 2011). Another advantage of pullulan is that it can be developed into various forms like nanoparticles, nanogels, microspheres etc.

Gupta and Gupta reported the (2004) synthesis of pullulan hydrogels for gene delivery purpose. They prepared pullulan nanoparticles by encapsulating pBUDLacZ inside the aqueous core of reverse micelles formed by aerosol-OT/n-hexane. Transfection efficiency of these nanoparticles was then evaluated in COS-7 and HEK293 cells lines in the presence of serum in order to closely mimic *in vivo* conditions. The results were compared with commercially available transfecting agent Lipofectamine 2000. Pullulan nanoparticles showed higher transfection efficiency in COS -7 cells and the results were comparable to that of Lipofectamine 2000. Moreover, these nanoparticles demonstrated excellent Cell viability in COS-7 cells as it exhibited 80% Cell viability even at 20 mg/ml polymer concentration (Gupta & Gupta, 2004).

Juan *et al*, (2007), synthesised diethyl amino ethyl pullulan (DEAE pullulan) incorporated 3 dimensional (3D) matrices for gene delivery in endoluminal vascular cells. These matrices are advantageous over other gene delivery systems as they eliminate the loss during the systemic circulation by concentrating the gene of interest near the target site. For this study, they grafted chloro – N, N- diethylamino ethyl hydrochloride to pullulan by activating its hydroxyl groups using sodium

hydroxide. The transfection efficiency of this cationised pullulan was first analysed in cultured rabbit SMCs by using pSEAP (the plasmid containing cDNA coding for the secreted form of alkaline phosphatase). This cationised pullulan was then incorporated into 3D matrices by cross-linking with dextran and pullulan in the weight ratio 1:2:7 using POCl_3 under alkaline conditions. The hydrogel was then cast into discs of 12mm diameter and 2mm thickness and loaded with 50 μg of pSEAP. This plasmid DNA impregnated discs exhibit higher transfection efficiency in cultured rabbit SMCs than that of the plasmid DNA alone and this may be due to the sustained release of the plasmid from the matrix. Moreover, these 3D matrices were also found to be non-toxic in these cultured cells.

Pullulan possesses higher affinity for liver cells especially towards hepatocytes and kupffer cells. This may be due to the presence of lectin receptors which shows the higher affinity towards sugar residues. In hepatocyte cells, asialoglycoprotein receptors play an important role in the endocytosis of this polysaccharide. Proper binding of pullulan to this receptor is facilitated by the orientation of hydroxyl groups that present in the pyranose rings which in turn promotes endocytosis. In a study conducted by Xi et al., found that intravenous administration of pullulan conjugated interferon found to be accumulating in liver cells more effectively than that of interferon alone. They conjugated interferon to pullulan through the cyanuric chloride method and this conjugate retains 7-19% biological activity of this protein. Enhanced 2-5A synthetase activity observed in the liver of mice administered with this pullulan conjugate. It was also noted that pullulan conjugated interferon required only in lower doses when compared to that of free interferon to induce the same

enzyme activity. Moreover, this activity was retained for 3 days in the mice administered with pullulan interferon conjugate while it was lost within 24 hrs in the mice that were administered with free interferon (Xi *et al*, 1996).

Among functional biomaterials, reduction sensitive biodegradable polymers and conjugates were found to be promising in the development of sophisticated drug and gene delivery systems. Generally, these biomaterials contain disulphide linkage either in the main chain/ side chain or in the crosslinker (Meng *et al*, 2009; Ferruti, 2013). These disulphide linkages are quite stable in the extracellular milieu while cleavable at the reductive environment that prevailing inside the cytoplasm and cell nucleus. In a reductive environment, these polymers undergo rapid cleavage via thiol- disulphide exchange reactions at a time scale from minutes to hours (Gilbert, 1995; Raina & Missiakas, 1997). This quick cleavage is advantageous over the other hydrolytically degradable polymers like polyesters and polycarbonates whose degradation kinetics ranges from days to weeks sometimes even months (Vert *et al*, 1992; Ikada & Tsuji, 2000). Yang *et al*, (2017) tailored biocleavable pullulan with reduction sensitive disulphide linkage for liver targeted gene delivery. They synthesised biocleavable comb-shaped pullulan poly (glycidyl) methacrylate ethanolamine (PUPGEA) vector by employing a two-step method. In the first step, hydroxyl groups of pullulan were modified with cystamine which imparts reduction sensitive disulphide linkage to this polysaccharide. In the second step, poly (glycidyl methacrylate) (PGMA) was grafted to this biocleavable pullulan via atom transfer radical polymerisation (ATRP) using this disulfide linkage as initiation site which was followed by subsequent functionalisation with ethanolamine. This biocleavable

pullulan exhibits excellent haemocompatibility when compared to that of PEI. Moreover, cellular uptake of this derivative was found to be higher in HepG2 cells than with HeLa cells which show their liver targetability (Yang *et al*, 2014).

Various groups have reported cationised pullulan which is modified using different cationic entities to effectively condense DNA and also to improve its gene transfection efficiency. Various molecules that studied to provide cationicity to pullulan include polyamines (spermine), peptides (poly-L-lysine), proteins (protamine) and also synthetic polymer (polyethyleneimine) (Thomsen *et al*, 2011; Park *et al*, 2012; Priya *et al*, 2014; Rekha & Sharma, 2011a). Gene transfection efficiency of spermine conjugated pullulan was studied by various groups in different cell lines for diverse applications. Thomsen *et al* studied the transfection efficiency of pullulan spermine conjugate in rat and human brain endothelial cells using pDNA encoding for human growth hormone 1 (hGH 1) (Thomsen *et al*, 2011). Kanatani *et al*, used pullulan spermine complex for transfecting T24 cells of human bladder cancer (Kanatani *et al*, 2006a) while Nagane *et al*, studied its gene transfection efficacy in bone marrow stromal cells using Notch intracellular domain gene (Nagane *et al*, 2009). Rekha *et al*., reported that cytotoxicity of PEI can be reduced to greater extent without compromising their gene transfection efficiency by pullulan modification (Rekha & Sharma, 2011a). They also observed that the liver targetability of pullulan, not get affected by this modification. They further modified this pullulan PEI conjugate with transferring as a ligand to target C6 glioma cells (Rekha & Sharma, 2011c).

2.1.2. Dextran

Dextran is a branched α -D-glucan of bacterial origin having a linear chain of anhydro-D- glucopyranose units linked together by α -1, 6 glycosidic linkages to which branches are connected mainly through α -1, 3 linkages although occasional α -1, 4 or α -1, 2 linkages are also present (Purama *et al*, 2009; Leathers, 2005). About 85% of branches are of 1 or 2 glucose residue length while the remaining 15% may have a length of 33 glucose residues. Dextran is synthesized by different strains of bacteria belonging to the family Lactobacillaceae especially by *Leuconostoc mesenteroids*, *Leucosnostoc dextranicum* and *Streptobacterium dextranicum* (Dhaneshwar *et al*, 2006; Sidebotham, 1974). Depending on the source of extraction, dextrans exhibit different chemical composition and physical properties like molecular weight, the degree of branching, solubility, optical activity and physiological action. Dextrans of pharmaceutical importance, mainly composed of 95% α -1, 6 glycosidic linkage and 5% of α -1, 4, α -1, 3 and a very few α -1, 2 linkages. This 95% linear linkages makes them as water soluble which is suitable for various applications (Purama *et al*, 2009; Varshosaz, 2012).

Dextran, the biodegradable neutral polysaccharide, has wider application in the field of medicine. Some of its applications include plasma volume expander, as antithrombotics and polymeric carrier for drug delivery systems. Pagano and Vaheri in 1965 were the first to explore the efficacy of cationised dextran in gene delivery. They studied the infectivity of Poliovirus RNA in both primate and non primate cell lines. They observed that infectivity of this nucleic acid increases in the presence of diethyl amino ethyl dextran (DEAE). Moreover, this cationised dextran also protects

RNA from ribonuclease degradation. Still, their transfection efficiency was not upto the mark when compared to that of viral counterparts (Pagano & Vaheri, 1965). Onishi et al (2007) tried to address this issue by modifying DEAE dextran with methyl methacrylate using ceric ammonium nitrate. They observed 16 fold rise in transfection efficiency of polymer derivative in HEK 293 cell line as compared to that of the parent chain. This may be due to the formation of more stable complexes which protects these nanoplexes from the degradation of DNase and dextran sucrose enzymes (Onishi *et al*, 2007).

Hosseinkhani *et al*, (2004) cationised dextran with natural oligoamine, spermine and explored its transfection efficiency both *in vitro* (HEK293 cell line) and *in vivo* (6 weeks old, DDy male mice) conditions using p-gal encoding plasmid DNA. The transfection efficiency of this dextran conjugates was comparable to that of the commercial transfecting agent, DOTAP/Chol 1/1 under serum free conditions. Moreover, these polymer derivatives also cause higher gene expression in the mice models when compared to that of naked DNA while administering via the intramuscular route. However, 80% of their transfection efficiency gets reduced while using serum containing medium and also during intravenous administration. Hence, they further modified these derivatives with PEG in order to improve the stability of these polymeric vectors in serum containing medium. These PEGyated derivatives exhibit higher gene transfection in liver cells while administering via the intravenous route. The reason for liver targeting by these polymer derivatives was also analysed by pretreating the animals with galactosylated and mannosylated agents that bind to galactose and mannose receptors present in the liver tissue

respectively. They found that gene expression in the liver tissues markedly gets reduced in the presence of galactose agents. Hence, they conclude that the galactose receptor present in the liver parenchymal cells may play an important role in the liver targeting of these polymer derivatives (Hosseinkhani *et al*, 2004).

Over these recent years, disulfide based bio-reducible polymeric vectors are receiving greater interest among non-viral gene delivery systems (Son *et al*, 2011). These vector systems make use of the reducing environment that prevails within the cell cytoplasm for gene delivery. The disulfide bonds present in these polymer derivatives were quite stable in the extracellular environment. However, the reducing environment prevailing within the cell's interior causes its cleavage which in turn promotes vector unpacking and the subsequent release of the gene cargo. Cytosol maintains a reducing environment with the help of the tripeptide called glutathione whose concentration in the cell's interior is 1000 times higher than that of the external environment (Lin & Engbersen, 2009).

Song *et al*, (2014) developed bio-reducible, disulfide-based cationic dextran conjugate for targeted gene delivery in ovarian cancer cells. First, they synthesised cationic polyamide (pSSBAP) having primary amine end groups from bis(p-nitrophenyl)-3,3'-dithiodipropionate and 1,4-bis(3-aminopropyl) piperazine (BAP) by a stepwise polycondensation reaction. This cationic polyamide then grafted to dextran and the transfection efficiency of these derivatives was evaluated in MCF-7 and SKOV-3 cell lines. This dextran conjugate effectively condensed DNA into nanosized complexes called polyplexes that exhibit good colloidal stability in the physiological environment. However, these polyplexes dissociate and release the

DNA under reducing environment. Gene transfection efficiency of these derivatives was comparable to that of linear polyethyleneimine or lipofectamine 2000 in SKOV-3 cell line. Moreover, these derivatives exhibit excellent cytocompatibility even at higher polymer concentrations i.e. 100 mg/L. They further modified this dextran conjugate with folate residues via carbodiimide chemistry in order to target ovarian cancer cells. Intravenous administration of this folate coupled dextran conjugates exhibits excellent gene transfection in SKOV-3 tumour xenografted, nude mouse model (Song *et al*, 2014).

In our lab, the gene transfection efficiency of dextran modified with the amino acid, histidine was evaluated under *in vitro* conditions using p53 plasmid in C6 glioma cells. The physiochemical properties, cellular uptake mechanisms, vector unpacking and transfection efficiency were studied in detail by Thomas *et al*, for this polymeric vector. Based on their findings, they elucidated the clathrin mediated endocytosis and macropinocytosis were the major routes by which this dextran derivative get internalised into the cells. They also proposed the possible role of histones in the vector unpacking. Moreover, this dextran histidine conjugate was found to be cytocompatible and also exhibited higher transfection efficiency in C6 glioma cells (Thomas *et al*, 2012). In another study, they modified dextran with protamine and explored its gene transfection efficiency. This derivative was found to be hemocompatible, non toxic and also exhibited excellent gene transfection efficiency in HepG2 cells (Thomas *et al*, 2010).

Effect of molecular weight and peptide grafting density on transfection efficiency was studied by Tang *et al* (2014) in ovarian carcinoma cell line, SKOV-3 using

oligopeptide grafted dextran. For this study, they have chosen dextran of 3 different molecular weights (10, 20 and 70 kDa) and modified with methacrylate. These polymer derivatives were further modified with the polypeptide, NH₂-RRRRRHHHHHC-COOH (R5H5) at different grafting densities via thiol-acrylate Michael type reaction. Higher transfection efficiency was observed for lower molecular weight dextran having higher grafting density when compared to that of higher molecular weight dextran with lesser grafting density. They discussed three possible reasons for this observation. Firstly, the weaker condensation of DNA by low molecular weight dextran favours vector unpacking which in turn improves their transfection efficiency. Secondly, their higher grafting density provides greater cationicity to these polymer derivatives and that helps in their effective cellular uptake. Thirdly, the higher buffering capacity possessed by these polymer derivatives assist in their endosomal escape once these polyplexes get internalised into the cells (Tang *et al*, 2014a).

2.2 Polyethylenimine (PEI) and gene delivery

PEI is considered as one of the golden standards in gene delivery as it transfects a wide variety of cell lines with reproducible results. Moreover, it is stable for years even at refrigerated conditions and also cost-effective (Zhao *et al*, 2014; Sou *et al*, 2013). Its molecular heterogeneity and the ease of chemical modification make it attractive in the field of gene delivery (Neuberg & Kichler, 2014). Due to the presence of a large number of amino groups, it readily forms complexes with DNA and condenses them into toroidal/globular shaped nanoplexes (Kichler, 2004b; Moghimi *et al*, 2005a). The application of PEI as gene delivery vector was first

studied by Boussif et al., and this polymer was found to be effective in transfecting both *in vitro* and *in vivo* conditions (Boussif *et al*, 1995a).

PEI is a versatile polymer available both in linear and branched form and also exist in a wide range of molecular weights. The branched PEI (bPEI) is synthesised by the polymerization of aziridine monomers either in controlled manner in an aqueous/alcoholic environment by adjusting temperature and the initiator concentration or in a vigorous manner using anhydrous aziridine at lower temperature (von Harpe *et al*, 2000; Kunath *et al*, 2003; Fischer *et al*, 1999). On the other hand, linear PEI (IPEI) was synthesised either from N(2-tetrahydropyranyl) aziridine or unsubstituted and two-substituted 2-oxazolines via cationic ring opening polymerization (Jones *et al*, 1944; Dick & Ham, 1970). The resultant N-substituted polymer is then subjected to acid or base-catalyzed hydrolysis to get the final product i.e. IPEI.

Branched PEI contains primary, secondary and tertiary amines in the ratio 1:2:1 while IPEI contains only primary and secondary amines. The success of gene delivery vector depends on how effectively it complexes with the gene of interest and safeguard them till they reach target site of action. As a gene delivery vector, bPEI condenses DNA more effectively to form compact structures and it also exhibit higher transfection efficiency as compared to that of IPEI (Kafil & Omid, 2011). The efficacy and cytotoxicity effects of bPEI based vectors widely depend on material characteristics (molecular weight, degree of branching, cationic charge density, buffering capacity), polyplex properties (particle size, zeta potential, DNA content) and also the environmental conditions during transfection experiments

(presence/absence of serum, incubation time, polyplex concentration). However, bPEI is highly toxic when compared to that of IPEI (Lungwitz *et al*, 2005).

Transfer of genetic materials from the site of administration to the target site of action is a herculean task as the gene delivery vectors have to face various obstacles to complete this task. Once these vectors reach the target cell, then it should interact with its plasma membrane to get internalised. Cationic polyplexes interact with plasma membrane via anionic proteoglycans that is present on the cell surface. Heparin sulphate proteoglycans (HSPG) are the major receptors involved in the uptake of these polyplexes. HSPG comprises of a wide variety of molecules such as beta glycan, also called as TGFR-3 (Zhang & Esko, 1994), CD44v3 (Brown *et al*, 1991), syndecans (SDCs) (Couchman, 2003), and glypicans (Lander & Selleck, 2000; Perrimon & Bernfield, 2000). Among these molecules, SDCs and glypicans are the two major cell surface HSPGs that widely expressed in mammalian cells and play an important role in the intake of the polyplexes formed with PEI (Kopatz *et al*, 2004). SDCs have four different forms namely SDC1, SDC2, SDC3 and SDC4 which are encoded by four different genes. Of these SDC1 and SDC2 play important roles in the endocytosis of PEI polyplexes. In a study conducted by Paris *et al.*, in HEK293 cells, they found that SDC1 enhances the gene transfection efficiency of PEI polyplexes by promoting endocytosis. On the other hand, SDC2 delays the endocytosis of these nanoplexes and have an inhibitory effect over the PEI mediated gene expression (Paris *et al*, 2008).

The large number of amino groups present in the PEI renders them high cationic charge density. Upon interactions with nucleic acid, this polymer forms positively

charged polyplexes which enters the cell via non-specific adsorptive endocytosis (Boussif *et al*, 1995a). The first step in the endocytosis of PEI/DNA polyplexes is their binding to syndecans, the HSGP that present in the cell surface. Clustering of syndecans around the polyplex triggers the cytoplasmic binding of these transmembrane proteins to actin filaments. This binding occurs via linker proteins which subsequently help in the uptake of these polyplexes through endocytic vesicles (Poon, 2007; Pichon *et al*, 2010; Demeneix & Behr, 2005). Once the vector gets internalised into the cell via the endocytic pathway, it experiences a drop in pH in this endosomal compartment. These endocytic vesicles then fuse with lysosome where the pH further drops in order to activate hydrolytic enzymes that present within these structures. So escape from these endocytic vesicles before its fusion with lysosomes is one of the critical steps for the success of gene delivery vector (Pack *et al*, 2005). It is generally believed that cationic vectors following internalization escapes from the endosomes either by destabilizing its membranes or by acting as proton sponge causing rupture of its membrane. PEI contains a protonable amino group in every third atom of its chain that renders this polymer excellent buffering capacity over a wide range of pH. PEI was hypothesised to act as proton sponge in the acidic environment that is prevailing within the endosomal compartment. As a result, ATPase proton pumps present in the endosomal membrane translocates more protons into the lumen in order to maintain its acidic pH. Electrical neutrality is then maintained by the influx of chloride ions. These events ultimately result in the osmotic swelling and rupturing of these vesicles causing the release of polyplexes into the cytoplasm (Akinc *et al*, 2005; Sonawane *et al*, 2003).

Hufnagel *et al*, (2009) observed that polyplexes of PEI-25/DNA having size ≥ 150 nm get internalised via distinct fluid-phase pathway, independent of clathrin and caveolin. They found that macropinosomes have a higher propensity to deliver PEI-25/DNA cargo than endosomes (Hufnagel *et al*, 2009). Evans *et al*, (2011) studied the PEI mediated entry of nanoparticles in neural cells via multimodal analysis. For this study, they synthesised fluorescent and magnetic polymer nanospheres by encapsulating magnetite (Fe_3O_4) nanoparticles within the fluorescently (rhodamine B dye) tagged poly (glycidyl methacrylate) (PGMA) nanospheres. PEI was then anchored to the epoxide groups present in the PGMA via simple ring-opening reaction. They used different techniques like relaxometry, correlated electron microscopy, fluorescence spectroscopy and microscopy to track the endocytic pathway of these nanoparticles. They found that PEI mediated nanosphere uptake involves three steps viz attachment to the cell membrane followed by clathrin and caveolin-independent endocytosis and final accumulation in membrane bound intracellular vesicles (Evans *et al*, 2011).

Once the polyplex gets released from the endosomes, then the viscous nature of cytoplasm imposes the next significant barrier. This diffusional barrier inflicted by the cytoplasm retards the nuclear transport of DNA. Nuclear translocation of plasmid DNA requires either disassembly of nuclear envelop that happens during cell division or through active intake by nuclear pore complex. A study conducted by Grandinetti *et al*, revealed that PEI possesses the ability to permeabilize the nuclear membrane. Polymer's ability to permeabilize the nuclear membranes is a boon and a curse. This is because nuclear membrane permeabilization increases the transfection

efficiency at the same time it will also cause toxicity. It can also damage the nuclei thereby triggering apoptosis of the cell. So care must be taken to tailor such polymers and there should be a balance between the cytotoxicity and transfection efficiency (Grandinetti *et al*, 2012a).

Despite its advantages, the use of PEI as gene delivery vector is hindered by their inherent cytotoxicity that scales with their transfection efficiency. Moghimi *et al*, (2005) studied the molecular basis of PEI mediated cytotoxicity in three different, clinically relevant human cell lines (Jurkat T cells, umbilical vein endothelial cells, and THLE3 hepatocyte-like cells). They used both branched (25 kDa) and linear (750 kDa) PEI as gene delivery vectors for this study. According to them, cytotoxicity induced by PEI follows a two-stage mechanism. In the phase I toxicity, the binding of PEI to the proteoglycans present in the cell surface causes their membrane destabilization. This, in turn, exposes phosphatidyl serine group that is present in the inner leaflet of cell membrane into the outer surface, leading to a rapid release of the enzyme lactate dehydrogenase. This early necrotic-like changes occur 30 min post transfection and it is the immediate response of the cell. Phase II toxicity occurs 24 h after transfection and it involves the activation of mitochondria mediated apoptotic programme. Here, the PEI interacts with the outer membrane of mitochondria and form channels through which proapoptotic cytochrome c get released into the cytoplasm. This, in turn, activates executioner caspase 3 whose translocation into the mitochondria alters their membrane potential and results in the production of reactive oxygen species. Hence PEI is found to act as an apoptotic agent (Moghimi *et al*, 2005a).

Another drawback of PEI based polyplexes while administering via systemic circulation is their non specific interactions with blood components, extracellular matrix and also the non targeted cells and tissues due to their higher charge density. Unmodified PEI/DNA polyplexes interacts with wide variety of proteins that present in the human plasma such as immunoglobulins (IgD, IgM), complement proteins (C3b,C4g), albumin, fibrinogen, apolipoproteins (apoA-I, A-II, H, C-III) and transthyretin (Ogris *et al*, 2003; Kursa *et al*, 2003). Adherence of complement components on the surface of these polyplexes activates the complement system. Subsequently, these complexes are cleared off from the systemic circulation by the reticuloendothelial cells (RES)(Plank *et al*, 1996). Interaction of PEI polyplexes with albumin results in the formation of ternary complexes. These complexes aggregate (Ogris *et al*, 1998; Ahn *et al*, 2002; Vinogradov *et al*, 1998; Tang *et al*, 2003; Nguyen *et al*, 2000) to form large structures which are easily removed from the bloodstream either by phagocytic cells engulfing or by the accumulation in capillary beds (Ogris *et al*, 1999). These interactions reduce the half life of PEI polyplexes in the systemic circulation thereby blocking their reach to the target tissue. Similarly, the interaction of these cationic polyplexes with blood cells especially with erythrocytes (Petersen *et al*, 2002b, 2002a) causes their aggregation which in turn obstructs the blood flow through blood vessel/ lung capillaries and that may result in pulmonary embolism (Ogris *et al*, 1999; Kircheis *et al*, 1999; Ogris *et al*, 1998).

Non specific interactions of PEI based polyplexes can be subdued by shielding the cationic surface charge with hydrophilic polymer either through covalent or non

covalent linkage. Some of the hydrophilic polymers used to shield cationic surface charge include polyethylene glycol (PEG), pluronic (Nguyen *et al*, 2000; Ochietti *et al*, 2002), dextran (Tseng & Jong, 2003), or dextran sulphates (Tiyaboonchai *et al*, 2003), polyacrylic acid (PAA), poly(N-(2-hydroxypropyl) methacrylamide) derived copolymers (Oupicky *et al*, 2002; Carlisle *et al*, 2004), transferring (Kircheis *et al*, 2001, 1999) or human serum albumin (Rhaese *et al*, 2003). The above mentioned modifications doesnot affect the solubility of polyplexes and also they retained their smaller size (Lungwitz *et al*, 2005).

Most of the clinical trials using PEI are in the initial phase. In cancer therapy, PEI and its derivatives were used to deliver the genes either to kill the cancer cells or to sensitize these cells to the chemotherapeutic drugs. Iwai *et al*, (2002) used PEI to deliver the suicide gene (Epstein- Barr virus based plasmid carrying the herpes simplex virus-1 thymidine kinase (HSV-1 Tk) to kill hepatocellular carcinoma (HCC) cells in mice models (Iwai *et al*, 2002). Gene therapy using PEI vectors found to hinder the proliferation of cancer cells and also promotes apoptosis in murine models of pancreatic tumors (Aoki *et al*, 2001; Vernejoul *et al*, 2002). In particular, Vernejoul *et al*, (2002) clearly demonstrated that PEI-based delivery of the somatostatin receptor 2 gene restored apoptosis at the same magnitude as that of adenoviral vectors (Vernejoul *et al*, 2002). Ovarian carcinoma is often characterized by their resistance to chemotherapy. The gene transfer efficiency of PEI based vectors was also explored in the cancer cells that developed resistance to chemotherapeutic drugs like that present in the ovarian carcinoma. In such cases, the goal of gene delivery is to restore chemosensitivity in these cells (Poulain *et al*, 2000;

Ziller *et al*, 2004). Clinical trials using PEI were also progressing in the field of DNA vaccine against HIV. Derma Vir is one such formulation comprising polyplexes of PEI mannose derivatives with plasmid DNA that encodes for 15 viral antigens to boost T cell responses against HIV. Gene delivery using PEI was also explored for treatment of acute myocardial infarction (Moon *et al*, 2014).

2.3 Significance of vinyl monomers

In order to impart specific functions, various vinyl monomers having biological significance were incorporated into the cationic polysaccharides as pendant groups. The vinyl monomers chosen for this study include vinyl imidazole (VI), ethylene glycol dimethacrylate (EGDMA), 2-diethyl amino ethyl methacrylate (DEAEM) and [2- (acryloyloxy) ethyl] trimethyl ammonium chloride (AOETMAC).

The imidazoles are aromatic heterocycles having two nitrogens separated with a methylene and they are ubiquitous in nature. This ring system is present as a part in various biological molecules such as histamine, histidine and plays an important role in the human body. Imidazoles are bioactive molecules having wider application in the field of biomedical research. They are also found to be promising as antibacterial, antifungal, anti inflammatory and anticancer agent. They are also quite stable to harsh chemicals such as strong acids/ bases and also resist hydrogenation (Bando & Sugiyama, 2006; Luca, 2005). The anticancer effect of imidazole is through the inhibition of post-translational farnesylation which is required for the activation of Ras proteins that involved in cancer cell proliferation (Luca, 2005).

Ihm *et al.*, (2003) synthesised poly (4-vinylimidazole) and evaluated its gene transfection efficiency using the luciferase gene in three different cell lines (HeLa, MC3T3E1 and 293 T). This polymer was found to be effective in condensing pDNA and formed 175nm sized complexes. These derivatives also exhibited above 70% Cell viability at the concentration 20 µg/ml which was higher when compared to that of PEI. Moreover, in all these cell lines tested, 3 fold rise in transfection efficiency was observed on comparison with that of PEI (Ihm *et al.*, 2003).

Asayama *et al.*, (2007) synthesised the pH sensitive, hepatocyte targeting gene delivery vector. For this study, they developed ternary complex consisting of lactosylated poly (L-lysine) (PLL-Lac), aminated poly (1-vinylimidazole) (PVIm-NH₂) and DNA. The imidazole groups present in the PVIm possess pKa around 6 and that accounts for its deprotonated state at physiological pH while get fully protonated at endosomal pH. Since the imidazole molecules that present in the PVIm exhibit negligible charge at pH 7.4, DNA molecules are anchored to the amino groups (-NH₂) as their pKa lies around 10. Once these ternary complexes reach endosome, imidazole moieties get fully protonated and dissociate with PLL-Lac. Hence, the binary complex (PVIm-NH₂ and DNA) alone gets released into the cytosol by disrupting the endosomal membrane. As far as Cell viability is concerned, these polymers exhibit no apparent toxicity even at the concentration 400 µg/ml. Moreover, their transfection efficiency was comparable to that of PEI (Asayama *et al.*, 2007).

Ethylene glycol dimethacrylate (EGDMA) is a diester synthesised by the condensation of two equivalents of methacrylic acid and one equivalent of ethylene

glycol and they are mainly used as cross linking agent. The transfection efficiency and cytotoxicity of PEI found to increase with the increase in their molecular weight. Dong et al., tried to address this issue by cross linking less toxic, low molecular weight PEI (2000 Da) via EGDMA to synthesise high molecular weight conjugates. The ester bonds that present in these crosslinker are cleavable at the physiological environment. Hence these high molecular weight conjugates revert back to the less toxic form once they reach the target site. They observed 60% transfection efficiency in B16F10, 293T, CHO, EL-4 and Hela cells and for former two cell lines, its transfection efficiency reached upto 80–90% (Dong *et al*, 2007a). A similar study was conducted by Forrest et al., using 800 Da PEI and 1,3-butanediol diacrylate/1,6-hexanediol diacrylate as cross linking agents (Forrest *et al*, 2003)

The water soluble nature together with the pH and thermoresponsive behaviour makes the diethylaminoethyl methacrylate (DEAEM) as an attractive molecule in the field of biomedical science (Nagasaki *et al*, 1997; Dai *et al*, 2008; A *et al*, 2015). Moreover, their polymeric form has the ability to transfect a wide variety of cell types. It was also reported in the literature, that they are capable of condensing DNA into nanosized structures and possess the ability to buffer the acidic pH that prevails within the endosomes. They also promote cellular entry by transiently disrupting lipid bilayer (van de Wetering *et al*, 1998; Takeda *et al*, 2004; Moselhy *et al*, 2007).

Sun *et al*, synthesised random copolymer, poly (2-aminoethyl methacrylate-co-2-(diethylamino) ethyl methacrylates) via atom transfer radical polymerization (ATRP) for gene delivery purpose. This copolymer effectively binds with the DNA and condense it into the spherical shaped nanosized complexes having a size around 400-

600 nm. Its transfection efficiency was almost comparable to that of PEI (25 kDa) in HEK 293T cells. And, this copolymer exhibit cytotoxicity much lower than that of 25 kDa PEI (Sun *et al*, 2015).

[2- (acryloyloxy) ethyl] trimethylammonium chloride (AOETMAC) is a cationic, bifunctional molecule containing pH-independent cationic head (quaternary ammonium) and a reactive acryloyl group. Mishra *et al*, (2014) developed [2- (methacryloyloxy) ethyl] trimethylammonium chloride (MAETAC) based hydrogels for targeted drug delivery in colon cancer cells. They synthesised pH responsive hydrogel by simple redox copolymerization reaction between MAETAC and polymethacrylic acid (PMAAc). Anticancer drug, 5- fluorouracil was subsequently loaded into this hydrogel. In vitro drug release, cellular entry and cytocompatibility of the hydrogels were studied in the human colon cancer cell lines (HT29 and HCT116 cells). This drug loaded hydrogels effectively kill human colon cancer cell lines than the healthy skin fibroblast cells (Mishra *et al*, 2014).

2.4 Role of p53 gene in cancer

The p53 gene, the tumour suppressor gene codes for a protein that plays an important role in the regulation of the cell cycle. This gene was first identified by Arnold Levine, David Lane and William Old in 1979 and initially thought to be an oncogene that accelerates cell cycle. Role of the p53 gene in tumour suppression was revealed in 1989 (Vogelstein *et al*, 2000). Regarding its pivotal role in preserving the genomic stability, this gene generally portrayed as “guardian of the genome” (Lane, 1992) and the “cellular gatekeeper” (Levine, 1997). In the human genome, p53 gene was located on the seventeenth chromosome.

p53 gene encodes for the phosphoprotein (p53 protein) that comprises of 393 amino acids. This protein act as a nuclear transcription factor that controls the expression of numerous genes that involved in the induction of cell cycle arrest/ and or apoptosis (Sionov & Haupt, 1999; Prives & Hall, 1999; Vousden & Lu, 2002; Ozaki & Nakagawara, 2011). In normal cells, the expression of p53 occurs in extremely low level due to the proteasomal degradation caused by RING-fingertype E3 ubiquitin protein ligase MDM2 (Kubbutat *et al*, 1997; Honda *et al*, 1997; Haupt *et al*, 1997). Moreover, this protein occurs in its functionally latent form in these cells. During cellular stress or damage conditions, this protein molecule gets converted into the active form through the post-translational modifications such as phosphorylation, acetylation and gets accumulated in the cell nucleus. Based on the degree of cell damage, the protein transactivates a set of target genes either to induce cell cycle arrest or to initiate apoptosis (Sionov & Haupt, 1999; Prives & Hall, 1999; Vousden & Lu, 2002; Ozaki & Nakagawara, 2011). Cell cycle arrest induced by the p53 protein allows the cells to repair the damaged gene. Once this task is completed, then these cells re-enter into the normal cell cycle. However, if the DNA damage goes beyond the cell's repair level, then this protein initiates apoptosis in order to maintain genomic integrity (Ozaki & Nakagawara, 2011).

Structure of p53 protein has 3 functional domains and several characteristic domains. The functional domains include NH₂-terminal acidic transactivation domain (TA), a DNA-binding domain (DB) and a COOH-terminal oligomerization domain (OD) that comprises amino acid residues 1-45,102-292 and 319-359 respectively. OD domain mediates the formation of functional p53 which is a homotetramer (Sionov & Haupt,

1999; Prives & Hall, 1999; Vousden & Lu, 2002; Ozaki & Nakagawara, 2011). In addition to these functional domains, p53 protein also possesses three nuclear localization signals (NLS) required for its efficient nuclear entry. These NLSs were recognized by importin α/β complex. Similarly, p53 protein also contains a Leu-rich nuclear export signal (NES) that recognized by CRM1 (chromosomal region maintenance 1), the nuclear export machinery (Fabbro & Henderson, 2003). This domain is masked during homotetramer formation of p53 protein. However, mono ubiquitination mediated by MDM2 at the COOH-terminal Lys residues exposes this domain by disrupting the tetramer formation (Stommel *et al*, 1999). This protein also has a Pro-rich domain comprising amino acids from 63 to 97 which are found to associate with pro-apoptotic function (Walker & Levine, 1996; Baptiste *et al*, 2002).

The gene targets of p53 protein which causes cell cycle arrest include p21^{WAF1}, 14-3-3 σ , p53R2 and Reprimo. Upregulation of p21^{WAF1} by p53 gene causes cell cycle arrest at G1 stage while 14-3-3 σ and p53R2 induce G2/M arrest (El-Deiry *et al*, 1993; Xiong *et al*, 1993; Hermeking *et al*, 1997; Tanaka *et al*, 2000). It is also reported that the 14-3-3 σ act as an antagonist for Mdm2-mediated p53 degradation and the nuclear export of p53 protein (Yang *et al*, 2003). Reprimo is an extensively glycosylated cytoplasmic protein which causes cell cycle arrest at the G2 stage (Ohki *et al*, 2000). MDM2 is one of the gene targets of p53 protein that tightly regulates the expression of this protein via participating in a negative autoregulatory feedback loop (Barak *et al*, 1993). p53 gene induces apoptosis via mitochondria mediated pathway. Hence the major gene targets of p53 gene for inducing apoptosis include BAX (Bcl2-associated X protein), p53 AIP1 (p53-regulated apoptosis-inducing protein 1),

NOXA (Latin for damage) and PUMA (p53upregulated modulator of apoptosis) (Ozaki & Nakagawara, 2011).

It was reported in the literature that more than 50% of human cancers have the loss of function mutations that occurs in *p53* gene (Nigro *et al*, 1989; Vogelstein, 1990; Hollstein *et al*, 1991). Of these, 95% occurs in the DNA binding domain and that causes the loss of sequence-specific transactivation ability in this mutant p53 protein (Vousden & Lu, 2002). The most commonly mutated amino acids in human cancer include Arg-175, Gly-245, Arg-248, Arg-249, Arg-273 and Arg-282 (Joerger & Fersht, 2007). The pro-apoptotic function of a p53 plasmid is closely associated with the ability to transactivate the specific sequence (El-Deiry *et al*, 1992; Pietenpol *et al*, 1994; Herskowitz, 1987). In addition, this mutant p53 protein forms the hetero-oligomer with wild type p53 protein and behaves as a dominant-negative inhibitor (Herskowitz, 1987). Moreover, certain cancer derived p53 mutants transactivate oncogenic genes, displays the chemo-resistant phenotype that leads to the formation of more aggressive cancer growth. Half life of this mutant p53 was also higher (2 to 12 h) when compared to the wild-type p53 (20 min) (V Crawford *et al*, 1984; Chen *et al*, 1990). Hence for efficient chemotherapy, the novel strategy should be developed to eliminate the influence of a mutant p53 gene on wild type p53 protein.

3. Materials and methods

This chapter comprises of detailed description of various experiments carried out to test the hypothesis and is divided into five sections. The first section deals with the synthesis and characterisation of cationised polysaccharides (CPs) i.e. Pullulan & Dextran modified with PEI. This CPs were further modified with four different vinyl monomers namely ethylene glycol dimethacrylate (EGDMA), (2-acryloyloxy ethyl) trimethyl ammonium chloride (AOETMAC), vinyl imidazole (VI) and 2-diethyl amino ethyl methacrylate (DEAEM). Synthesis and characterisation of these vinyl monomers modified CPs are discussed in the successive sections.

3.1 Cationisation of polysaccharides – Pullulan & Dextran

3.1.1 Materials

Pullulan (MW 280,000 Da) and dextran (MW 16,000 Da) were bought from SRL and Fluka respectively. Branched polyethyleneimine (PEI, MW 10, 000 Da), 1,1'-carbonyldiimidazole (CDI), Dulbecco's modified Eagle's medium (DMEM)/F12 Ham, Minimum essential medium (MEM) and 3-(4,5-dimethylthiazol- 2-yl)-2,5-diphenyl-tetrazolium bromide (MTT) were purchased from Sigma – Aldrich Chemicals Co, US. Foetal bovine serum (FBS) obtained from GIBCO (USA). Live Dead assay kit and other fluorescent stains like YOYO iodide, Hoechst 33342 were bought from Invitrogen. Calf thymus DNA purchased from Worthington Biochemical Corp., p53 Dominant-Negative Vector from Clontech, USA. Dimethyl sulfoxide, borax (disodium tetraborate) and acetone were obtained from Merck, India. Cell lines - C6 glioma, HeLa and L929 cells were obtained from the National

Centre for Cell Science (NCCS), Pune, India. All other chemicals were of analytical grade available in India.

3.1.2 Synthesis

Polysaccharides - pullulan and dextran were cationised with PEI using CDI chemistry to form pullulan PEI (PP) and dextran PEI (DP) respectively. In brief, 250 mg polysaccharide (pullulan/dextran) was dissolved in 12.5 ml DMSO and 23 mg CDI was added in order to activate their hydroxyl group. The solution was kept at 37°C under stirring for 2 hrs. To this solution, 100 mg PEI dissolved in 10 ml, 20 mM borax was added slowly and the reaction was kept at room temperature for overnight. CP was then precipitated from the reaction mixture by adding 50 ml acetone. This step was repeated twice with 25 ml acetone to completely remove unreacted reactants and CDI. The precipitate was then filtered and dissolved in 25 ml distilled water (Mitha & Rekha, 2014). CP was further purified by dialysing in distilled water for 24 hours with water change at fixed intervals.

3.1.3 Fourier transform infrared spectroscopy (FTIR)

Grafting of PEI to pullulan and dextran was evaluated by Fourier transform infrared (FTIR) technique. The thin film of PP, DP along with their parent polymers- pullulan, dextran and PEI were analysed by ATR method over the scan range 400 – 4000 cm^{-1} using Nicolet 5700 spectrophotometer.

3.1.4 Proton nuclear magnetic resonance (^1H NMR)

For the ^1H NMR study, polymer samples – DP and PP were concentrated using filters having molecular weight cut off of 30,000 and 50,000 Da respectively and

then dissolved in deuterated water. The ^1H NMR spectra of the samples were recorded using a 500 MHz FTNMR (Brucker AV500) at 25°C. The ^1H NMR spectra of parent molecules- pullulan, dextran and PEI were also analysed after dissolving in D_2O . Chemical shifts (δ) of ^1H NMR spectra were calculated downfield from SiMe_4 (δ 0.0) and expressed as parts per million (ppm).

3.1.5 Determination of free amino groups

Free amino groups present in the CPs were determined by CuSO_4 assay. PEI standard solution was prepared at a concentration of 2 mg/ml using distilled water in a volumetric flask. From this solution, working standards were prepared at the concentration range of 0.2-2 mg/ml solutions. From each of these working standards, 500 μL was pipetted and optical density (OD) was measured at 285 nm after adding 5 ml copper (II) sulphate solution (0.145 mg/ml in distilled water). The standard curve was plotted by taking concentration on X axis and OD on Y axis. From this graph, free amino groups available in the CPs were determined by carrying out the experiment with 500 μL polymer solution (1mg/ml).

3.1.6 Buffering capacity

The buffering capacities of PP, DP and PEI were determined by simple acid–base titration. Briefly, 25ml polymer solution (0.1mg/ml) was prepared in normal saline and the pH was adjusted to 10 using 0.1 N NaOH. The titration was carried out by the sequential addition of 50 μL 0.01 N HCl and each time pH of the solution was measured using a pH meter. This procedure was continued until the pH of the solution reached 4 (Benns *et al*, 2002). A graph was plotted with pH against the

volume of 0.01N HCl consumed during this titration and assessed the buffering capacity of the corresponding polymer.

3.1.7 Preparation of polymer/ ctDNA nanoplexes

Nanoplexes of polymer with ctDNA was prepared at six different weight ratios (0.5:1, 1:1, 2:1, 3:1, 4:1, 5:1) by vortexing different volumes of 1mg/ml polymeric solutions with fixed amount (10 μ L) of 1 mg/ml ctDNA solution for 30 s and thereafter incubation for 20 min at room temperature (Casé *et al*, 2009).

3.1.8 Size and zeta potential

Nanoplexes of PP, DP and PEI were prepared at different weight ratios as mentioned in the section 3.1.7. Hydrodynamic size and zeta potential of these nanoplexes were then determined using Zetasizer Nano ZS (Malvern Instruments Ltd., UK). He-Ne laser beam of 633 nm wavelength with a detection angle of 173° was used to analyse the size of the nanoplex. For each sample, three measurements were taken with average 12 runs per measurement. The same equipment was used to measure the zeta potential of these nanoplexes.

3.1.9 DNA binding ability and effect of plasma on nanoplex stability

The extent of association between cationic polymer (PP, DP and PEI) and ctDNA was analysed by agarose gel electrophoresis (AGE). The polyplexes prepared with ctDNA at various weight ratios were loaded on to 1% (w/v) agarose gel stained with EtBr (0.5 μ g/mL) and electrophoresed at 100 V in 1X Tris-acetate-EDTA buffer for 15 min using Bio-Rad Mini-PROTEAN III electrophoresis system (Bio-Rad Laboratories, CA, USA). The gel was then visualized and captured the image using

image analyzer (FUJIFILM FLA- 5100). Nanoplex stability was also evaluated in the presence of plasma protein by running AGE.

3.1.10 Nanoplex stability in the presence of digestive enzyme, DNase

CPs ability to protect the DNA in the presence of DNase was also analysed. For this study, nanoplexes were prepared at various weight ratios as mentioned in the section 3.1.6. These nanoplexes were then treated with 4 μ L DNase (1mg/ml) prepared in digestion buffer (0.1M sodium acetate, 5mM MgSO₄, pH 7.4) and incubated for 15 min at 37°C. The reaction was stopped by the addition of 3 μ L termination buffer (equal volume of 0.5M EDTA, 2M NaOH& 0.5M NaCl). AGE was carried out as mentioned in the section 3.1.9. Further, 5 μ L heparin (1000 IU) added to the remaining nanoplex and incubated for 30 min at room temperature in order to release the DNA from the polymer (Srinivasachari *et al*, 2007). AGE once again carried out and the gel image was photographed using FUJIFILM FLA- 5100 image analyser.

3.1.11 Polymer interactions with plasma proteins

Interaction of cationic polymers with plasma proteins was investigated. For this, 1 mg/ml solution of polymer in normal saline (100 μ L) was prepared and incubated with 20 μ L of human plasma. This was then centrifuged at 5000 rpm for 10 min. From this, 20 μ L of supernatant was collected and mixed with 1X sample loading buffer. This was then loaded into the gel composed of 4% stacking gel and 7% resolving gel along with positive (plasma treated with PEI) and negative (plasma in normal saline) controls. Electrophoresis was performed in Mini-Protean II electrophoresis system (Bio-Rad, CA, US) at 240 V for 30 min. Gel was stained with

Coomassie blue to visualize the protein bands and the image was captured using Fuji LAS 4000 image analyzer.

3.1.12 Cell culture studies

Performance of CPs as gene delivery vectors was analysed in the *in vitro* conditions using different cell lines. Cytocompatibility was assessed in two different cancer cell lines (C6, HeLa) and in a normal cell line (L929). Cellular internalisation and gene transfection efficiency of CPs were analysed using ctDNA and p53 plasmid respectively. C6 glioma cells are cultured in medium containing F12 Ham/DMEM and MEM in the ratio 1:1 with 10% FBS while HeLa and L929 cells were cultured in MEM medium containing 10% FBS. These cells were cultured in the T-25 flask and kept in the CO₂ incubator at 37°C. Cells were trypsinised and transferred to multi well dish at required cell density prior to each experiment as detailed below.

3.1.13 Cell viability

MTT assay was carried out both in cancer cells (C6 and HeLa) and normal cell line (L929) in order to assess the percentage viability of these cells in the presence of cationic polymers. These cells were seeded onto a 96-well plate at a concentration of 1×10^4 cells/well in 200 μ L culture medium (DMEM/F12 Ham and MEM in the ratio 1:1 for C6 cells while MEM for HeLa and L929 cells) containing 10% FBS and allowed to adhere overnight. The next day, the growth medium was removed and the cells were then incubated either with cationic polymers at four different concentrations i.e. 25, 50, 75 and 100 μ g/mL or with their corresponding nanoplex prepared with ctDNA at optimum weight ratios (5:1 for PP and DP while 2:1 for

PEI) for 24 h. After treatment, polymer or polyplex solution was removed and the cells were then incubated with 100 μ L of 0.5 mg/mL, MTT solution prepared using sterile PBS for another 3 h at 37°C in CO₂ incubator. After removing the MTT solution, formazan crystals produced by the live cells were dissolved in 200 μ L of dimethyl sulfoxide (DMSO) and absorbance was measured at 570 nm using a microplate reader. The relative percentage Cell viability was then calculated in comparison with the untreated cells by using the formula,

$$\text{Percentage Cell viability} = \frac{\text{Abs. of test}}{\text{Abs. of control}} \times 100$$

where Abs. is the absorbance at 570 nm.

3.1.14 Cellular uptake of polyplexes

Cellular internalisation of cationic polymers was studied in C6, HeLa after tagging ctDNA with YOYO Iodide. Polyplexes are prepared at optimum weight ratio by using fluorescently tagged ctDNA. Cells grown overnight in four well plate having 80% confluency were exposed to fluorescently tagged polyplexes in such a way that each well receive 2.5 μ g of ctDNA. After 2.5 h of transfection at 37 °C, 7 μ l of nuclear stain Hoechst 33342 (1 mM) was added and the cells were incubated for another 30 min at similar conditions. On completion of 3 hours of exposure, nanoplex containing culture medium was then removed and washed with PBS. Cells were then fixed using 1% formaldehyde solution in PBS, visualized and photographed using fluorescence microscope (Leica DMI 3000B, Germany). YOYO Iodide positive cells were also quantified using flow cytometer (FACS Canto II, BD Biosciences, Franklin Lakes, NJ).

3.1.15 Polymer trafficking studies

CPs and PEI were tagged with an amino reactive labelling reagent, TRITC (tetramethyl rhodamine isothiocyanate) in order to track the movement of polymer inside the cell. For this analysis, 200 μL of 0.2 M sodium bicarbonate buffer having pH 9 was added to 2 mg/ml polymer solution. To this reaction mixture, 50 μL TRITC (1mg/ml solution prepared in DMSO) was added and incubated for 2 h at room temperature. Addition of 50 μL , 1 M ammonium chloride stops the reaction which was then dialysed at 4°C in distilled water in order to remove the unbound TRITC. C6 cells were trypsinised and seeded onto the four well plate at a cell density of 1×10^5 cells/well and incubated overnight in the CO₂ incubator maintained at 37°C. Nanoplexes are prepared by vortexing TRITC tagged polymer and YOYO tagged ctDNA at their optimum weight ratio (5:1 for DP and PP while 2:1 for PEI). These nanoplexes were then added to the cells and incubated for 2.5 h at 37°C. The nucleus was counterstained using Hoechst 33342 and incubated for another 30 min at the similar conditions. After PBS wash, cells were fixed with 1 % formaldehyde prepared in PBS and the images were captured using the confocal microscope.

3.1.16 Gene transfection

In vitro gene transfection efficacy of cationic polymers was determined using p53 plasmid whose expression leads to apoptosis of cancer cells. Gene transfection efficiency of DP, PP and PEI were analysed in cancer cells (C6, HeLa). Cells were seeded onto a four well plate at a density of 1×10^5 cells/well in 0.5 mL of culture medium. After overnight incubation at 37 °C and 5% CO₂, cells were treated with polyplexes containing the p53 plasmid (prepared at their optimum weight ratio, 5:1

for CPs and 2:1 for PEI). After 5 h of incubation, the transfecting media was replaced with 0.5 ml of fresh complete media and the cells were once again incubated for 19 h. In the subsequent step, cells were stained using 2 μ M calcein AM and 4 μ M ethidiumhomodimer (EthD-1). Cell status was then observed and photographed using Leica DMI 3000B, fluorescence microscope (Germany) after fixing with 1% formaldehyde solution. Number of dead cells was also quantified by using fluorescence activated cell sorting (FACS) technique after staining with propidium iodide (PI).

3.1.17 Annexin V staining

Apoptosis induced by nanoplexes of CPs and PEI with p53 plasmid was studied by staining cells with Annexin V. This study was carried out in HeLa cells which were seeded onto the 24 well plate at the cell density of 1×10^5 cells/well. After overnight incubation at 37°C, cells were treated with nanoplexes prepared with p53 plasmid at their optimum weight ratios i.e. 5:1 for DP and PP while 2:1 for PEI and incubated for another 5h. Polyplex containing medium was then replaced with 0.5ml of fresh culture medium and incubated for 19 h at 37°C in CO₂ incubator. After PBS wash, cells were trypsinised and centrifuged at 5000 rpm for 10 min. Cells pellet was resuspended in 100 μ L of Annexin- V – Flous labelling solution and incubated for 15 minutes at dark. For flow cytometry analysis 400 μ L incubation buffer (10 mM HEPES/NaOH, pH 7.4, 140 mM NaCl and 5 mM CaCl₂) was added and fluorescence was detected using flow cytometer.

3.2 Synthesis and characterisation of ethylene glycol dimethacrylate (EGDMA) cross linked cationised polysaccharides

3.2.1 Materials

Ethylene glycol dimethacrylate, 3-(4,5-dimethylthiazol-2-yl)-2,5-diphenyl-tetrazoliumbromide (MTT), cell culture medium like Dulbecco's modified Eagle's medium (DMEM)/F12 Ham, Minimum essential medium (MEM) were obtained from Sigma – Aldrich Chemicals Co, US. Fetal bovine serum (FBS) obtained from GIBCO (USA). Trypsin, Live Dead assay kit and fluorescent stains like YOYO iodide, Hoechst 33342 were procured from Invitrogen. Nucleic acids used in this study were obtained from Worthington Biochemical Corp. (ctDNA) and Clontech, USA (p53 Dominant-Negative Vector). Cell lines - C6 glioma, HeLa and L929 cells were supplied by the National Centre for Cell Science (NCCS), Pune, India. Rest of the chemicals used in this study, were of analytical grade locally purchased in India.

3.2.2 Synthesis

Cationic polymers modified with EGDMA were synthesised via aza - Michael addition reaction mediated by ceric ammonium nitrate as catalyst in water (Varala *et al*, 2006). To 100 mg pullulan PEI, 200 μ L and 300 μ L of EGDMA (98%) were added and synthesised two different polymer derivatives- PPE I and PPE II respectively. The reaction was carried out at 60°C by continuous stirring of polymer solution with monomer in the presence of catalyst for 2 h. The final product was purified by methanol precipitation followed by thorough dialysis in distilled water. Similarly EGDMA modified DP derivatives were synthesised but the end product

turned out to be hydrophobic in nature due to extensive cross linking. Hence they were not taken up for further studies as it is focussed on hydrophilic polymers.

3.2.3 Fourier transform infrared spectroscopy (FTIR)

FTIR spectrum of the PPE was recorded using Thermo Nicolet 5700 spectrometer over the scan range $400\text{--}4000\text{ cm}^{-1}$ by ATR method and the data was analysed using the Omnic software.

3.2.4 Proton nuclear magnetic Resonance (^1H NMR)

^1H NMR spectrum of PPE was recorded using BrukerAvance II 500 NMR spectrometer at 25°C . For this analysis, polymer sample was dissolved in D_2O .

3.2.5 Determination of free amino groups

The unreacted free amino groups present in the EGDMA derivatives were determined by copper sulphate assay. This assay was carried out by adding freshly prepared, 0.145mg/ml copper (II) sulphate solution (5 ml) to $500\text{ }\mu\text{l}$ polymer solution (1mg/ml). After vortexing, OD was measured at 285nm using water as the blank. From the standard graph, plotted between the known concentration of PEI and their corresponding OD, the percentage of free amino groups present in the sample was determined.

3.2.6 Buffering capacity

Acid – base titration was carried out to analyse the buffering capacities of EGDMA derivatives (PPE I & PPE II). For this analysis, 0.1mg/ml polymer solution was prepared in normal saline and the pH was adjusted to 10 using 0.1N NaOH. This pH

was then brought down to 4 by sequential addition of 0.01N HCl (50 μ L). Each time, the pH change of the solution was noted using pH meter (Benns *et al*, 2002). Buffering capacity was assessed from the graph plotted between volume of 0.01N HCl consumed versus change in pH.

3.2.7 Polymer/ctDNA polyplexes preparation

Polyplexes were prepared at various weight ratios (0.5:1, 1:1, 2:1, 3:1, 4:1 & 5:1) by mixing the different amount of PPE I and PPE II with the fixed amount of ctDNA and incubating for 20 min at room temperature (Casé *et al*, 2009).

3.2.8 Size and zeta potential

The nanoplex size was measured using Malvern Zetasizer NS, UK, at 25 °C (He Ne laser, 633 nm). Backscattered light was detected at the 173° angle. Hydrodynamic diameters (Z average mean) measurements were taken in triplicate. For every sample, three measurements each having 12 runs of 10 s duration were taken in order to elucidate the hydrodynamic diameters (Z average mean) and polydispersity indices (PDI) of the nanoplexes.

Zeta potential was also measured using the same equipment by utilising Laser Doppler Electrophoresis technique. The nanoplex solution was taken in a capillary cell (DTS1070) and duration of measurement was set as automatic. The instrument was calibrated using polystyrene beads having zeta potential -52 mV. Smoluchowski model was used to analyze the data.

3.2.9 DNA binding ability and effect of plasma on nanoplex stability

The strength of association between cationic polymers (PPE I, PPE II) with ctDNA was assessed by carrying out agarose gel electrophoresis. Nanoplexes of these cationic polymers were prepared with ctDNA at different weight ratios as mentioned above. Nanoplexes loaded onto a 1% agarose gel stained with ethidium bromide (EtBr) and electrophoresis was conducted at 100 V for 15 min in 1X Tris Acetate EDTA (TAE) buffer using Mini-PROTEAN III electrophoresis apparatus (Bio-Rad, USA). The affinity between EGDMA derivatives and ctDNA was also analysed by running agarose gel electrophoresis in the presence of plasma proteins.

3.2.10 Polymer interactions with plasma proteins

The nature of polymer protein interaction in the case of EGDMA derivatives was investigated. For this analysis 100 µg polymer solution prepared in normal saline was incubated with human plasma (20µL) for 30 min. This was then centrifuged at 5000 rpm for 10 min and supernatant was collected which was then loaded along with 1X sample loading buffer into the 4% stacking gel. The protein bands were then resolved into single bands by 7% resolving gel. Electrophoresis was carried out at 240 V for 30 min using Mini-Protean II electrophoresis system (Bio-Rad, CA, US). Coomassie blue used to stain the protein bands in the gel and image was procured using Fuji LAS 4000 image analyzer.

3.2.11 Cell culture studies

EGDMA derivatives efficacy to perform as gene delivery vector was evaluated in cancer cell lines – C6 and HeLa. Cytocompatibility of these polymers and also their

nanoplexes were evaluated both in cancer cell lines (C6 and HeLa) as well as in normal cell line (L929). Cellular internalisation and gene transfection efficiency of these derivatives were analysed in cancer cell lines using ctDNA and p53 plasmid respectively. HeLa and L929 cells were cultured in MEM containing 10% FBS while C6 cells required a combination of F12 Ham/DMEM and MEM in the ratio 1:1 and 10% FBS for their growth. These cells were initially cultured in T-25 flasks and based on necessity; cells were trypsinised and transferred to the multi well plate.

3.2.12 Cell viability

Percentage Cell viability of both cancer cells (C6 and HeLa) and also the normal cell line (L929) was assessed both in the presence of cationic polymers – PPE I, PPE II at different concentrations and also with their nanoplexes using MTT assay. To perform this assay, cells were seeded at a density of 10^4 cells/well on to a 96 well plate in 200 μ L culture medium containing 10% FBS and incubated overnight at 37°C at 5% CO₂ in order to get 70-80% confluency. Culture medium was chosen based on the cell type used. For HeLa and L929 cells, MEM is the culture medium while for C6 cells, a mixture of DMEM/F12 Ham and MEM in the ratio 1:1 is used as the culture medium. These cells were then treated with either cationic polymers at four different concentrations (25, 50, 75 and 100 μ g/ml) or with their corresponding nanoplexes prepared at their optimized weight ratio i.e. 5:1 and incubated for another 24 h in the CO₂ incubator under similar conditions. After removing culture medium, 100 μ L of 0.5mg/ml MTT solution prepared in sterile PBS was added to each well and incubated for 3 h. The reduction of yellow coloured MTT reagent into insoluble purple coloured formazan crystals signifies the number of living cells present in each

well. These formazan crystals were then solubilised in DMSO and quantified spectrophotometrically by reading absorbance at 570nm. Percentage Cell viability was calculated using the following equation,

$$\text{Percentage Cell viability} = \frac{\text{Abs. of test}}{\text{Abs. of control}} \times 100$$

where Abs. is the absorbance at 570nm.

3.2.13 Cellular uptake of polyplexes

Cellular internalisation of nanoplexes was studied both in C6 and HeLa cell lines. This study was carried out in four well plates seeded with 10^5 cells in 0.5 ml of their corresponding culture medium. Once the cells attained 70-80% confluence, they were treated with nanoplexes of cationic polymers (PPE I, PPE II) prepared with YOYO Iodide (2.5 μ L of 10 μ M YOYO Iodide for 1.0 μ g DNA) tagged ctDNA at their optimised weight ratio (5:1). These cells were then incubated at 37°C for 2.5 h in 5% CO₂ incubator. Nuclear stain, Hoechst was added and incubated for another 30 min. Culture medium containing stain was then removed and cells were fixed with 1% formaldehyde containing PBS. Images were then captured using (Leica DMI 3000B, fluorescence microscope, Germany).

3.2.14 Gene transfection

Gene transfection efficiency of these polymer derivatives was analyzed using the p53 plasmid in cancer cells – C6 & HeLa whose expression will lead to apoptosis in these cells. To execute this study, cancer cells were seeded at the density of 10^5 cells/ well onto the four well plate and incubated overnight at 37°C in the CO₂ incubator.

Nanoplexes of cationic polymers prepared with p53 plasmid at their selected weight ratio were added to these cells in 250 μ L in their respective culture medium devoid of FBS. After 5 h of incubation, nanoplex containing culture medium was replaced with 0.5 ml of fresh medium and incubated at 37°C for another 24 h in the CO₂ incubator. Cells were then stained with calcein AM and ethidium homodimer (EthD-1) at a concentration of 2 μ M and 4 μ M respectively. After the incubation time, the cells were washed thoroughly with PBS thrice and were fixed with 1% formaldehyde. These cells were then observed under the fluorescence microscope, Leica DMI 3000B (Germany) and images were taken.

3.3 Synthesis and characterisation of [2-(Acryloyloxy) ethyl] trimethylammonium chloride (AOETMAC) grafted cationised polysaccharides

3.3.1 Materials

2-(Acryloyloxy) ethyl) trimethylammonium chloride (AOETMAC), Cerium ammonium nitrate (CAN), Dulbecco's modified Eagle's medium (DMEM)/F12 Ham, Minimum Essential Medium (MEM) and 3-(4,5-dimethylthiazol-2-yl)-2,5-diphenyl-tetrazolium bromide (MTT) were procured from Sigma – Aldrich Chemicals Co, US. Fetal bovine serum (FBS) was purchased from GIBCO (USA). Trypsin, Live Dead assay kit, fluorescent stains like YOYO iodide, Hoechst 33342 were obtained from Invitrogen. Nucleic acids like Calf thymus DNA, p53 Dominant-Negative plasmid Vector were purchased from Worthington Biochemical Corp. and Clontech (USA) respectively. National Centre for Cell Science (NCCS), Pune, India

supplied the cell lines - C6 glioma, HeLa and L929 required for this study. All other chemicals utilised in this study were of analytical grade, available in India.

3.3.2 Synthesis

AOETMAC was grafted to DP and PP at three different weight ratios 10:0.01, 10:0.015, 10:0.0025 to form six different polymer derivatives namely DPA I, DPA II, DPA III, PPA I, PPA II, PPA III. Polymer derivatives were synthesised by adding 200 μ l, 300 μ l and 50 μ l of AOETMAC (80%) to 100 mg of CPs (DP and PP). Michael addition reaction was carried out at room temperature by continuously stirring cationic polysaccharide with AOETMAC for 72 h (Escalante *et al*, 2008). The final product was thoroughly dialysed in distilled water in order to remove the unreacted monomer molecules.

3.3.3 Fourier transform infrared spectroscopy (FTIR)

FTIR spectra of AOETMAC grafted polymer derivatives – PPA and DPA were analysed over the scan range 400 – 4000 cm^{-1} using Nicolet 5700 spectrophotometer. Polymer samples are prepared as thin film and the study was carried out by ATR method. Data was analysed using Omnic software.

3.3.4 Proton nuclear magnetic resonance (^1H NMR)

Proton Nuclear Magnetic Resonance (^1H NMR) spectra of DPA and PPA were recorded at 25°C using 500 MHz BrukerAvance II NMR spectrometer. This study was carried out using concentrated polymer solutions dissolved in D_2O .

3.3.5 Determination of free amino groups

Determination of free amino groups present in the AOETMAC derivatives was done by copper sulphate assay. Freshly prepared, 0.145mg/ml copper (II) sulphate solution (5 ml) was added to 500 µl polymer solution (1mg/ml). After thorough mixing, OD was taken at 285nm. Percentage free amino group present in the polymer sample was then determined from the standard graph plotted with known concentration of PEI versus their corresponding OD.

3.3.6 Buffering capacity

Acid – base titration was used to analyze the buffering capacity of AOETMAC grafted cationic polymers. For this analysis, 0.1mg/ml of polymer was prepared in normal saline. Initially, pH of the solution was adjusted to 10 using 0.1N NaOH which was then brought down to 4 by the sequential addition of 50 µL 0.01N HCl. Every time, the pH change of the solution was measured using pH meter(Benns *et al*, 2002). The buffering capacity of AOETMAC derivatives was then assessed from the graph plotted with volume of 0.01N HCl consumed versus the pH change of the solution.

3.3.7 Polymer/ctDNA polyplexes preparation

Polymer/ctDNA nanoplexes were prepared at six different weight ratios by vortexing various amount of 1mg/ml polymer solution (5, 10, 20, 30, 40 & 50 µL) with fixed amount of ctDNA (10 µg) for 30 s followed by 20 min incubation at room temperature (Casé *et al*, 2009).

3.3.8 Size and zeta potential

Nanoplexes of AOETMAC grafted cationic polymers prepared with ctDNA at different weight ratios as mentioned in the section 3.3.6 and the hydrodynamic size, zeta potential were analysed using the equipment Malvern Zetasizer NS, UK. Measurements were taken in triplicate at 25°C each having 12 runs with run duration of 10 s for every polymer sample. HeNe laser of wavelength 633 nm was used to detect the hydrodynamic size of the nanoplexes. Back scattered light from the nanoplexes was detected at the angle of 173° in order to avoid multiple scattering and to reduce effects from dust contaminants. Zeta potential of these nanoplexes were measured based on Laser Doppler Electrophoresis technique using the same equipment.

3.3.9 DNA binding ability and effect of plasma on nanoplex stability

DNA binding ability of AOETMAC grafted cationic polymers was evaluated by agarose gel electrophoresis. Nanoplexes of these cationic polymers were prepared at six different weight ratios with ctDNA. Electrophoresis was carried out at 100 V for 15 min in 1X TAE buffer using EtBr stained 1% agarose gel loaded with these nanoplexes and control DNA. These gels are then visualized under UV for DNA and photographed using image analyzer (FUJIFILM FLA- 5100). Stability of nanoplexes in the presence of plasma proteins were also studied by carrying out agarose gel electrophoresis.

3.3.10 Polymer interactions with plasma proteins

Compatibility with blood plasma is important for polymers that are intended for systemic delivery. Hence, AOETMAC derivatives interactions with plasma proteins were studied by carrying out nativePAGE. For this analysis, samples were prepared by incubating 100 µg of polymer solution in normal saline with 20 µL human plasma for 30 min at room temperature. Supernatant was collected after centrifugation at 5000 rpm for 10 min and mixed with 1X sample loading buffer. This was then loaded into the gel comprising 7% resolving gel and 4% stacking gel. Electrophoresis was carried out at 240 V for 30 min along with positive and negative controls which were plasma treated with PEI and saline respectively. Gel was stained with Coomassie blue and image was captured using Fuji LAS 4000 image analyser.

3.3.11 Cell culture studies

Cancer cell lines are used as models to evaluate the *in vitro* performance of AOETMAC derivatives as gene delivery vectors. Cytocompatibility of these derivatives and their correspondingnanoplexes were determined in three different cell lines – C6, HeLa and L929. Plasmid trafficking and transfection efficiency of these polymers were determined by preparing polyplexes with YOYO iodide tagged ctDNA and p53 plasmid respectively. Combination of F12 Ham/DMEM and MEM in the ratio 1:1 with 10% was used as the culture medium for C6 cells while HeLa and L929 cells were cultured in MEM containing 10% FBS. Initially, T-25 flasks were used to culture these cells which are later transferred to the multi well plate at required cell density preceding to each experiment.

3.3.12 Cell viability

Percentage Cell viability of L929, HeLa and C6 glioma cells were analysed in the presence of AOETMAC grafted cationic polymers and their nanoplexes by MTT assay. To perform this assay, cells were seeded onto the 96 well plate at the density 10^4 cells/well and 200 μ L corresponding culture medium was added. These cells were then incubated overnight at 37°C in CO₂ incubator. Once the cells reached 70-80% confluency, the culture medium was removed and cells treated either with polymer solution at different concentrations (25, 50, 75 & 100 μ g/ml) or with their nanoplexes (prepared at their optimized weight ratio i.e. 5:1). These cells were then incubated for another 24 h under similar conditions. After incubation, the culture medium was replaced with 100 μ L of 0.5 mg/ml solution of MTT prepared in sterile PBS and the cells were further incubated for 3 h in CO₂ incubator. The insoluble formazan crystals thus formed through the reduction of MTT by live cells were then dissolved in 200 μ L of DMSO. The absorbance was then taken at 570nm using automated microplate reader (Bio Tek, Synergy H1, US). Percentage Cell viability was then calculated in relative to untreated cells as the control using the following equation

$$\text{Percentage Cell viability} = \frac{\text{Abs. of test}}{\text{Abs. of control}} \times 100$$

where Abs. is the absorbance at 570nm.

3.3.13 Cellular uptake of polyplexes

Cancer cell lines – C6 glioma and HeLa were seeded onto a four well plate at the cell density 10^5 cells/well and incubated overnight at 37 °C in CO₂ incubator in order to

attain 80% confluency. ctDNA was then tagged with YOYO Iodide dye. Nanoplexes of AOETMAC grafted cationic polymers were prepared at the weight ratio 5:1 by using this fluorescently tagged ctDNA. The cells were then transfected using these nanoplexes and incubated for 2.5 h at 37 °C in CO₂ incubator. Nuclear stain, Hoechst 33342 (7µl of 1 mM solution) was then added to these cells and incubated for another 30 min at same conditions. After PBS wash, cells were fixed with 1% formaldehyde and photographed using Leica DMI 3000B, fluorescence microscope (Germany).

3.3.14 Gene transfection

Gene transfection efficiency of AOETMAC grafted cationic polymer was analyzed using p53 plasmid whose expression causes cell death in cancer cells. To execute this study, cancer cell lines C6 and Hela were seeded onto the four well plate at the density 10⁵ cells/ well and incubated overnight at 37 °C in CO₂ incubator. Once these cells reached 70-80% confluency, the nanoplexes of AOETMAC grafted cationic polymer with p53 plasmid prepared at the weight ratio 5:1 was added and incubated for 5 h in CO₂ incubator. After incubation, nanoplexes containing culture medium was replaced with 0.5 ml fresh complete medium and incubated for another 19 h at similar conditions. Live and dead cells present in the culture plate were then differentially stained using Live Dead Assay Kit following the manufacturer protocol. Briefly cells are treated with solution containing 2 µM calcein AM and 4 µM ethidium homodimer (EthD-1) dissolved in PBS. The cells were then fixed using 1% HCHO and visualized under fluorescence microscope (Leica DMI 3000B, Germany).

3.4 Synthesis and characterisation of vinyl imidazole (VI) grafted cationised polysaccharides

3.4.1 Materials

Vinyl imidazole (VI), 3-(4,5-dimethylthiazol-2-yl)-2,5-diphenyl-tetrazolium bromide (MTT) and cell culture medium like DMEM and MEM were obtained from Sigma – Aldrich Chemicals Co, US. Fetal bovine serum (FBS) was purchased from GIBCO (USA). Fluorescent stains like YOYO iodide, Hoechst 33342, Live Dead assay kit and trypsin were procured from Invitrogen. Calf thymus DNA obtained from Worthington Biochemical Corp., while p53 Dominant-Negative plasmid Vector was purchased from Clontech (US). Cell lines (C6 glioma, HeLa and L929) used in this study were purchased from National Centre for Cell Science (NCCS), Pune, India. All other chemicals were of analytical grade, purchased in India.

3.4.2 Synthesis

Vinyl imidazole (VI) grafted to cationised polysaccharides - DP and PP by free radical addition reaction using ceric ammonium nitrate (CAN) as initiator (Caner *et al*, 2007). Grafting of VI to DP and PP was carried out at 3 different weight ratios each viz 0.005: 10, 0.01:10 and 0.02:10 to yield 6 different grafted polymers namely DPI I, DPI II, DPI III, PPI I, PPI II and PPI III respectively. Polymer derivatives were synthesised by adding 100 μ L, 200 μ L and 500 μ L of VI (99%) to 100 mg of cationised polysaccharides and the reaction was carried out at 60°C for 2 h under inert atmosphere. VI grafted cationic polymers were then purified by acetone precipitation followed by extensive dialysis in distilled water.

3.4.3 Fourier transform infrared spectroscopy (FTIR)

FTIR spectroscopy of VI grafted cationic polymers were conducted using Nicolet 5700 spectrophotometer by ATR method. Thin films of polymer samples were analysed over the scan range $400 - 4000\text{cm}^{-1}$ with Omnic software.

3.4.4 Proton nuclear magnetic resonance (^1H NMR)

^1H NMR spectra of VI grafted cationic polymers were recorded using BrukerAvance II NMR spectrometer at $25\text{ }^\circ\text{C}$ and 500 MHz frequency. Samples were concentrated using appropriate filters and then dissolved in deuterated water (D_2O) for this analysis.

3.4.5 Buffering capacity

Buffering capacity of VI derivatives was assessed by acid base titration over the pH range 10 – 4 by preparing 0.1mg/ml polymer solution in normal saline. Titration was performed by sequential addition of 50 μL 0.01 N HCl and every time change in the solution pH was noted using pH meter(Benns *et al*, 2002). The graph plotted with volume of 0.01N HCl consumed versus pH change reveals the buffering capacity of the corresponding polymer.

3.4.6 Preparation of polymer/DNA polyplexes

The polymer/ctDNA nanoplexes of different weight ratios were prepared by mixing varying amount of 1mg/ml of polymeric solutions (5 μL , 10 μL , 20 μL , 30 μL , 40 μL , 50 μL) with fixed volume(10 μL) of 1mg/ml ctDNA solution by gently vortexing for 30 s and then incubating for 20 min at room temperature(Casé *et al*, 2009).

3.4.7 Size and zeta potential

Polyplexes of VI derivatives were prepared with ctDNA at six different ratios as mentioned above. Hydrodynamic size and zeta potential of these nanoplexes were analysed using Zetasizer Nano ZS (Malvern Instruments, Malvern, U.K.) at 25 °C by dynamic light scattering (DLS) method. Three measurements, each having 12 runs of 10 s duration were taken to analyse size of nanoplexes. Zeta potential was measured using Laser Doppler Electrophoresis technique in which sample was taken in a capillary cell (DTS1070).

3.4.8 DNA binding ability and effect of plasma on nanoplex stability

Binding strength of VI derivatives with ctDNA was assessed by running agarose gel electrophoresis. Nanoplexes prepared with ctDNA at different weight ratios were loaded onto 1% agarose gel containing EtBr and electrophoresis was carried out at 100 V in 1X TAE buffer using Bio-Rad, Mini-PROTEAN III gel electrophoresis apparatus (USA). DNA was then visualised under UV and images were taken using image analyser (FUJIFILM FLA- 5100). Agarose gel electrophoresis was also carried out to determine the stability of nanoplexes in the presence of plasma proteins.

3.4.9 Nanoplex stability in the presence of digestive enzyme, DNase

Vinyl imidazole derivatives ability to protect DNA from the degradation caused by the enzyme DNase was analysed by agarose gel electrophoresis. For this analysis, polyplexes of VI derivatives were prepared at different weight ratios as mentioned in the section 3.4.6. These polyplexes were then treated with 4 μ L of DNase (569 U/mL)

prepared in digestion buffer (0.1M sodium acetate, 5mM MgSO₄, pH 7.4) and incubated for 15 min at 37°C. The reaction was stopped by the addition of 3 µL termination buffer that containing equal volumes of 0.5 M EDTA, 2 M NaOH and 0.5 M NaCl. Agarose gel electrophoresis was carried out as mentioned in the section 3.4.9, and the image was captured using FUJIFILM FLA- 5100 image analyser. To the remaining polyplex solution, 5µL heparin (1000 IU) was added and incubated for another 30 min at room temperature (Srinivasachari *et al*, 2007). Agarose gel electrophoresis was once again carried out and the gel image was captured.

3.4.10 Polymer interactions with plasma proteins

Plasma protein interactions with VI derivatives were analysed by performing native PAGE. Gel was casted with 7% resolving gel and 4% stacking gel. Polymer solution (100 µL of 1mg/ml solution in normal saline) was incubated with 20 µL human plasma for 30 min. After centrifugation at 5000 rpm for 10 min, supernatant was collected and mixed using 1x sample loading buffer. This was then loaded onto the gel along with the positive (PEI) and negative (normal saline) controls. The electrophoresis was carried out at 240 V for 30 min using Mini-Protean II electrophoresis system (Bio-Rad, CA, US). Coomassie blue was used to stain the gel and the image was captured using an image analyser (LAS 4000, Fuji).

3.4.11 Cell culture studies

The efficacy of VI derivatives as gene delivery vector was assessed using cancer cell lines as *in vitro* models. Cytocompatibility of these polymers and also their nanoplexes were assessed using three different cell lines namely C6, HeLa and L929.

Cellular internalisation mechanism and also their transfection efficiency were studied by using cancer cell lines – C6 and HeLa. C6 cells requires a combination of F12 Ham/DMEM and MEM in the ratio 1:1 with 10% FBS for their growth and maintenance while HeLa and L929 cells were cultured in MEM containing 10% FBS. T-25 flasks are used to culture these cells. Prior to the start of each experiment, these cells were trypsinised and seeded to multi well plate at required cell density.

3.4.12 Cell viability

Cell viability in the presence of VI derivatives and also the corresponding nanoplexes were analysed in three different cell lines viz C6 glioma, HeLa and L929 by MTT assay. These cells were seeded at the density 10^4 cells/well onto a 96 well plate and incubated overnight at 37°C in a humidified atmosphere with 5% CO₂ in 200 µL culture medium. These cells were then treated with either polymer at four different concentrations i.e. 25, 50, 75 & 100µg/ml or with their nanoplexes prepared with ctDNA at their optimised weight ratio. After 24 h of incubation at similar conditions, the culture medium was replaced with 100 µL of MTT solution (0.5 mg/mL) prepared in sterile PBS was added and incubated for another 3 h in CO₂ incubator. Thereafter, the insoluble formazan crystals produced by the live cells from the reduction of MTT reagent was dissolved in 200 µL of DMSO and absorbance was measured at 570 nm using automated microplate reader (Bio Tek, Synergy H1, US). The relative cell viability was then calculated by taking untreated cells as the control using the following equation

$$\text{Percentage Cell viability} = \frac{\text{Abs. of test}}{\text{Abs. of control}} \times 100$$

where Abs. is the absorbance at 570nm.

3.4.13 Cellular uptake of polyplexes

Cellular internalisation of nanoplexes prepared from the VI derivatives with YOYO I tagged ctDNA was studied in cancer cells – C6 glioma and HeLa cells. This study was carried out in four well plate seeded with 10^5 cells/well in 0.5ml corresponding culture medium. After overnight incubation at appropriate conditions, the cells were treated with polyplexes containing culture medium and incubated for another 2.5 h at 37°C in CO₂ incubator. The cells were then stained with 7µg of Hoechst 33342 and incubated for 30 min under similar conditions. Visualisation of cellular internalisation and imaging of these cells were carried out using fluorescence microscope, Leica DMI 3000B (Germany) after fixing with 1% formaldehyde solution. Cells that internalised nanoplexes were also quantified by flow cytometry (Becton Dickinson FACS Aria, USA).

3.4.14 Cellular uptake in the presence of endocytotic inhibitors

Cellular uptake mechanism of nanoplexes prepared with VI derivatives was studied in C6 cells using different endocytotic inhibitors. For this study, cells were seeded at a density of 10^5 cells/well onto a 24-well plate and incubated overnight at 37 °C in CO₂ incubator. Once it reached 80% confluency, the cells were treated with various endocytotic pathway inhibitors like chlorpromazine, filipin and amiloride at a concentration of 4 µg/mL, 5 µg/mL and 2.25 µg/mL respectively and incubated for

30 min under similar conditions (Rekha & Sharma, 2009b). Nanoplexes of VI derivatives prepared at the weight ratio 5:1 with YOYO I tagged ctDNA were then added to these cells and incubated for another 3 h. Flow cytometry analysis was carried out using Becton Dickinson FACS Aria (US) in order to quantify the cells that internalised the nanoplexes.

3.4.15 Gene transfection

Cancer cells - C6 glioma and HeLa as well as normal cells – L929 were harvested from the culture flask having confluent growth and seeded at a density of 1×10^5 cells/well in a 4-well plate. The cells were cultured in 0.5 ml of corresponding culture medium supplemented with 10% FBS in CO₂ incubator at 37°C to attain 70 – 80% confluency. These cells were then treated with nanoplexes of VI derivatives prepared with p53 plasmid at their optimised weight ratio and incubated under similar conditions. After 5 h incubation, transfection media was replaced with 0.5 ml of fresh culture media and cells were incubated for another 19 h at 37°C. The culture plate were then differentially stained using Live Dead Assay kit containing calcein AM and ethidium homodimer (EthD-1) in order to distinguish live cells from dead ones. The cell status was then visualised and photographed using Leica DMI 3000B fluorescence microscope (Germany). Dead cells were also quantified by flow cytometry using Becton Dickinson FACS Aria (US) by staining with propidium iodide (PI).

3.5 Synthesis and characterisation of 2-Diethyl amino ethyl methacrylate (DEAEM) grafted cationised polysaccharides

3.5.1 Materials

2-Diethyl amino ethyl methacrylate (DEAEM), 3-(4,5-dimethylthiazol-2-yl)-2,5-diphenyl-tetrazolium bromide (MTT) and cell culture medium like Dulbecco's modified Eagle's medium (DMEM)/F12 Ham, Minimum Essential Medium (MEM) were obtained from Sigma – Aldrich Chemicals Co, US. Fetalbovine serum (FBS) procured from GIBCO (USA) while trypsin, Live Dead assay kit; fluorescent stains like YOYO iodide, Hoechst 33342 were purchased from Invitrogen. Calf thymus DNA (ctDNA) was brought from Worthington Biochemical Corp. Dominant-Negative plasmid Vector of p53 was purchased from Clontech (USA) respectively. Cell lines required for this study (C6 glioma, HeLa and L929) were procured from National Centre for Cell Science (NCCS), Pune, India. All the other chemicals were of analytical grade, available in India.

3.5.2 Synthesis

Cationised polysaccharides – DP and PP grafted with 2- DEAEM at two different weight ratios (10:0.01 and 10:0.005) by Michael addition reaction. In brief, 100mg of cationic polysaccharide – DP and PP stirred with 200 and 100 μ g of 2- DEAEM in the presence of methanol and stirred for 72 h at room temperature to synthesis DPD I, DPD II, PPD I and PPD II respectively (Escalante *et al*, 2008). The solution was then thoroughly dialysed in distilled water in order to remove unreacted monomer molecules.

3.5.3 Fourier transform infrared spectroscopy (FTIR)

Fourier transform infrared spectroscopy (FTIR) was recorded using Nicolet 5700 spectrophotometer over the scan range 400 – 4000 cm^{-1} by ATR method. For this analysis, samples were prepared as thin films.

3.5.4 Proton nuclear magnetic resonance (^1H NMR)

Proton nuclear magnetic resonance (^1H NMR) spectra of the samples were analysed using a 500 MHz FTNMR (Bruker AV500) at 25°C. To execute this study, polymer solutions were concentrated using appropriate filters and then dissolved in deuterated water.

3.5.5 Determination of free amino groups

Free amino groups present in the DEAEM derivatives were determined by copper sulphate assay. As detailed in section 3.1.5, a standard curve using PEI standard was developed. The copper sulphate analysis was carried out by adding 5 ml of the reagent to 500 μl of polymer solution (1mg/ml). The OD was measured at 285 nm and the free amino groups present in the DEAEM derivatives were determined from the standard curve.

3.5.6 Buffering capacity

The buffering capacity of DPD I, DPD II, PPD I and PPD II was determined over the pH range from 10 to 4 by acid–base titration assay. Briefly, 0.1 mg/ml polymer solution was prepared in normal saline (0.9 % NaCl) and the pH was adjusted to 10 using 0.1N NaOH. The pH was then brought down to 4 by the sequential addition of

0.01N HCl and change in pH was monitored using pH meter (Benns *et al*, 2002). Buffering capacity of the polymer solution was then assessed from the graph plotted between volume of 0.01N HCl consumed and pH change.

3.5.7 Polymer/ctDNA polyplexes preparation

Nanoplexes of DEAEM derivatives of cationic polymers were prepared with ctDNA at 6 different weight ratios (polymer: ctDNA) viz 0.5:1, 1:1, 2:1, 3:1, 4:1 and 5:1. These nanoplexes were prepared by gently vortexing different amounts of polymer solutions (1mg/ml) with fixed amount of ctDNA and complexes were allowed to form by incubating at room temperature for 20 min (Casé *et al*, 2009).

3.5.8 Size and zeta potential

The size and zeta potentials of the nanoplexes were measured at 25°C by using a Zetasizer Nano ZS (Malvern Instruments, Malvern, U.K.) provided with He Ne laser having beam wavelength of 633 nm. Back scattered light from the nanoplexes were detected at an angle of 173° and three mean hydrodynamic diameter (Z-average) measurements were recorded each from 12 runs having 10s duration. Zeta potential of the nanoplexes was also measured at 25°C using the same equipment by taking sample in a capillary cell (DTS1070).

3.5.9 DNA binding ability and effect of plasma on nanoplex stability

Binding strength of the complexes formed between 2- DEAEM grafted cationic polymers and ctDNA was analysed by conducting agarose gel electrophoresis. To this study, nanoplexes prepared at different weight ratios were loaded on to a 1%

agarose gel containing EtBr. Electrophoresis was carried out in Mini-PROTEAN III gel electrophoresis apparatus (Bio Rad, USA) at 100 V for 15 min using 1X TAE buffer. DNA smear present in the gel was then visualized under UV and the image was captured using FUJIFILM FLA- 5100, image analyzer. The association strength between DEAEM derivatives and ctDNA was also evaluated in the presence of plasma protein by carrying out agarose gel electrophoresis.

3.5.10 Nanoplex stability in the presence of digestive enzyme, DNase

The potential of DEAEM derivatives to protect the DNA was assessed in the presence of DNase enzyme. Polyplexes were prepared at different weight ratios (as mentioned in the section 3.5.6) and treated with 4 μ L of DNase (569 U/mL) prepared in digestion buffer (0.1M sodium acetate, 5mM MgSO₄, pH 7.4). After 15 min incubation at 37°C, 3 μ L termination buffer (equal volume of 0.5M EDTA, 2M NaOH& 0.5M NaCl) was added to stop the reaction. As mentioned in the section 3.5.9, AGE was carried out and the gel image was captured using FUJIFILM FLA-5100 image analyser. Further, 5 μ L heparin (1000 IU) was added to the remaining nanoplex solution in order to release the DNA from the polyplex (Srinivasachari *et al*, 2007). After 30 min incubation, electrophoresis was once again carried out and gel image was photographed using the image analyser.

3.5.11 Polymer interactions with plasma proteins

Native PAGE was carried out to analyse the plasma proteins interactions with polymer. Polymer sample (100 μ g) was incubated with 20 μ L of human plasma for 30 min at room temperature. The samples were then centrifuged at 5000 rpm for 10

min and 20 μ L supernatant along with sample loading buffer loaded on to wells in 4 % stacking gel. To separate the protein bands, 7% resolving gel was used and the electrophoresis was carried out at 240 V for 30 min using Mini-Protean II electrophoresis system (Bio-Rad, CA, US). The gel image was documented using an image analyser (LAS 4000, Fuji) after staining with Coomassie blue. PEI interacts with plasma protein which was taken as positive control while normal saline that shows no interaction with plasma protein serves as negative control.

3.5.12 Cell culture studies

The efficacy of DEAEM derivatives to deliver gene was evaluated in the *in vitro* conditions using 3 different cell lines namely C6, HeLa and L929. These cells were initially cultured and maintained in T-25 flask and based on necessity, these cells were trypsinised and transferred to multi well plate at required cell density. Rat C6 glioma cells required culture medium containing equal volumes of F12 Ham/DMEM and MEM with 10% FBS for their growth while MEM alone with 10% FBS is enough to culture HeLa and L929 cells.

3.5.13 Cell viability

MTT assay was carried out in C6, HeLa and L929 cells in order to assess percentage Cell viability in the presence of 2- DEAEM grafted cationic polymers and also with their nanoplexes prepared at their optimum weight ratio. This study was carried out in 96 well plate seeded with 10^4 cells/well and incubated overnight in CO₂ incubator at 37°C and humidified atmosphere. Cells were then treated either with cationic polymers at different concentrations (25, 50, 75 & 100 μ g/ml) or with their

corresponding nanoplexes once they attained 70-80% confluency. These cells are then incubated under similar conditions for 24 h. After that culture medium was removed and 100 μ L of MTT solution (0.5 mg/mL) prepared in sterile PBS was added to each well. Following 3 h incubation, the formazan crystals produced by the live cells were then dissolved in 200 μ L of DMSO and the absorbance was measured using automated microplate reader (Bio Tek, Synergy H1, US) at 570 nm. By considering untreated cells as control, the percentage Cell viability was calculated using the following equation

$$\text{Percentage Cell viability} = \frac{\text{Abs. of test}}{\text{Abs. of control}} \times 100$$

where Abs. is the absorbance at 570nm.

3.5.14 Cellular uptake of polyplexes

Nanoplexes were prepared with DEAEM grafted cationic polymers with YOYO I tagged ctDNA analysed for cellular internalisation in C6, HeLa and L929 cells. To execute this study, cells were seeded onto a four well plate at the density 10^5 cells/well in 0.5ml corresponding culture medium and incubated overnight at 37 °C in CO₂ incubator. Once the cells attained 80% confluency, then it was treated with nanoplexes of DEAEM derivatives prepared at their optimum weight ratio (5:1) and incubated for 2.5 h under similar conditions. Nucleus of these cells were then stained with Hoechst and incubated for another 30 min. On completion of three hours of incubation with nanoplex, the cells were thoroughly washed three times with PBS. Cellular uptake of nanoplexes was then visualised and imaged using fluorescence microscope, Leica DMI 3000B (Germany) after fixing with 1% HCHO. Percentage

of cells that nanoplexes get internalised were quantified by flow cytometry (Becton Dickinson FACS Aria, USA).

3.5.15 Cellular uptake in the presence of endocytotic inhibitors

C6 cells were seeded to a 24-well plate at a density of 10^5 cells/well and incubated overnight at 37 °C in CO₂ incubator under humidified atmosphere until 80% cell confluency. The cells were then treated with clathrin inhibitor chlorpromazine, caveolae inhibitor filipin, macropinocytosis inhibitor amiloride at a concentration of 4 µg/mL, 5 µg/mL and 2.25 µg/mL respectively (Rekha & Sharma, 2009b; Kanatani *et al*, 2006b). After 30 min incubation, these are treated with nanoplexes of DEAEM derivatives prepared with YOYO I tagged ctDNA at the weight ratio 5:1 and incubated for another 3 h. Nanoplexes internalised cells were then quantified by flow cytometry (Becton Dickinson FACS Aria,USA) by counting ten thousand cells for each measurement.

3.5.16 Intra cellular trafficking of polymer

Intracellular trafficking of the polymer was studied in C6, HeLa and L929 cells by tagging DPD II and PPD II with TRITC (tetramethyl rhodamine isothiocyanate) using the protocol that mentioned in the section 3.1.15. Cells were seeded at the density of 10^5 cells/well and incubated overnight in order to achieve 80 % cell confluency. The cells were then treated with nanoplexes prepared at the weight ratio 5:1 using this TRITC tagged polymer with YOYO I tagged ctDNA and incubated for 2.5 h in the CO₂ incubator. Nuclear stain Hoechst was added and incubated for another half an hour under similar conditions. After PBS wash, cells were fixed using

1% HCHO. These cells were then visualized and photographed using a confocal microscope.

3.5.17 Gene transfection

Cell lines - C6, HeLa and L929 were seeded onto a four well plate at the density of 10^5 cells/well and incubated overnight at 37 °C in CO₂ incubator under humidified atmosphere. These cells were then treated with nanoplexes of DEAEM derivatives (DPD I, DPD II, PPD I and PPD II) prepared with p53 plamid at their optimised weight ratio i.e. 5:1. After 5 h of incubation in CO₂ incubator, nanoplex containing medium was replaced with 0.5ml of full growth culture medium and incubated for another 24 h under similar conditions. Live Dead Assay Kit containing 2 µM calcein AM and 4 µM ethidium homodimer (EthD-1) was used to stain the live and dead cells present in the culture plate respectively. Visualization of cells and its imaging were carried out using Leica DMI 3000B, fluorescence microscope (Germany) after fixing the cells with 1% HCHO. Dead cells were also quantified using flow cytometry (Becton Dickinson FACS Aria, USA).

3.5.18 Annexin V staining

The efficiency of DEAEM derivatives to deliver p53 plasmid was studied in HeLa cells by annexin V staining. Cells were seeded at the cell density onto a 24 well plate and incubated overnight at 37°C in CO₂ incubator. Nanoplexes of DPD II and PPD II derivatives were prepared with p53 plasmid at their optimum weight ratios (i.e. 5:1). The cells treated with these nanoplexes were incubated under similar conditions. After 5 h incubation, polyplex containing medium was replaced with 0.5ml fresh

culture medium and the incubation was continued for next 19 h at similar environment. Cells are then washed with PBS, trypsinised and centrifuged at 5000 rpm for 10 min to pellet down the cells. Resuspended the cell pellet using 100 μ L Annexin- V – Flous labelling solution and incubated for 15 min at dark conditions. After adding, 400 μ L incubation buffer (10 mM Hepes/NaOH, pH 7.4, 140 mM NaCl and 5 mM CaCl_2), the annexin V and propidium iodide positive cells were quantified by flow cytometer (Becton Dickinson FACS Aria,USA).

3.5.19 Immunostaining

Immunostaining was done in C6 cells in order to confirm the expression of p53 plasmid delivered by DEAEM derivatives. For this analysis, C6 cells were transfected with nanoplexes of DPD II and PPD II prepared with p53 plasmid at their optimum weight ratio i.e. 5:1. After 24 h incubation at 37 °C in CO_2 incubator, cells were washed with PBS and then fixed using 1% formaldehyde. Cells were once again subjected to PBS wash followed by cell permeabilisation using 0.2% Triton X-100 prepared in blocking solution (1% BSA in PBS) and incubated for 20 min. In the subsequent step, 0.2% Triton X-100 solution was replaced with 250 μ L blocking solution and incubated for another 30 min at room temperature. After removing the blocking solution, cells were incubated overnight with 200 μ L p53 antibody (200 μ g/1ml in PBS) at 4°C. Cells were once again treated with blocking solution as mentioned before which was followed by 1h incubation with 250 μ L FITC tagged anti rabbit IgG (200 μ g/ 1ml in PBS) at room temperature. In the subsequent step, cells were washed with PBS and the images were captured using confocal microscope.

3.5.20 Biodistribution studies

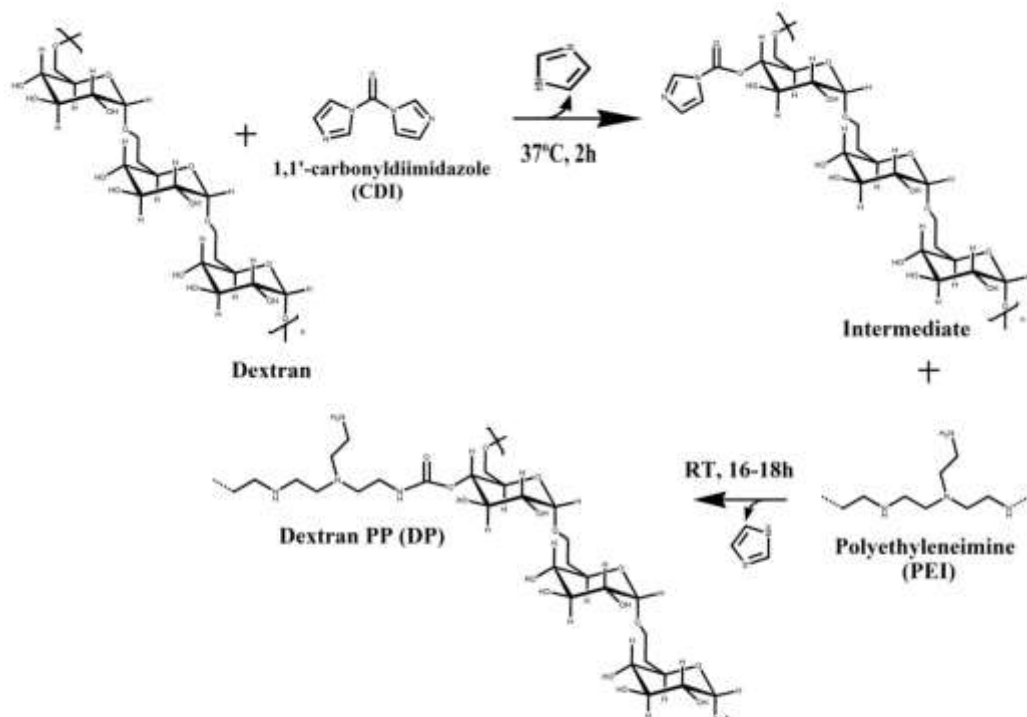
Biodistribution of DPD II and PPD II were analysed in BALB/c mice at various time periods (SCT/IEAC-158/July/2015/88, 28.7.15). For this study, polymer was tagged with Alexa fluor 790 dye by stirring 2 mg/ml polymer solution prepared in Na₂CO₃ buffer (pH 8) with 100 µg dye prepared in anhydrous DMSO for 1h at 90 rpm. In order to remove the excess dye molecules, the polymer solution was then dialysed in normal saline using membrane having molecular cut off, 2500. The tagged polymer (100 µg) was then injected to the adult mice via tail vein. These mice were then euthanized at four different time periods – 15 min, 3 h, 6 h and 24 h. Organs like liver, kidney, spleen, lungs, heart and brain were collected from these deceased animals and images were captured using *In vivo* imaging system (IVIS, Xenogen) at the Ex/Em 745/820 nm.

4. Results

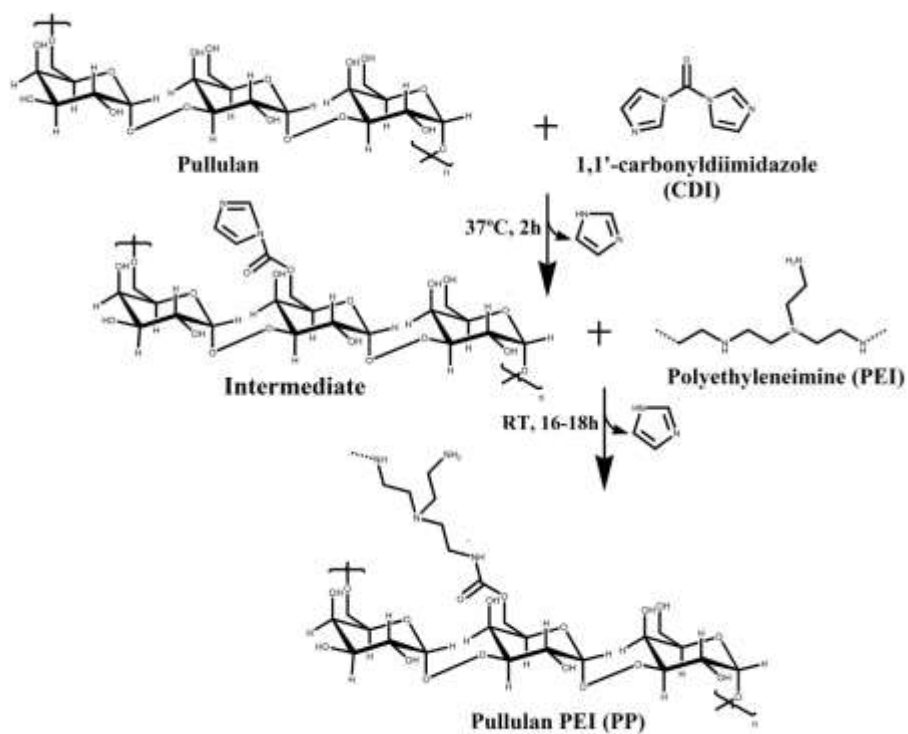
4.1 Cationisation of polysaccharides – Pullulan & Dextran

4.1.1 Synthesis

The first and foremost matter that should be considered while designing a polymeric gene delivery vector is that it should possess enough cationic charge so as to condense the negatively charged DNA. The cationic charge is also essential for proper cellular internalisation as the plasma membrane of the cell is negatively charged. Herein, the polysaccharides pullulan and dextran were modified with PEI in order to provide the cationicity required for DNA condensation and also to assist in cellular internalisation. CPs were prepared by grafting PEI with polysaccharides using CDI as the coupling agent. Based on the standardization studies, PEI to polysaccharide weight ratio was optimised as 1: 2.5. At this ratio, CPs exhibit higher transfection efficiency with lower cytotoxicity. The reaction scheme is depicted in scheme1 in which PEI is grafted to the polysaccharides through the carbamate linkage. CPs prepared at this optimised weight ratio was used for further modifications with vinyl monomers whose synthesis and characterisation are discussed in the subsequent sections.



A



B

Scheme 1: Schematic representation of synthesis of cationised polysaccharides (CPs) by CDI chemistry- (A) Dextran PEI, (B) Pullulan PEI

4.1.2 Fourier transform infrared spectroscopy (FTIR)

Functional groups present in the polysaccharides, PEI and CPs were evaluated by FTIR spectroscopy. In the figure 1, PEI shows characteristic bands at 3276 cm^{-1} , 2934 cm^{-1} , 1595 cm^{-1} , 1456 cm^{-1} and $1350\text{--}1000\text{ cm}^{-1}$ corresponding to --N--H stretching, --C--H stretching, --N--H bending, --C--H bending and --C--N stretching respectively (Wang *et al*, 2012). In the FTIR spectra of dextran, appearance of broad band at 3272 cm^{-1} corresponds to --O--H stretch while methylene stretch observed at 2930 cm^{-1} .

In the case of pullulan, the stretching vibrations of these groups appear at 3295 cm^{-1} and 2928 cm^{-1} respectively (Nikonenko *et al*, 2000; Shingel, 2002). The appearance of several bands over the region, $1175\text{--}1140\text{ cm}^{-1}$ ascribed to the formation of glycosidic linkage in these polysaccharides. The characteristic band at 995 cm^{-1} in the FTIR spectra of PP corresponds to the bending vibrations of C-OH group present at the C-6 carbon. At this position, the primary hydroxyl groups are absent in the structure of dextran as they are involved in the formation of α (1-6) glycosidic linkage (Nikonenko *et al*, 2000; Shingel, 2002). The appearance of additional bands in the FTIR spectra of DP and PP, corresponding to the formation of carbamate linkage (i.e. C=O stretching near 1650 cm^{-1} and C-N stretching vibrations in combination with --NH bending around 1570 cm^{-1}) confirms the grafting of PEI in these polysaccharides.

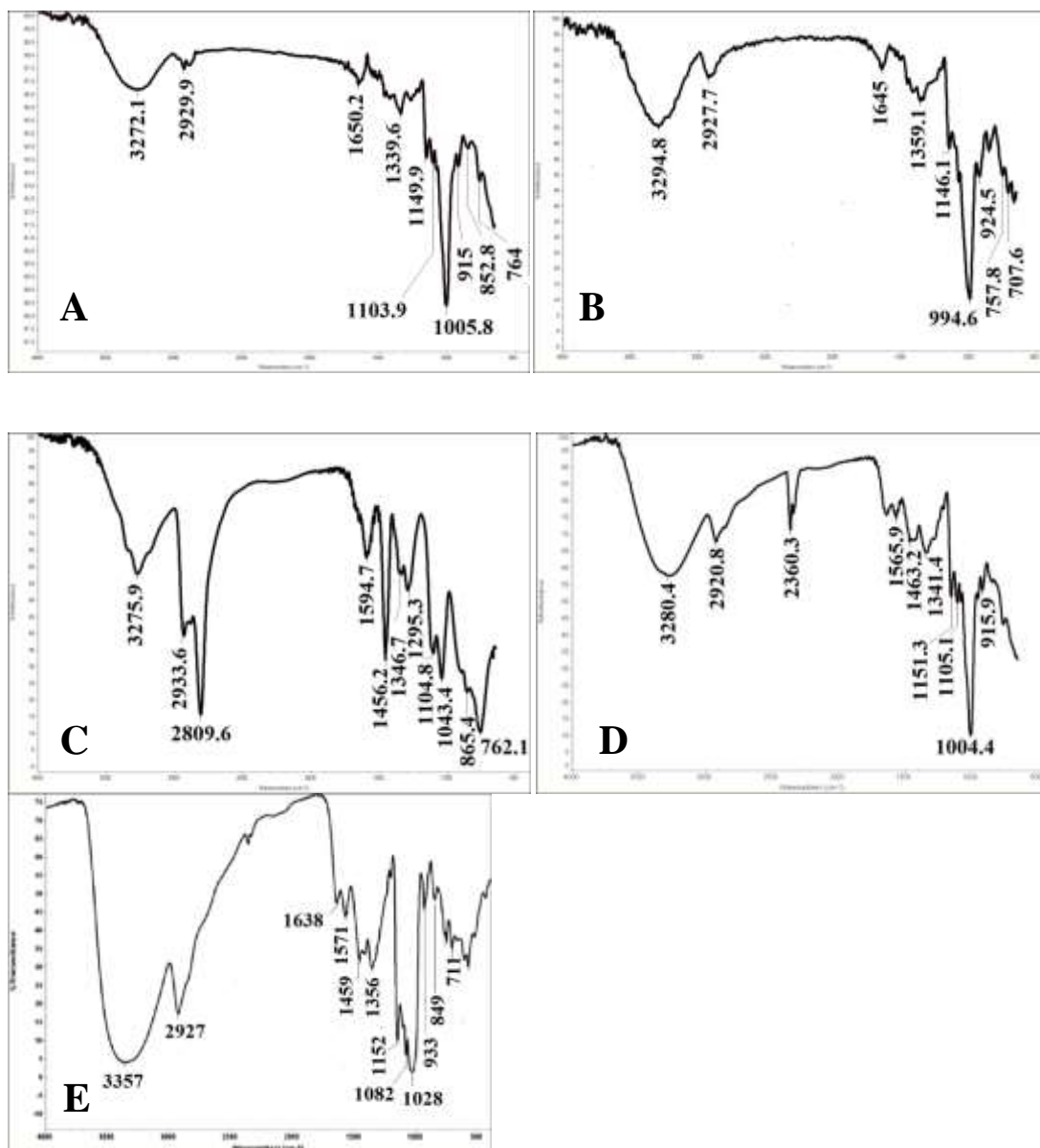
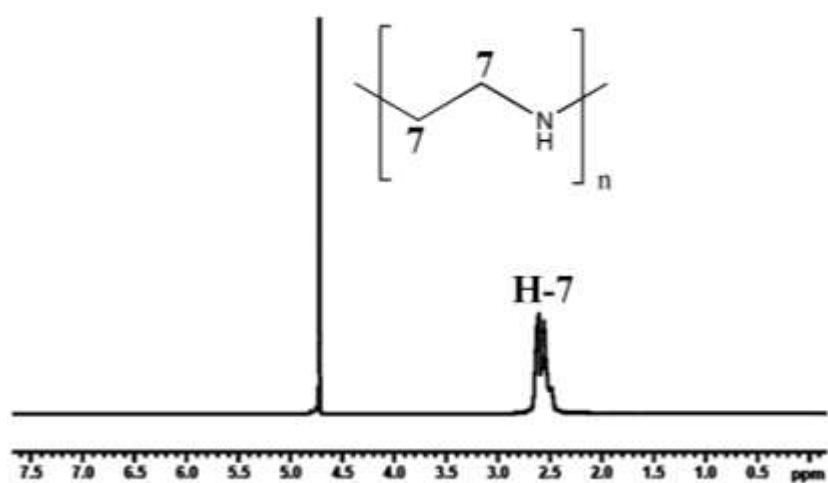


Figure 1: FTIR spectra for evaluation of functional groups in PEI, native polysaccharides and their cationised derivatives- (A) dextran (B) pullulan (C) PEI (D) dextran PEI, DP (E) pullulan PEI, PP.

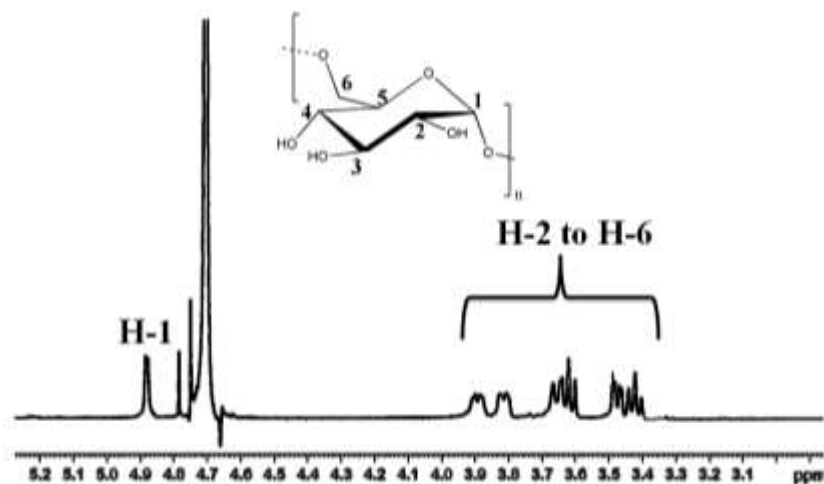
4.1.3 Proton nuclear magnetic spectroscopy (^1H NMR)

^1H NMR spectra further confirmed the grafting of PEI to the polysaccharides (dextran and pullulan). In figure 2, PEI shows chemical shifts around the region 2.5-2.8 ppm corresponding to the resonance of protons in the group ($-\text{CH}_2-\text{CH}_2-\text{N}$) while

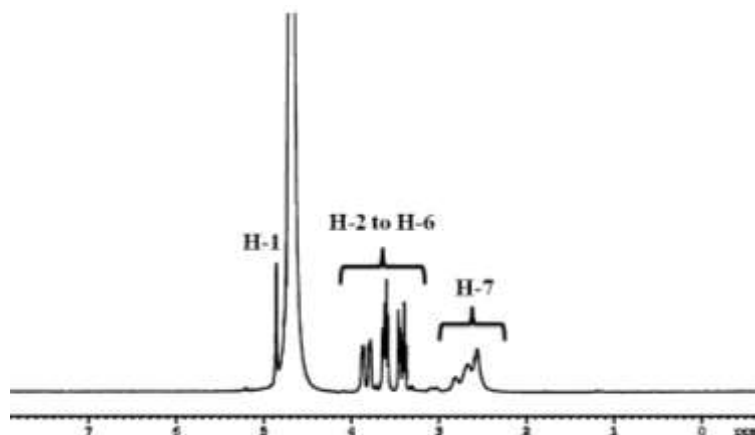
polysaccharides exhibit shifts around the region 3.4-4.0 ppm and 4.8-5.4 ppm which are associated with protons of C₂ to C₆ carbons and C₁ carbon of glucose units respectively. In the spectra of the CPs (DP and PP), the appearance of new peaks around the region 2.5-2.8 ppm in addition to the characteristic polysaccharides shifts confirm the grafting of PEI to these polysaccharides.



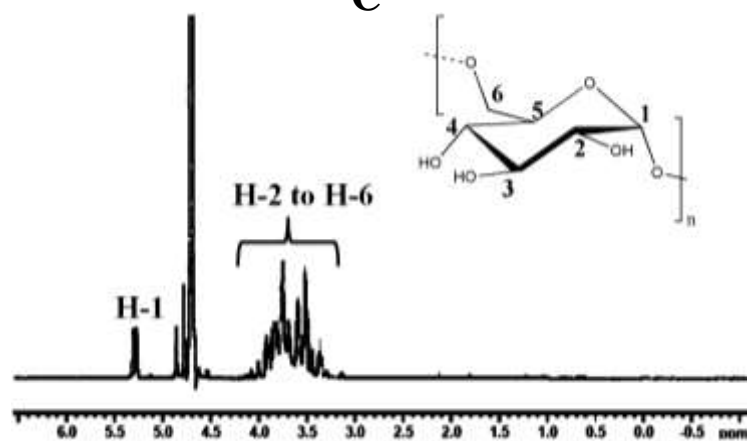
B



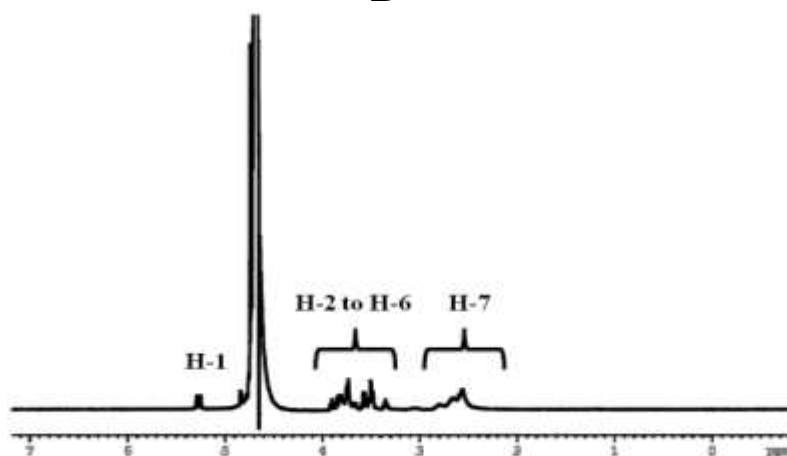
B



C



D



E

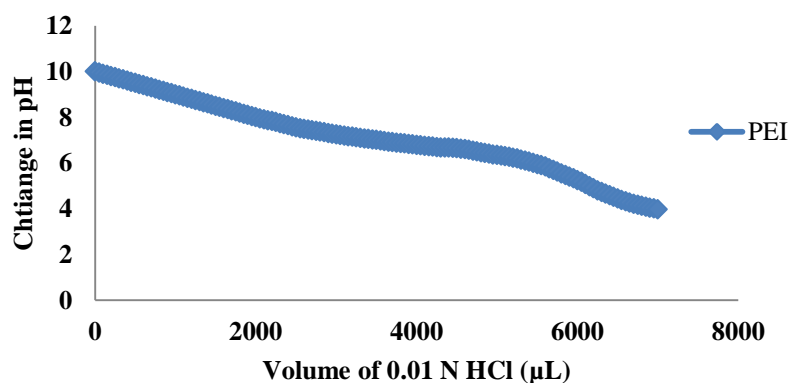
Figure 2: Proton NMR spectra of polysaccharides, PEI and CPs. (A) PEI (B) dextran(C) dextran PEI, DP (D) pullulan (E) pullulan PEI, PP. H-1 and H-2 to H-6 are the protons associated with C-1 and C-2 to C-6 carbons that present in the glucose units of polysaccharides while H-7 is the protons present in the methylene group of PEI.

4.1.4 Copper sulphate assay

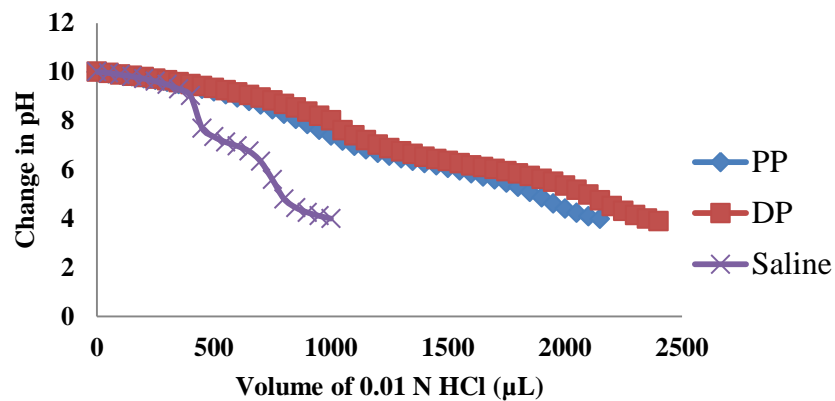
The extent of PEI grafting in DP and PP was determined by estimating the total amino groups present in these CPs by copper sulphate assay. The basic principle behind this assay includes the formation of coloured product by the reaction of copper ions with amino groups which was quantified by measuring optical density (OD) at 285 nm. As dextran and pullulan have no amino groups of their own, that present in the CPs was directly proportional to the PEI grafting density and it was estimated as $29.73 \pm 0.47\%$ for PP and $26.56 \pm 0.8\%$ for DP.

4.1.5 Buffering capacity

Buffering capacities of CPs and PEI were determined over the pH range 10 to 4 by acid - base titration. PEI exhibits excellent buffering capacity over wider pH range such that 7 ml of 0.01N HCl were consumed to bring down its pH from 10 to 4 (figure 3). On the other hand, CPs exhibit lower buffering capacity as compared to that of PEI but still they possess the appreciable level of buffering capacity over the endosomal pH range i.e. 6 to 4.



A

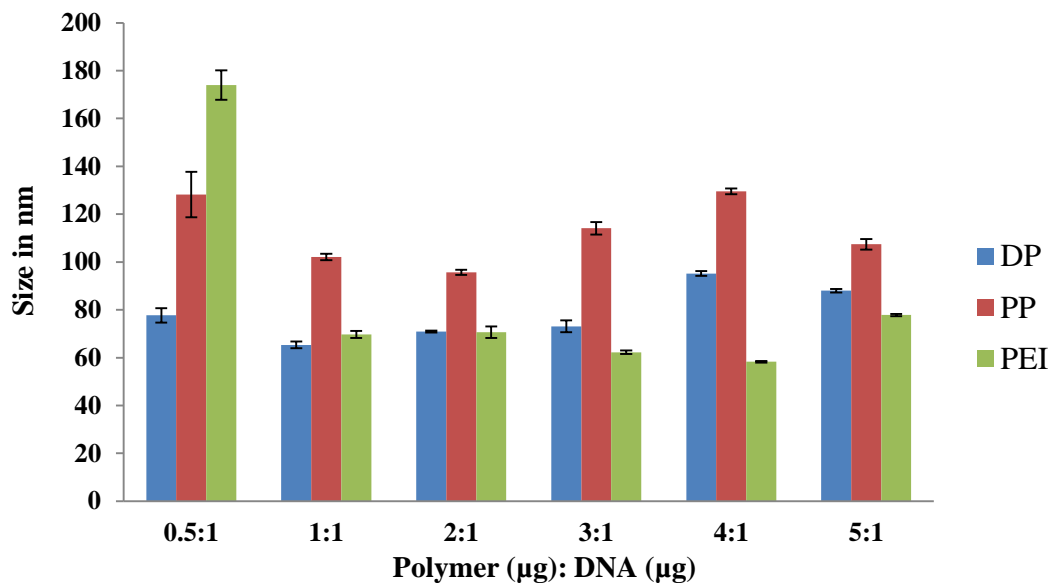


B

Figure 3: Buffering capacities of cationic polymers and saline over the pH range 10 to 4 which was determined by acid base titration. (A) PEI, (B) cationised polysaccharides (DP, PP) and saline.

4.1.6 Size and zeta potential

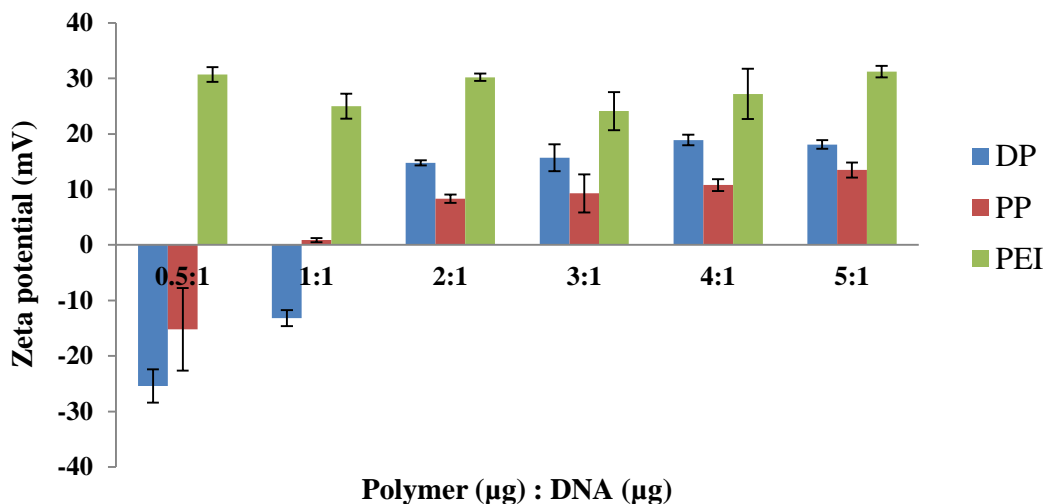
Nanoplexes of cationic polymers were prepared with ctDNA at different weight ratios. Size distribution of these nanoplexes was then analysed by dynamic laser scattering experiments. As figure 4 (A) shows all the cationic polymers effectively condense ctDNA and form smaller sized nanoparticles below 150 nm range. Of these, PEI forms the smallest nanoplexes of size below 80 nm (except at 0.5:1 weight ratio) which was followed by DP and PP that form nanoplexes of size below 100 and 150 nm respectively. Hydrodynamic size of these nanoplexes decreased with the increase in the polymer to DNA weight ratio which could be attributed to the formation of more condensed structures.



A

Figure 4(A): Hydrodynamic sizes of the polyplexes that prepared by complexing cationic polymers (DP, PP & PEI) with ctDNA at different weight ratios.

Polyplexes of PEI exhibit positive zeta potential even at the lower weight ratio i.e. 0.5:1 and this value found to be stable (i.e. around +30 mV). Further addition of the polymer did not influence this zeta potential value (Figure 4.B). However, the zeta potential of CPs found to increase with increase in the polymer/DNA weight ratios. Polyplexes of CPs exhibit negative zeta potential at the lower weight ratios and turns to be positive at the higher weight ratios. Steep rise in zeta potential observed at the weight ratio, 2:1 for both CPs and after that only slight increase in zeta potential was observed. Highest positive zeta potential was observed at the weight ratio, 5:1 and at this ratio, DP and PP exhibit a zeta potential of 18.1 ± 0.79 mV and 13.5 ± 1.35 mV respectively.



B

Figure 4(B): Zeta potential measurements of polyplexes prepared at different weight ratios by complexing different volumes of 1mg/ml cationic polymer solutions with fixed amount of ctDNA.

4.1.7 DNA binding ability and effect of plasma on nanoplex stability

Agarose gel electrophoresis was carried out in order to analyse the binding strength of cationic polymers with ctDNA. For this analysis, nanoplexes of cationic polymers were prepared with ctDNA at different weight ratios (0.5:1, 1:1, 2:1, 3:1, 4:1 & 5:1) and electrophoresis was carried out by loading onto the 1% gel. From the figure 5(A-C), it is clear that the association between cationic polymers and ctDNA is tight enough to retard the mobility of the latter under the electric field. However, for CPs, slight DNA leach out was observed at lower weight ratios especially at the 0.5:1 ratio. Nanoplexes stability was also established in the presence of plasma proteins as these proteins are negatively charged; there is a possibility to displace DNA from the nanoplexes by interacting with these cationic polymers. Figure 5 (D-F) shows that both CPs and PEI forms a tight complex with ctDNA. They are quite stable even in

the presence of plasma proteins and the results are similar with that of nanoplex alone.

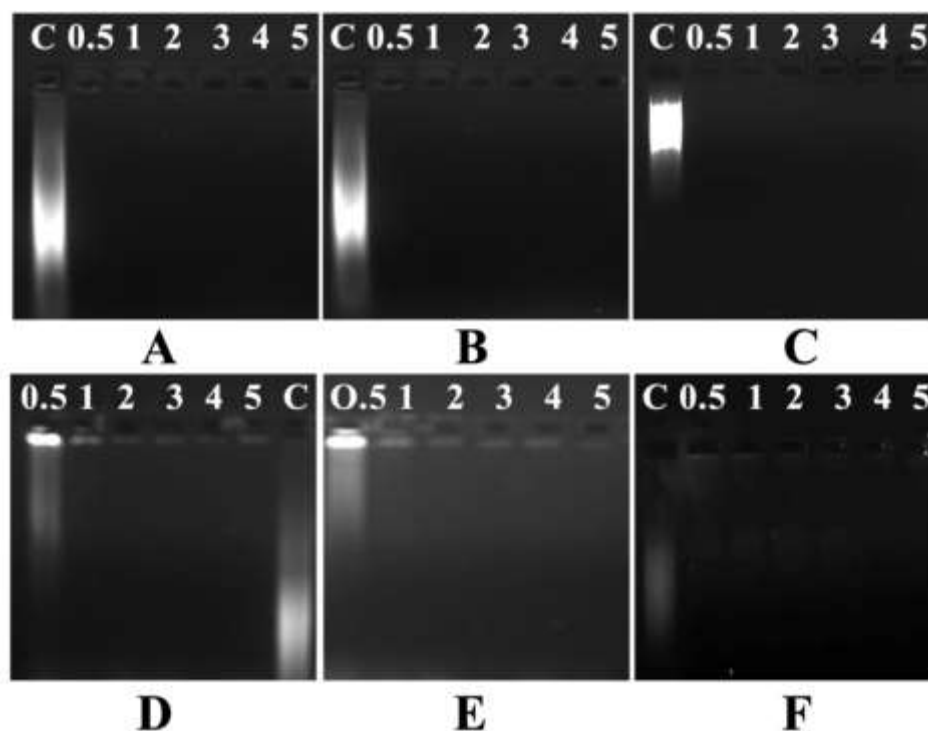


Figure 5: Stability of the nanoplexes and the ability of cationic polymers to retard the movement of DNA under electric field were assessed by agarose gel electrophoresis. A, B, C are nanoplexes of cationic polymers- PEI, DP and PP prepared with ctDNA at different weight ratios (0.5:1 to 5:1). D, E, F are the stability assessment of nanoplexes of PEI, DP and PP in the presence of plasma proteins respectively. Lane C is the control DNA i.e.without any treatment.

4.1.8 Nanoplex stability in the presence of digestive enzyme, DNase

The ability of cationic polymers to protect the DNA from nuclease degradation was assessed by incubating polyplexes with DNase, the digestive enzyme. Agarose gel electrophoresis was then performed in order to evaluate whether DNase has the access to digest the ctDNA present in the nanoplex. In figure 6 (A, B) control DNA without any treatment appears as smear while that treated with DNase show degradation and appeared as a band in the gel. No DNA degradation was observed in

the lanes loaded with nanoplexes prepared at higher weight ratios. However, nanoplexes that were prepared at lower weight ratio (i.e. 0.5:1) showed slight degradation as thin smear appears in their lane. The integrity of protected DNA by these cationic polymers was then analysed by adding heparin to the remaining polyplexes. This negatively charged glycosaminoglycan competes with the DNA for binding with the cationic polymer. As a result, the DNA get displaced from the polyplex and appeared as the smear in the lane on carrying out agarose gel electrophoresis. From figure (C, D) it was clear that CPs protect DNA more efficiently at all weight ratios except the one that prepared at the lower weight ratio (0.5:1).

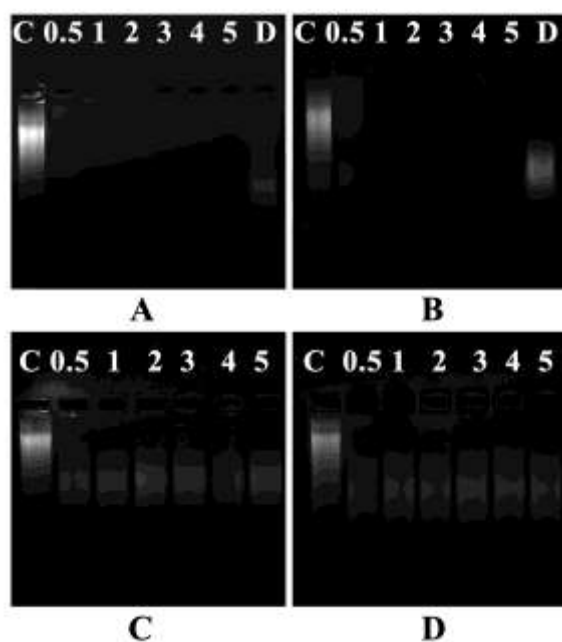


Figure 6: Nanoplexes of CPs were prepared with ctDNA at different weight ratios (0.5:1 to 5:1) and treated with 4 μ L DNase (569 U/mL). The images (A) and (B) shows nanoplexes of DP and PP treated with DNase. To check the integrity of protected DNA, these nanoplexes were further treated with heparin which releases DNA from the nanoplex by neutralising cationic charge. C and D are the nanoplexes of DP and PP treated with heparin respectively. Lane C is the control ctDNA without any treatment while lane D is that treated with DNase.

4.1.9 Polymer interactions with plasma proteins

Interaction of cationic polymers with plasma proteins is very critical as it determines their half-life in the systemic circulation. As saline shows no interactions with plasma proteins, saline-treated plasma was taken as negative control. Figure 7 reveals that PEI shows strong interaction with plasma proteins as most of the protein bands are missing when compared to that of the negative control, saline. CPs also exhibit slight interactions with plasma proteins but most of the protein bands remained intact as that of negative control.

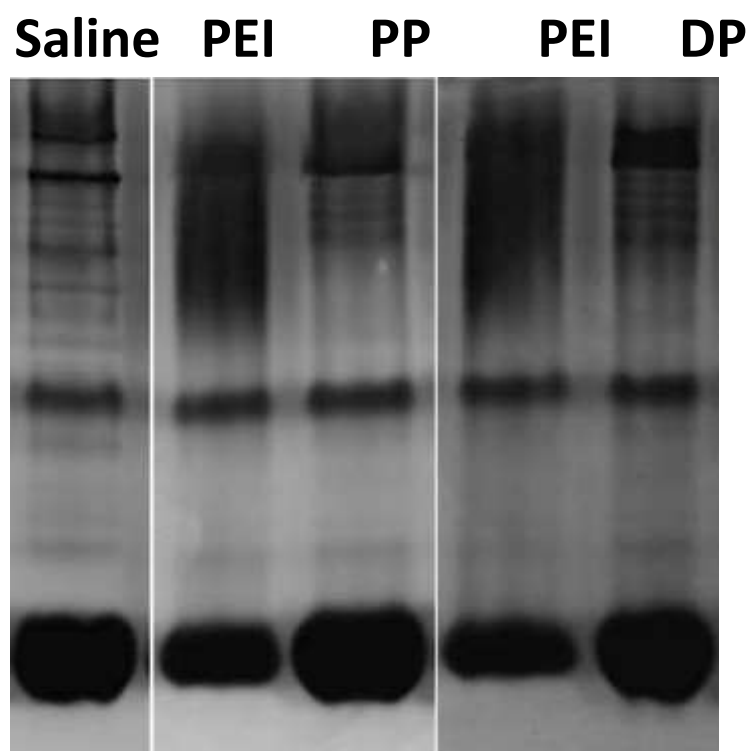
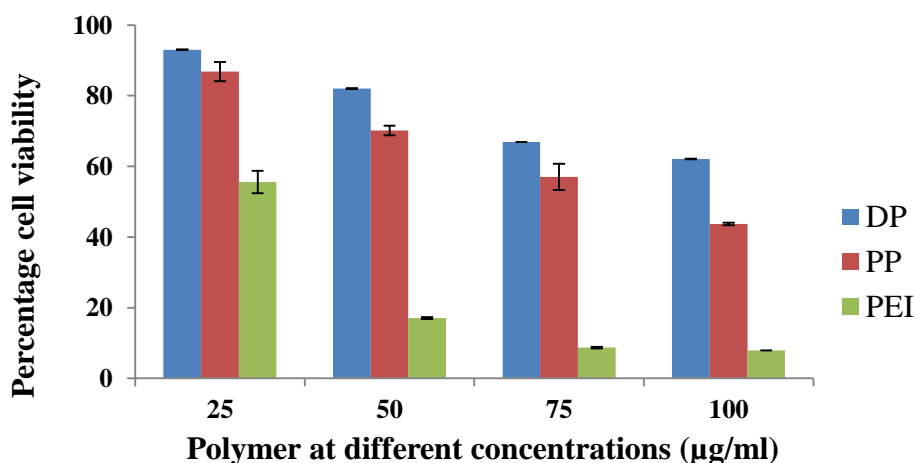
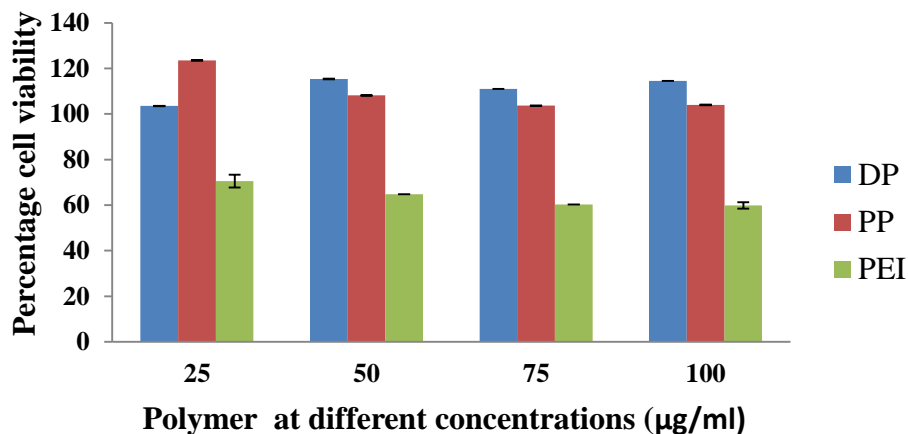


Figure 7: Interaction of cationic polymers with plasma proteins was evaluated by poly acrylamide gel electrophoresis following incubation of plasma with the respective polymers.

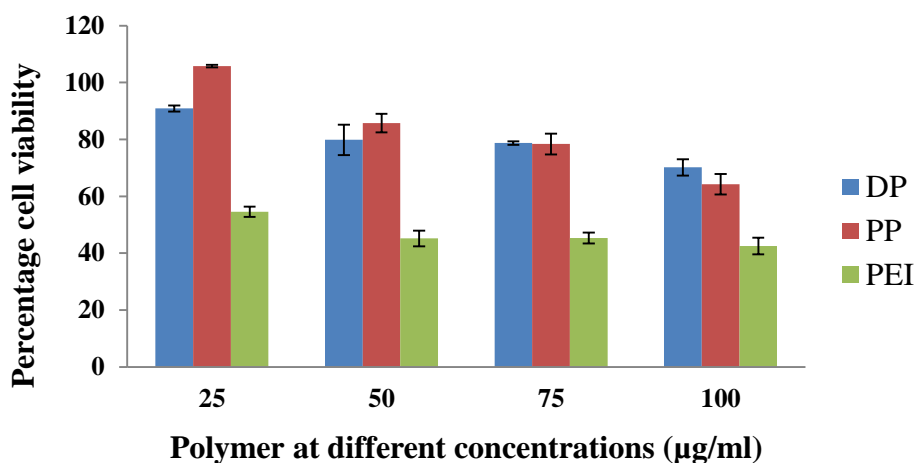
4.1.10 Cell viability

Inherent cytotoxicity is one of the major drawbacks of cationic polymers that are intended for gene delivery. So cytocompatibility of both cationic polymers and also their polyplexes were analysed in three different cell lines viz C6, HeLa and L929. These cells were either incubated with cationic polymers at four different concentrations or with their nanoplexes prepared with ctDNA at their optimised weight ratio (i.e. 5:1 for CPs and 2:1 for PEI). PEI was found to be toxic to all these cell lines even at lower concentrations (figure 8). On the other hand, CPs exhibited toxicity only at higher concentrations in C6 and L929 cells. CPs exhibit above 75% cell viability in L929 cell lines even at the polymer concentration 75 $\mu\text{g}/\text{ml}$ while in C6 cells, DP and PP found to be toxic after the polymer concentrations 50 $\mu\text{g}/\text{ml}$ and 25 $\mu\text{g}/\text{ml}$ respectively. However, these polymer derivatives are quite compatible with HeLa cells and exhibit 100% cell viability in this cell line even at their higher polymer concentrations. Polyplexes prepared from these cationic polymers found to be cytocompatible as they exhibit above 75% cell viability in all the three cell lines tested.





B



C

Figure 8: Cytocompatibility of cationic polymers evaluated by MTT assay in three different cell lines – (A) C6, (B) HeLa and (C) L929 cell lines at four different polymer concentrations (25, 50, 75 and 100 µg/ml).

4.1.11 Cellular uptake of polyplexes

Cationic polymers without any targeting ligands enter the cell via non specific endocytosis mechanism. Size and surface charge potential of the polyplexes plays an important role for this type of entry. To analyse the polyplexes efficiency to get internalised, cellular uptake studies were performed in two different cancer cell lines namely C6 and HeLa. These cells were transfected with polyplexes of cationic

polymers prepared at their optimised weight ratio (i.e. 5:1 for CPs while 2:1 for PEI) with YOYO I tagged ctDNA. Figure 9 shows good cellular internalisation of polyplexes in both C6 glioma and HeLa cell lines. It was also observed that ctDNA get localized into the cell nucleus which is essential for gene to get expressed. In figure 9, the appearance of green fluorescence in the nuclear region confirms the entry of ctDNA into the nucleus.

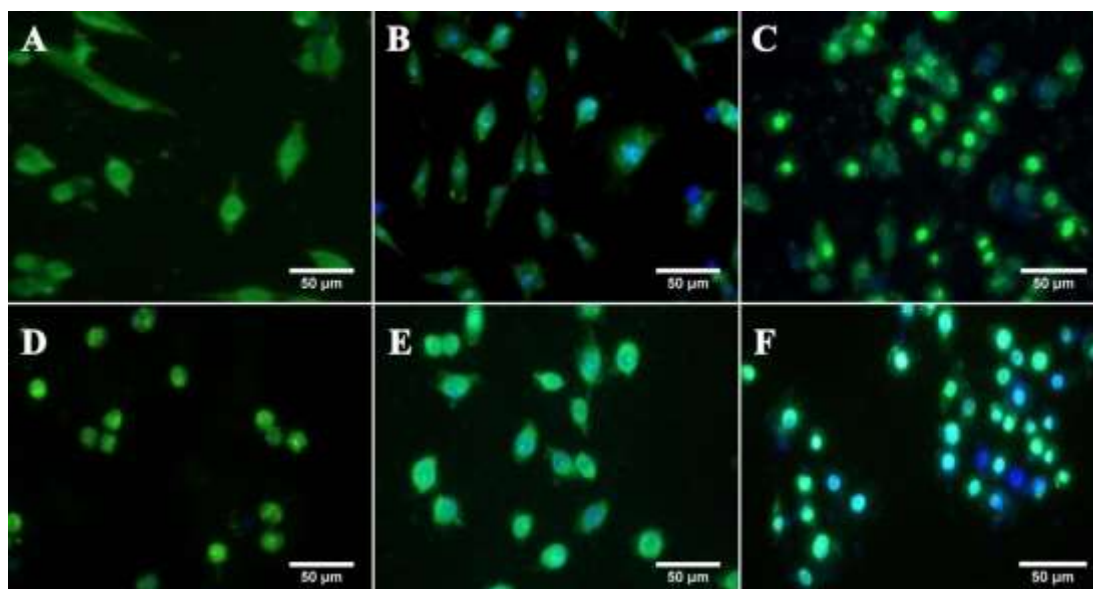


Figure 9 : Cellular uptake studies of cationic polymers in C6 glioma and HeLa cell lines. Polyplexes were prepared with YOYO I tagged ctDNA which emits green fluorescence. Cells nuclei were stained with Hoechst that emits blue fluorescence. A, B and C are the C6 cells treated with the polyplexes of DP, PP and PEI respectively while D, E and F are that in HeLa cells.

4.1.12 Polymer trafficking studies

Vector unpacking is one of the crucial steps in gene delivery as it determines the transfection efficiency. The release of DNA from the cationic polymers is assumed to be occurring in the cytoplasm by the interactions of polyplexes with the anionic cytosolic proteins. So, in order to elucidate the polymer status within the cell, CPs

and PEI were tagged with TRITC which emits red fluorescence. The cellular uptake study was then performed using polyplexes prepared with this tagged polymer. From figure 10, it is observed that PEI gets into the nucleus while CPs remains in the cytoplasm. This study confirms that the vector unpacking of CPs happens in the cytoplasm while polyplexes of PEI as such get into the nuclear compartment.

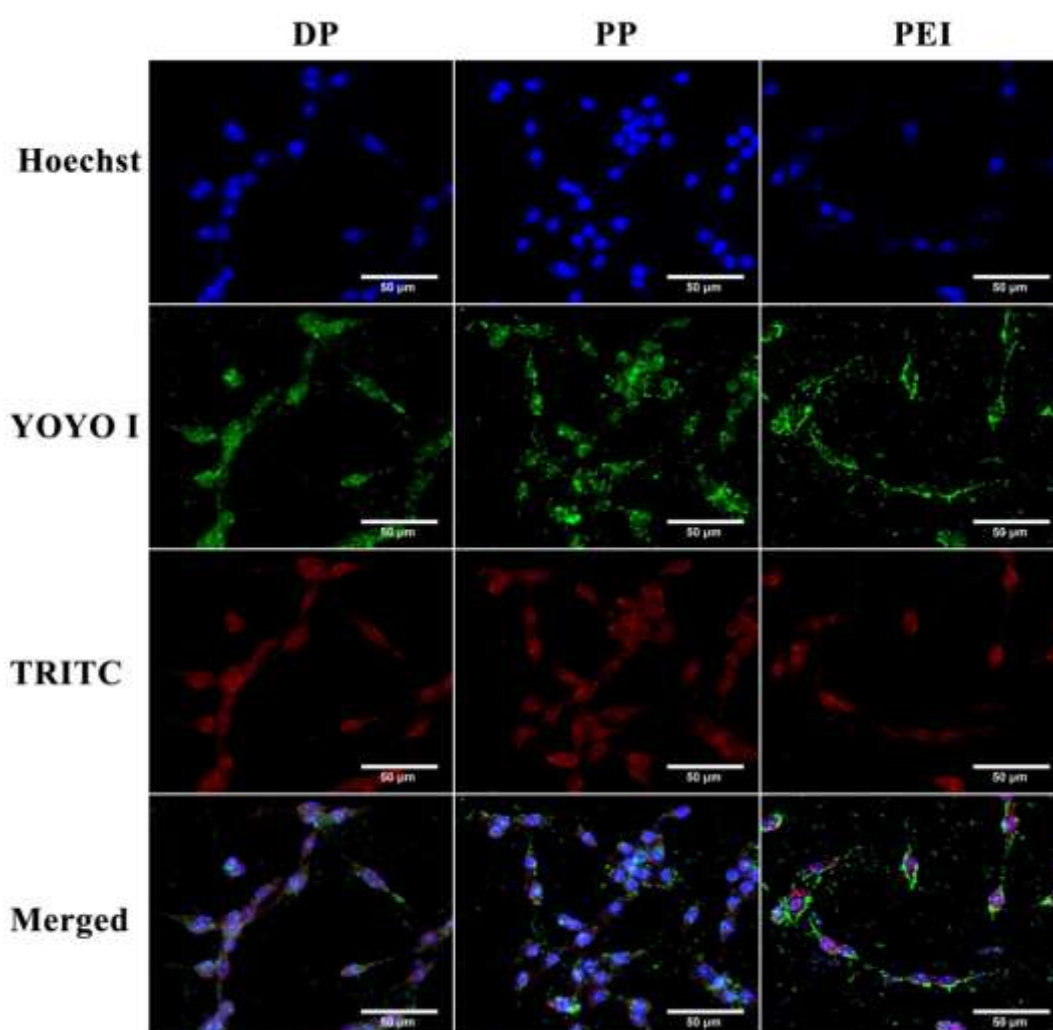


Figure 10: Polymer trafficking studies in C6 cells. Nucleus was stained with Hoechst while ctDNA and polymer were tagged with YOYO I and TRITC that emits green and red fluorescence respectively.

4.1.13 Gene transfection

The success of gene delivery vectors relies on how efficiently the delivered gene gets expressed. In this study, gene expression was studied using p53 plasmid whose expression leads to apoptosis of the cancer cells. Live and dead cells in the cell culture plate were distinguished by differential staining with Calcein AM and ethidium bromide respectively. Cellular death destabilises the plasma membrane which in turn allows the ethidium bromide to get into the cell and produces red fluorescence by binding with the cellular DNA. On the other hand, live cell emits green fluorescence by the action of intracellular esterase. Calcein AM and produces highly fluorescent, hydrophilic calcein.

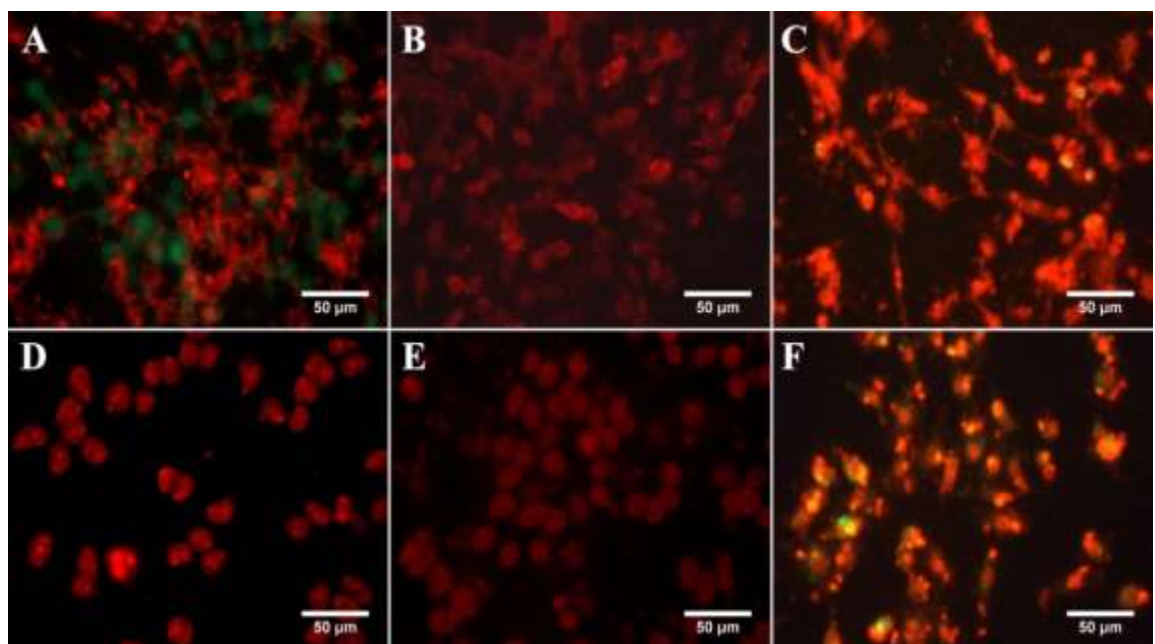


Figure 11: Assessment of transfection efficiency of CPs and PEI using p53 plasmid. A, B, C are C6 cells and D, E, F are HeLa cells transfected with polyplexes of DP, PP and PEI respectively. Dead cells emit red fluorescence while live cells are stained green.

To analyse the transfection efficiency of cationic polymers (CPs and PEI), C6 and HeLa cell lines were transfected with polyplexes that are prepared with p53 plasmid at their optimised weight ratio (5:1 for CPs and 2:1 for PEI). From the figure 11, it is clear that, these cationic polymers exhibit good transfection efficiency in both C6 and HeLa cell lines. This is evidenced by the appearance of more dead cells in these transfected cell lines.

4.1.14 Annexin V staining

Annexin V staining was done in order to confirm the death that occurred in the cells transfected with nanoplexes of cationic polymer prepared with p53 plasmid was through the induction of apoptosis. From the flow cytometric data (figure 12), it is clear that most of the cells transfected with PEI were in late apoptotic stage while that transfected with CPs were equally distributed in early and late apoptotic stage. The cells that was transfected with polyplexes of DP, PP and PEI had a population of 31.77 ± 6.49 %, 42.4 ± 6.38 %, 60.37 ± 6.87 % late apoptotic cells and 39.7 ± 12.36 %, 40.33 ± 2.82 %, 35.37 ± 6.95 % early apoptotic cells respectively. The occurrence of necrosis in these transfected cells was less than 1% for all these cationic polymers tested. Live cells were also observed in these transfected cells and their percentage was in the order DP > PP > PEI.

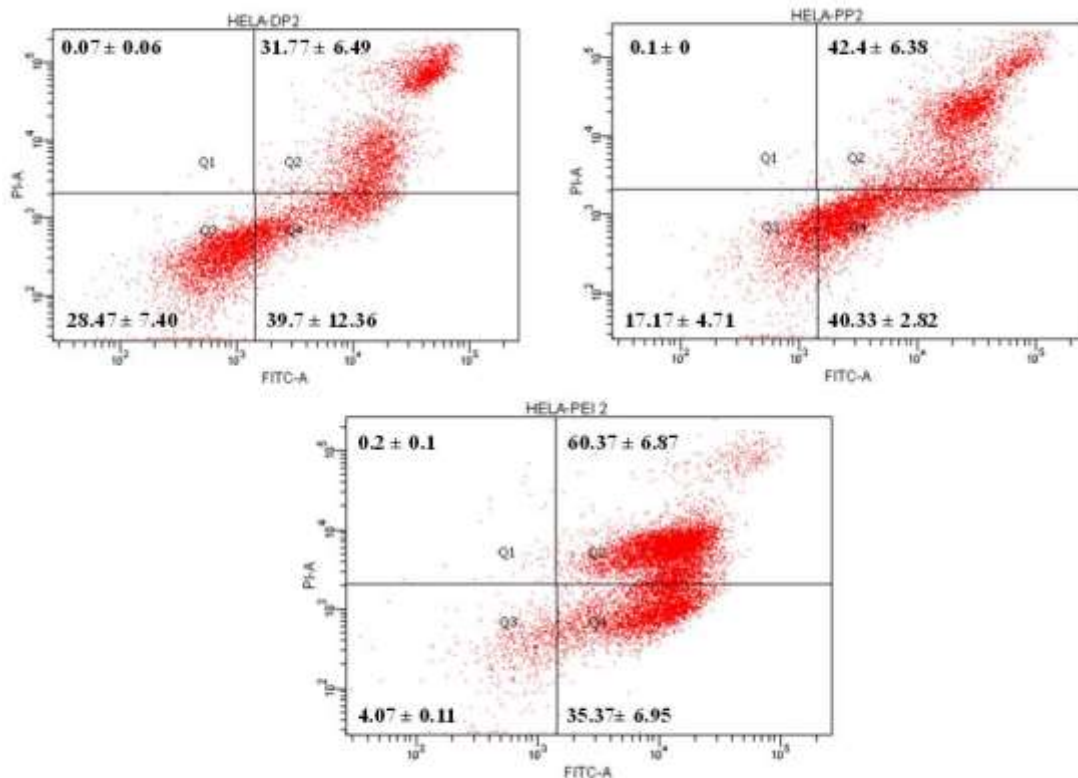


Figure 12: Flow cytometric data of HeLa cells transfected with polyplexes of cationic polymers prepared with p53 plasmid. Apoptotic and necrotic cells were distinguished with differential staining using FITC tagged Annexin V (Anx) and propidium iodide (PI) respectively. Quadrant 1 (Q1) is the Anx⁻/PI⁺ region and it indicates necrotic cells while quadrant 2 (Q2) and 4 (Q4) are Anx⁺/PI⁺, Anx⁺/PI⁻ regions that indicate late and early apoptotic cells respectively. Quadrant 3 is Anx⁻/PI⁻ region that signifies live cells.

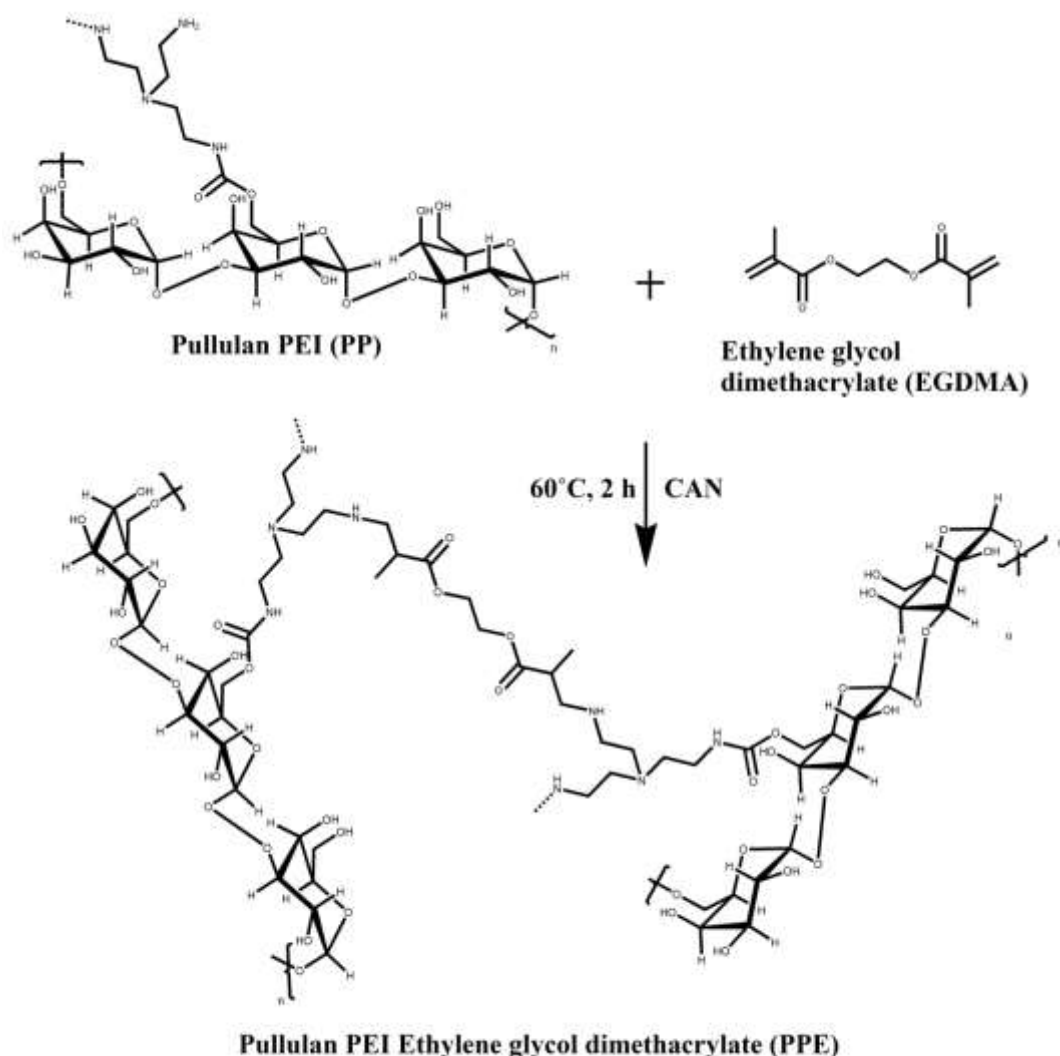
4.2 Synthesis and characterisation of ethylene glycol dimethacrylate

(EGDMA) cross linked cationised polysaccharides

4.2.1 Synthesis

EGDMA was introduced into the CPs in order to improve their cytocompatibility and also to avoid unwanted interactions with plasma proteins. EGDMA crosslinked PP was synthesised at two different weight ratios, 0.01:10 and 0.015:10 via aza Michael addition mechanism using CAN as catalyst and the resulting polymer derivatives

were named as PPE I and PPE II respectively. The reaction mechanism was depicted in the scheme 2. Similarly, DP derivatives were also synthesised but the end product turned out to be hydrophobic due to extensive crosslinking. As the derivatives were too hydrophobic and difficult to dissolve in any media it was found unsuitable towards gene delivery purpose. Hence, in this section, further work was carried out only with PP derivatives.



Scheme 2: Schematic representation of synthesis of PPE. Pullulan PEI (PP) was crosslinked with EGDMA using ceric ammonium nitrate (CAN) as the catalyst.

4.2.2 Fourier transform infrared spectroscopy (FTIR)

The FTIR spectrum of PPE is shown in the figure 13. In this spectrum, absorption bands corresponding to the parent chain (i.e. PP) appears at 3396 cm^{-1} (-O-H and -N-H stretch), 2981 cm^{-1} and 2889 cm^{-1} (-C-H stretch). The absorption band at 1647 cm^{-1} is ascribed to C=O stretching while that at 1541 cm^{-1} attributed by the combinations of -N-H bending and -C-N stretching vibrations in carbamate linkage. FTIR bands corresponding to the ester group (around 1740 cm^{-1}) in EGDMA moiety found to overlaps with the carbonyl group of the carbamate linkage.

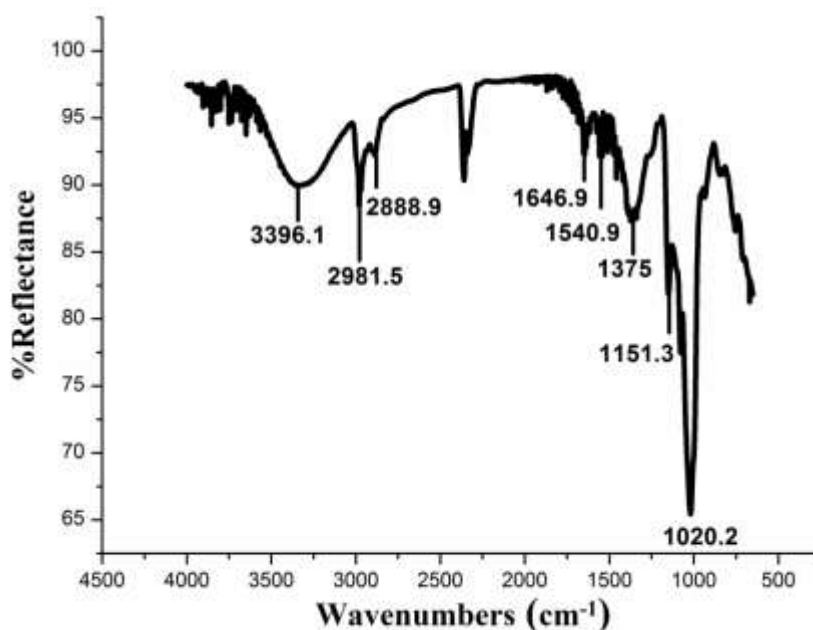


Figure 13: FTIR spectrum of pullulan PEI ethylene glycol dimethacrylate (PPE)

4.2.3 Proton nuclear magnetic spectroscopy (^1H NMR)

Crosslinking of EGDMA moieties in PP was confirmed by proton NMR spectra. In this spectrum (figure 14), the appearance of additional peaks around 4.688 ppm ascribed to the protons present in the (-COO- CH_2 -) group of EGDMA. Moreover,

in addition to the peaks of PP that are described in the section 4.1, the shifts around 3.01 to 3.2 ppm correspond to the protons present in the methylene carbon that links EGDMA with the primary amino group of PP. This confirms the cross linking of this vinyl monomer.

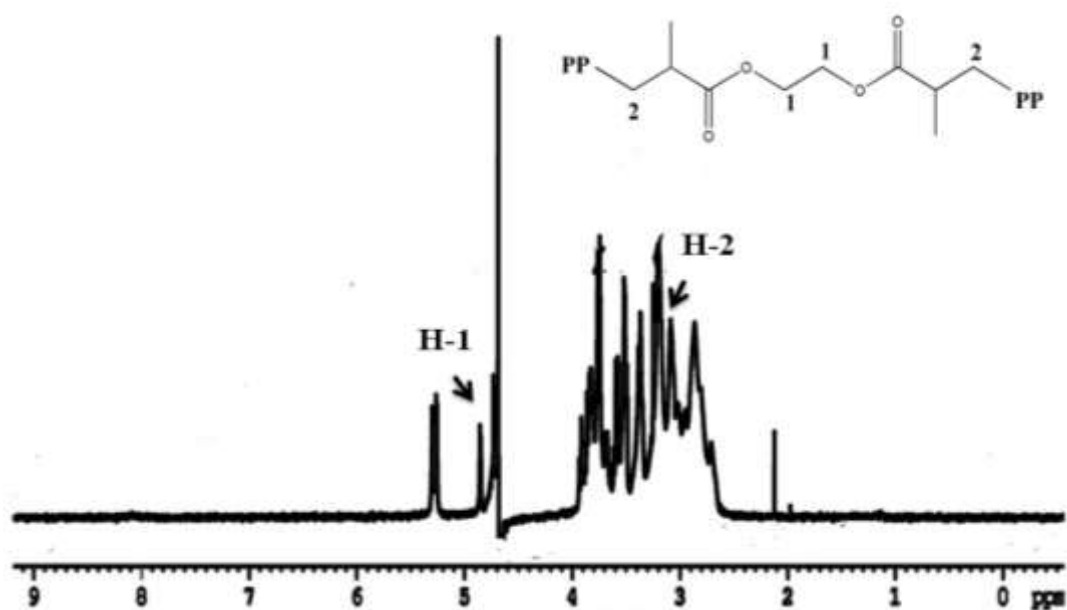


Figure 14: Proton NMR spectra of PPE in deuterated water.

4.2.4 Copper sulphate assay

Cross linking of EGDMA moieties occurs between the amino groups of the PP. Hence the extent of EGDMA cross linking in the resultant polymer derivatives was determined indirectly by calculating the reduction in amino groups of the parent chain, PP. Copper sulphate assay was used to determine amino groups present in the PPE I and PPE II and the results were compared with that of the corresponding parent polymer. Percentage crosslinking of EGDMA moieties was found to be $1.9 \pm 0.53\%$, $2.36 \pm 0.35\%$, for PPE I and PPE II derivatives respectively.

4.2.5 Buffering Capacity

Cationic polymers which enter the cell through non specific interactions with plasma membrane exploit endocytosis as the major route of internalisation. These polymers are usually entrapped in the endosomes where they experience a drop in pH from 7.4 to 5. PEI based cationic polymers are assumed to escape from these endosomal compartments through the proton sponge mechanism. Basic amino groups present in the PEI resist the pH drop experienced within the endosomes by absorbing the protons. In order to maintain the acidic pH, ATPase proton pump translocates more protons into the lumen of endosomes. Simultaneously, to maintain electrical neutrality, there is a concurrent influx of chloride ions and water molecules into the lumen of endosomes. This will develop osmotic pressure within this compartment which ultimately result in their rupture and the release of polyplexes into the cytoplasm (Boussif *et al*, 1995a). Therefore, one of the most important parameters should be considered while designing cationic polymers for gene delivery is that they should possess buffering capacity over the pH range 7 to 5 in order to resist the pH drop experienced within the endosome (Lin *et al*, 2008). Hence in this study, the buffering capacity of EGDMA derivatives was analysed by acid - base titration. From the figure 15, it is clear that both PPE I and PPE II derivatives exhibit significant buffering capacity over endosomal pH range i.e. 7 to5.

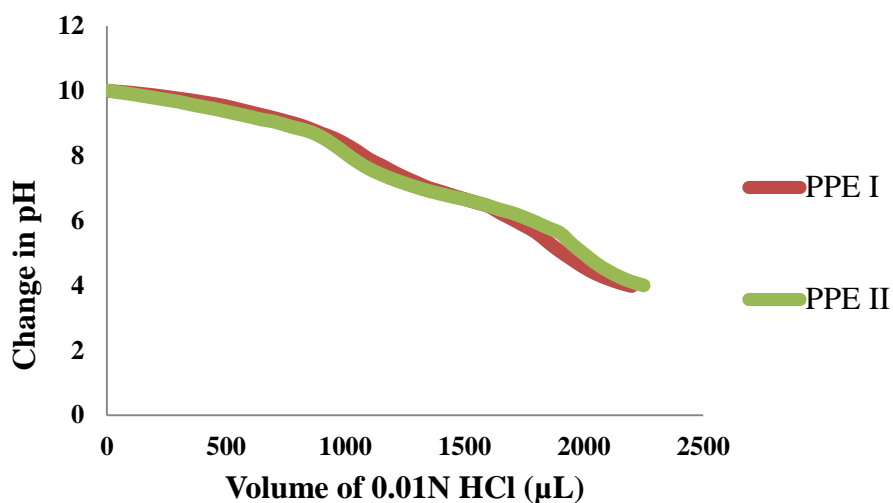
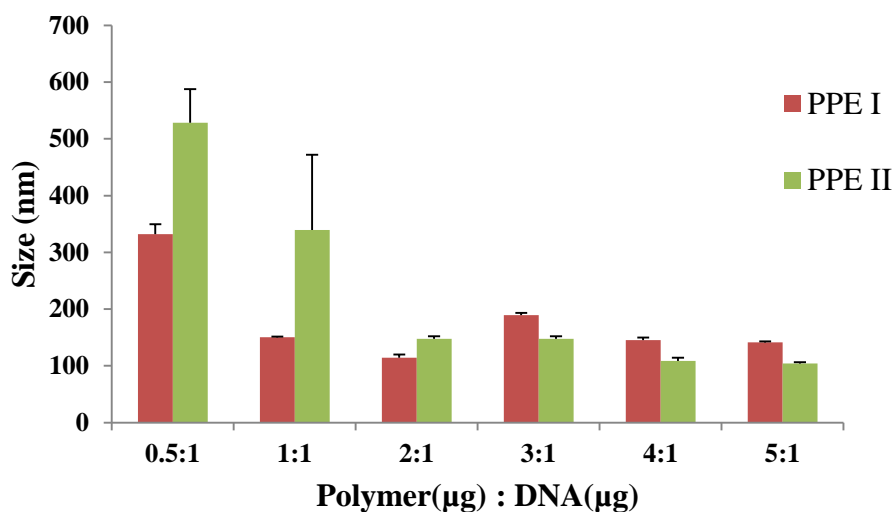


Figure 15: Buffering capacities of EGDMA derivatives of PP over the pH range 10 to 4 by acid base titration.

4.2.6 Size and zeta potential

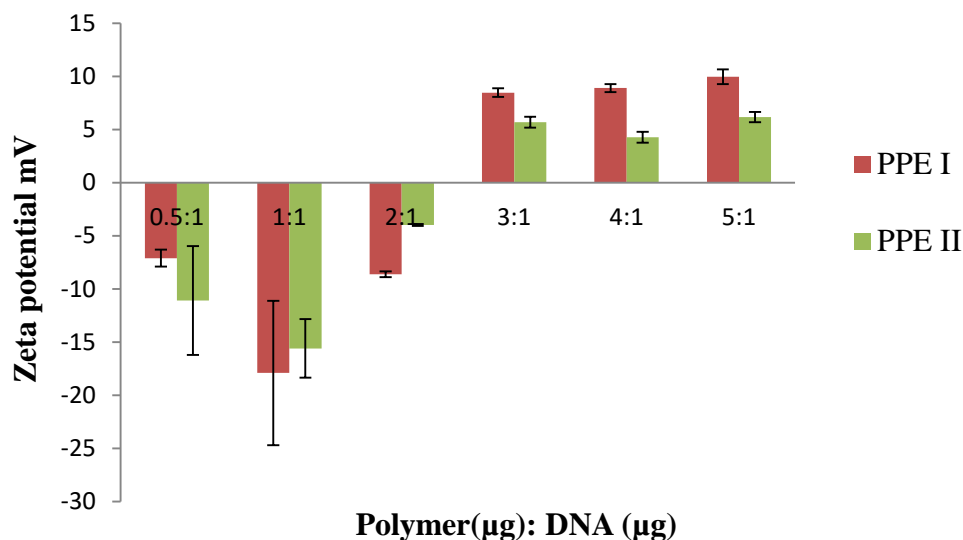
The electrostatic interactions between cationic polymers with negatively charged DNA leads to the formation of more condensed structures. Size and zeta potential of EGDMA derivatives were analysed by preparing their nanoplexes with ctDNA at six different ratios. Nanoplexes size distribution was then analysed by dynamic laser light scattering experiments. Size of these nanoplexes was found to be decreasing with the increase in the polymer to DNA weight ratio (figure 16A). Both PPE I and PPE II derivatives condensed ctDNA more effectively at the weight ratio 5:1 and formed around < 150 nm sized nanoplexes. PDI values were around 0.3 at this weight ratio and that indicates the formation of a more homogenous population.



A

Figure 16(A): Hydrodynamic diameter of PPE polyplexes prepared with ctDNA at different weight ratios.

Electrostatic interaction between EGDMA derivatives of PP with ctDNA neutralises the negative charge of the later and exhibit a positive zeta potential at higher polymer concentrations. Figure 16(B) shows that zeta potential of both EGDMA derivatives increase with an increase in the polymer to ctDNA weight ratio. Polyplexes prepared at the lower weight ratios exhibit negative zeta potential (until 2:1 ratio) and after that sharp increase in zeta potential was observed. Polyplexes of both PPE I and PPE II exhibited the highest positive zeta potential at the weight ratio of 5:1. At this ratio, polyplexes of PPE I exhibit higher zeta potential and it was around 9.96 mV while for PPE II, it was around 6.16 mV. Based on size, PDI and zeta potential values, nanoplexes prepared at the 5:1 weight ratio was optimised for further studies with EGDMA derivatives.



B

Figure 16(B): Zeta potential measurements of PPE polyplexes prepared with ctDNA at six different weight ratios.

4.2.7 DNA binding ability and effect of plasma on nanoplex stability

The strength of association between EGDMA derivatives and DNA was analysed by performing agarose gel electrophoresis. Strong electrostatic interactions between cationic polymer and DNA retard the mobility of latter under the external electric field. To evaluate the binding strength of EGDMA derivatives with ctDNA, nanoplexes were prepared at different weight ratios and loaded onto the 1% gel along with control DNA and electrophoresis was performed at 100 mV. From the figure 17 (A and B), it was clear that the polyplexes prepared at the lower weight ratios (i.e. below 2:1 ratio) was not stable enough to retard the mobility of DNA which was evidenced from the appearance of DNA smear in these lanes. However, the nanoplexes prepared at higher weight ratios are quite stable as they prevent the mobility of DNA towards the anode. In these lanes, the occurrence of fluorescence

inside the well signifies the retention of DNA within the polyplexes. Nanoplex stability was also evaluated in the presence of plasma proteins by incubating with human plasma. Figure 17 (C and D) shows that plasma proteins interact with polyplexes and displaces DNA from loosely bound complexes from the EGDMA derivatives owing to their anionic nature. As a result DNA smear appears even at the 3:1 weight ratio which indicates that stable nanoplexes are formed only at higher weight ratios (i.e. 4:1 and 5:1 weight ratios).

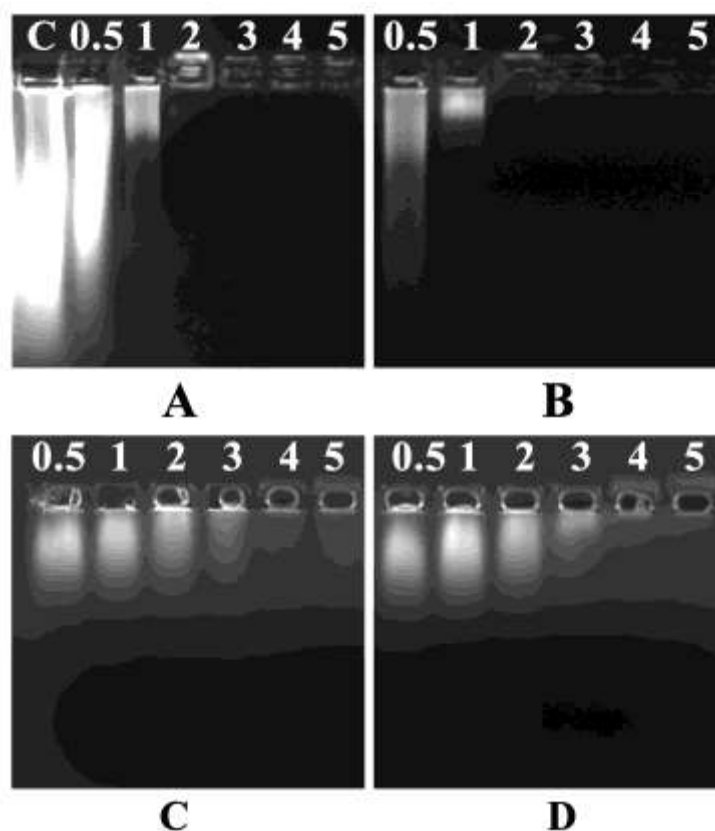


Figure 17: Stability of PPE polyplexes to retain ctDNA under electric field was assessed by gel retardation assay. (A) and (B) are polyplexes of PPE I and PPE II derivatives prepared with ctDNA at six different weight ratio (0.5:1 to 5:1) while (C) and (D) are that in the presence of plasma proteins respectively.

4.2.8 Polymer interactions with plasma proteins

In vivo biodistribution of cationic polymers depends on their interactions with plasma proteins. Polyacrylamide gel electrophoresis was performed in order to analyse the interactions of EGDMA derivatives with plasma proteins by incubating these polymers with human plasma. PEI due to their higher cationic charge density binds strongly with plasma proteins and as a result protein bands are missing in this lane. On the other hand, saline treated with plasma show no interactions and it serves as the negative control. Among EGDMA derivatives, as seen in figure 18, PPE I exhibit slight interactions with plasma proteins. No interactions were observed for the plasma treated with PPE II derivatives and protein bands were similar as that of negative control, saline.”

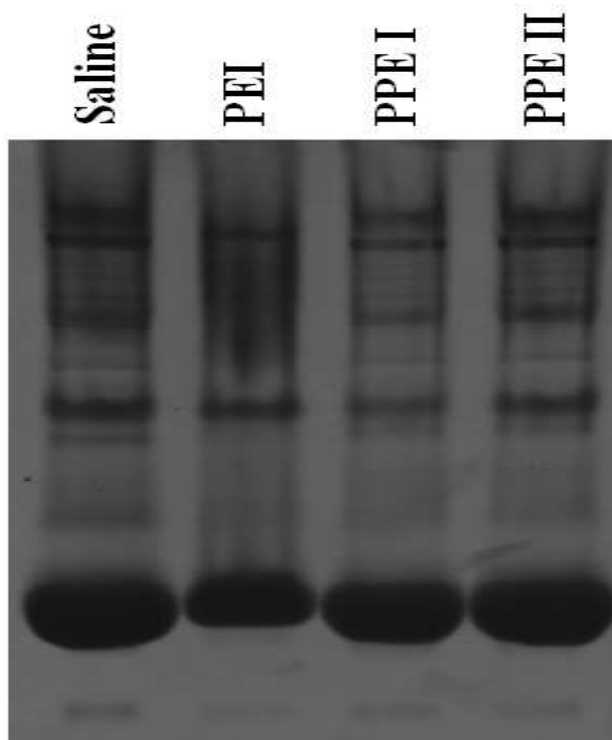
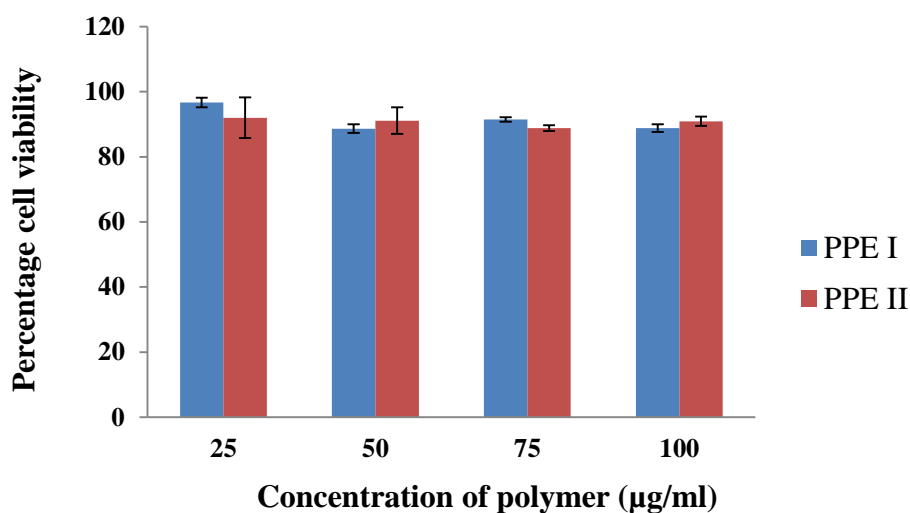


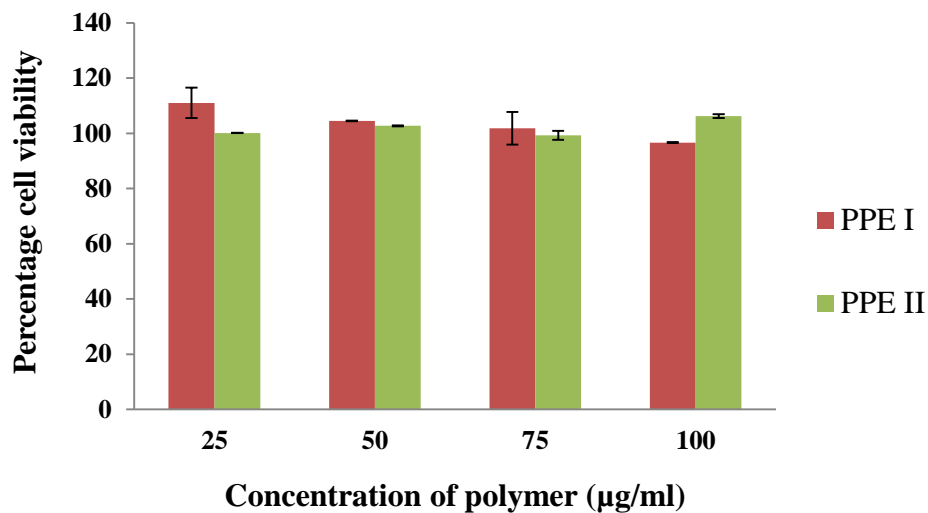
Figure 18: Plasma protein interactions of PPE derivatives was studied by performing poly acrylamide gel electrophoresis.

4.2.9 Cell viability

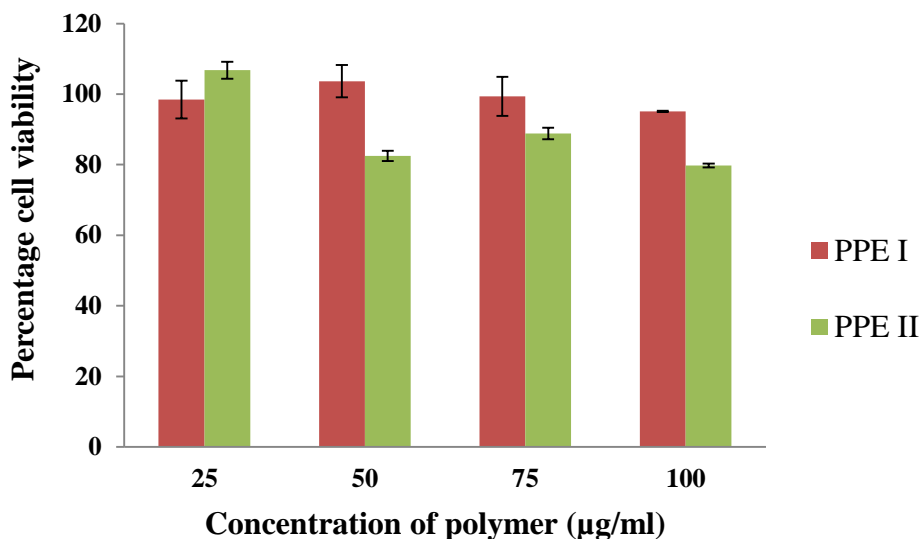
Cytocompatibility of EGDMA derivatives was studied in three different cell lines (C6, HeLa and L929) by performing MTT assay. For this analysis, cells were grown overnight and were incubated with EGDMA derivatives at four different polymer concentrations (25, 50, 75 and 100 $\mu\text{g/ml}$). After 24 h of incubation, percentage Cell viability of these cells was calculated relative to the control cells (without any treatment). EGDMA derivatives exhibit about 80% cell viability in all these cell lines even at the higher polymer concentrations (Figure 19). Percentage cell viability was also evaluated for the PPE II polyplexes prepared with ctDNA at their optimised weight ratio (5:1). Nanoplexes of this polymer derivative was also found to be cytocompatible as they exhibit above 95% cell viability in all these cell lines tested.



A



B



C

Figure 19: Cytocompatibility of PPE derivatives was evaluated by MTT assay in (A) C6, (B) HeLa and (C) L929 cells.

4.2.10 Cellular uptake of polyplexes

Cellular internalisation is one of the rate limiting steps in gene delivery as it determines the transfection efficiency of the vector. Cellular uptake of EGDMA derivatives was analysed in cancer cell lines (C6 glioma and HeLa) by preparing

polyplexes with YOYO I tagged ctDNA at 5:1 weight ratio. Polyplexes of EGDMA derivatives exhibited good cellular internalisation in C6 cells (figure 20). Here, the ctDNA get into the nucleus which is evidenced by the appearance of green fluorescence in this compartment. But in HeLa cells, poor cellular internalisation observed for the nanoplexes prepared with these polymer derivatives.

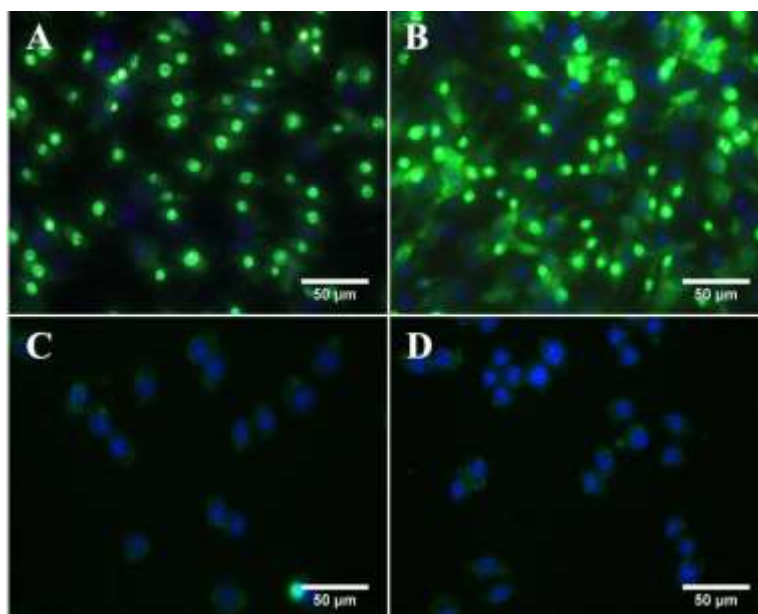


Figure 20: Cellular uptake of PPE polyplexes prepared at 5:1 ratio with YOYO I tagged ctDNA that emits green fluorescence. Cells nuclei were stained with Hoechst that emits blue fluorescence. (A) and (B) are C6 cells transfected with polyplexes of PPE I and PPE II while (C) and (D) are that in HeLa cells respectively.

4.2.11 Gene Transfection

Transfection efficiency of EGDMA derivatives was analysed in HeLa and C6 glioma cell lines by using p53 plasmid. Expression of the p53 gene induces apoptosis in the cancer cells. So the cell death that occurs in the cells transfected with polyplexes prepared with p53 plasmid signifies the transfection efficiency of these polymer derivatives. In this study, Live Dead Assay kit containing Calcein AM and EtBr was

used to differentially stain live and dead cells. The assay principle is based on the difference in the morphology and physiology of the live and dead cells. Live cell contains intracellular esterase enzymes that cleave acetoxy methyl ester linkage present in the calcein AM and produces hydrophilic calcein that emits green fluorescence. On the other hand, in dead cells, the loss of membrane integrity allows the entry of EtBr within the cell which binds with DNA to produce red fluorescence. Figure 21 shows that EGDMA derivatives exhibit good transfection efficiency in C6 cells while they fail to transfect HeLa cells. The transfection efficiency of EGDMA derivatives was also quantified in C6 cells by carrying out flow cytometry analysis and was found to be 65.56% for PPE I and 72.53% for PPE II (figure 22) which further coincides with fluorescence microscopic data.

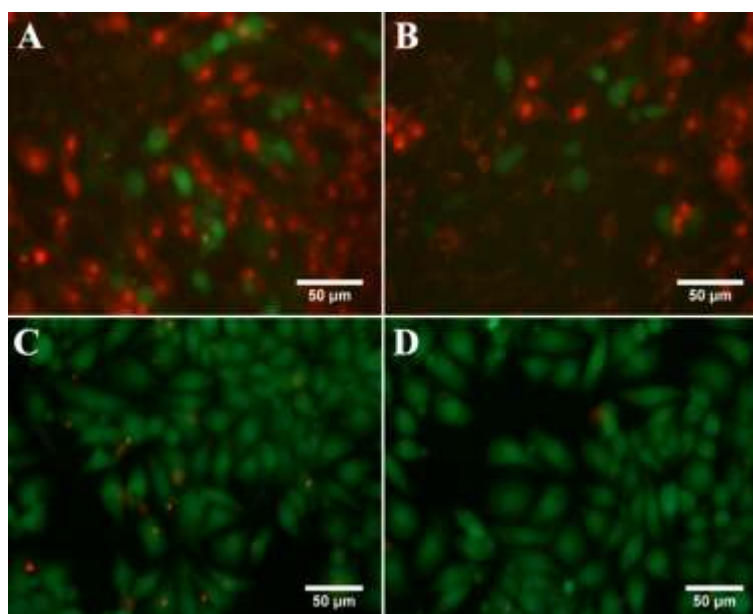


Figure 21: Transfection efficiency of EGDMA derivatives were assessed by using p53 plasmid whose expression induces apoptosis in cancer cells. (A) and (B) are C6 cells while (C) and (D) are HeLa cells transfected with polyplexes of PPE I and PPE II respectively.

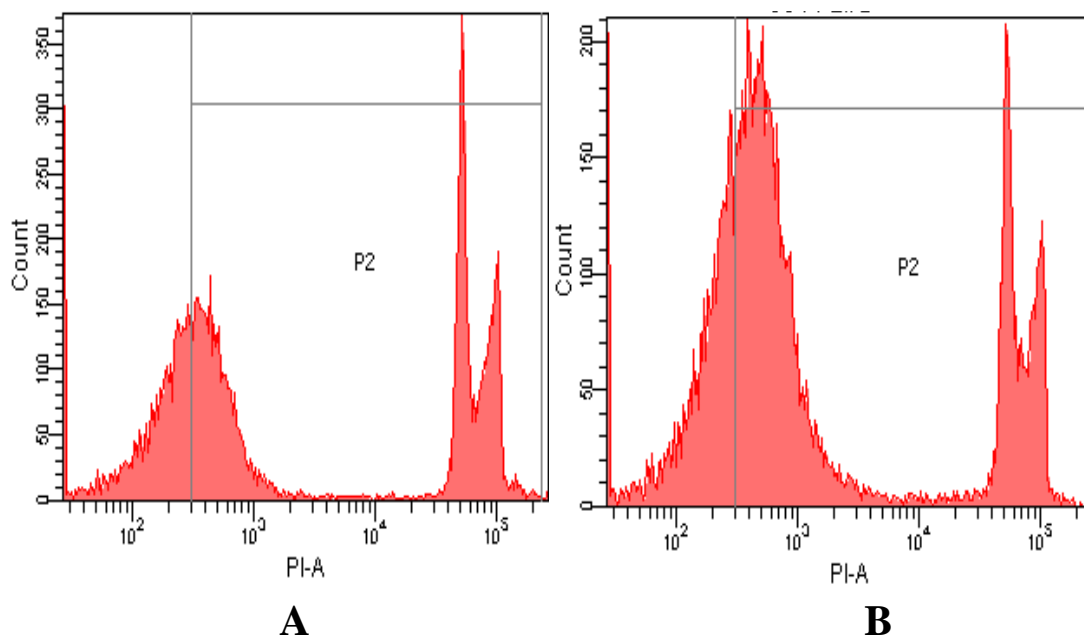
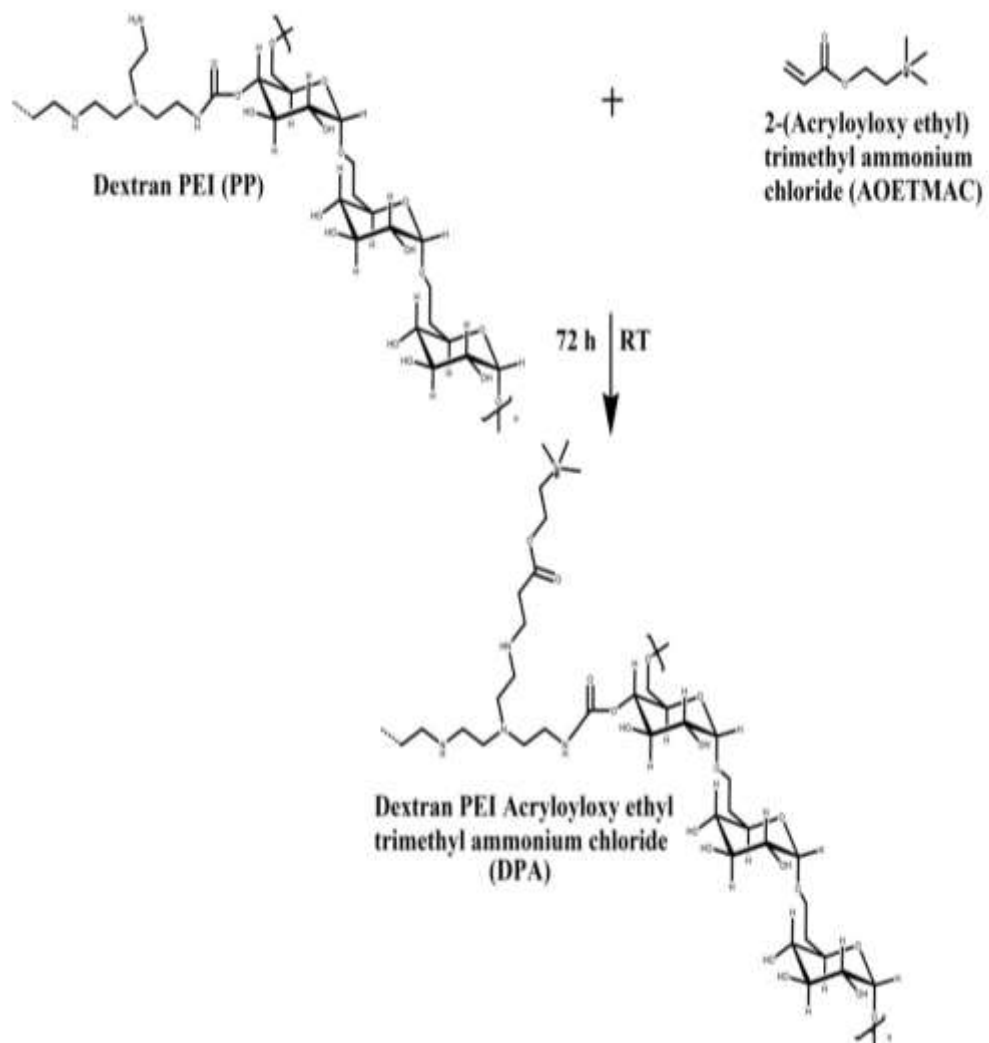


Figure 22: Flow cytometric quantification of cell death that occurred in C6 cells after transfecting with polyplexes of PPE I (A), PPE II (B) that prepared with p53 plasmid at the weight ratio 5:1. Dead cells were stained with propidium iodide.

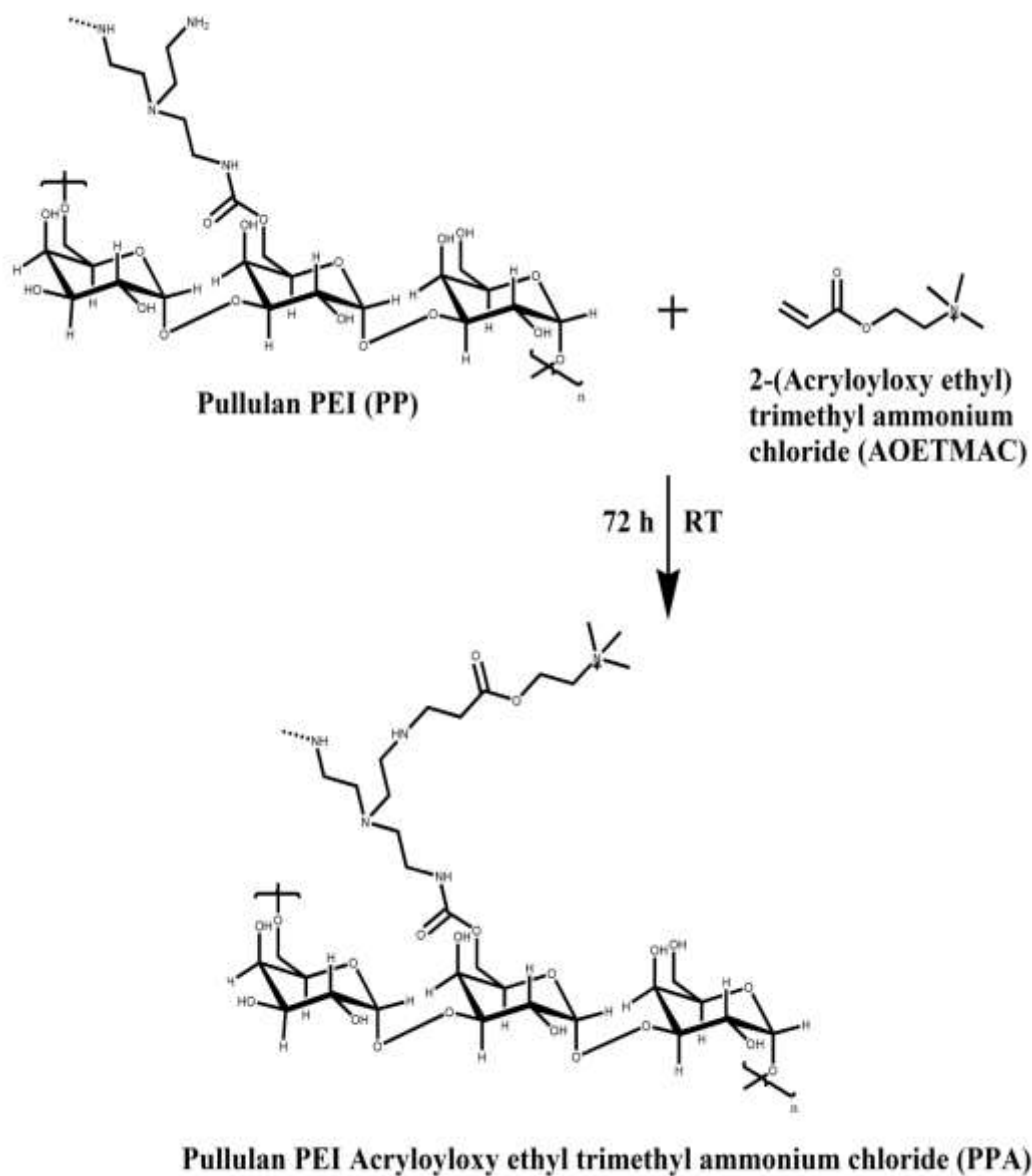
4.3 Synthesis and characterisation of [2-(Acryloyloxy) ethyl] trimethylammonium chloride (AOETMAC) grafted cationised polysaccharides

4.3.1 Synthesis

Introduction of AOETMAC moieties as pendent group in the polymeric chain of CPs can improve their blood circulation time by preventing unwanted interactions with plasma proteins. The monomer units were grafted to each of these CPs i.e. DP and PP via Michael addition reaction at three different weight ratios namely 0.01:10, 0.015:10 and 0.0025:10 to synthesis six different derivatives which were coded as DPA I, DPA II, DPA III, PPA I, PPA II and PPA III respectively. Scheme 3 depicts the reaction mechanism of the synthesis of AOETMAC derivatives.



A



B

Scheme 3: Schematic representation of the synthesis of AOETMAC derivatives by Michael addition reaction - (A) Dextran PEI acryloyloxy ethyl trimethyl ammonium chloride (DPA), (B) Pullulan PEI acryloyloxy ethyl trimethyl ammonium chloride (PPA).

4.3.2 Fourier transform infrared spectroscopy (FTIR)

FTIR bands corresponding to carbonyl stretch (1740 cm^{-1}) and quarternary amino groups (948 cm^{-1}) that are present in the AOETMAC molecules overlaps with the functional groups (carbonyl group present in the carbamate linkage and -OH bending vibrations) present in the parent chains (DP and PP). Hence, in the FTIR spectra (figure 23) of AOETMAC derivatives, no new bands appeared corresponding to the grafting of this monomer units.

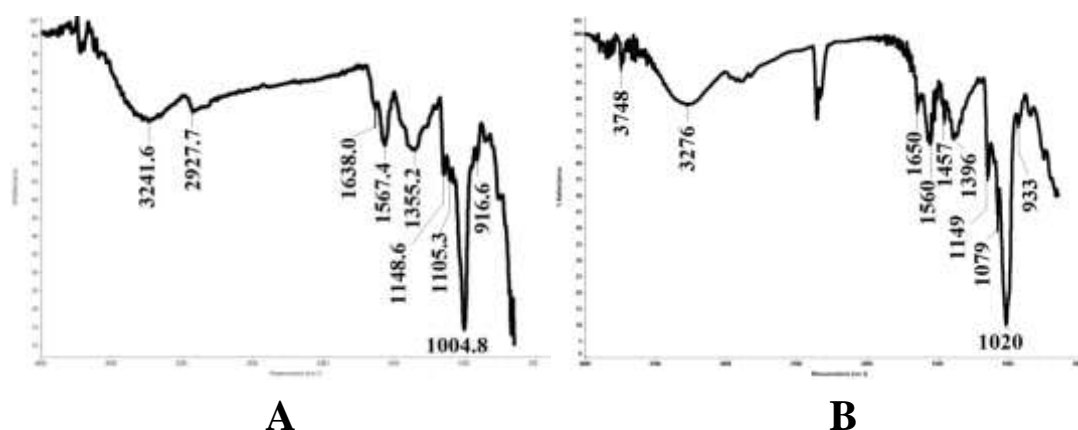
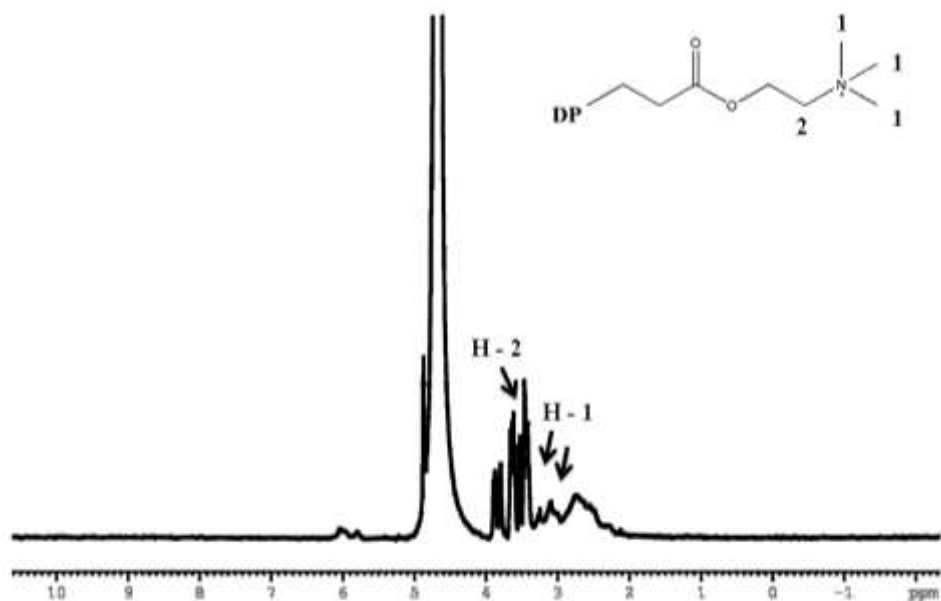


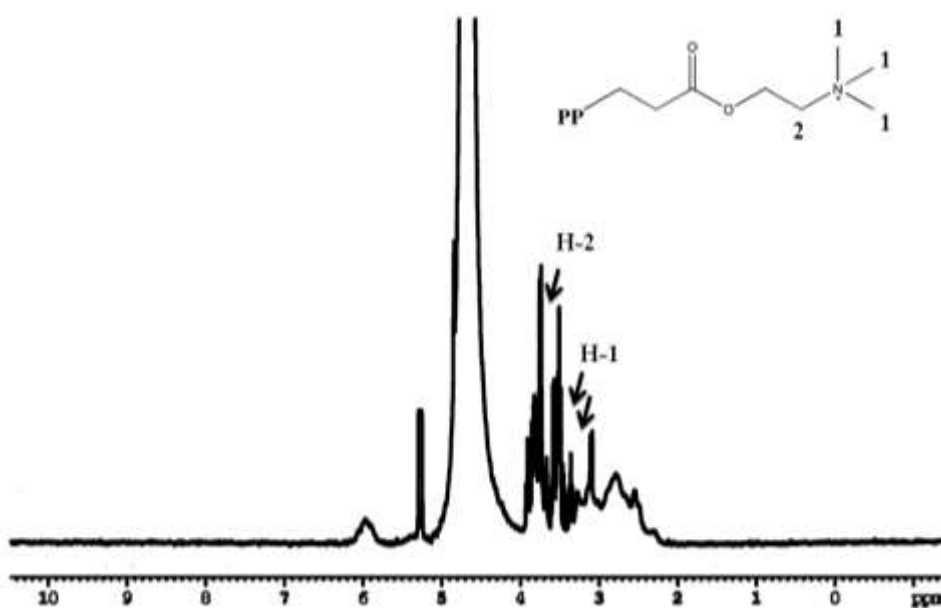
Figure 23: FTIR spectrum of AOETMAC derivatives (A) DPA (B) PPA.

4.3.3 Proton nuclear magnetic spectroscopy (^1H NMR)

Grafting of AOETMAC monomers in polymeric chains of CPs were established by proton NMR spectra. In figure 24, in addition to the peaks attributed by the parent chains (PP and DP), the appearance of peaks specific to AOETMAC confirms its grafting to these CPs. In the NMR spectra of DPA and PPA, the shift around 3.2 to 3.3ppm corresponds to the protons of methyl groups that present in $\text{-N}^+(\text{CH}_3)_3$ while that around 3.52 is ascribed to the protons present in the methylene group attached to the quaternary ammonium group in AOETMAC.



A



B

Figure 24: ^1H NMR spectra of AOETMAC derivatives- (A) DPA (B) PPA

4.3.4 Copper sulphate assay

AOETMAC moieties are grafted to CPs via nucleophilic addition reaction that occurs in the primary amino group of CPs. Their grafting reduces percentage amino

groups present in the CPs. So by comparing the amino groups present in the parent chain with that in the grafted polymer, grafting density of AOETMAC in each of these polymer derivatives can be calculated. Amino groups present in the grafted polymers were colorimetrically estimated by copper sulphate assay and the results are tabulated in table 1.

Polymer	Initial monomer feed amount (μL)	Percentage reduction in amino group
DPA I	200	4.17 ± 0.78
DPA II	300	5.29 ± 0.6
DPA III	50	3.18 ± 0.34
PPA I	200	4.66 ± 0.46
PPA II	300	5.05 ± 0.76
PPA III	50	1.23 ± 0.55

Table 1: Percentage reduction in amino groups present in the CPs after AOETMAC grafting.

4.3.5 Buffering Capacity

Escape from the endosomal compartment is one of the critical factors that determine the gene delivery by cationic polymers. Endosomal release of polyplexes formed using cationic polymers is proposed to be mediated by the proton sponge effect. The buffering abilities of these polymeric vectors over the pH range 5-7 induce the swelling and rupture of endosomes thereby releasing the nucleotide cargo into the cytosol. So in order to elucidate the buffering capacity of AOETMAC derivatives,

acid – base titration was carried out over the pH range 10 to 4. From figure 25, it was clear that all the AOETMAC derivatives exhibit good buffering capacity over the pH 10-7 and not in the endosomal pH range. Among these six AOETMAC derivatives, PPA III exhibits the highest buffering capacity which was followed by DPA derivatives. Between PPA I and PPA II, the later shows better buffer capacity.

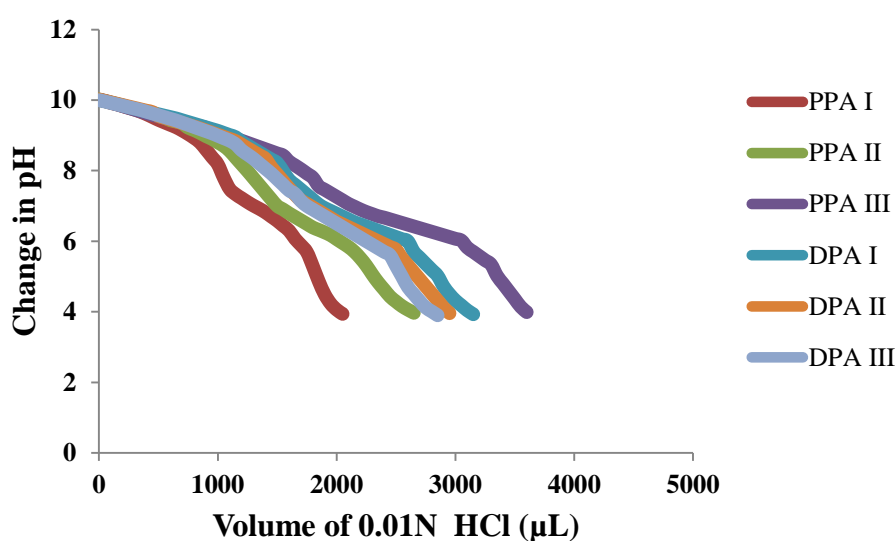
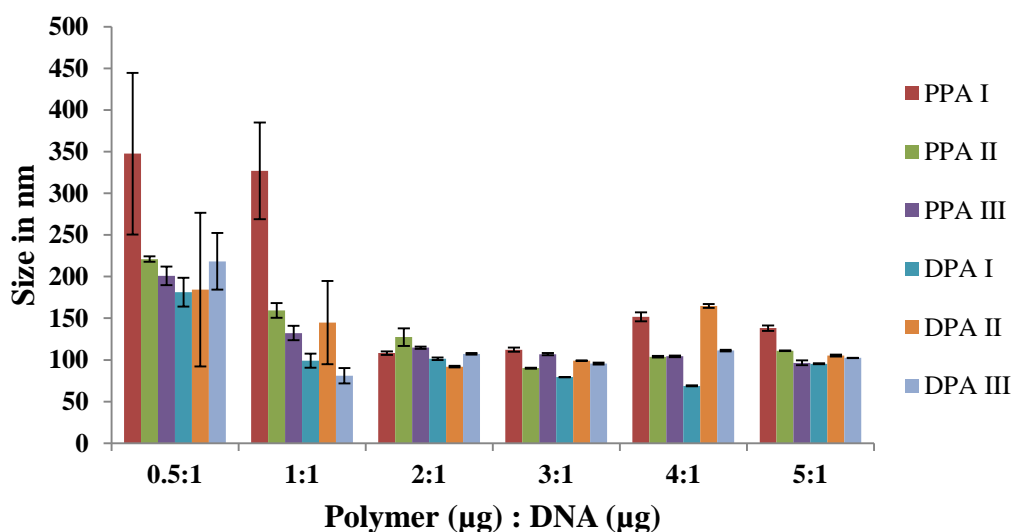


Figure 25: Buffering capacities of AOETMAC derivatives of CPs over the pH range 10-4 by acid-base titration

4.3.6 Size and zeta potential

Cationic polymers condense negatively charged DNA through electrostatic interactions into nano sized complexes called polyplexes. The size and zeta potential of these nanoplexes are very important as it determines their half life in blood circulation and also the cellular entry. To analyse size and zeta potential, polyplexes of AOETMAC derivatives were prepared with ctDNA at six different weight ratios (0.5:1 to 5:1). Hydrodynamic size of these nanoplexes were analysed by performing dynamic light scattering experiments. As from figure 26.A no specific trend appear

in the size distribution of these AOETMAC derivatives except PPA III. Hydrodynamic size of nanoplexes of PPA III derivative found to be decrease with the increase in the polymer to ctDNA weight ratio. At the 5:1 weight ratio, these derivatives form nanoplexes having size below 140nm range and PDI values lies between 0.05 and 0.2.



A

Figure 26(A): Hydrodynamic size of nanoplexes of AOETMAC derivatives prepared with ctDNA at different weight ratios.

The nanoplexes which enters into the cell through non specific endocytosis mediated pathway requires a positive zeta potential in order to interact with anionic plasma membrane and to get internalised. Figure 26.B shows that PPA I and PPA II exhibit negative zeta potential at lower weight ratios and turns to be slightly positive at the weight ratio 4:1 which further increases at the weight ratio 5:1. Unlike PPA I and PPA II, nanoplexes of PPA III derivatives exhibit positive zeta potential at the weight ratio 2:1 and found to increase with the increase in the weight ratio. Zeta

potential of AOETMAC derivatives of DP (except DPA II) found to be negative even at the weight ratio 5:1.

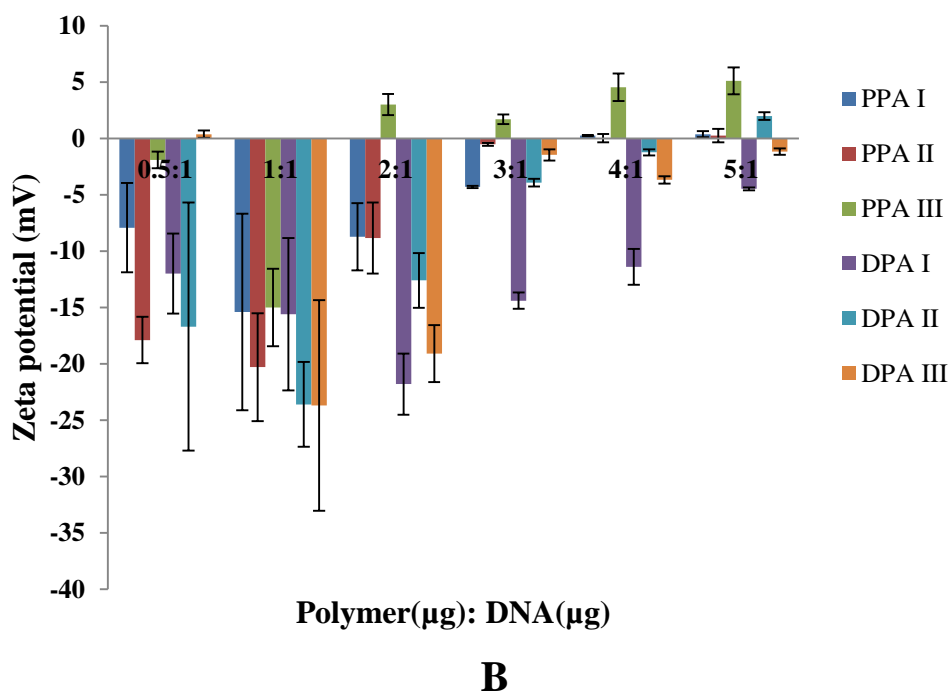


Figure 26(B): Zeta potential measurements of AOETMAC derivatives nanoplexes prepared with ctDNA.

4.3.7 DNA binding ability and effect of plasma on nanoplex stability

The binding strength of AOETMAC and ctDNA was analysed by carrying out agarose gel electrophoresis. Nucleic acids owing to their anionic nature move towards the anode under the application of an external electric field. Strong association between cationic polymer and ctDNA hinders the movement of latter under the electric field. To assess the stability of nanoplexes formed by AOETMAC derivatives with ctDNA, nanoplexes were prepared at six different ratios and loaded onto 1% agarose gel. As seen in figure 27, all the AOETMAC derivatives except

PPA III form loose complexes with ctDNA even at higher weight ratio. It was evidenced by the appearance of DNA smears in these lanes. PPA III form tight complexes with ctDNA and it retard the mobility of ctDNA even at the weight ratio 2:1. Stability of AOETMAC nanoplexes was also evaluated in the presence of plasma protein and similar results were observed as that of nanoplex alone (figure 28).

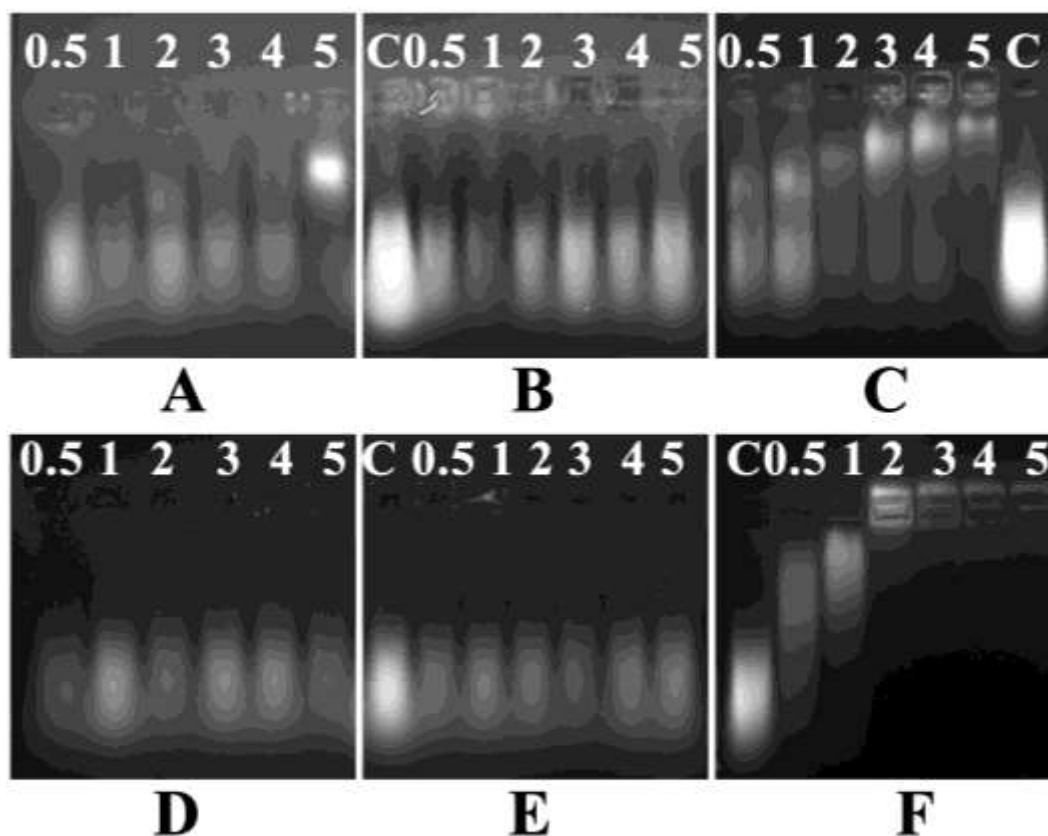


Figure 27: Nanoplex stability of AOETMAC derivatives assessed by agarose gel electrophoresis. (A), (B), (C), (D), (E), (F) are stability of nanoplexes formed by DPA I, DPA II, DPA III, PPA I, PPA II and PPA III respectively. Lanes 0.5 to 5 are nanoplexes of AOETMAC derivatives prepared with ctDNA at different weight ratios. Lane C is the naked ctDNA.

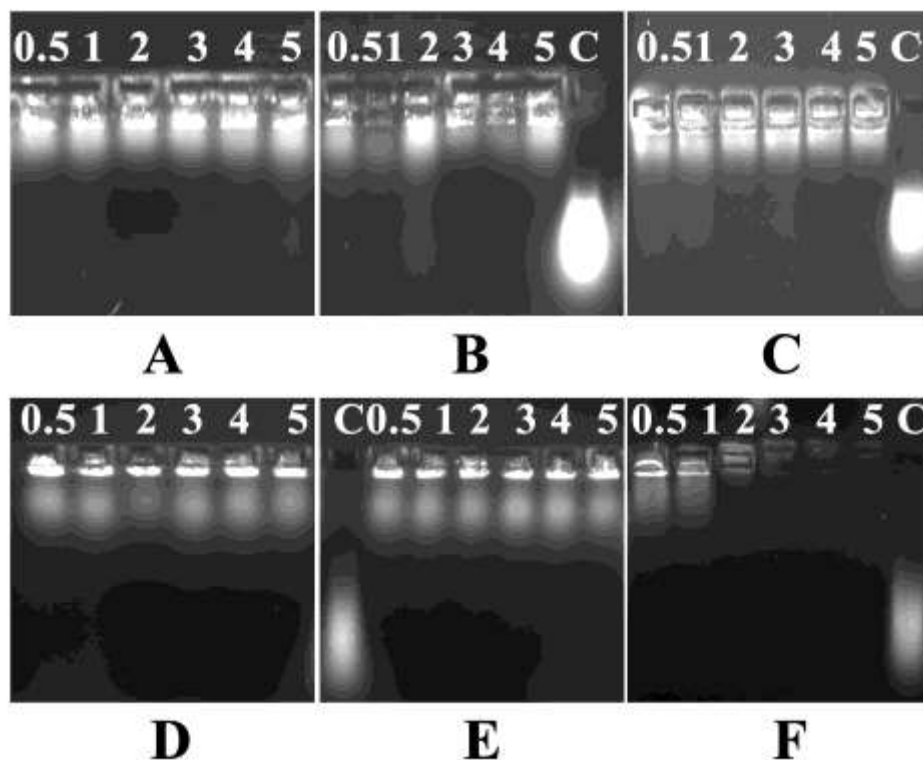


Figure 28: Nanoplex stability of AOETMAC derivatives assessed in the presence of plasma proteins by agarose gel electrophoresis. (A), (B), (C), (D), (E), (F) are stability of nanoplexes formed by DPA I, DPA II, DPA III, PPA I, PPA II and PPA III respectively. Lanes 0.5 to 5 are nanoplexes of AOETMAC derivatives prepared with ctDNA at different weight ratios. Lane C is the ctDNA alone.

4.3.8 Polymer interactions with plasma proteins

Half life of cationic polymers in the systemic circulation depends on their interactions with plasma proteins. The nature of interaction of AOETMAC derivatives with plasma proteins were studied by performing polyacrylamide gel electrophoresis. For this analysis, plasma treated cationic polymers was loaded onto a 4% stacking gel which was then resolved by 7% gel. Plasma treated with PEI and saline act as positive and negative controls respectively. From figure 29, it was clear that all the six AOETMAC derivatives show minimal interactions with plasma proteins as most of the bands showed similar intensity as that of negative control

saline. As expected, PEI exhibited strong interactions with human plasma as most of the protein bands are missing in this lane.

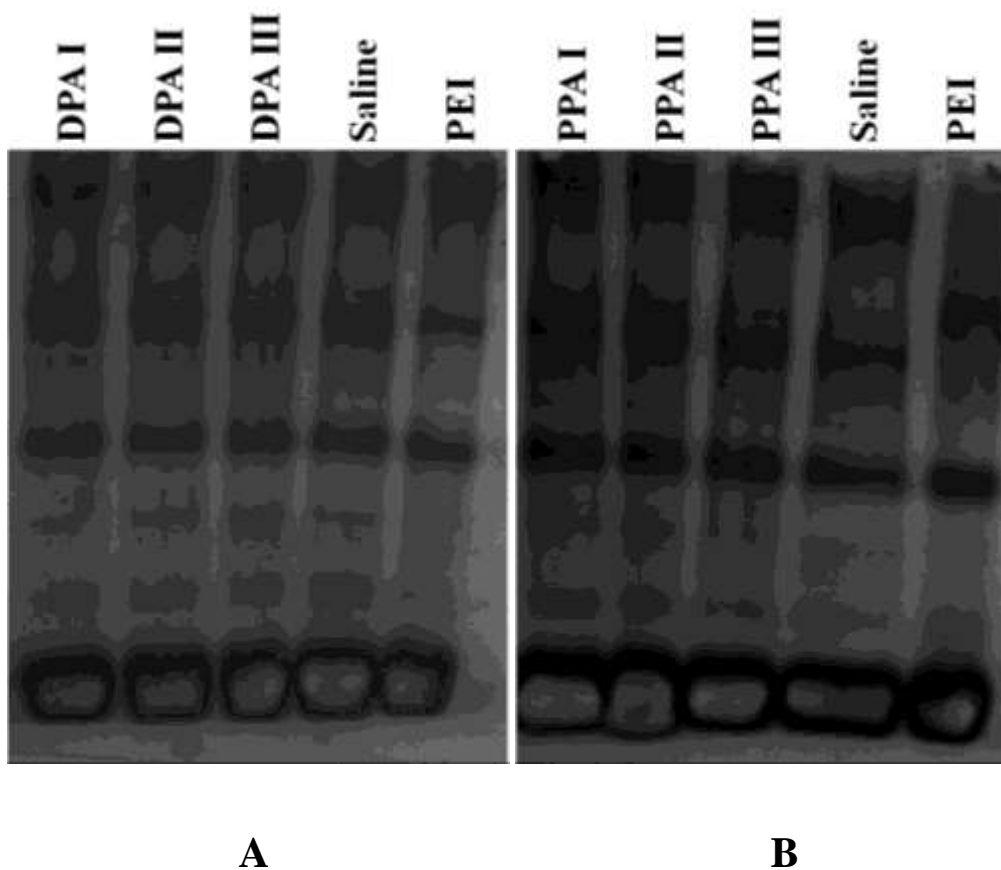
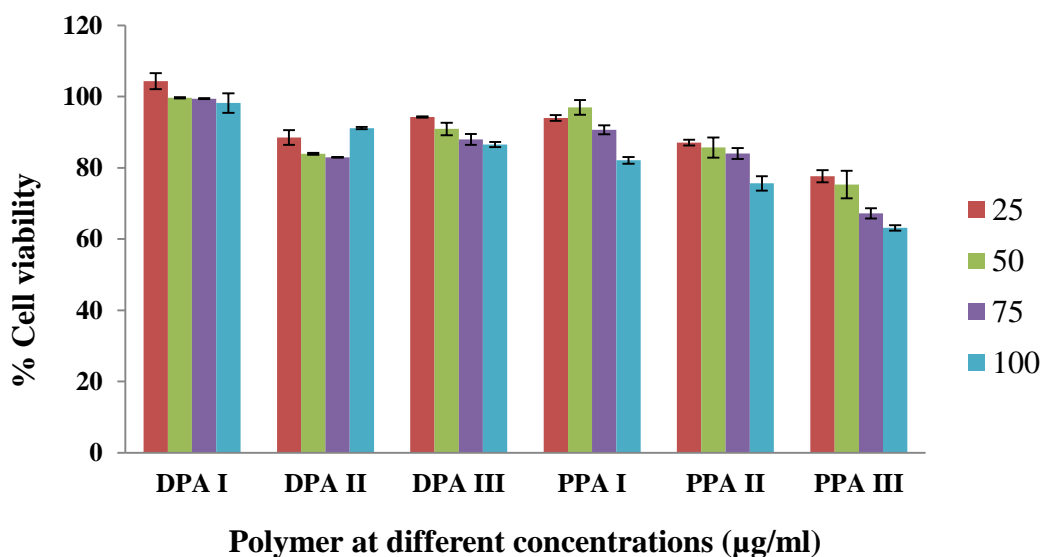


Figure 29: Interactions of AOETMAC derivatives with plasma proteins studied by performing polyacrylamide gel electrophoresis. Saline with plasma protein is taken as negative control while PEI that shows strong interactions with plasma proteins is taken as positive control.

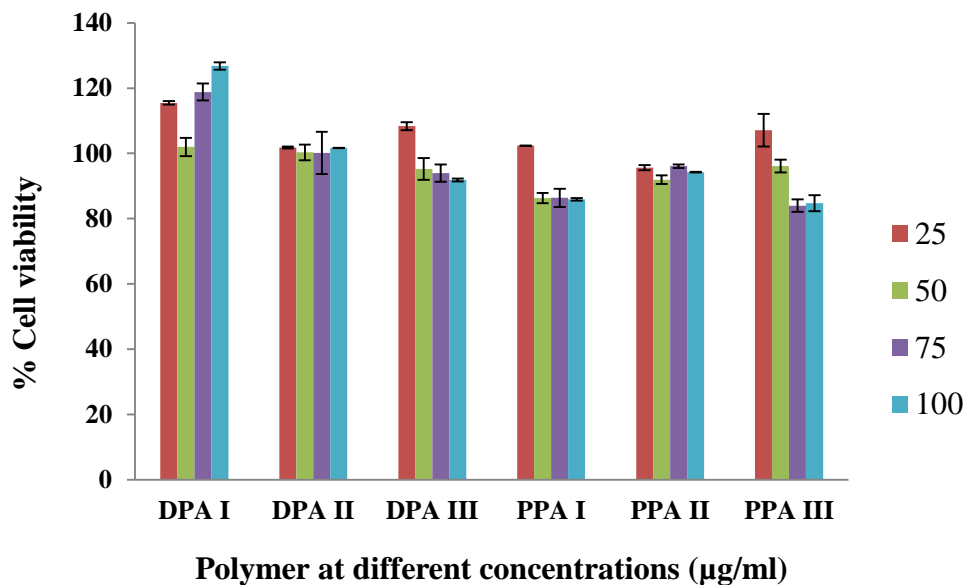
4.3.9 Cell viability

Cytotoxicity is one of the major drawbacks that hinder the application of cationic polymers as gene delivery vectors. Hence in this study, cytocompatibility of AOETMAC derivatives was evaluated in two different cancer cell lines – C6 and HeLa using MTT assay. Cytocompatibility of DPA I and PPA I was also evaluated in

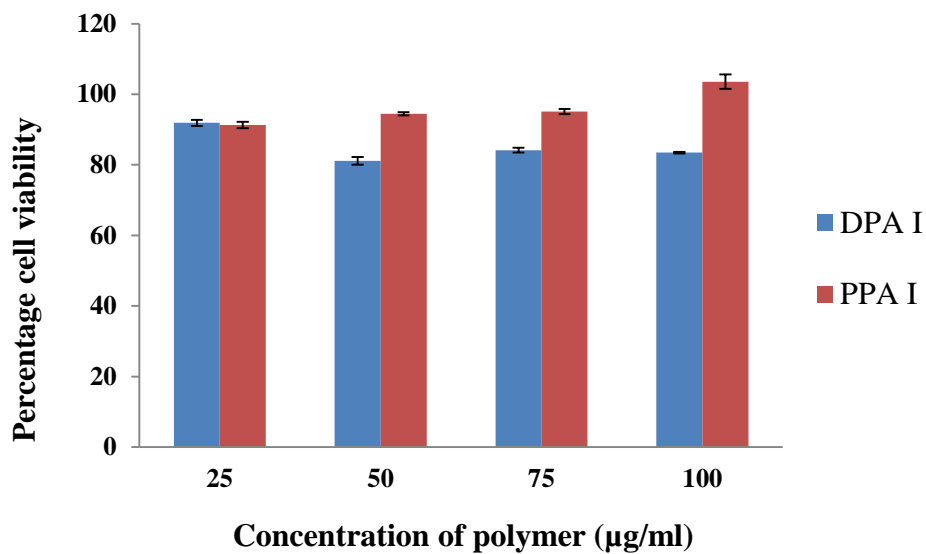
L929 cells as the representatives of AOETMAC derivatives. The nanoplexes of these derivatives prepared with ctDNA were also evaluated for cytocompatibility in all these three cell lines. Overnight grown cultures of these cell lines were treated either with these polymer derivatives at four different polymer concentrations (25, 50, 75 and 100 µg/ml) or with their polyplexes prepared at their optimised weight ratio (5:1) with ctDNA. All the AOETMAC derivatives except PPA III exhibit above 75% cell viability in C6 while the later found to be toxic at higher polymer concentrations (figure 30). In HeLa cells, all these polymer derivatives including PPA III exhibit above 80% cell viability. DPA I and PPA I exhibit above 80% and 90% cell viability in L929 cells even at higher polymer concentrations. Nanoplexes of DPA I and PPA I derivatives exhibit above 90% cell viability in all these cell lines tested.



A



B



C

Figure 30: Cytocompatibility of AOETMAC derivatives in three different cell lines- (A) C6 (B) HeLa (C) L929 at four different polymer concentrations i.e. 25, 50, 75 and 100 µg/ml.

4.3.10 Cellular uptake of polyplexes

Cellular uptake of nanoplexes determines the transfection efficiency of polymeric vector since the expression of foreign gene in the host cell depends on the number of particles that get internalised. Furthermore, the cellular uptake mechanism may also determine the intracellular trafficking and the final fate of these vectors. In this study, cellular uptake of AOETMAC derivatives were studied in C6 and HeLa cells by preparing nanoplexes with fluorescently tagged ctDNA at their optimised weight ratio (5:1). Figure 31 and 32 shows that nanoplexes of these derivatives express good cellular internalisation in C6 cells while poor cellular uptake was observed for HeLa cells (except PPA III).

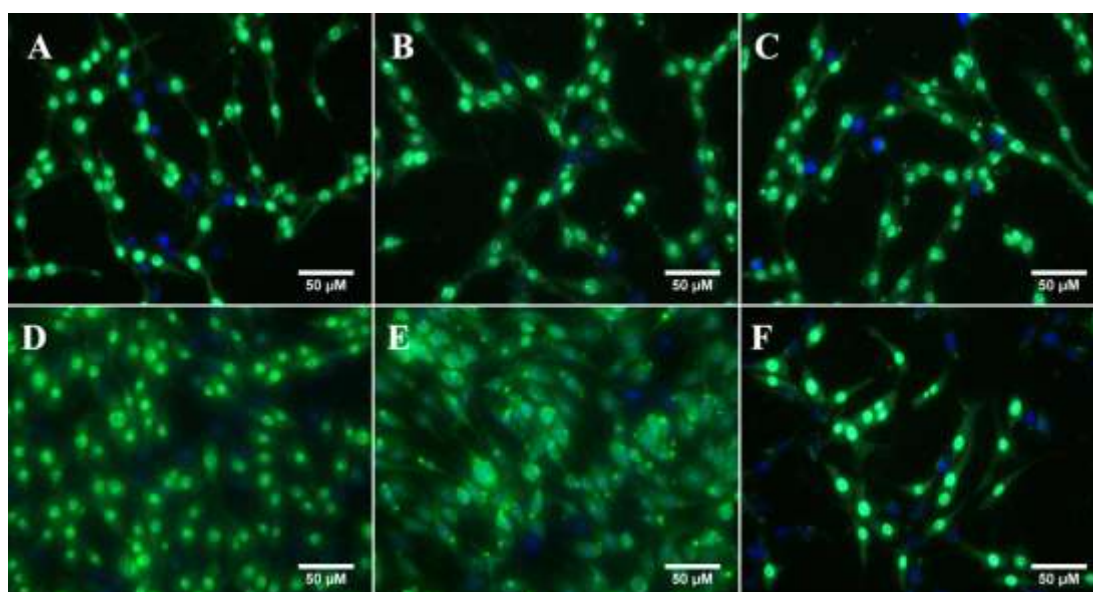


Figure 31: Cellular uptake of nanoplexes of AOETMAC derivatives prepared with YOYO I tagged ctDNA (green fluorescence) at the optimised weight ratio i.e. 5:1 in C6 cells. Nuclei of these cells were stained with Hoechst (blue fluorescence). A, B, C, D, E, F are the cells transfected with nanoplexes of DPA I, DPA II, DPA III, PPA I, PPA II and PPA III respectively.

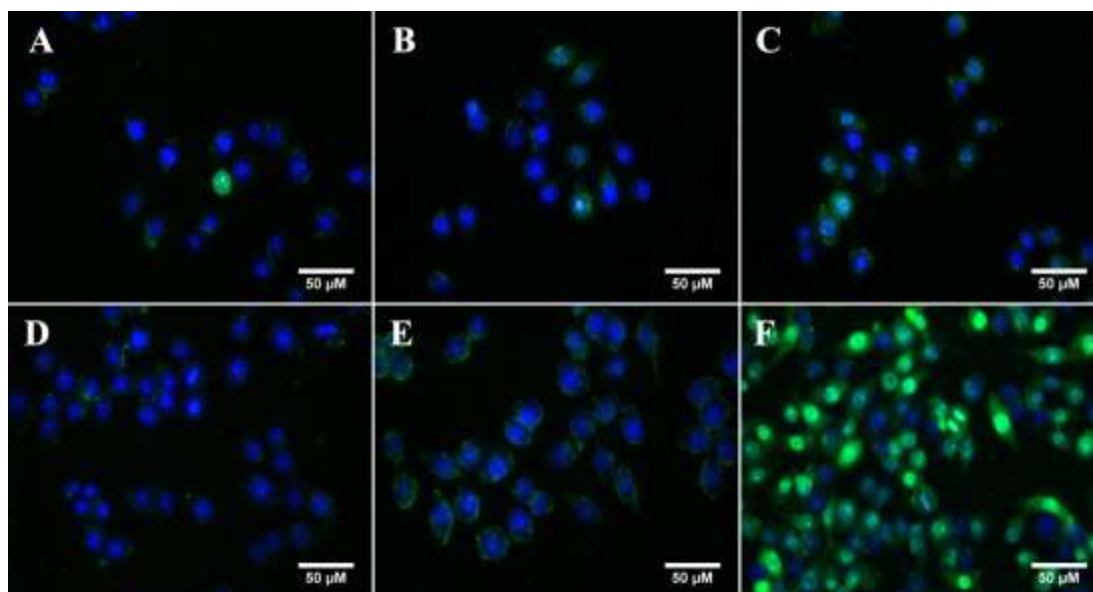


Figure 32: Cellular uptake of AOETMAC derivatives in HeLa cells. Polyplexes were prepared with YOYO I tagged ctDNA (green fluorescence) at the weight ratio, 5:1. Nuclei of these cells were stained with Hoechst (blue fluorescence). A, B, C, D, E, F are the cells transfected with nanoplexes of DPA I, DPA II, DPA III, PPA I, PPA II and PPA III respectively.

4.3.11 Gene transfection

Transfection efficiency of AOETMAC derivatives was evaluated in C6 cells using p53 plasmid. Expression of this plasmid DNA is expected to induce apoptosis in transfected cells. However, these polymeric vectors exhibit poor transfection efficiency in C6 cells and most of the transfected cells remain alive. The representative image was shown in the figure 33.

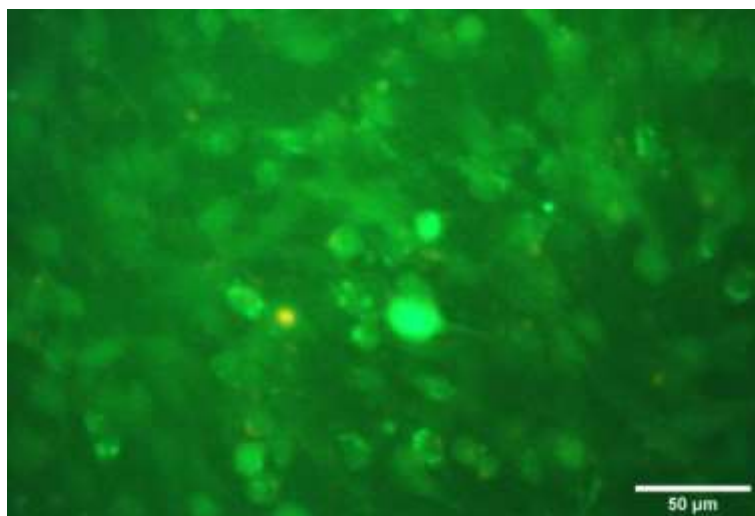


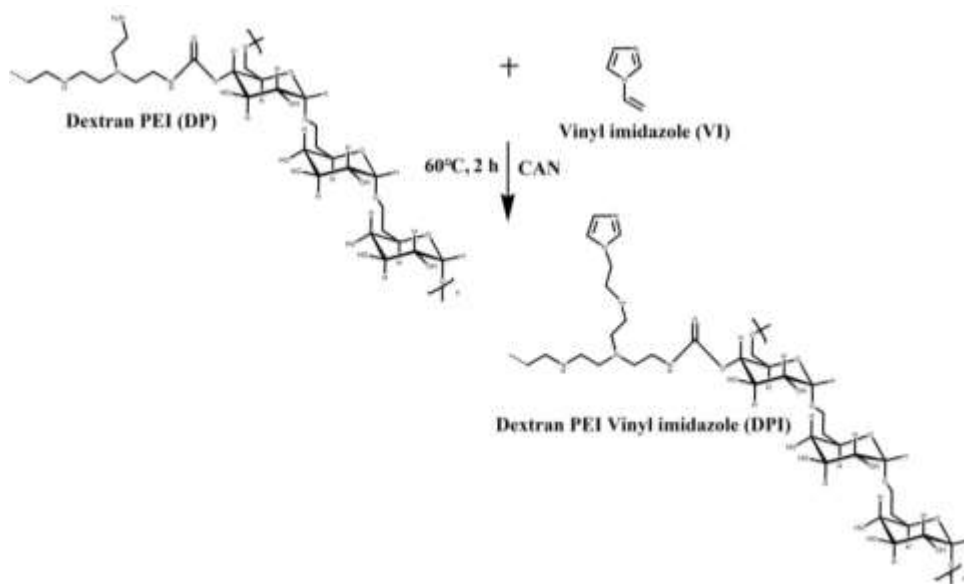
Figure 33: Live dead assay in C6 cells transfected with polyplexes of PPA II prepared with p53 plasmid at the weight ratio 5:1.

4.4 Synthesis and characterisation of vinyl imidazole grafted cationised polysaccharides

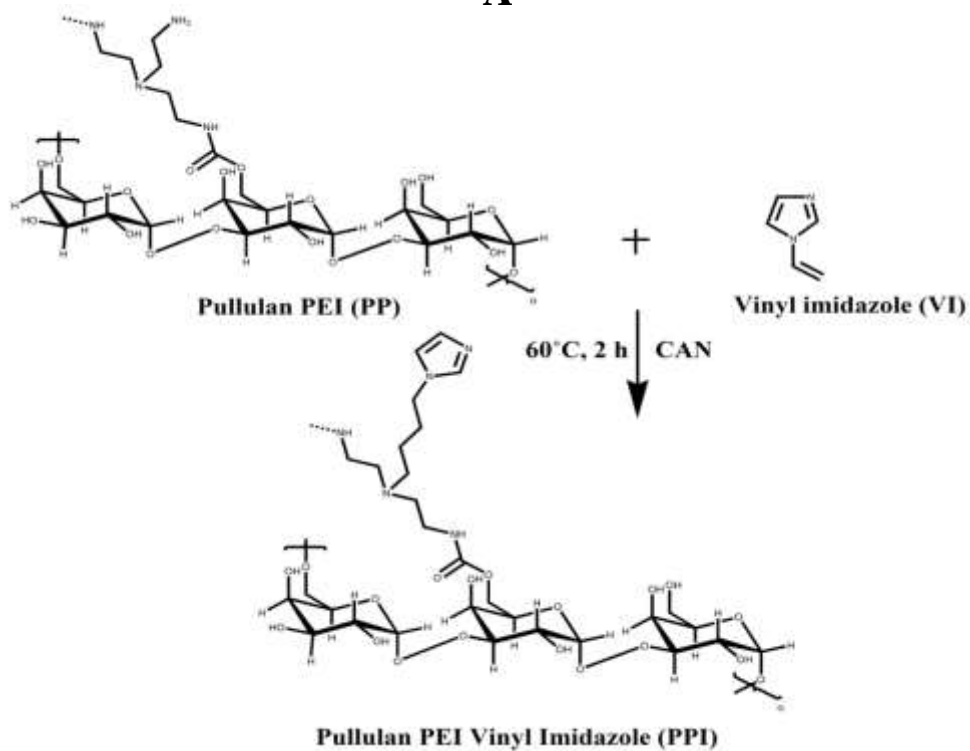
4.4.1 Synthesis

Cationic polymers were modified with imidazole moieties in order to improve the endosomal escape and also to improve their cytocompatibility. Moreover, these moieties also help in vector unpacking as their pKa is around 6, they show weak interactions with DNA at the physiological pH due to the negligible charge. In this study, DP and PP are modified with VI at three different weight ratios viz 10:0.005, 10:0.01, 10:0.02 and synthesised six different polymer derivatives namely DPI I, DPI II, DPI III, PPI I, PPI II and PPI III respectively. The reaction mechanism is depicted in the scheme 4 in which VI is grafted to cationic polymers through free radical addition reaction using CAN as the initiator. The grafted polymer was then

purified by acetone precipitation which was followed by dialysis against distilled water.



A



B

Scheme 4: Schematic representation of synthesis of (A) DPI and (B) PPI by free radical addition reaction using CAN as the initiator.

4.4.2 Fourier transform infrared spectroscopy (FTIR)

In the FTIR spectra (figure 34) of VI derivatives, the characteristic C=O stretching and N-H bending vibrations of carbamate bond that is present in the CPs got reduced to a single band by the grafting of vinyl imidazole. Moreover, the appearance of FTIR bands at 668cm^{-1} , 822cm^{-1} in PPI and 669cm^{-1} , 822cm^{-1} in DPI corresponding to the puckering vibration and out of plane bending vibration of imidazole ring respectively, further confirms the grafting of VI to these CPs (Talu *et al*, 2015; Lippert *et al*, 1985).

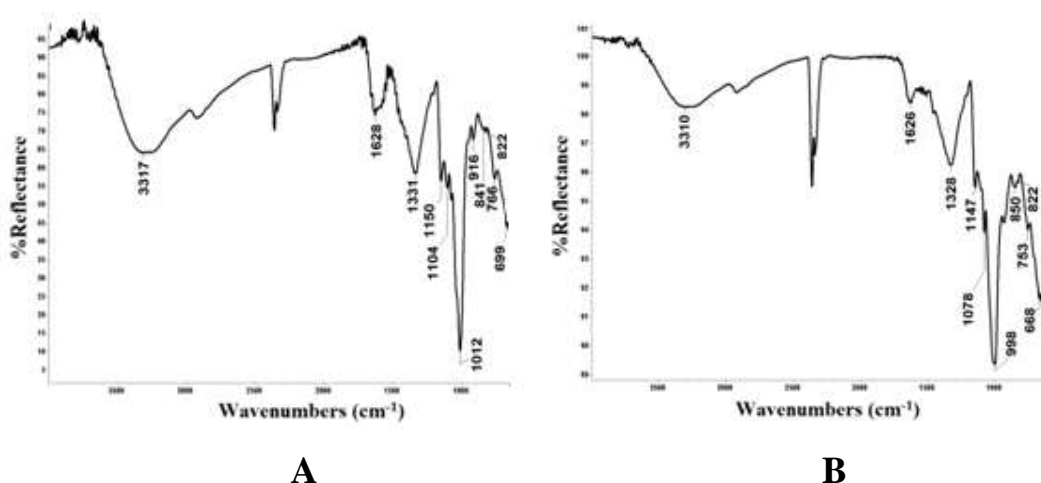


Figure 34: FTIR spectra of VI derivatives. (A) DPI (B) PPI

4.4.3 Proton nuclear magnetic resonance spectroscopy (¹H NMR)

NMR spectra further confirm the grafting of VI to these cationic polymers. In figure 35, shifts around 6-8 ppm is associated with the protons present in the imidazole ring while that around 2.5-2.8 ppm corresponds to the resonance of protons in the methylene group of PEI. Signals from the protons attached to the C2 to C6 carbons and C1 carbon of hexose units of polysaccharides were observed around the region

3.4-4.0 ppm and 4.8- 5.4 ppm respectively (Jiang & Salem, 2012a; Asayama *et al*, 2010a).

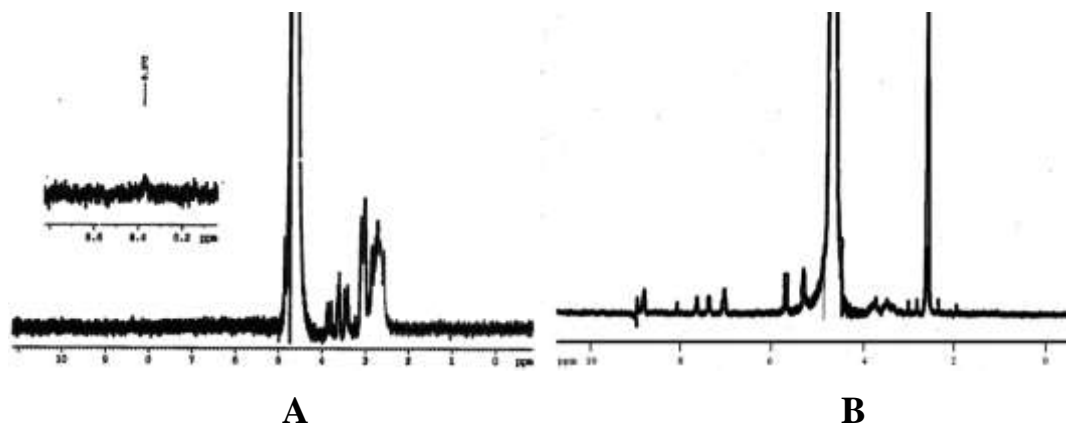


Figure 35: ^1H NMR spectrum of (A) Dextran PEI Imidazole (DPI), (B) Pullulan PEI Imidazole (PPI) in D_2O .

4.4.4 Buffering capacity

Polymeric vectors which are designed to enter the cell via the endocytotic pathway should possess buffering capacity near acidic pH, in order to release the DNA into the cytosol and also to protect it from the degradation caused by the lysosomal enzymes. As compared to the parent chain, VI derivatives exhibit lower buffering capacity. However, these derivatives resist pH change near endosomal pH i.e. around 5 to 7 range as evidenced from the data shown in figure 36. Among PPI and DPI derivatives, later exhibit good buffering capacity as compared to that of the former.

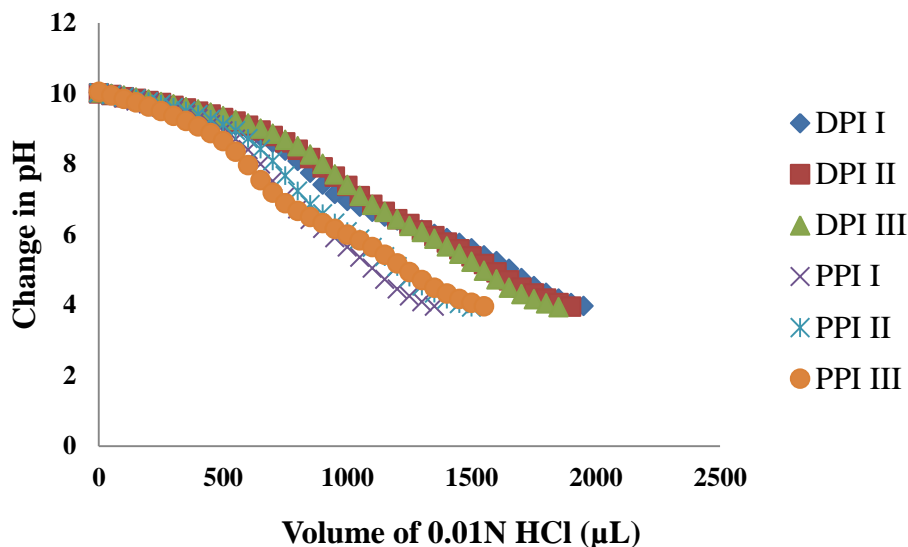
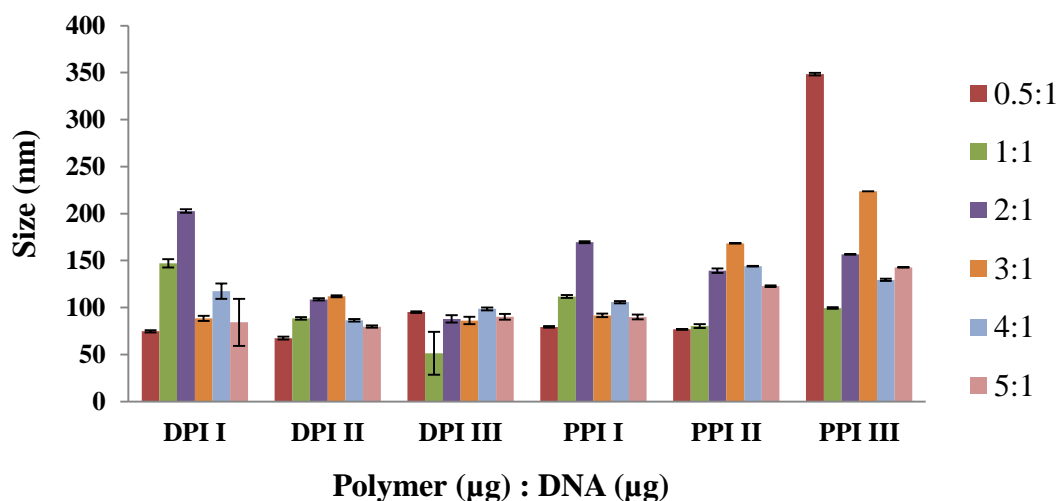


Figure 36: Buffering capacity of VI derivatives over the pH range 10-4 determined via acid-base titration by sequential addition of 0.01N HCl (50 µL).

4.4.5 Particle size and zeta potential

Particle size and zeta potential are the two major parameters that determine the fate of nanoparticles under *in vivo* conditions which are analysed via Zetasizer Nano ZS (Malvern, UK). Nanoplexes were prepared by vortexing polymers with ctDNA at 6 different weight ratios (0.5:1, 1:1, 2:1, 3:1, 4:1 and 5:1) for 30s followed by 20min incubation at room temperature. VI derivatives formed smaller sized nanoparticles of the range 70-150nm (Figure 37.A) while complexing with ctDNA. Nanoplexes prepared at the higher polymer to DNA weight ratios (i.e., from 3:1 to 5:1) exhibit narrow polydispersity index (PDI) that ranges between 0.1 to 0.3 which indicates the formation of the more homogenous population at these ratios. Smaller sized nanoparticles with narrow PDI of 0.1 to 0.2 observed at the weight ratio, 5:1 which was optimised for further studies of VI derivatives. At their optimised weight ratio,

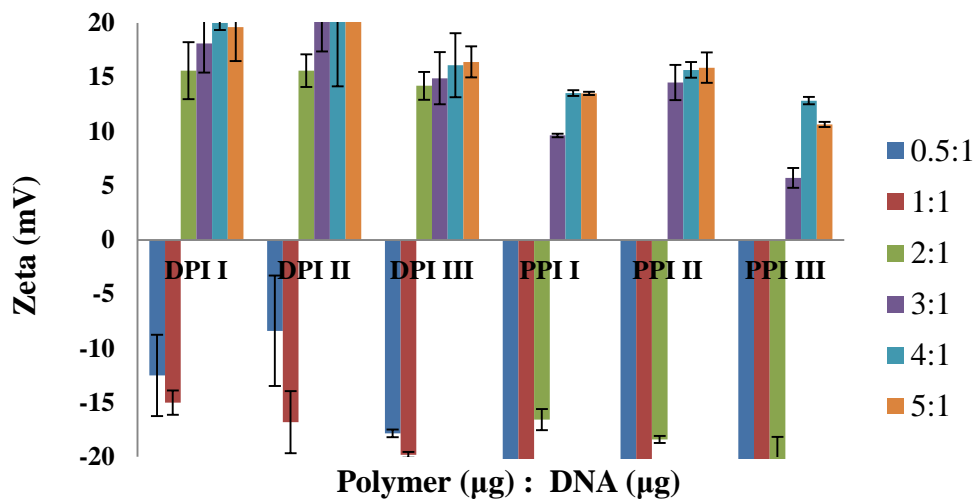
DPI II form the smallest size nanoplex with ctDNA and the order was DPI II < DPI I < PPI I < DPI III < PPI II < PPI III.



A

Figure 37(A): Hydrodynamic size of polyplexes prepared from DPI and PPI derivatives by complexing with ctDNA at six different weight ratios (0.5:1 to 5:1).

Zeta potential is another major factor that determines nanoplex size, stability, blood circulation time, intracellular trafficking as well as the toxicity of the polymer which was analysed using Zetasizer, Nano ZS. Both PPI and DPI derivatives exhibited negative zeta potential at the lower (polymer to DNA) weight ratio while it changes to positive at higher polymer concentration (Figure 37.B). On comparing the zeta potential values of nanoplexes prepared at their optimised weight ratio (i.e.5:1), DPI II exhibit higher positive zeta potential and they follow the order, DPI II > DPI I > DPI III > PPI II > PPI I > PPI III. Among DPI and PPI derivatives, the former possess higher positive zeta potential which is around 16 to 22 mV while PPI derivatives exhibit zeta potential of around 10 to 16 mV.



B

Figure 37(B): Zeta potential measurements of nanoplexes prepared by complexing VI derivatives with ctDNA at six different polymer to DNA weight ratios.

4.4.6 DNA binding ability and effect of plasma on nanoplex stability

Cationic polymers interact with ctDNA through the electrostatic interactions. The strength of these interactions is quite important as it determines the stability of these nanoplexes. Agarose gel electrophoresis was carried out in order to evaluate the nanoplex stability. From the figure 38, it was clear that VI derivatives form tight complexes with ctDNA as they retard the mobility of later under the electric field even at lower weight ratio of 1:1.

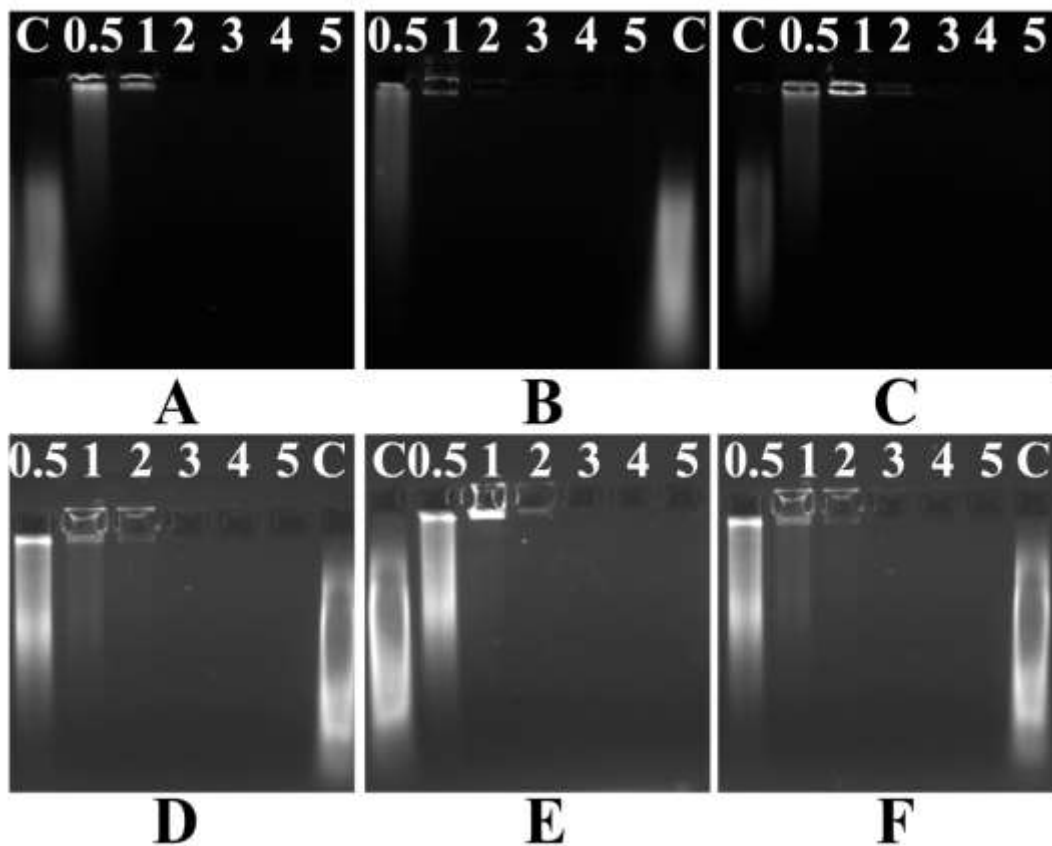


Figure 38: Nanoplex stability of VI derivatives analysed by performing agarose gel electrophoresis. Nanoplexes prepared at six different weight ratios 0.5:1, 1:1, 2:1, 3:1, 4:1, 5:1 were loaded on the lanes 0.5 to 5. Lane C was the control ctDNA. A,B,C,D, E, F were the gels loaded with the nanoplexes of DPI I, DPI II, DPI III, PPI I, PPI II and PPI III derivatives respectively.

These nanoplexes are also stable in the presence of plasma proteins as seen in figure 39 which shows similar results as that of nanoplex alone.

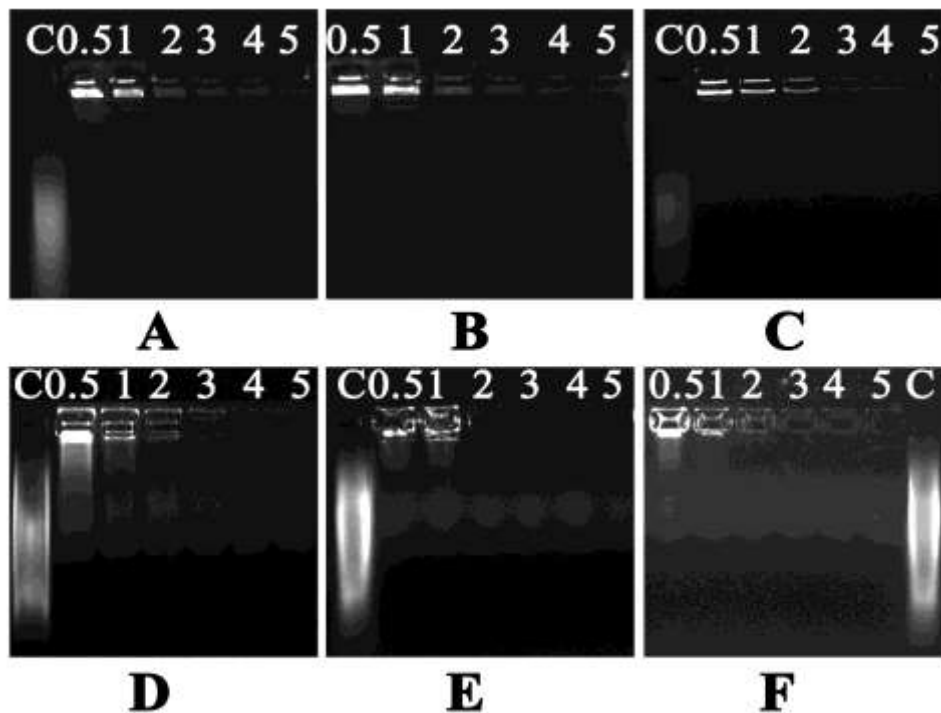


Figure 39: Stability of the nanoplexes of VI derivatives prepared with ctDNA in the presence of plasma proteins. A,B,C,D, E, F were the gels loaded with the nanoplexes of DPI I, DPI II, DPI III, PPI I, PPI II and PPI III derivatives respectively. Lane C was the control ctDNA while lanes 0.5 to 5 were loaded with nanoplexes prepared at six different weight ratios (i.e. 0.5:1, 1:1, 2:1, 3:1, 4:1, and 5:1).

4.4.7 Nanoplex stability in the presence of digestive enzyme, DNase

The success of a gene delivery vector depends on how efficiently it protects the gene of interest from the degradation caused by the nucleases present in the biological systems. For this analysis, polyplexes were incubated with DNase and then agarose gel electrophoresis was carried out in order to evaluate whether ctDNA present in the nanoplex gets degraded by the action of this enzyme. From the figure 40, it was clear that no degradation bands observed in the lanes loaded with nanoplexes prepared at higher weight ratios (3:1, 4:1 and 5:1). However, thin DNA smear appeared in the lanes that were loaded with nanoplexes prepared at lower ratios. The naked DNA

treated with DNase enzyme show extensive degradation. In order to counter check the integrity of protected DNA by these VI derivatives, heparin was added to the polyplex solution and once again agarose gel electrophoresis was performed. From the figure 41, it is obvious that the DNA remains intact within these polyplexes.

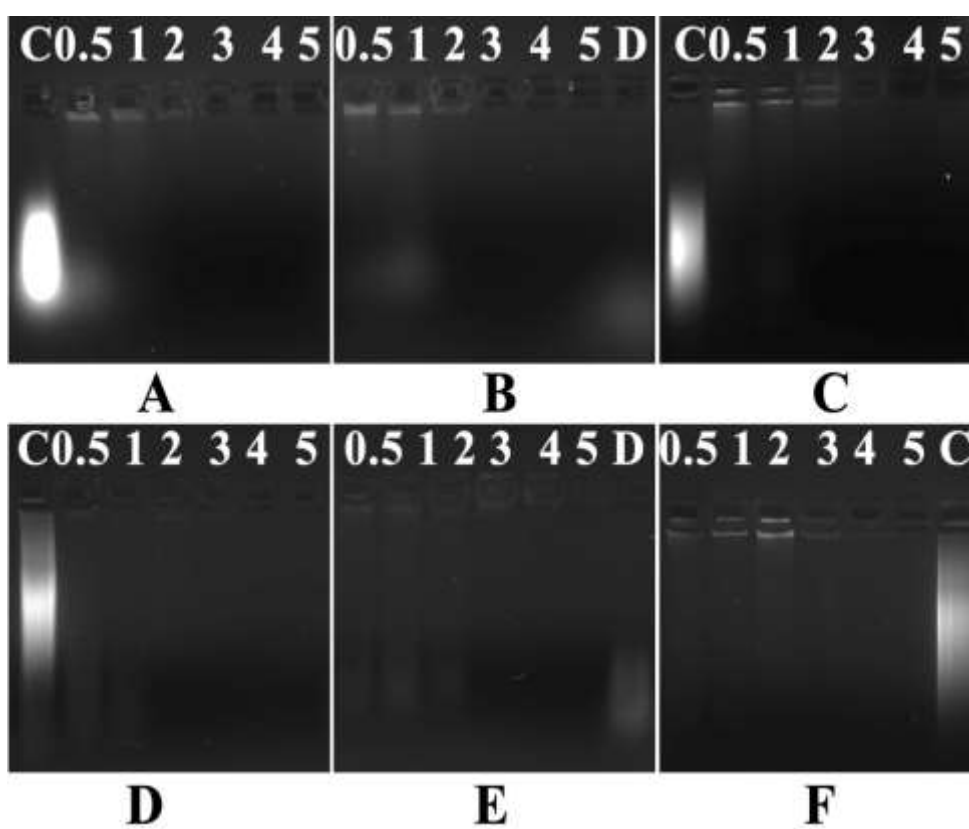


Figure 40: Nanoplex stability of VI derivatives prepared with ctDNA at six different weight ratios (0.5 to 5) was analysed in the presence of the digestive enzyme, DNase. A, B, C, D, E, F are the agarose gel loaded with the nanoplexes of DPI I, DPI II, DPI III, PPI I, PPI II and PPI III respectively.

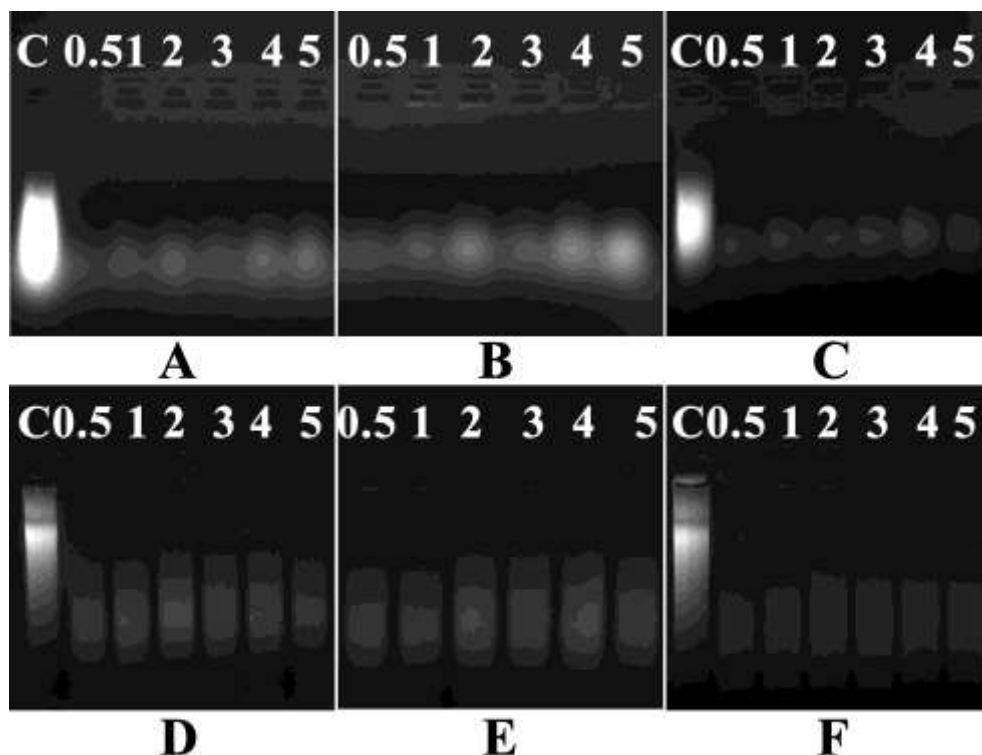
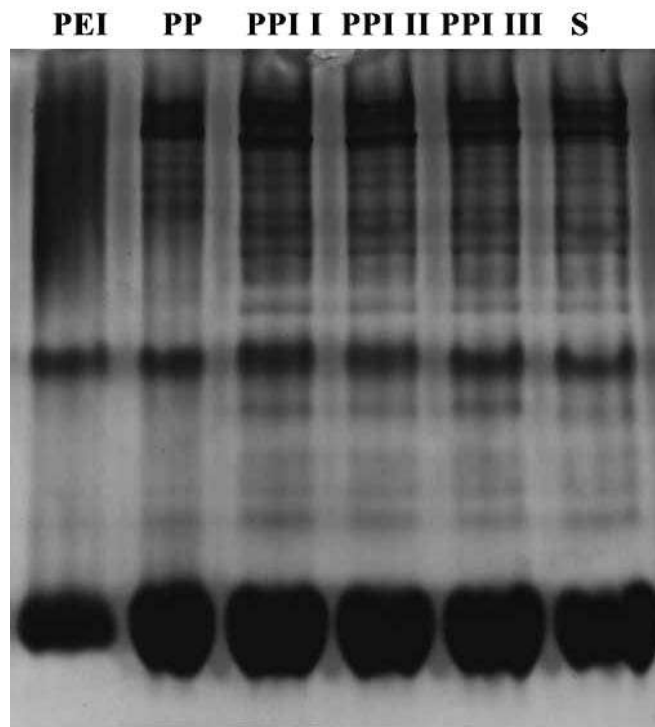


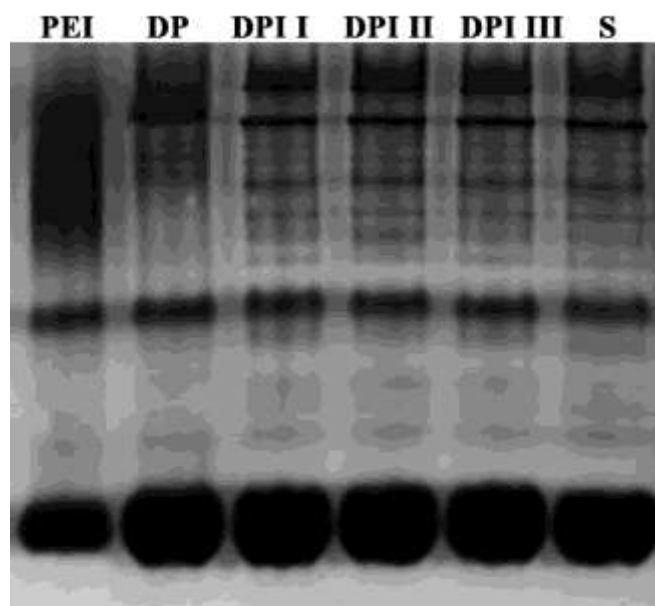
Figure 41: Decondensation of nanoplexes of VI derivatives in the presence of anionic polysaccharide, heparin. A, B, C, D, E, F are the agarose gel loaded with the nanoplexes of DPI I, DPI II, DPI III, PPI I, PPI II and PPI III respectively. Lane C was the control ctDNA while lanes 0.5 to 5 were the nanoplexes that prepared at six different ratios (i.e. 0.5:1, 1:1, 2:1, 3:1, 4:1 and 5:1).

4.4.8 Polymer interactions with plasma proteins

The study of plasma protein interactions with cationic polymers are of great interest as it determines the half-life of these polymers in the systemic circulation. Saline does not show any interactions with plasma proteins and hence saline treated plasma taken as negative control. On the other hand, PEI shows strong interactions with plasma proteins, and was taken as positive control. From the figure 42 (A and B), it was obvious that PPI and DPI derivatives do not show any interactions with plasma proteins and the protein bands are similar as that of the negative control, saline.



A

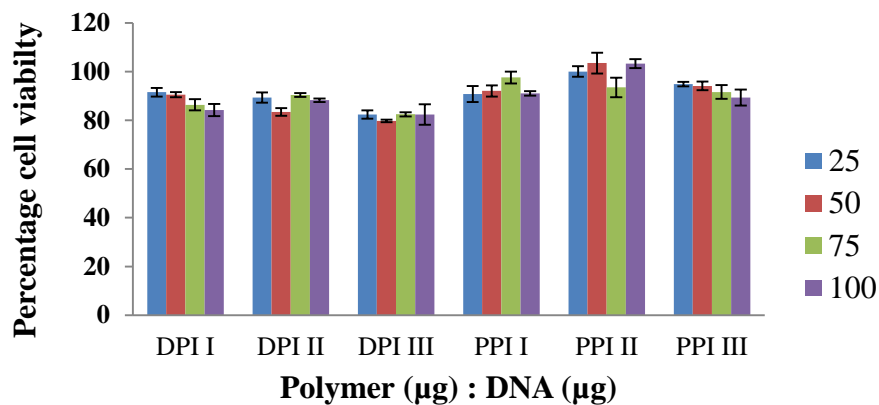


B

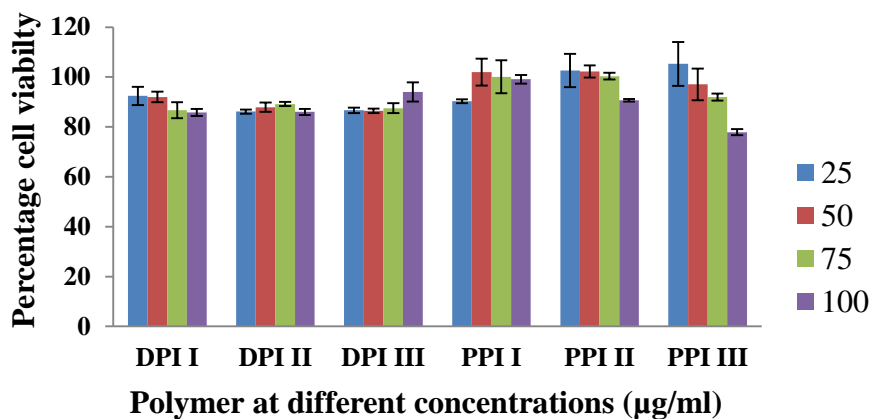
Figure 42: Plasma protein interactions with VI derivatives. (A) Pullulan derivatives
(B) Dextran derivatives

4.4.9 Cytotoxicity studies –MTT assay

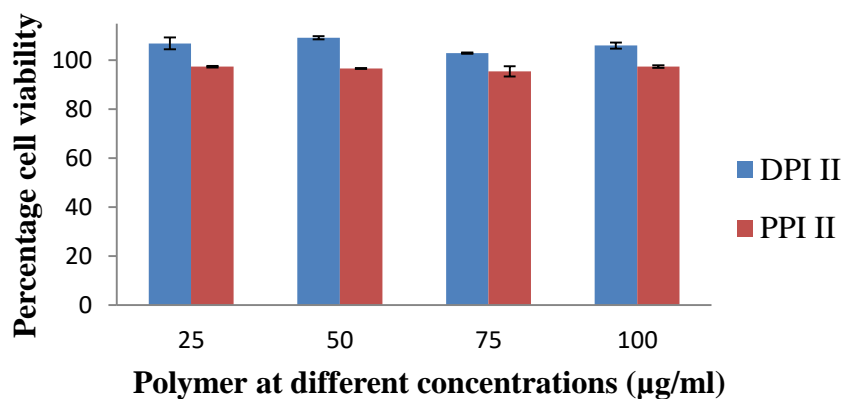
Cytotoxicity is one of the major drawbacks that limit the use of cationic polymers as gene delivery vector. The cytocompatibility of these VI derivatives was evaluated in both cancer (C6 and HeLa) and normal cell lines (L929). MTT assay was used to determine the percentage cell viability of these cell lines by assessing their metabolic activity in the presence of polymer at four different concentrations. Cytocompatibility was also evaluated for the polyplexes of DPI and PPI derivatives prepared at their optimised weight ratios (i.e. 5:1). From figure 43, it is clear that VI modification improves the percentage viability of the cells when compared to that of parent chains (DP and PP). Both DPI and PPI derivatives are cytocompatible as they possess above 75% cell viability even at higher polymer concentration. PPI II and PPI III exhibit above 90% cell viability which is slightly higher when compared to that of DPI derivatives which show above 80% cell viability in both the cell lines (C6 and HeLa). DPI derivatives shows better compatibility with HeLa cells as compared with that of C6 cells. Cytocompatibility of DPI II and PPI II were also evaluated in L929 cells and these derivatives exhibit above 95% cell viability. Nanoplexes of these selected VI derivatives (DPI II and PPI II) were also found to be cytocompatible as they exhibited above 75% cell viability in all the three cell lines tested.



A



B



C

Figure 43: MTT assay was used to analyse the percentage cell viability of three cell lines- C6 (A), HeLa (B) and L929 (C) by incubating with VI derivatives at four different polymer concentrations. These derivatives shows above 75% cell viability in C6 and HeLa cell lines while above 95% cell viability observed in L929 cells.

4.4.10 Cellular uptake of polyplexes

Intracellular trafficking of nanoplexes was studied in both C6 and HeLa cell lines by tagging ctDNA with fluorescent dye YOYO I. Presence of green fluorescence in both cytoplasm and nucleus confirms the cellular internalisation of these nanoplexes (Figure 44 and 45). VI derivatives show similar cellular uptake in both the cell lines while morphology gets slightly or heavily get affected in cells treated with DPI derivatives. Cellular internalisation of nanoplexes of PPI derivatives was also quantified flow cytometrically and it was found to be above 90% in both C6 and HeLa cell lines (table 2). The flow cytometry data substantiate the fluorescence microscopic data.

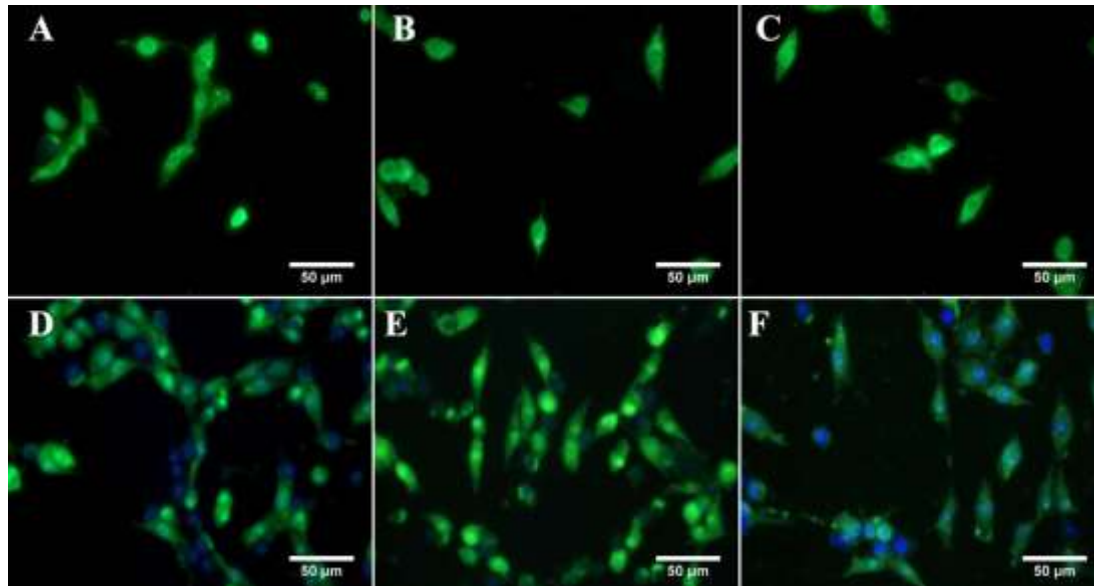


Figure 44: Cellular internalization of nanoplexes in C6 cells. Nanoplexes of VI derivatives were prepared with YOYO I tagged ct DNA (green) at the weight ratio, 5:1. The nucleus was stained with Hoechst which emits blue fluorescence. A, B, C, D, E, F are cells treated with nanoplexes of DPI I, DPI II, DPI III, PPI I, PPI II, PPI III respectively.

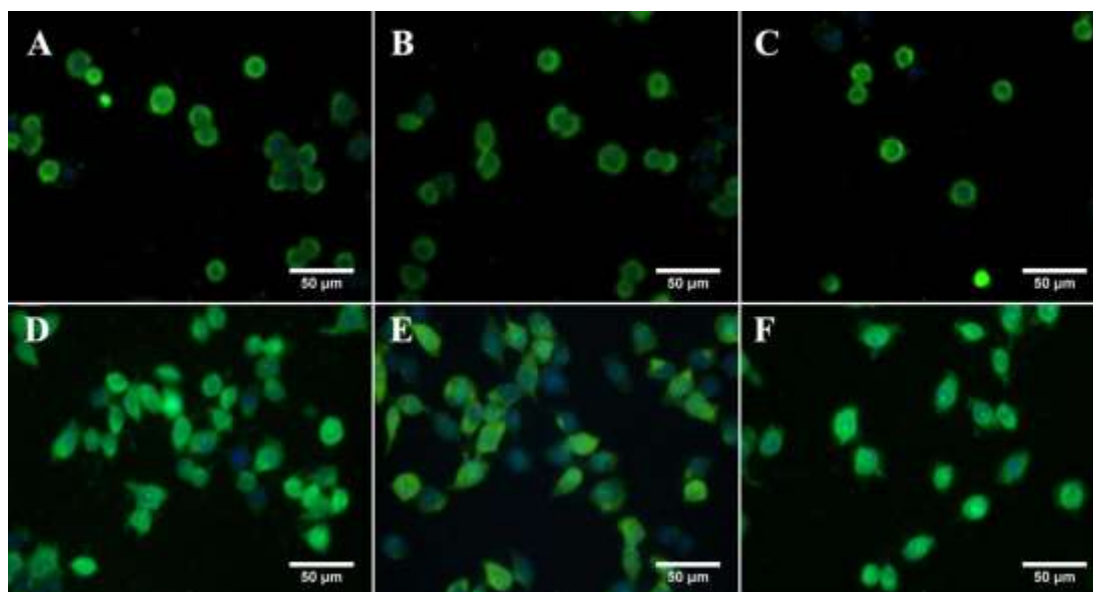


Figure 45: Cellular internalization of nanoplexes of VI derivatives prepared at the weight ratio, 5:1 with YOYO I tagged ct DNA (green). The nucleus was stained with Hoechst (blue). A, B, C, D, E, F are HeLa cells treated with nanoplexes of DPI I, DPI II, DPI III, PPI I, PPI II, PPI III respectively.

Polymer	% Cellular internalization	
	C 6	HeLa
PPI I	96.23±0.71	90.73±3.72
PPI II	98.67±0.32	94.37±1.17
PPI III	99.13±0.25	95.37±0.9

Table 2: Cellular internalisation of nanoplexes of PPI derivatives prepared with YOYO I tagged ctDNA were quantified in C6 and HeLa cell lines by flow cytometric analysis.

4.4.11 Cellular uptake in the presence of endocytic inhibitors

Cellular intake mechanism by which the nanoplexes of VI derivatives get into the cell was elucidated by studying cellular uptake in the presence of certain chemicals that inhibit specific endocytic pathways. Three inhibitors viz amiloride, chlorpromazine and filipin were chosen for this study which inhibits macropinocytosis, clathrin, and caveolae mediated pathways respectively. C6 cells were treated with these inhibitors individually half an hour prior to the incubation with polyplexes. The cellular uptake of nanoplexes was then estimated by flow cytometric analysis and the results were tabulated (table 3). Cellular uptake doesnot get affected in the presence of any of these inhibitors.

Inhibitor	Mode of action	Concentration (µg/ml)	% Cellular internalisation
Amiloride	Macropinocytosis (-)	2.25	96.75±1.06
Chlorpromazine	Clathrin (-)	2	96.75±0.35
Filipin	Caveolae (-)	5	96.25±0.21

Table 3: Flow cytometric data of cellular uptake of nanoplexes of PPI II prepared with ctDNA at the 5:1 weight ratio in the presence of various endocytotic inhibitors.

4.4.12 Gene transfection

Transfection efficiency of VI derivatives was assessed by transfecting both C6 and HeLa cell lines with p53 plasmid whose expression leads to the apoptosis in these cell lines. Live cells were stained green by Calcein-AM while dead cells are stained

red with EtBr. From the figure 46 and 47, it is clear that VI derivatives transfect cells more efficiently.

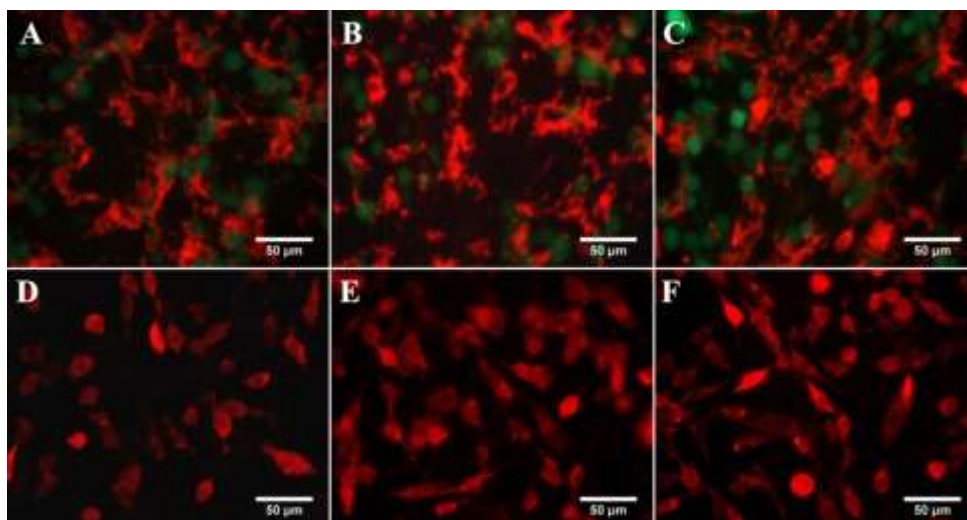


Figure 46: Live/dead assay in C6 cells transfected with nanoplexes of VI derivatives prepared with p53 plasmid at the weight ratio 5:1 (polymer to DNA). Live and dead cells are differentially stained with calcein AM and ethidium bromide that emits green and red fluorescence respectively. A to F are the cells transfected with nanoplexes of DPI I, DPI II, DPI III, PPI I, PPI II and PPI III respectively.

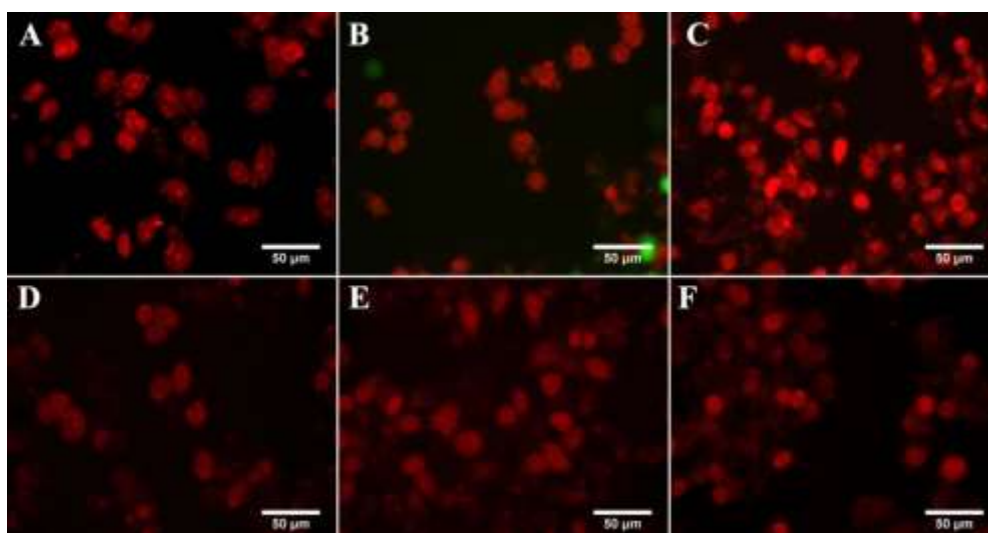


Figure 47: Live/dead assay in HeLa cells transfected with nanoplexes of VI derivatives. Nanoplexes were prepared with p53 plasmid at the weight ratio 5:1. Live are stained green with calcein AM and dead cells are stained red with ethidium bromide. A to F are the cells transfected with nanoplexes of DPI I, DPI II, DPI III, PPI I, PPI II and PPI III respectively.

On comparing DPI and PPI derivatives, the later exhibit higher transfection efficiency and also they are more consistent when compared to that of the former. Hence, the number of cell deaths occurred was quantified flow cytometrically only for that transfected with PPI derivatives. Flow cytometry results (figure 48 and table 4) further corroborated the fluorescence microscopic data. Among PPI derivatives, PPI II possess the highest transfection efficiency followed by PPI III while comparing between cell lines, transfection efficiency was higher in the C6 cell as compared to that of HeLa cells.

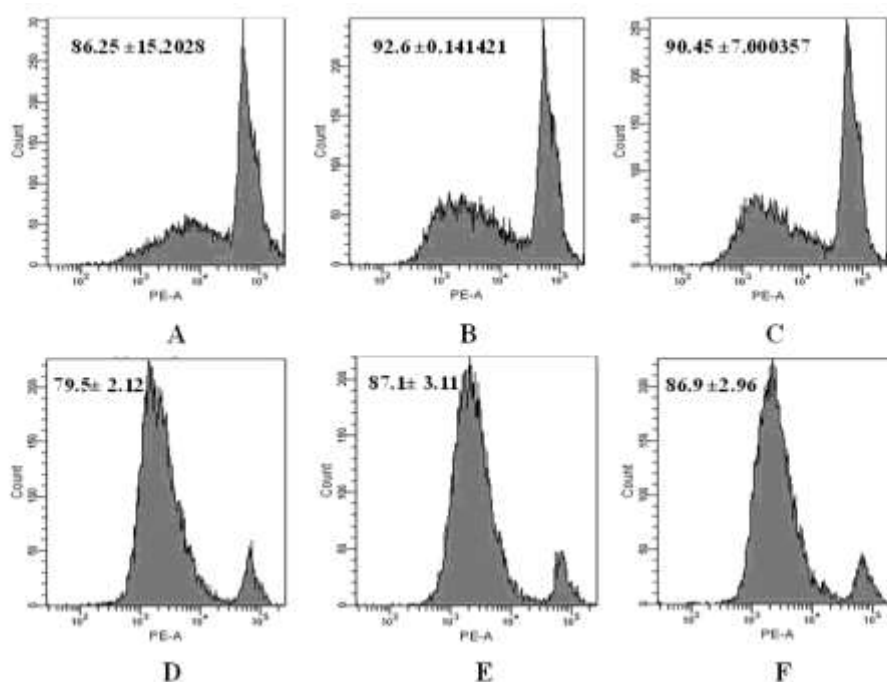


Figure 48: Flow cytometric quantification of cell death in C6 (A-C) and HeLa (D-F) cells by transfecting with polyplexes of PPI I, PPI II and PPI III that prepared with p53 plasmid at the weight ratio 5:1 by propidium iodide staining.

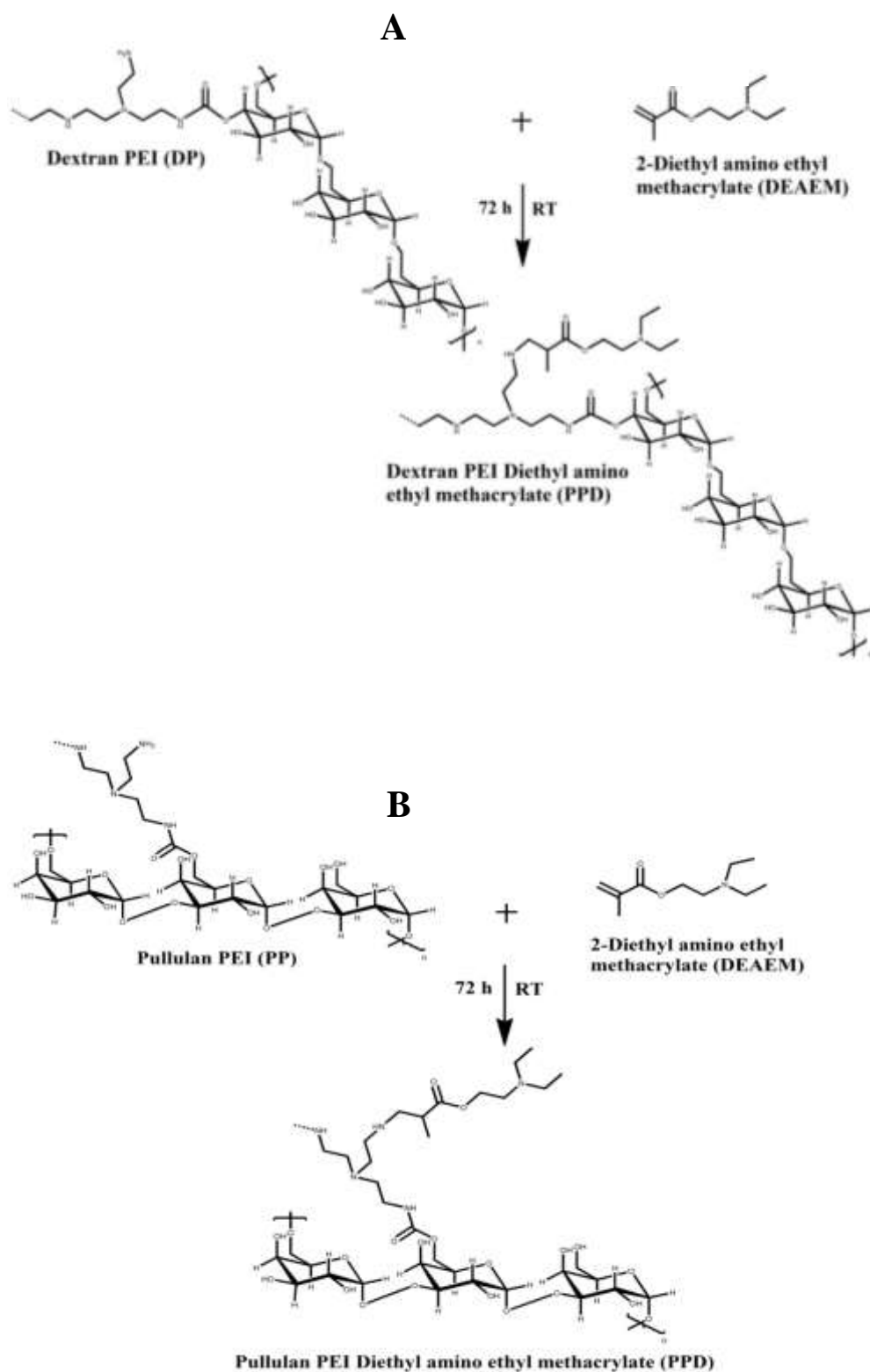
Polymer	% Transfection Efficiency	
	C 6	HeLa
PPI I	86.25±15.2	79.5±2.12
PPI II	92.6±0.14	87.1±3.11
PPI III	90.45±7	86.9±2.97

Table 4: Transfection efficiency of PPI derivatives was analysed in C6 and HeLa cells by using p53 plasmid whose expression triggers apoptosis in these cell lines. Dead cells are quantified using flow cytometer by staining with propidium iodide.

4.5 Synthesis and characterisation of 2- diethyl amino ethyl methacrylate (DEAEM) grafted cationised polysaccharides

4.5.1 Synthesis

2- Diethyl amino ethyl methacrylate was grafted to cationised polysaccharides to improve their buffering capacity and also to assist in cellular uptake as these molecules have the capacity to transiently disrupt the lipid bilayer. This vinyl monomer was grafted to DP and PP via Michael addition reaction at two different weight ratios 10 : 0.01 and 10 : 0.005 and synthesised four different polymer derivatives viz DPD I, DPD II, PPD I and PPD II respectively. The reaction mechanism is illustrated in the scheme 5. Grafted polymer was thoroughly dialysed in distilled water in order to remove the unreacted monomer molecules.



Scheme 5: Schematic representation of synthesis of 2-diethyl amino ethyl methacrylate (DEAEM) derivatives- (A) dextran PEI diethyl amino ethyl methacrylate (DPD), (B) pullulan PEI diethyl amino ethyl methacrylate (PPD)

4.5.2 Fourier transform infrared spectroscopy (FTIR)

Chemical structure of DEAEM derivatives were analysed by FTIR spectroscopy. In these spectra (Figure 49), characteristic bands of the parent chains (DP and PP) corresponding to the carbamate linkage appears in the region around 1640 cm^{-1} (C=O stretch) and 1566 cm^{-1} (C-N stretching vibrations in combination with -NH bending vibrations). The ester group present in this vinyl monomer which is expected to give band around 1740 cm^{-1} was found to overlap with the carbonyl group in the carbamate linkage. Hence, no new band appear in these spectra specific to the grafting of this vinyl monomer.

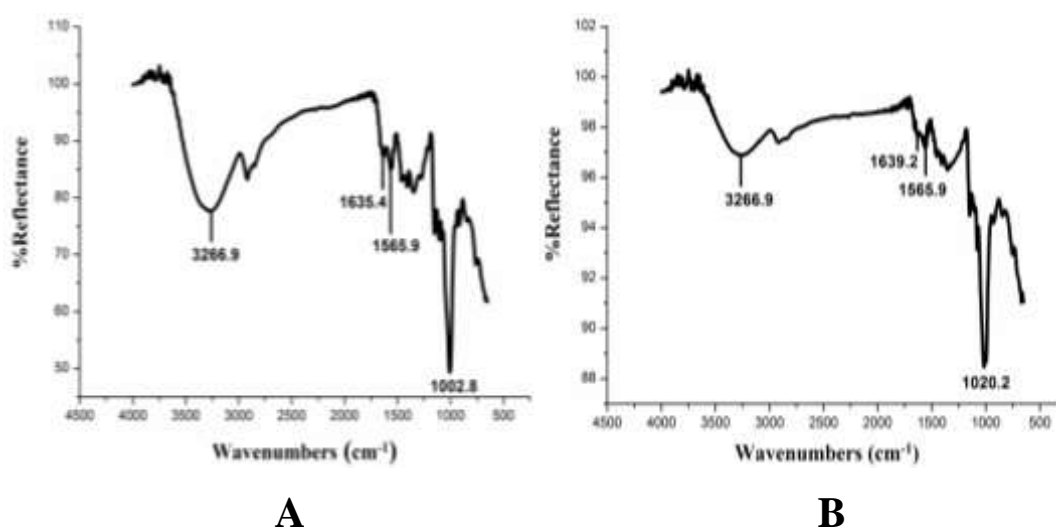
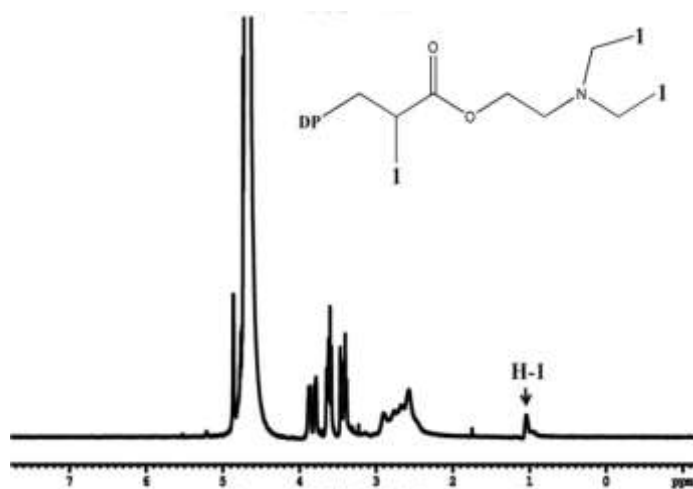


Figure 49: FTIR spectra of 2-diethyl amino ethyl methacrylate (DEAEM) derivatives- (A) dextran PEI diethyl amino ethyl methacrylate (DPD), (B) pullulan PEI diethyl amino ethyl methacrylate (PPD)

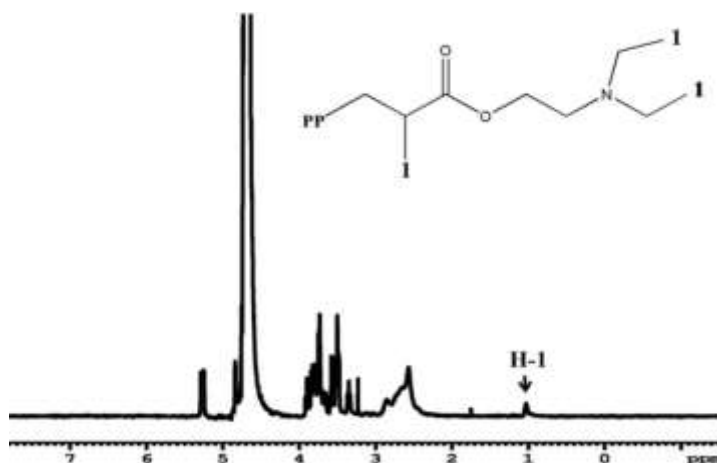
4.5.3 Proton nuclear magnetic spectroscopy (¹H NMR)

¹H NMR spectra of DEAEM derivatives confirmed the grafting of this vinyl monomer to the CPs (DP and PP). In these spectra (figure 50), the appearance of chemical shifts around region 2.5-2.8 ppm corresponds to the resonance of protons

in the methylene group of PEI while that around the region 3.4-4.0 ppm and 4.8-5.4 ppm are associated with protons of anomeric carbons, C₂ to C₆ carbons and C₁ carbon of polysaccharides respectively. In addition to these chemical shifts, the appearance of new peak around 1 ppm confirms the grafting of this vinyl monomer as it is attributed by the resonance of protons in methyl group of DEAEM molecule.



A



B

Figure 50: ¹H NMR spectra DEAEM derivatives. (A) DPD (B) PPD. H-1 is the protons associated with methyl group of DEAEM molecules.

4.5.4 Copper sulphate assay

Grafting percentage of DEAEM molecules to the CPs were determined indirectly by calculating the reduction in amino groups as their addition occurs at the primary amino groups of CPs. The amino groups present in the polymer derivatives were determined by copper sulphate assay. The grafting percentage was then calculated by comparing these values of DEAEM derivatives with that of parent chains (DP and PP). Grafting density of this vinyl monomer was found to $6.5 \pm 0.36\%$, $2.4 \pm 0.01\%$, $3.89 \pm 0.17\%$ and $2.06 \pm 0.5\%$ for DPD I, DPD II, PPD I and PPD II respectively.

4.5.5 Buffering capacity

Buffering capacities of DEAEM derivatives were determined over the pH range 10 to 4 by acid - base titration. These polymer derivatives exhibit lower buffering capacity (figure 51) as compared to that of the parent chains (DP and PP). However, these derivatives exhibit moderate buffering capacity over acidic pH and the order is PPD I > DPD I > PPD II = DPD II.

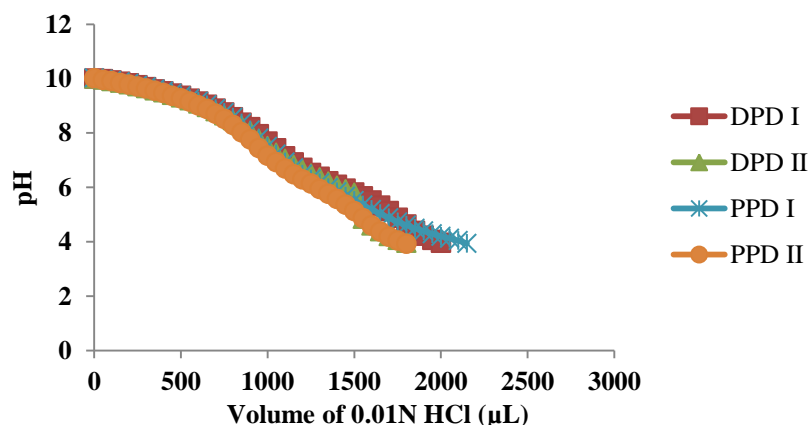
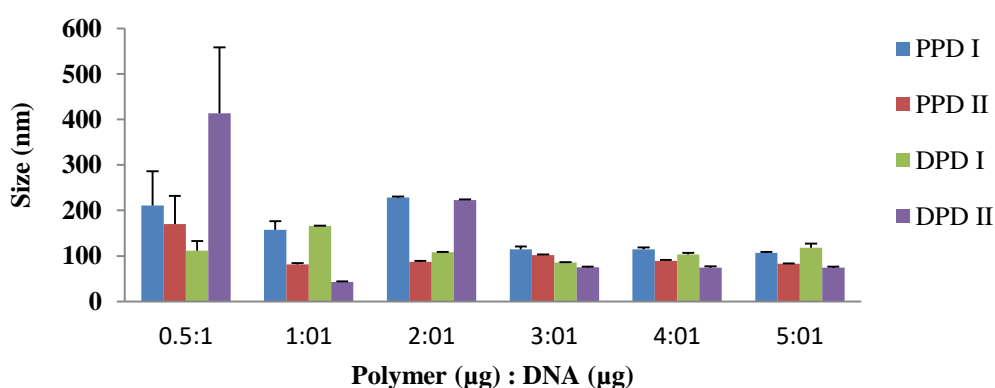


Figure 51: Buffering capacities of DEAEM derivatives over the pH range 10 to 4 determined by the acid base titration.

4.5.6 Size and zeta potential

Nanoplexes of DEAEM derivatives were prepared with ctDNA at six different weight ratios (0.5:1 to 5:1). Hydrodynamic size of these nanoplexes was analysed by dynamic laser scattering experiments. From figure 52 (A), it was clear that size of these nanoplexes decreased with increase in the polymer to DNA weight ratio. At the weight ratio, 5:1, they effectively condense ctDNA and form smaller sized nanoparticles below 120 nm range and the PDI value ranges from 0.1 to 0.2. Of these, DPD II forms the smallest nanoplexes of size below 75 nm and the order was DPDI > PPD II > PPD I > DPD I.

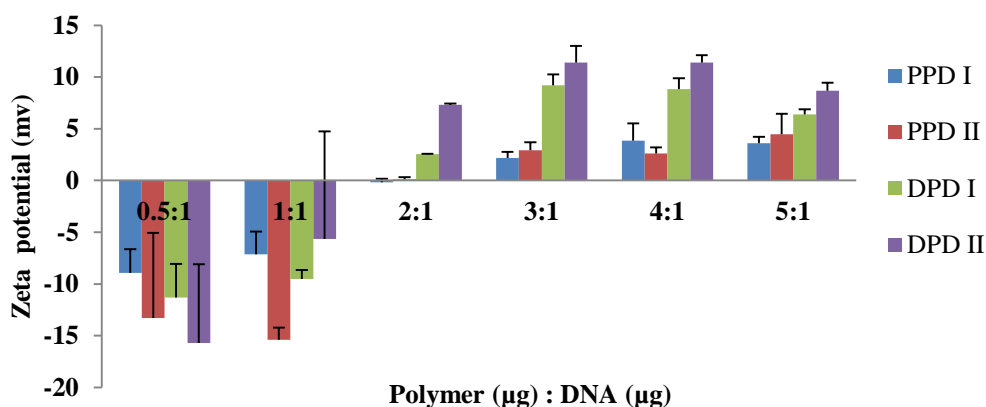


A

Figure 52(A): Hydrodynamic sizes of the polyplexes formed by the DEAEM derivatives with ctDNA at different weight ratios polymer to DNA weight ratios.

Polyplexes of DEAEM derivatives exhibit negative zeta potential till the weight ratio 1:1 and after that this value turns either to positive or nearer to zero (figure 52.B). Zeta potential generally found to increase with increase in the polymer to DNA weight ratio. These polymer derivatives form nanoplexes of around +3 to +9 mV zeta

potential at the weight ratio, 5:1. DPD II derivatives exhibit higher positive zeta potential of around +9 mV at the 5:1 weight ratio and it was followed by the DPD I, PPD II and PPD I.



B

Figure 52(B): Zeta potential measurements of nanoplexes of DEAEM derivatives prepared with ctDNA at different weight ratios.

4.5.7 DNA binding ability and effect of plasma on nanoplex stability

Binding strength of DEAEM derivatives to form nanoplexes with ctDNA was analysed by agarose gel electrophoresis. Nanoplexes of these polymer derivatives were prepared with ctDNA at six different weight ratios (0.5:1, 1:1, 2:1, 3:1, 4:1 & 5:1) and electrophoresis was carried out at 100 V by loading these nanoplexes onto the 1% gel. Figure 53 (A-D), reveals that DEAEM derivatives form strong complexes with ctDNA that prevents the later's mobility under electric field. However, slight DNA leach out observed at lower weight ratios especially at the 0.5:1 ratio for these polymer derivatives. The stability of these nanoplexes was also studied in the presence of plasma proteins. Since these proteins are anionic in nature, they possess the capacity to displace DNA from these polyplexes. Figure 53 (E-H)

shows that nanoplexes of DEAEM derivatives found to stable complexes even in the presence of plasma proteins and the results are similar to that of nanoplex alone.

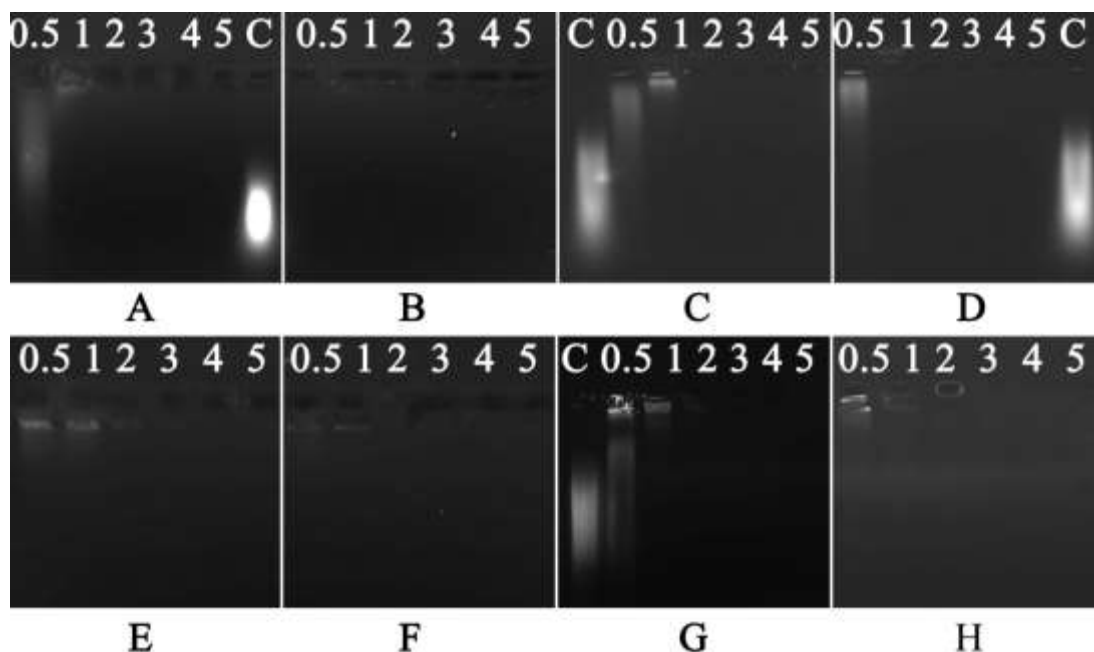


Figure 53: DEAEM derivatives ability to retard the movement of DNA under electric field was assessed by agarose gel electrophoresis. A – D are nanoplexes of DEAEM derivatives prepared with ctDNA at different weight ratios (0.5:1 to 5:1) while E- H the stability assessment of nanoplexes of DPD I, DPD II, PPD I and PPD II in the presence of plasma proteins respectively. Lane C is the control DNA (without any treatment).

4.5.8 Nanoplex stability in the presence of digestive enzyme, DNase

The ability of DEAEM derivatives to protect the DNA from the degradation by the nuclease enzyme was analysed by performing agarose gel electrophoresis after incubating the polyplexes with digestive enzyme, DNase. In figure 54 (A-D), control DNA appeared as smear while that treated with DNase show degradation and visualised as a band in the gel. However, no DNA degradation was observed in the lanes loaded with nanoplexes of DEAEM derivatives even at lower weight ratios. The results were counter checked by adding heparin to the remaining polyplex

solution. This anionic glycosaminoglycan competes with DNA for binding with the DEAEM derivatives and as a result, the DNA get displaced from these polyplexes and appeared as the smear in the lane while performing agarose gel electrophoresis. Hence the integrity of DNA protected by these derivatives from the degradation caused by the enzyme, DNase can be checked by this assay. DEAEM derivatives efficiently protect the DNA from the degradation caused by the digestive enzyme even at the lower weight ratio which was evidenced by the appearance of intact DNA as smear in these lanes in the figure 54 (E-H).

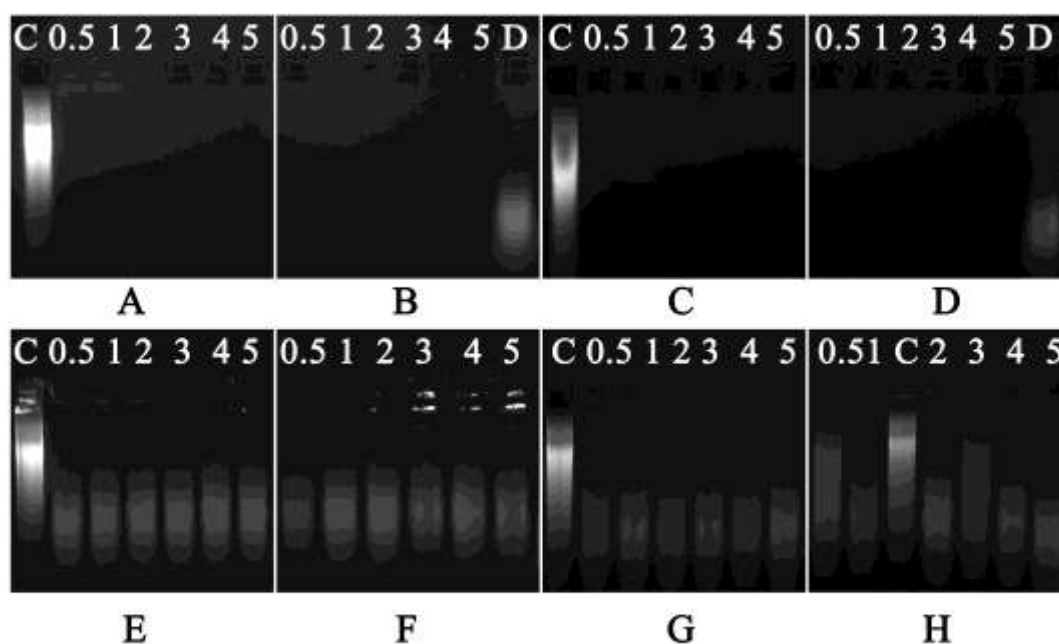


Figure 54: (A-D) are DNase treated nanoplexes of DPD I, DPD II, PPD I and PPDI derivatives respectively. Lanes 0.5:1 to 5:1 are that loaded with nanoplexes of DEAEM derivatives prepared with ctDNA at different weight ratios. Control DNA alone and that treated with DNase were loaded to the lanes C and D respectively. (E-H) are heparin treated nanoplexes of DPD I, DPD II, PPD I and PPD II derivatives respectively.

4.5.9 Polymer interactions with plasma proteins

Plasma protein interactions with DEAEEM derivatives were analysed by performing polyacrylamide gel electrophoresis as they determine the half life of this polymer derivatives in the systemic circulation. Saline treated with plasma have no interactions with these proteins and hence it is taken as negative control. On the other hand, PEI shows strong interactions with plasma proteins and it is taken as positive control. From figure 55, it was clear that DEAEEM derivatives show no interactions with plasma proteins and the bands were similar to that of the negative control, saline.

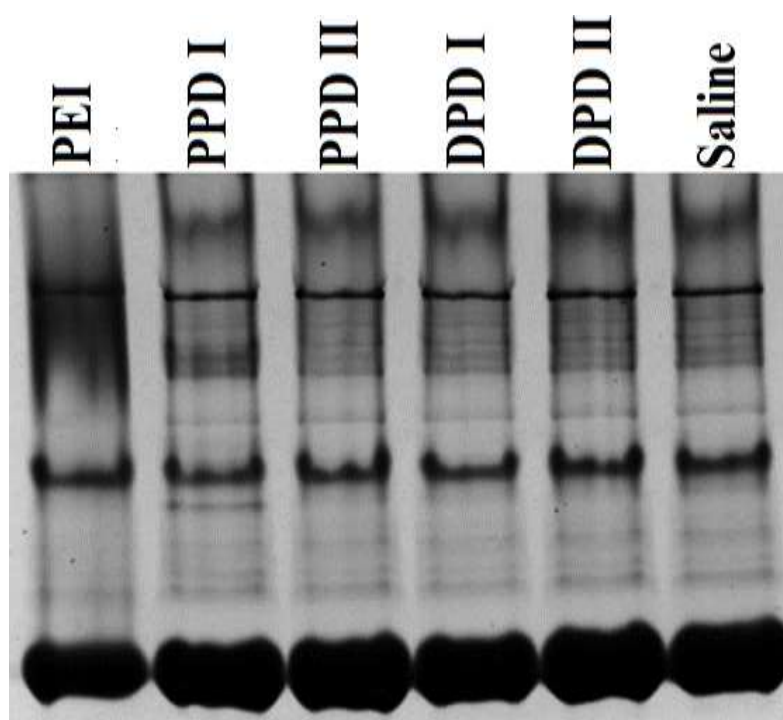
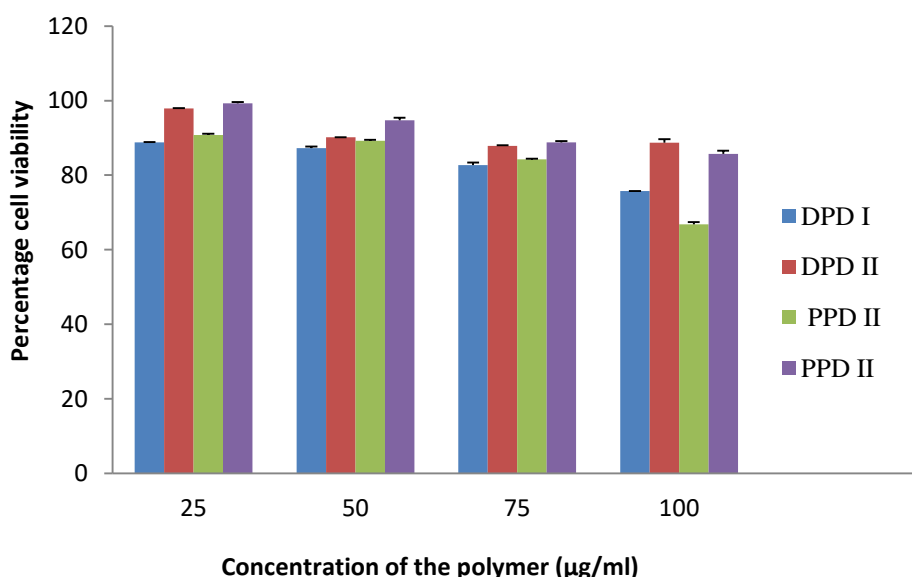


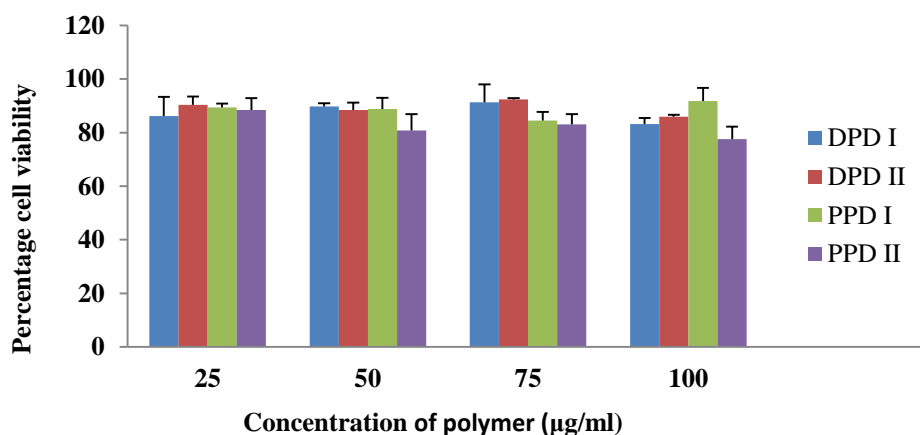
Figure 55: Interactions of plasma proteins with DEAEEM derivatives were analysed by polyacrylamide gel electrophoresis after incubating the respective polymers with plasma.

4.5.10 Cell viability

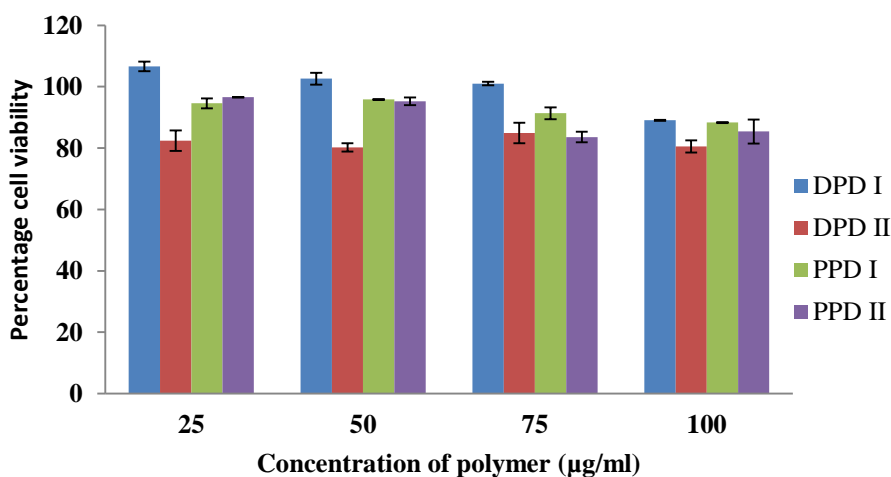
Cationic polymers intended for gene delivery are usually associated with inherent cytotoxicity. So cytocompatibility of DEAEM derivatives was determined by MTT assay in three different cell lines viz C6, HeLa and L929. These cells were incubated with these polymer derivatives at four different concentrations. DEAEM derivatives found to be cytocompatible and exhibit above 80% Cell viability in all these cell lines tested even at higher polymer concentrations (figure 56). Among these polymer derivatives, DPD II exhibit highest Cell viability (90%) and it was followed by PPD II (85%). DPD I and PPD I exhibit almost similar Cell viability of 80% in C6 and HeLa cell lines. Nanoplexes of DPD II and PPD II prepared with ctDNA at the weight ratio 5:1 were also evaluated for cytocompatibility and found to exhibit above 95% cell viability in all these three cell lines tested.



A



B



C

Figure 56: MTT assay to determine cytocompatibility of DEAEM derivatives at four different polymer concentrations (25, 50, 75 and 100 µg/ml) in the cell lines – (A) C6, (B) HeLa and (C) L929.

4.5.11 Cellular uptake of polyplexes

Non specific endocytosis mechanism is the predominant way of cellular internalisation opted by the cationic polymers which have no targeting ligands for their internalisation. Size and zeta potential of these nanoplexes plays significant role in the determination of this type of cellular entry. DEAEM derivatives ability to get

internalised into the cells was analysed in C6, HeLa and L929 cells by preparing polyplexes with YOYO I tagged ctDNA at the weight ratio 5:1. As from the figure 57, it was clear that these polymer derivatives readily get internalised into C6 and HeLa cells. The DNA also gets into the nucleus which was evidenced by the appearance of green fluorescence in the nuclear compartment of these cells. However, DEAEM derivatives exhibit poor cellular uptake in L929 cells. The cellular uptake in C6 and HeLa cells was further confirmed by the flow cytometric data which shows above 95% cellular intake in these cell lines (figure 58) and that corroborates with fluorescence microscopy data.

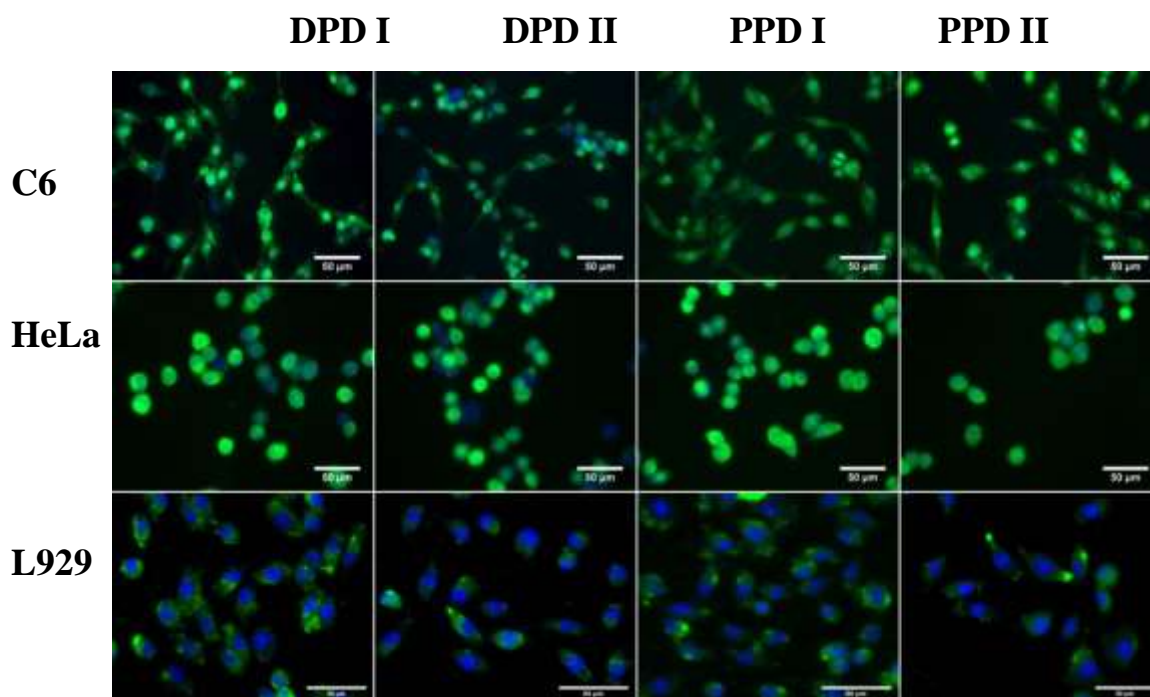


Figure 57: Cellular uptake of polyplexes of DEAEM derivatives prepared with YOYO I tagged ctDNA (green) at the weight ratio 5:1 in C6, HeLa and L929 cell lines. Nuclei of these cell lines were stained with Hoechst which emits blue fluorescence.

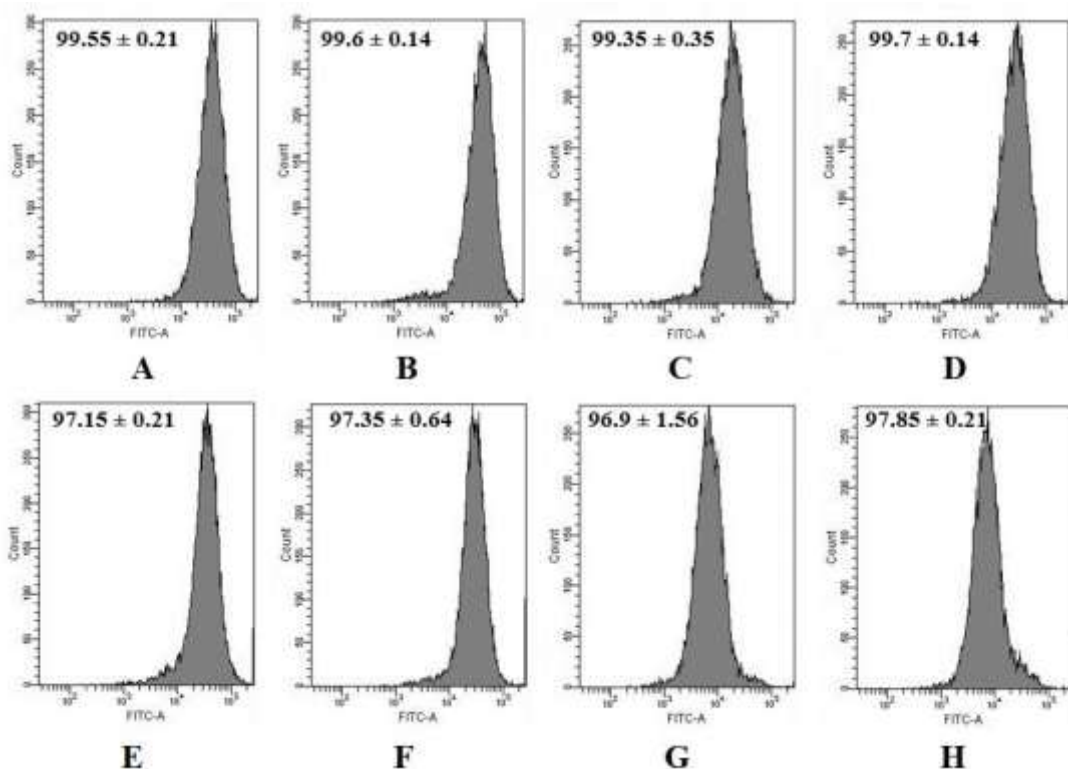


Figure 58: Flow cytometric quantification of cellular uptake of nanoplexes of DEAEM derivatives prepared with YOYO I tagged ctDNA at the weight ratio 5:1. (A-D) and (E-H) are cellular uptake in C6 and HeLa cells that treated with polyplexes of DPD I, DPD II, PPD I and PPD II respectively.

4.5.12 Cellular uptake in the presence of endocytic inhibitors

Endocytic pathway by which nanoplexes of DEAEM derivatives get internalised was determined by carrying out cellular uptake study in C6 cells that priorly treated with certain chemicals that inhibit specific endocytic pathways. For this study, three inhibitors - amiloride, chlorpromazine and filipin were chosen to specifically inhibit macropinocytosis, clathrin, and caveolae mediated pathways respectively. Cellular uptake of these nanoplexes was quantified by flow cytometric analysis. From the results (table 5), it was clear that, cellular uptake of DEAEM derivatives doesnot get

affected in the presence of any of these inhibitors. These results indicate that the polyplexes of these polymer derivatives get enter into the cell via multiple pathways.

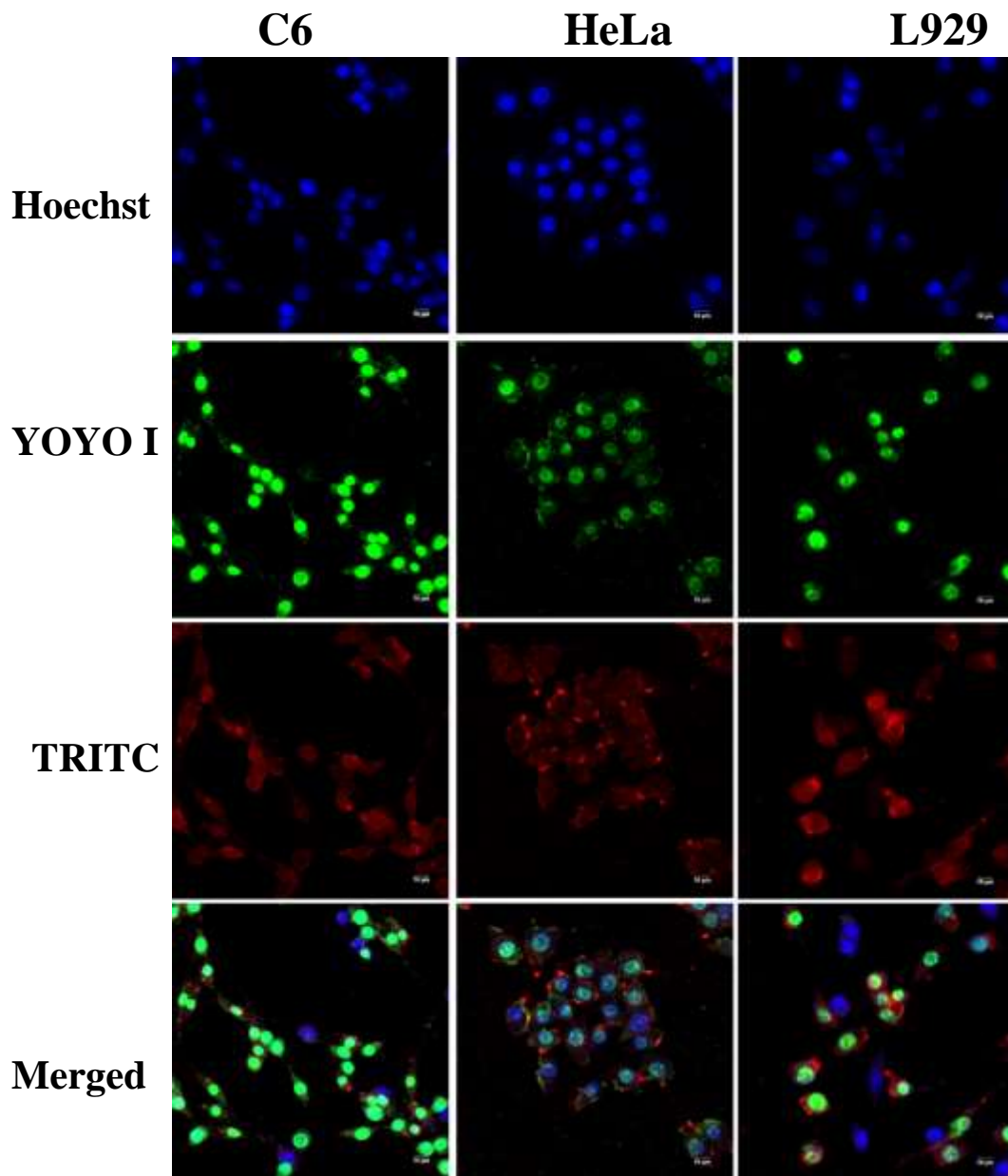
Inhibitor	Mode of action	Concentration ($\mu\text{g/ml}$)	% Cellular internalisation	
			PPD	DPD
Amiloride	Macropinocytosis(-)	2.25	96.65 \pm 0.07	98.37 \pm 0.31
Chlorpromazine	Clathrin(-)	4	98.5 \pm 0.28	99.27 \pm 0.15
Filipin	Caveolae(-)	5	99.75 \pm 0.21	99.3 \pm 0.1

Table 5: Flow cytometric quantification of cellular uptake of nanoplexes of DEAEM derivatives in C6 cells in the presence of various endocytic inhibitors.

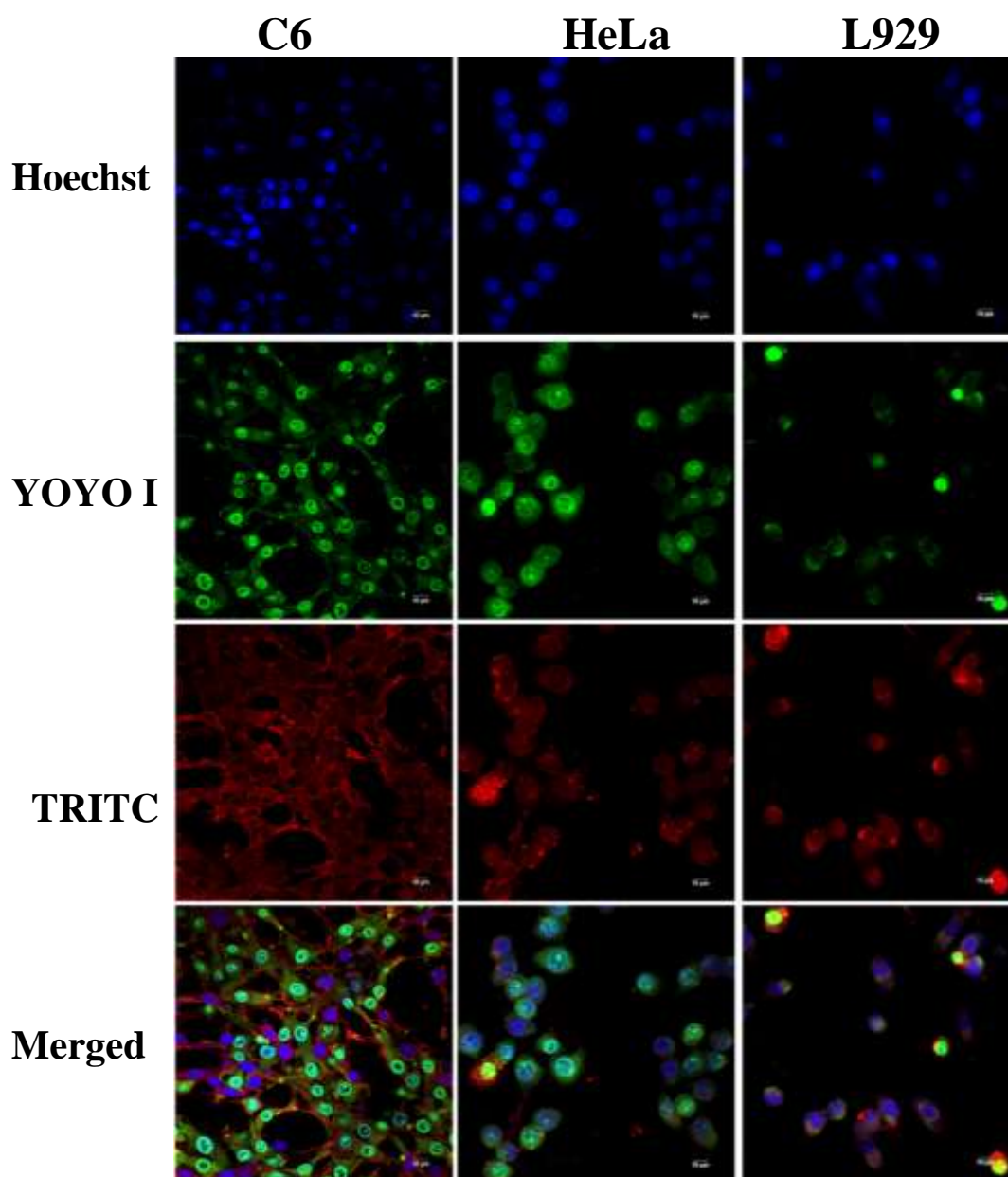
4.5.13 Polymer trafficking studies

Transfection efficiency of the polymeric vector depends on how efficiently it decondenses and releases the gene of interest to the target so that it gets expressed. Hence, vector unpacking is very crucial for the gene delivery vectors as it determines their transfection efficiency. It is reported in the literature, that vector unpacking of cationic polymers occurs by their interactions with anionic components present in the cytosol. So in order to study the status of DEAEM derivatives inside the cell, these polymer derivatives were tagged with TRITC, a fluorescent dye emitting red fluorescence. The cellular uptake study conducted using this tagged polymer reveals that vector unpacking of this polymeric derivative occurs in the cytoplasm as red

fluorescence appears only in the cytosol while DNA alone gets into the nucleus (figure 59).



A



B

Figure 59: Confocal microscopic images of trafficking DEAEM derivatives in C6, HeLa and L929 cells. Cells nuclei, ctDNA and polymer were stained blue, green and red with Hoechst, YOYO I and TRITC respectively. (A) and (B) are polymer trafficking of DPD II and PPD II respectively. Scale bar is of 10 μm length for all the images.

4.5.14 Gene transfection

The success of gene delivery vector relies on how efficiently it delivered the gene of interest in transcriptionally active form. Gene transfection efficiency of DEAEM derivatives was evaluated in C6, HeLa and L929 using p53 plasmid. The expression of this gene induces apoptosis in cancer cells while causes reversible cell cycle arrests in normal cells. Hence, the gene transfection efficiency of DEAEM derivatives was determined in cancer cells by performing live dead assay (LDA). Live cells are distinguished from the dead cells using differential staining technique. Live cells are stained green with calcein AM while dead cells appear red by ethidium bromide. From the figure 60, it was clear that DEAEM derivatives exhibit good transfection efficiency in both C6 and HeLa as most of these cells stained red. However, they exhibit poor transfection efficiency in L929 cells as most of the cells remain as green.

Transfection efficiency of DEAEM derivatives in C6 and HeLa was also quantified flow cytometrically by staining dead cells with propidium iodide (PI). Nanoplexes of these polymeric derivatives causes above 90% cell death (except DPD I derivative) in C6 cells while above 95 % cell death occurs in HeLa cells (figure 61). So in order to confirm, the cell death induced by these nanoplexes is through the expression of p53 plasmid and not by toxicity caused either by these polymer derivative or it nanoplexes, LDA experiments repeated using polymer alone in C6 cells (figure 62) and nanoplexes of DPD II and PPD II prepared with ctDNA in C6 and HeLa cells (figure 63). However, the cells treated with polymer alone and also that transfected

with polyplexes prepared with ctDNA remains alive which further confirms that the cell death in figure is due to the expression of p53 plasmid.

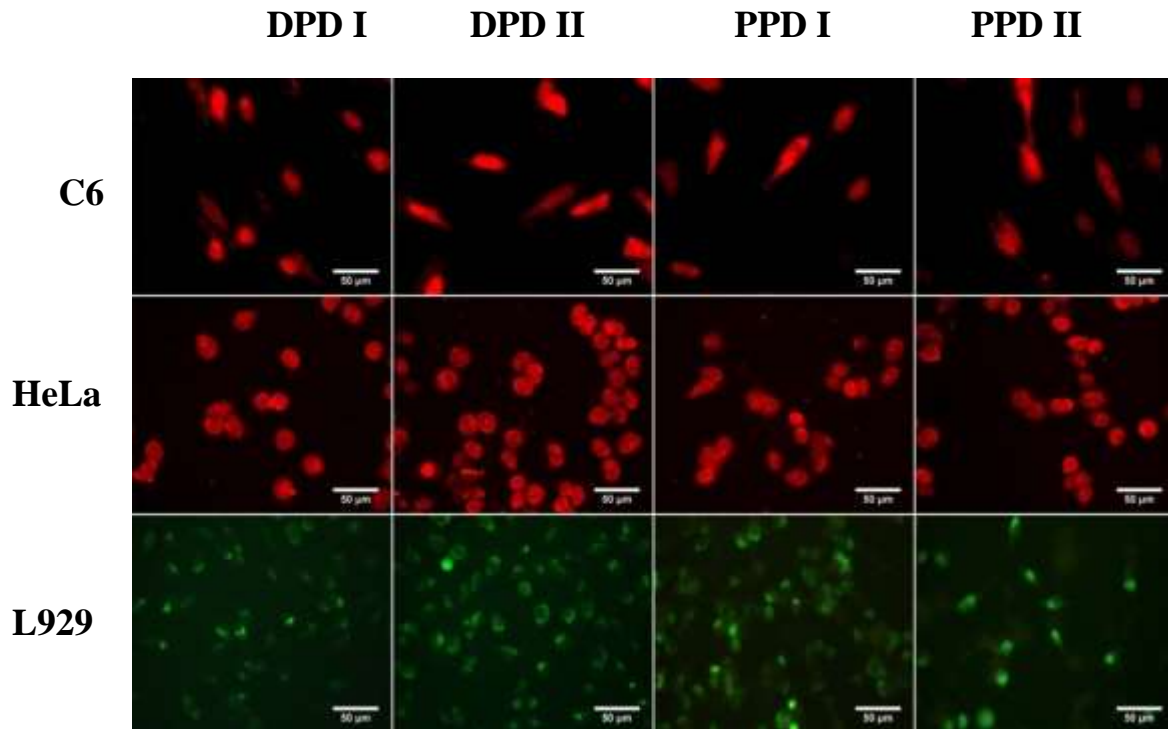


Figure 60: Transfection efficiency of DEAEM derivatives assessed by using p53 plasmid in C6, HeLa and L929 cells. Dead cells are stained red with ethidium bromide while live cells are stained green with calcein AM.

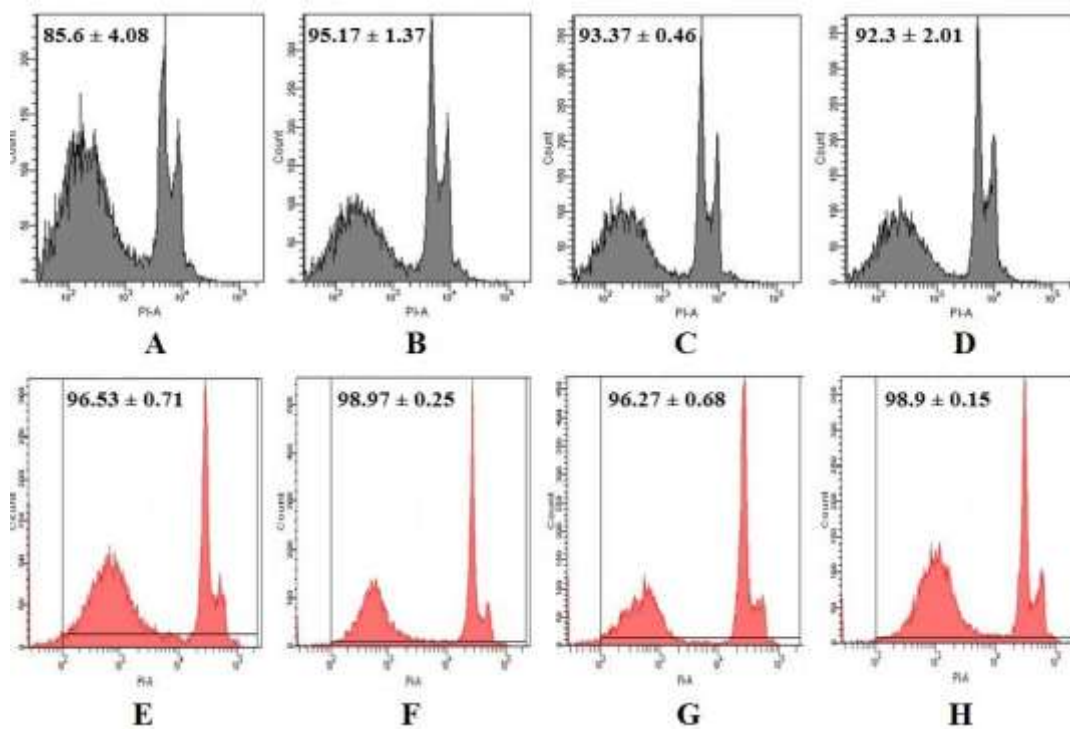


Figure 61: Flow cytometric quantification of cell death by propidium iodide staining. (A-D) and (E-H) are C6 and HeLa cells transfected with polyplexes of DPD I, DPD II, PPD I and PPD II prepared with p53 plasmid at the weight ratio 5:1, respectively.

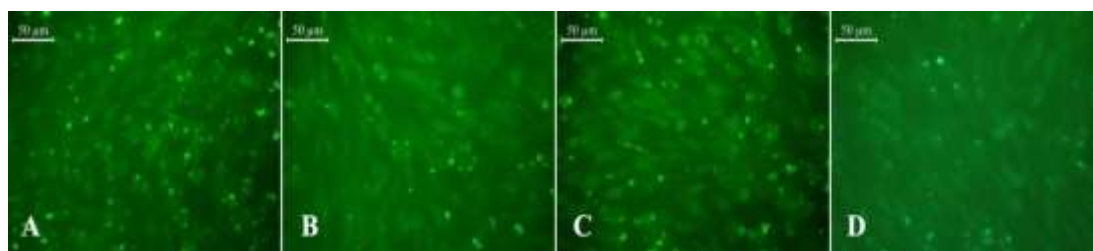


Figure 62: (A -D) Live dead assay in C6 cells treated with DEAEM derivatives DPD I, DPD II, PPD I and PPD II respectively.

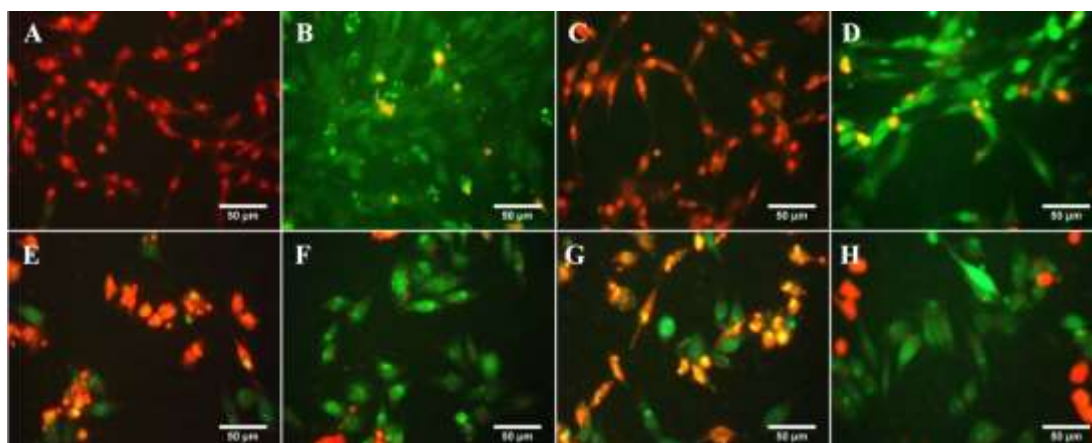


Figure 63: Live dead assay in C6 (A-D) and HeLa cells (E-H) transfected with polyplexes of DEAEM derivatives and their parent chains (DP and PP) prepared with ctDNA. A,B,C, D are C6 cells that transfected with nanoplexes of DP, DPD II, PP, PPD II while E,F,G,H are that in HeLa cells respectively.

4.5.15 Annexin V staining

In order to confirm the cell death that occurred in HeLa cells transfected with polyplexes of DEAEM derivatives prepared with p53 plasmid was through the induction of apoptosis, Annexin V staining was done. Flow cytometric data (figure 64 and table 6), reveals that most of the transfected cells were either in early or in late apoptotic stage for both PPD I and DPD II derivatives. Percentage cell death that occurs by necrosis in these transfected cells was below 1%. Occurrence of live cells was higher for those transfected with DPD II derivatives and it was around $42.17 \pm 7.11 \%$ while that for PPD II derivatives, it was around $26 \pm 6.02 \%$.

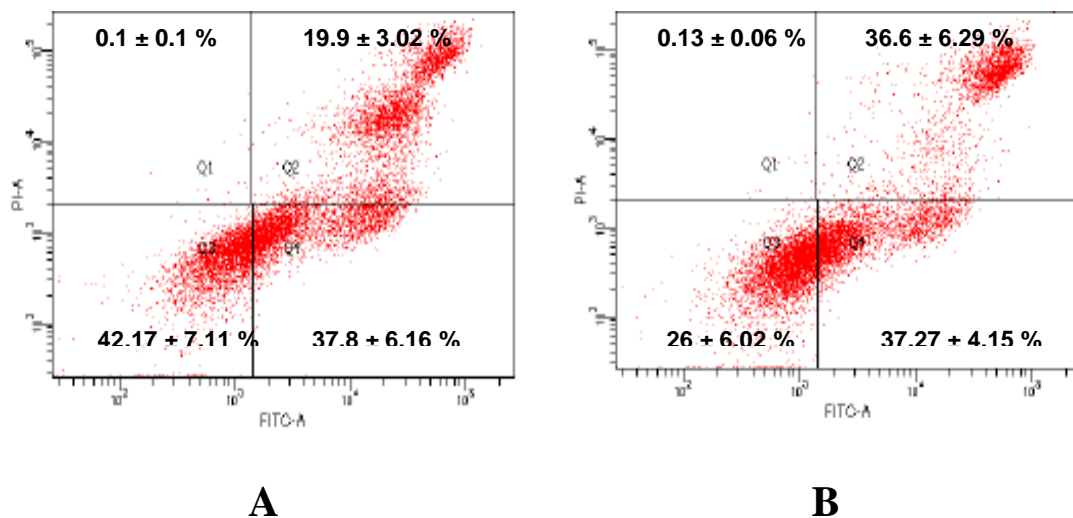


Figure 64: Flow cytometric data of HeLa cells transfected with polyplexes of DEAEM derivatives that are prepared with p53 plasmid. FITC tagged Annexin V (Anx) and propidium iodide (PI) used to differentiate apoptotic from necrotic cells. Quadrant 1 (Q1) depicts necrotic cells (Anx⁻/PI⁺ region), Quadrant 3 (Q3) signifies live cells (Anx⁻/PI⁻ region) while quadrant 2 (Q2) and quadrant 4 (Q4) are Anx⁺/PI⁺, Anx⁺/PI⁻ regions that indicate late and early apoptotic cells respectively. (A) DPD II (B) PPD II

Polymer	Live cells %	Early apoptotic cells %	Late apoptotic cells %	Total apoptotic cells %	Necrotic cells %
DPD II	42.17 ± 7.11%	37.8 ± 6.16 %	19.9 ± 3.02 %	57.7	0.1
PPD II	26 ± 6.02 %	37.27 ± 4.15 %	36.6 ± 6.29%	73.87	0.13

Table 6: Live, apoptotic (early and late), necrotic cells in C6 that occurred by the transfection with polyplexes of DEAEM derivatives analysed by annexin V staining. Nanoplexes are prepared with p53 plasmid at the weight ratio, 5:1.

4.5.16 Immunostaining

Immunostaining experiments were carried out in C6 cells in order to confirm the expression of p53 gene delivered by these DEAEM derivatives. For this analysis, C6 cells were transfected with the nanoplexes of this polymer derivatives prepared with p53 plasmid at weight ratio, 5:1. The results were compared with that of PEI 10 K as it transfect cells more effectively. In figure 65, the appearance of green fluorescence in the C6 cells confirms the expression of p53 gene. However, the expression of this protein was higher in the cells that are transfected with PEI. The p53 protein found to be uniformly distributed throughout the cell.

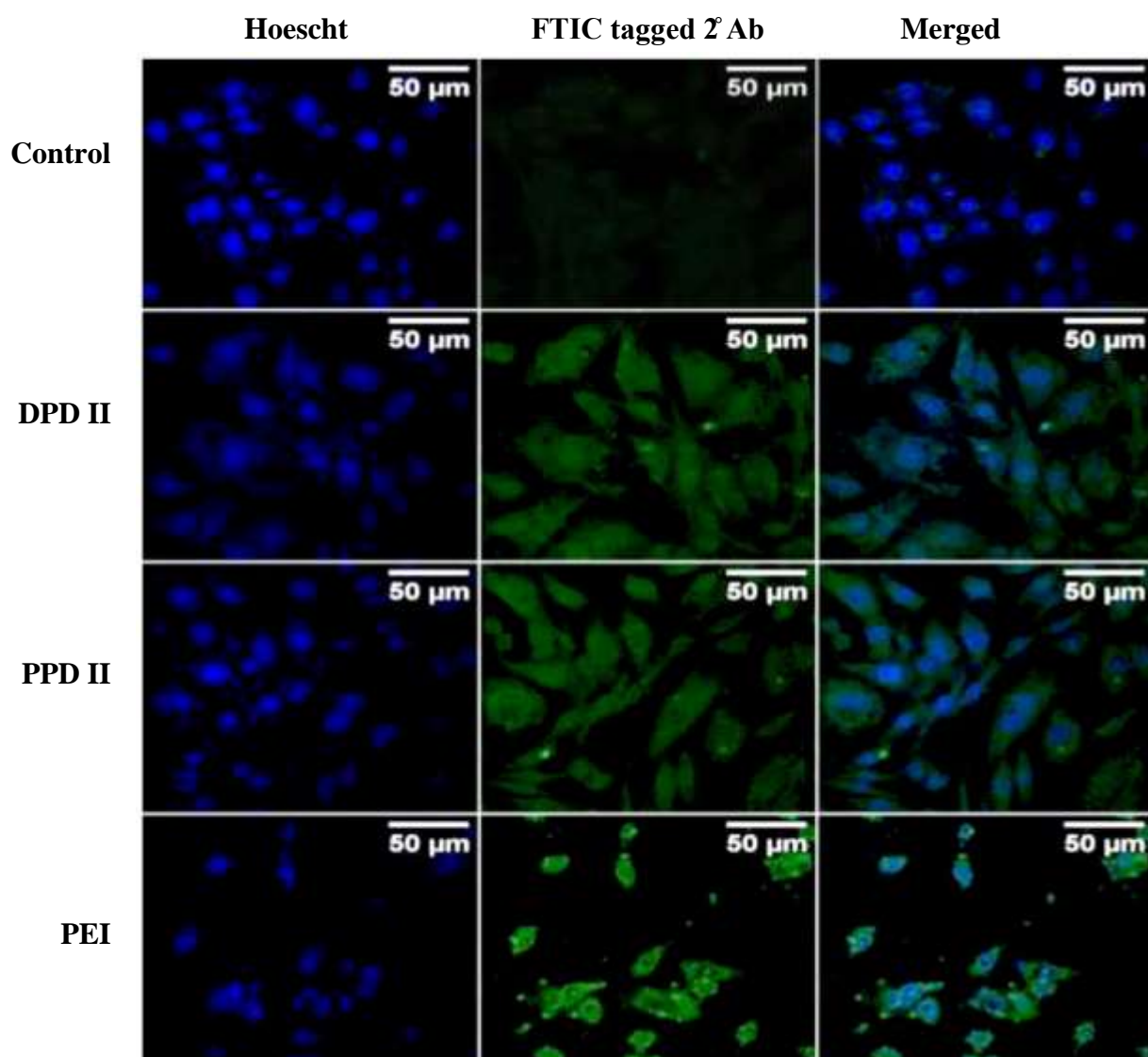


Figure 65: Immunostaining of C6 cells that transfected with polyplexes of DPD II, PPD II and PEI prepared with p53 plasmid. Nanoplexes were prepared at the weight ratio, 5:1 for DEAEM derivatives and 2:1 for PEI.

4.5.17 Biodistribution studies

Biodistribution of DEAEM derivatives was performed in BALB/c mice by administering, Alexa flour 790 tagged DPD II and PPD II derivatives via tail vein injection. The animals were the euthanised in CO₂ chamber at four different time

periods namely 15 minutes, 3 h, 6 h and 24 h and internal organs like kidney, liver, heart, spleen, brain and lungs were collected. These organs were imaged using *in vivo* imaging system (IVIS, Xenogen) at the Ex/Em 745/820 nm. At the initial time period (15 min post intra venous administration), these two derivatives found to accumulate in the kidney cells while negligible fluorescence observed in lungs and liver tissue (figure 66). During the 3 h, DPD II derivatives found to accumulate in the liver tissue. However, PPD II derivatives take 6 h to enter the liver tissue. Both these derivatives exhibit good renal clearance as the fluorescence observed in the kidney cells till 6th h. At 24th hour, fluorescence in the kidney cells gets reduced while a little fluorescence retained in the liver tissue.

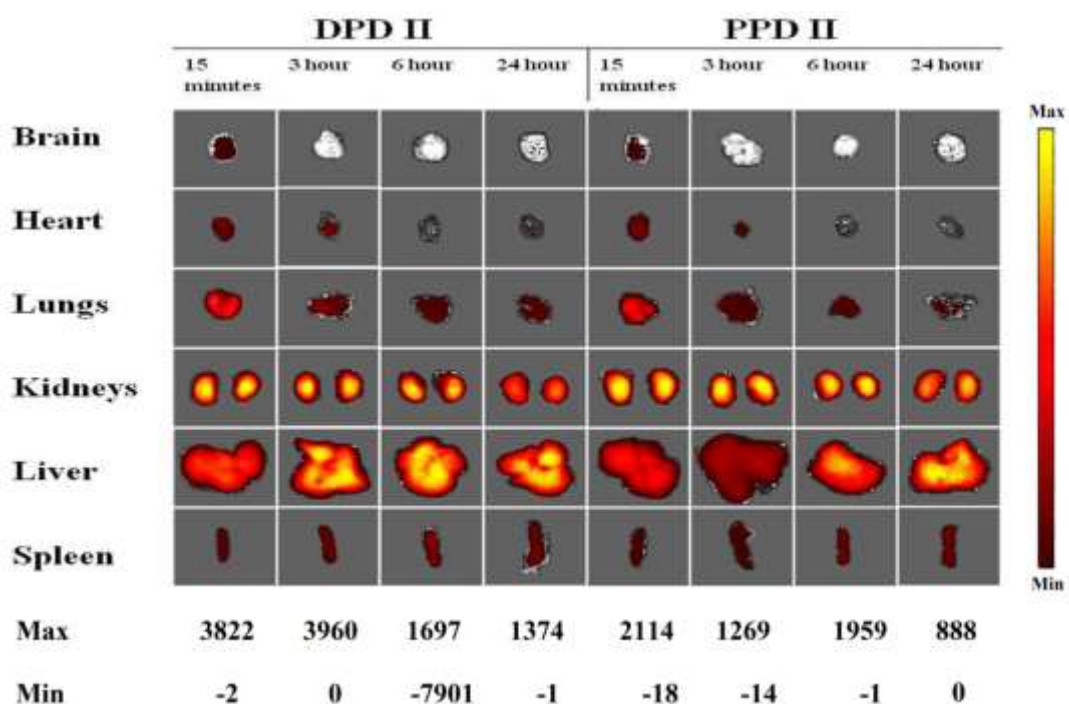


Figure 66: Biodistribution of DEAEM derivatives in BALB/c mice at 4 different time periods.

5. Discussion

5.1 Cationisation of polysaccharides – Pullulan & Dextran

Polymeric vector intended for gene delivery should possess enough cationic charge density in order to condense the negatively charged DNA. The cationic charge is also essential for proper cellular internalisation as the plasma membrane of the cell is negatively charged. Herein, the polysaccharides pullulan and dextran were modified with PEI in order to provide the cationicity required for DNA condensation and also to assist in cellular internalisation. PEI was grafted to these polysaccharides (pullulan and dextran) at the weight ratio 1:2.5 by using CDI as the coupling agent. CDI introduces carbonyl group to the oxygen atom of hydroxyl group present in the polysaccharides which then attacks primary amino group present in the PEI to form the carbamate linkage. PEI to polysaccharide weight ratio is very critical as it determine the properties of the grafted polymer. If the PEI grafting density is higher, then the resulting polymer turns to be cytotoxic and if it is lower, then it adversely affects their transfection efficiency. Following many standardisation studies, PEI to polysaccharide weight ratio was optimised as 1:2.5 since CPs exhibit appreciable level of transfection efficiency with minimum cytotoxicity at this weight ratio.

The total free amino groups present in the CPs were determined by the copper sulphate assay. Amino groups present in the CPs were directly proportional to the PEI grafting density and the naive polysaccharides – pullulan and dextran does not possess any amino groups of their own. So by determining the amino groups present

in the CPs, the grafting density of PEI in DP and PP can be calculated and it was found to be $26.56 \pm 0.8\%$ and $29.73 \pm 0.47\%$ respectively.

Grafting of PEI to the polysaccharides - dextran and pullulan was further confirmed by FTIR and NMR spectroscopy. In FTIR spectra, the appearance of shoulder like bands at 1654 cm^{-1} , 1566 cm^{-1} in DP and 1638 cm^{-1} , 1571 cm^{-1} in PP corresponding to the carbamate linkage confirms the grafting of PEI (figure 1). NMR spectra of DP and PP further confirm the grafting of this polymer to these polysaccharides (figure 2). In these spectra, appearance of additional peaks over 2.5 ppm to 2.8 ppm, corresponds to the resonance of protons in the methylene groups of PEI moiety, which confirms its conjugation to these polymers.

Polymeric gene delivery vector exploits endocytosis as the major route of cellular internalisation. Initially, these vectors are entrapped in early endosomes where the pH drops from neutral to acidic pH 6 and once they get matured into late endosomes, the pH further drops to 5-6 by the action of ATPase proton pump. These late endosomes then fuse with lysosomes that containing hydrolytic enzymes and here the pH further reduces to 4.5 facilitating substrate denaturation and subsequent degradation. So, the prerequisite for an ideal gene delivery vector is that it should resist the drop in pH within these endosomes and also should escape from these compartments before their fusion with lysosomes (Jones *et al*, 2013b; Sun *et al*, 2013). The primary, secondary and tertiary amino groups present in the PEI offers excellent buffering capacity over the wider pH range especially between 7.5 and 3. The unprotonated amino groups present in the PEI act as proton sponge that absorbs excess protons present in the endosomal compartment as a part of their acidification.

This triggers ATPase proton pump to import more protons into the lumen of endosome in order to maintain its pH. The electrical neutrality was maintained by the subsequent inflow of counter ions (Cl^{-1} ions). This influx of ions elevates the osmotic pressure prevailing within the endosomes that finally leads to their swelling and eventual rupture (Behr, 1997; Benjaminsen *et al*, 2013).

Titration study revealed that CPs exhibits much lower buffering capacity when compared to that of PEI alone and this could be attributed to the reduction/masking of the amino groups by these polysaccharide modifications (figure 3). However, these CPs exhibit appreciable levels of buffering capacity over the endosomal pH range i.e. 6.5 to 5. Although, the efficient buffering capacity of cationic polymer is essential for the endosomal release of polyplexes into the cytoplasm, there are some published reports in which reduced buffering capacity also favours the *in vitro* gene transfection. In a study conducted by Forrest *et al*, they found that altering the protonation properties of PEI (25 KDa) by acetylation decreases its buffering capacity and pKa but still this modification greatly enhances the transfection efficiency of the polymer (Forrest *et al*, 2004). Similar results were obtained in a study conducted by Jun Sun *et al*, in which they modified PEI (25 KDa) with poly-(2-methacryloyloxyethyl phosphorylcholine) (PMPC) via tert-butyl hydroperoxide (TBHP) -initiated polymerization reaction. They found that, although this grafted polymer exhibits reduced buffering capacity, their transfection efficiency was higher in the presence of serum as compared to that of PEI alone (Sun *et al*, 2013).

Cationic polymers without any targeting ligands enter the cell via non specific endocytosis mechanism. Size and surface charge potential of the polyplexes plays an

important role for this type of entry. The size requirement for this type of endocytosis varies along with different cell lines, but for most cell types, it is of the order of 200 nm or less (Jones *et al*, 2013b; Zauner *et al*, 1998). As far as polymeric gene delivery systems are concerned, their ability to form complexes with nucleic acid and thereby condensing them into compact structures (polyplexes) is the first and foremost criteria for efficient gene delivery (Namvar *et al*, 2015). Polymers interact with DNA through electrostatic interactions and they form nanosized particles called polyplexes. The particle size of these polyplexes depends on various factors like the polymer to DNA weight ratio, pH, temperature and also the media used for their preparation. Herein, the hydrodynamic sizes of the polyplexes of PEI and CPs formed with ctDNA in aqueous media were analysed by dynamic light scattering experiments. PEI condenses DNA more effectively which was evidenced by the formation of < 80 nm sized polyplexes even at the lower polymer to DNA weight ratio i.e. 1:1 (figure 4.A). Moreover, the poly dispersity index (PDI) values of these polyplexes lie between 0.1 and 0.3 which indicates the formation of more homogenous populations. Polyplexes of CPs are found to possess larger size when compared to that of PEI and this may be due to the masking of its cationic charge by these polysaccharides (pullulan and dextran). However, hydrodynamic size of the polyplexes formed with CPs found to be decreasing with the increase in the polymer to DNA weight ratio. DP and PP form polyplexes of size below 90 nm at the weight ratio 5:1 and this values lies within the required range for the effective cellular internalisation happening via endocytosis.

CPs and PEI condense anionic DNA through electrostatic interactions. Zeta potential measurements revealed that the ionic complex formation of cationic polymers with ctDNA neutralises their negative charge and converts to positive for the polyplexes prepared at the higher polymer to DNA weight ratio. Nanoplexes developed with PEI exhibited positive zeta potential even at the lower weight ratio i.e. 0.5:1 and this value was found to be stable since no further increase in zeta potential observed at the addition of excess polymer (Figure 4.B). These results infer that amino group present in the PEI are capable of neutralising twice its amount DNA and also to render positive charge to these polyplexes. In the case of DP, zeta potential remains negative till the weight ratio 1:1 and after that, it shoots up abruptly to a positive zeta potential of 14.8 mV at the weight ratio, 2:1. Thereafter a moderate increase in zeta potential is observed for the further addition of polymer. Similarly, PP exhibit negative zeta potential at the weight ratio of 0.5:1 and it turns out to be slightly positive at the weight ratio 1:1. Zeta potential of these polyplexes increased steeply at the weight ratio 2:1, after that only a slight increase is observed for the polyplexes prepared at the higher polymer to DNA weight ratios. These results infer that anionic DNA rapidly get neutralised by CPs at the weight ratio 1:1 after that the addition of excess polymer rapidly over charges these polyplexes. The weight ratio at which these cationic polymers form stable, smaller sized, homogenous populations with positive zeta potential was optimised for further studies and it was 5:1 for CPs and 2:1 for PEI.

The stability of the polyplexes formed by the PEI and CPs with ctDNA was analysed by agarose gel electrophoresis. The binding strength between the polymer and the

DNA depends on the number of charges per molecule that is involved in binding and also the charge distribution over the polymer chain i.e. the charge density (Strand *et al*, 2005; Geall & Blagbrough, 2000; Zelikin *et al*, 2002; Vijayanathan *et al*, 2005). Gel retardation assay reveals that PEI and CPs form tight complexes with ctDNA as they completely retard the mobility of latter under an external electric field even at the weight ratio, 0.5:1 (figure 5). The association strength between these cationic polymers and DNA was very strong that it prevents the access of EtBr to intercalate with DNA. As a result, the presence of DNA was not visible even in the wells. Stability of these polyplexes was also evaluated in the presence of plasma proteins. As these proteins are anionic in nature, there is a possibility to compete with DNA for polymer binding and thereby displacing DNA from these complexes. In this study, both PEI and CPs form tight complexes with ctDNA as a result these polyplexes are quite stable even in the presence of plasma proteins. However, there was slight DNA leach out in the lane loaded with polyplexes of CPs prepared at the weight ratio, 0.5:1 and this may be due to the formation of loose complexes at these lower weight ratios.

The stability of CP polyplexes prepared with ctDNA at various weight ratios were also evaluated in the presence of DNase I enzyme. Gel retardation assay reveals that CPs form tight complexes with DNA and they protect the latter from the degradation caused by the nuclease enzyme (figure 6). However, nanoplexes of CPs prepared at the lower weight ratio i.e. 0.5:1 show slight degradation as thin smear appears in this lane. On the other hand, the naked DNA treated with this enzyme shows complete degradation. DNase treated ctDNA appear as band in the gel rather than as smear

and that indicates its degradation. These results were counter checked by performing agarose gel electrophoresis and this time, heparin was added to the remaining polyplex solution. Heparin, the anionic glycosaminoglycans destabilize these polyplexes by competing with DNA for binding with polymer and thereby causing the release of DNA from these polyplexes by lowering their electrostatic interactions (Vader *et al*, 2012). Polyplexes of CPs treated with heparin releases the intact DNA which further confirms that these polymers protect DNA from the nuclease degradation.

Interaction with plasma proteins is one of the major hurdles that are encountered by the polymeric gene delivery vectors under the *in vivo* conditions. A wide variety of proteins present in the serum, found to possess ability to bind with these polymeric vectors and thereby determining their fate. Some of these interactions either inhibit the biological activity of these vectors or sequester them for degradation and/ or removal (Gottfried & Dean, 2013). Some of the proteins that is present in the plasma play a key role in binding with these vectors and that include albumin, immunoglobulins, fibronectin, apo lipoproteins, complement system, C-reactive protein, and b2-glycoprotein (Semple *et al*, 1998). Proteins interactions with cationic polymers (PEI and CPs) were studied by performing native PAGE. This analysis was carried out after incubating cationic polymers with plasma and the results were compared with that of the negative control, saline. PEI shows strong interactions with plasma proteins as most of the protein bands are missing when compared to that of the saline (figure 7). In a study conducted by Zhong *et al*, they identified about 41 proteins in the blood plasma that found to possess some sort of interactions with

PEI (Zhong *et al*, 2013). However, in CPs, these interactions are reduced to the greater extent and this may be due to the stealth effect offered via polysaccharide modification (Guhagarkar *et al*, 2010; Doh & Yeo, 2012; Rekha & Sharma, 2011b). The non ionic, hydrophilic nature of polysaccharides (dextran and pullulan) enhance the blood circulation time of CPs by preventing unwanted interactions with serum proteins (Doh & Yeo, 2012; Passirani *et al*, 1998).

One of the major drawback of PEI based gene delivery vector is their inherent cytotoxicity owing to their higher cationic charge density (Fischer *et al*, 1999; Florea *et al*, 2002). Moghimi *et al*, studied the molecular basis behind the PEI mediated cytotoxicity. They proposed a two step mechanism for PEI mediated toxicity. Phase I is the immediate response that occurs after 30 min post transfection. Here, early necrotic like changes occurs – loss of membrane integrity, release of lactate dehydrogenase enzyme and the exposure of phosphatidyl serine group from the inner membrane towards outside. Phase II is the delayed one that occurs after 24 h post transfection and here mitochondrially mediated apoptotic response occurs. Here, PEI interacts with mitochondrial membrane and induces channel through which cytochrome C get released. This in turn activates the executioner caspase 3 that triggers the apoptosis (Moghimi *et al*, 2005a).

In this study, cytocompatibility of the cationic polymers (PEI and CPs) and their polyplexes were analysed both in normal (L929) as well as cancer cell lines (C6 and HeLa). As expected, PEI found to be toxic in all these cell lines tested even at the lower polymer concentration (figure 8). On the other hand, CPs exhibit toxicity only at higher concentrations in C6 and L929 cells while they are quite compatible with

HeLa cells even at their higher polymer concentrations. These cationic polymers exhibit cell type dependent cytocompatibility. Normal cell lines are usually more sensitive to chemicals when compared to that of cancerous or transformed cell lines (Sarmiento & Neves, 2012). Hence L929 cells are more vulnerable to the toxic effects of these cationic polymers when compared to that of the cancerous cell lines. Moreover, in a study conducted by Williams *et al*, (2005) they found that cell proliferation rate plays a significant role in determining their sensitivity to toxic chemicals. Cells with higher doubling time found to be more resistant to toxic materials (Williams *et al*, 2005a). Among C6 and HeLa cells, the latter exhibits higher doubling time and hence they are more resistant to toxic chemicals when compared to that of the former.

However, the polyplexes prepared from these cationic polymers with ctDNA at the optimised weight ratio (2:1 for PEI and 5:1 for CPs) found to be cytocompatible in all the three cell lines tested. This may be due to the reduction in the cationic charge density of the polymer by their binding with DNA.

Cellular internalization of the polyplexes is the next important barrier that determines the transfection efficiency of these polymeric gene delivery systems. Depending on the cell type and also the nature of the cargo (polyplex size and zeta potential), cellular uptake of these polyplexes occurs via different routes. Most common route for the internalisation of positively charged macromolecules has been reported to occur via pinocytosis or fluid-phase uptake. Of these, polyplexes having size above 1 μ m enters via macropinocytosis while that having ≤ 120 nm and ≤ 90 nm sizes enter the cell through clathrin-mediated and caveolin-mediated endocytic

mechanisms respectively (Conner & Schmid, 2003; Doherty & McMahon, 2009; Rejman *et al*, 2005a; Evans *et al*, 2011). Endocytosis of the polyplexes of PEI initiated by their binding to syndecans, the negatively charged heparin sulfate proteoglycans (HSPGs) that present in the cell membranes (Poon & Gariépy, 2007; Pichon *et al*, 2010; Demeneix & Behr, 2005). This in turn activates actin filaments that subsequently help in the uptake of these polyplexes through endocytic vesicles.

Cellular uptake of PEI and CPs was studied in the cancer cell lines (C6 and HeLa) by preparing polyplexes at their optimised weight ratios (2:1 for PEI and 5:1 for CPs) using YOYO I tagged ctDNA. In these cell lines, good cellular internalisation observed for the polyplexes of both PEI and CPs (figure 9). However, the cell morphology gets disrupted for the cells transfected with PEI and this may be due to the inherent toxicity exhibited by this polymer owing to their higher cationic charge density. On the other hand, presence of polysaccharide in CPs reduced the toxic effect of PEI to a greater extent. Moreover, it was also observed that tagged DNA enter into the nucleus while transfecting with these cationic polymers. In order to establish whether DNA alone get into the nucleus or it enters along with these polymeric vectors, cellular uptake experiments were repeated using TRITC tagged cationic polymers. These results reveal that, polyplexes of PEI as such get into the nucleus owing to their membrane permeabilising effect (Prevette *et al*, 2010; Grandinetti *et al*, 2012b). On the other hand, cells transfected with polyplexes of CPs, DNA alone get into the nucleus while the polymer remains in the cytoplasm (figure 10). These results infer that the vector unpacking happens in the cytoplasm for the cells transfected with CPs. This vector unpacking could be attributed to

destabilisation of these polyplexes by their interactions with anionic proteins that present in the cytosol (Chen *et al*, 2008; Okuda *et al*, 2004).

The success of gene delivery vectors relies on how efficiently the delivered gene gets expressed. In this study, gene expression was studied using p53 plasmid whose expression leads to apoptosis of the cancer cells. Live and dead cells in the cell culture plate were distinguished by differential staining with Calcein AM and ethidium bromide respectively. Cellular death destabilises the plasma membrane which in turn allows the ethidium bromide to get into the cell and produces red fluorescence by binding with the cellular DNA. On the other hand, live cell emits green fluorescence by the action of intracellular esterase. This enzyme cleaves the acetoxy methyl group that is present in the hydrophobic Calcein AM and produces highly fluorescent, hydrophilic calcein. CPs and PEI exhibit good transfection efficiency in both C6 and HeLa cells which was evidenced by the presence of dead cells (figure 11). However, the toxic nature of PEI may also contribute for the death of the cells transfected with polyplexes of this polymer (Prevette *et al*, 2010; Grandinetti *et al*, 2012b).

Annexin V staining was done in order to confirm whether the death that occurred in the cells transfected with nanoplexes of cationic polymer prepared with p53 plasmid was brought about by the induction of apoptosis. Annexin V detects early apoptotic cells where the plasma membrane remains intact and prevents the entry of propidium iodide while their cell membrane phospholipids asymmetry will be lost. At this stage, the phosphatidyl serine which is usually present in the inner leaflet of the plasma membrane, facing the cytoplasm flips to the outer surface. FITC tagged annexin V

bind to this early apoptotic marker in the presence of divalent ions like Ca^{2+} and produces fluorescence. Annexin V staining revealed that HeLa cells transfected with PEI undergoes apoptosis more effectively when compared to that of CPs as most of these cells exist in late apoptotic stage (figure 12). On the other hand, cells transfected with CPs contains almost equal number of early and late apoptotic cells. Moreover, the percentage of live cells also higher for CPs when compared to that of PEI. This study reveals that transfection efficiency was higher for PEI which was followed by PP and the order is $\text{PEI} > \text{PP} > \text{DP}$.

To summarize, polysaccharide modification reduces the strong interactions of PEI with plasma proteins and also improves the cytocompatibility of this cationic polymer. However, these CPs still exhibit toxicity at higher polymer concentrations and interactions with plasma proteins are not fully addressed.

5.2 Ethylene glycol dimethacrylate (EGDMA) cross linked cationised polysaccharide for gene delivery

When it comes to polymeric gene delivery vectors, the balance between cytotoxicity and transfection efficiency is the major issue that should be addressed for their success in gene therapy (Godbey *et al*, 1999a; Boussif *et al*, 1995b). PEI is considered as one of the golden standards among the various polymeric gene delivery vectors developed as they exhibit higher transfection efficiency (Godbey *et al*, 1999b; Kichler, 2004a). However, their higher cationic charge density imparts toxicity to this polymer that limits their use as a gene delivery vector. It was reported in the literature that molecular weight plays an important role in the determination of

their cytotoxicity and transfection efficiency of this polymer (M. Laird Forrest *et al*, 2003; Patnaik *et al*, 2010). High molecular weight PEI (i.e. 25KDa) is found to transfect cells more effectively when compared to that of lower molecular weight PEI (2000 Da). However, the former exhibit poor cytocompatibility when compared to that of the later. (Dong *et al*, 2007b) tried to address these issues by combining the advantages of both low and high molecular weight PEI by cross linking 2000 Da PEI to high molecular structures using ethylene glycol dimethacrylate (EGDMA) (Dong *et al*, 2007b). Ester bond that is present in the EGDMA cleave at the physiological conditions and thereby reverting back to the cytocompatible low molecular weight counterparts. Hence, by cross linking cationised polysaccharide with EGDMA, cytocompatibility of this cationic polymer may be improved without altering its transfection efficiency.

EGDMA cross linked pullulan PEI (PP) was synthesised by Michael addition reaction using CAN as catalyst at two different weight ratios (0.01:10 and 0.015:10). Similarly EGDMA cross linked dextran derivatives were also synthesised. However, these dextran derivatives were found to be insoluble due to extensive cross linking. Chemical structure of the PPE derivatives was then studied by FTIR and NMR spectroscopy. In the FTIR spectrum of PPE, the –N-H bending and –C=O stretching vibrations of carbamate linkage owing to the PEI grafting to pullulan appears in the region 1647 cm^{-1} and 1541 cm^{-1} respectively (figure 13). The FTIR band corresponding to the ester group of EGDMA was found to overlap with the carbonyl group present in the carbamate linkage of the parent chain. It was reported in the literature that the ester peak which is expected to occur around 1740 cm^{-1} may shift

to the lower wave numbers and overlaps with vibrations of carbonyl group in the carbamate linkage i.e. around 1650cm^{-1} owing to the hydrogen bonds of the later (Coleman *et al*, 1994; Wang *et al*, 2017). However, the NMR spectrum confirms the crosslinking of this vinyl monomer to the PP. In this spectrum, shift at 4.688 ppm corresponds to the protons present in the methylene group that is attached to the ester carbon of the EGDMA (figure 14). The shifts between 3.01 and 3.2 ppm contributed by the protons in the methylene group that connecting PP with EGDMA.

Amino groups present in the PP were the cross linking sites of the EGDMA derivatives. Hence the cross linking percentage of EGDMA moieties can be determined indirectly by estimating the percentage reduction in the amino groups that present in the PP by their cross linking. Amino groups present in the EGDMA derivatives were estimated by copper sulphate assay. Cross linking percentage was then calculated by comparing the amino groups present in the EGDMA with that of the parent chain, PP and it was found to be 1.9%, 2.36%, for PPE I, PPE II derivatives respectively.

Polymeric gene delivery vectors without any targeting ligand enter the cell via non specific endocytotic mechanism. Once the polyplexes get internalised by this pathway, they experience drop in pH within the endosomal compartment. During the maturation process of these endosomes, acidic pH further drops and they finally fuse with lysosomes that containing hydrolytic enzymes. So escape from this endosomal compartment is very critical for efficient gene delivery of polymeric vectors. PEI based cationic polymers act as proton sponge and absorb the excess protons prevailing within this acidic compartment. So, in order to maintain the homeostasis,

ATPase pumps present in the endosomal membrane translocate more protons into the lumen. This, in turn, triggers the influx of chloride ions and water molecules into this compartment which leads to the osmotic swelling and subsequent rupturing of this endosomes. This sequence of events finally causes the release of the polyplexes into the cytosol (Lin & Engbersen, 2008; Varkouhi *et al*, 2011). So polymeric vectors intended for gene delivery should possess buffering capacity over the acidic pH in order to resist pH drop experienced in this compartment and also for their release into the cytosol. In this present study, even though, EGDMA cross linking reduces the amino groups, the buffering capacity of these PPE derivatives does not get affected. PPE derivatives exhibit almost similar buffering capacity as that of their parent chain, PP (figure 15). This may due to the cleavage of ester bond that present in the EGDMA cleaves at this acidic pH and thereby reverting back to their original state, i.e. PP (Dong *et al*, 2007b; M. Laird Forrest *et al*, 2003).

Polymer/DNA complex size plays an important role in the endocytosis and efficient gene transfection of the polymericvectors. Previous reports suggest that for the efficient endocytosis of polyplexes, small and compact complexes of below 200 nm size was found to be optimum (Boussif *et al*, 1996; Godbey *et al*, 2000). Moreover,the particle size of polyplexes also determines their half-life in the systemic circulation andtissue distribution of these nanoplexes (Ahl *et al*, 1997; Kong *et al*, 2000; Prabha *et al*, 2002). EGDMA derivatives interact with ctDNA through electrostatic interactions and form more condensed structures called polyplexes. Dynamic laser light scattering experiments were carried out to determine the size distribution of these polyplexes prepared with ctDNA at six different weight

ratios. PPE I and PPE II derivatives exhibit a different pattern in their size distribution owing to their different cross linking percentage. PPE I show similar size pattern as that of the parent chain (PP) due to their lesser EGDMA cross linking percentage (figure 16.A). However, PPE II derivatives exhibit a different pattern in which nanoplex size was found to be decreased with the increase in the polymer to DNA weight ratio. This variation may be due to the difference in the molecular structure of these derivatives owing to different EGDMA cross linking percentages. Both these derivatives formed smaller sized polyplexes with lower PDI at the weight ratio, 5:1 which was chosen for further cell studies. At this weight ratio, PPE II form smaller sized particles as compared to that of PPE I.

Binding of EGDMA with ctDNA neutralises the negative charge of the later and form positively charged polyplexes at the higher polymer concentrations. Increase in the zeta potential was observed for PPE derivatives when polymer to ctDNA weight ratio increases from 0.5:1 to 5:1 (figure 16.B). At the lower weight ratios, polyplexes formed by these derivatives exhibit a negative zeta potential, however, after 2:1 weight ratio, a sharp rise in zeta potential was observed. The highest positive zeta potential was observed at the weight ratio 5:1 for the polyplexes of EGDMA derivatives. At this weight ratio, polyplexes of PPE I exhibited higher positive zeta potential as compared to the polyplexes of PPE II. The reason may be due to the greater reduction in the amino groups in PPE II caused by extensive cross linking of EGDMA when compared to that of PPE I derivative. The polymer to DNA weight ratio, 5:1 was chosen and optimised for further studies because at this weight ratio

both PPE I and PPE II derivatives form homogenous, smaller sized (below 150 nm), polyplexes having positive zeta potential of around 10 mV.

The efficiency of polymeric gene delivery vector depends on its ability to form stable complexes with DNA. This process is essential as it helps to deliver the intact DNA to the target cell by protecting the DNA from the degradation caused by the nucleases that present in the extracellular milieu. The stability of polyplexes formed by EGDMA derivatives was checked by performing agarose gel electrophoresis. Polyplexes of both PPE I and PPE II prepared at the higher weight ratios (i.e. from 2:1 onwards), retard the mobility of DNA towards cathode under an external electric field (figure 17). However, in these gels, DNA appeared as a smear, from the wells loaded with the polyplexes prepared at the lower weight ratios (i.e. 0.5:1 and 1:1). These results reveal that EGDMA derivatives effectively neutralise the anionic nature of ctDNA and form stable complexes at the higher polymer to DNA weight ratio. At the lower weight ratios, the polyplexes formed are loosely bound and possess negative zeta potential. As a result, polyplexes prepared at these weight ratios fail to retard the mobility of the DNA under the electric field. Stability of these nanoplexes was also analysed in the presence of plasma proteins. Owing to the anionic nature of the plasma proteins, interactions of the nanoplexes with these proteins may cause the displacement of DNA from the loosely bound complexes. As expected, DNA leached out from the wells loaded with polyplexes prepared at the lower weight ratio (i.e. 0.5:1 and 1:1). In addition, the polyplexes that prepared at the weight ratios 2:1 and 3:1 also failed to retard the mobility DNA under the electric field. Irrespective of their positive charge, polyplexes prepared at the 3:1 ratio failed

to retard the mobility of DNA. One of the possible explanations for this observation is that the primary amino groups present in the surface of PP largely get reduced by EGDMA cross linking (Nouri *et al*, 2017). Hence, these polymer derivatives are required in an excess amount to fully condense the DNA molecules. Even though, positive zeta potential observed at the weight ratio, 3:1, the concentration of these polymer molecules is not sufficient for the efficient condensation of DNA molecules. This leads to the formation of large sized, unstable complexes at this weight ratio. Hydrodynamic size data further supports this observation. Hence, EGDMA derivatives form stable complexes with ctDNA only at higher weight ratios (i.e. 4:1 and 5:1).

Stability of polyplexes in the systemic circulation and their half life depends on their interactions with the plasma proteins. So, protein-polymer interactions of EGDMA derivatives with plasma proteins were studied by performing polyacrylamide gel electrophoresis. From the results, it was clear that EGDMA cross linking prevents interactions with plasma proteins and the protein bands were remained intact as that of the negative control, saline (figure 18). However, PPE I owing to their lesser crosslinking percentage, show slight interactions with plasma proteins. Due to their higher cationic charge density, positive control PEI show strong interactions with plasma proteins. Non specific interactions with proteins occur as a result of the formation of hydrogen bonds, charge interactions or non polar interactions (Ross & Subramanian, 1981). Hydrophilic nature of polysaccharides (pullulan and dextran) minimise these non specific interactions to an extent. However, as evidenced from the plasma protein interactions studies of CPs (section 4.1.9), polysaccharide

modifications do not completely eliminate the problem. It is reported in the literature that ethylene glycol moieties have inherent capacity to avoid non specific interactions with proteins (Charles *et al*, 2009; Xu *et al*, 2008). Hence by cross linking pullulan PEI (PP) with EGDMA helps to improve the blood circulation time.

One of the major drawbacks of using cationic polymers as gene delivery systems is their inherent toxicity owing to their higher charge density. The cytotoxic effects of these cationic polymers are usually associated with their interactions either with plasma membranes or with the anionic cellular components and proteins (Moghimi *et al*, 2005; Kafil & Omid, 2011; Xiong *et al*, 2007). Hence, cytocompatibility of EGDMA derivatives was evaluated in three different cell lines – C6, HeLa and L929 cells. Here, the metabolic activity of these cells was analysed in the presence of EGDMA derivatives at four different concentrations using MTT assay. Exposure of the cells to these derivatives exhibited above 75% cell viability in all the three cell lines tested (figure 19). PPE I and PPE II exhibit almost similar cytocompatibility in C6 and HeLa cell lines. However, in L929 cells percentage cell viability is slightly higher for PPE I derivatives when compared to that of PPE II. It is reported in the literature, that the molecular weight, cationic charge density and also the arrangement of cationic groups in the three dimensional matrix all together contributes for the cell damaging effects of the cationic polymers (Fischer *et al*, 2003b). However, cross linking with EGDMA moieties greatly improved the cytocompatibility of the cationised pullulan.

Once the polyplex reaches the target cell, then the semi permeable nature of plasma membrane pose another significant barrier for its entry into the cell. Cationic

polymers without any targeting ligand enter the cell via interactions with anionic proteoglycans such as heparin sulphate proteoglycans (HSPG) that is present in the cell membrane (Poon & Gariépy, 2007; Pichon *et al*, 2010; Demeneix & Behr, 2005). Transfection efficiency of the polymeric gene delivery vector depends on how readily it get internalised into the cell and delivered the gene of interest to the target site for its expression. Hence, cellular internalisation of EGDMA derivatives was studied in both C6 and HeLa cell lines by preparing polyplexes with YOYO I tagged ctDNA at the optimised weight ratio 5:1. Both PPE I and PPE II readily get internalised into C6 cells, however, poor cellular uptake observed for HeLa cells (figure 20). Cellular internalisation of non targeted nanoplex occurs via endocytosis which is an active process. However, this step is preceded by the passive adsorption of particles on to cell surface. Differential cellular uptake in C6 and HeLa cells can be explained based on the difference in the composition of the plasma membrane and glycocalyx in these cell lines (Zhang *et al*, 2019; Kettler *et al*, 2014). Moreover, EGDMA cross linking also prevent the interaction with most of the proteins and that was evidenced by the plasma protein interaction studies. Hence this property of EGDMA derivatives may prevent their interactions with proteins present in the cell surface of the HeLa cells and thereby blocking their entry in this cell line.

Transfection efficiency of EGDMA was also evaluated in these cell lines (C6 and HeLa) using therapeutic gene, p53 plasmid. The expression of these plasmids leads to apoptosis in cancer cells while causes reversible cell cycle arrest in the normal cells. For this analysis, cells were transfected with polyplexes prepared with p53 at the weight ratio 5:1 and incubated for 24h. Post transfection, live and dead cells in

the culture plate were distinguished by differential staining using calcein AM and EtBr that stains these cells with green and red fluorescence respectively. PPE I and PPE II derivatives exhibit almost similar transfection efficiency in C6 cells which was also quantified by flow cytometry analysis (figure 21 & 22). As expected, owing to their poor cellular uptake, these derivatives exhibited poor transfection efficiency in HeLa cells. To summarize, EGDMA modification improves the cytocompatibility of CPs and minimizes the protein interactions. These derivatives exhibit good cellular uptake and transfection efficiency in C6 cells while that get compromised in HeLa cells by this modification.

5.3 [2- (acryloyloxy) ethyl] trimethylammonium chloride (AOETMAC) grafted cationised polysaccharides for gene delivery

[2- (acryloyloxy) ethyl] trimethyl ammonium chloride (AOETMAC) is a cationic, amphoteric molecule containing pH-independent cationic head (quaternary ammonium) and a reactive acryloyl group. Grafting of this vinyl monomer to the chitosan molecule offers pH dependent swelling properties to this matrix (Lee *et al*, 2011). Moreover, the antifouling and antibacterial properties of this vinyl monomer makes it attractive in the field of biomedical sciences (Deng *et al*, 2016). [2- (methacryloyloxy) ethyl] trimethyl ammonium chloride (MAETAC) based hydrogels developed by Mishra *et al*, for targeted drug delivery in colon cancer cells. The pH responsive hydrogel was synthesized by simple redox copolymerization reaction between MAETAC and polymethacrylic acid (PMAAc) and loaded with anticancer drug, 5- fluorouracil. They observed effective killing of human colon cancer cell lines by these drug loaded hydrogels (Mishra *et al*, 2014).

AOETMAC grafted cationised polysaccharides were synthesised at three different ratios viz 0.01:10, 0.015:10 and 0.0025:10 via Michael addition reaction to synthesis six different derivatives which are DPA I, DPA II, DPA III, PPA I, PPA II and PPA III respectively. Chemical structure of these AOETMAC derivatives were analysed by FTIR and NMR spectroscopy. In FTIR spectra, bands corresponding to the C=O stretching and –NH bending that present in the carbamate linkage of the parent chain occurs at 1638 cm^{-1} and 1567 cm^{-1} in DPA while around 1650 cm^{-1} and 1560 cm^{-1} in PPA (figure 23). FTIR bands corresponding to the functional groups of the AOETMAC molecules i.e. carbonyl stretch and the quaternary amino group found to overlap with that present in the parent chains (DP and PP). Hence, no new bands appeared in the FTIR spectra of these AOETMAC derivatives in response to the grafting of this monomer unit. However, in NMR spectra, the grafting of AOETMAC monomers were confirmed by the appearance of the shift around 3.2 to 3.3 corresponding to the protons of methyl groups that present in $-\text{N}^+(\text{CH}_3)_3$ (quaternary ammonium group). Moreover, that around 3.52 attributed by the protons present in the methylene group connected to the quaternary ammonium group (figure 24).

Grafting of AOETMAC molecules occurs at the primary amino group present in the parent chain. Hence, the grafting density of this monomer molecule was estimated indirectly by determining the reduction in the amino group by copper sulphate assay. It was found to $4.16 \pm 0.78\%$, $5.29 \pm 0.6\%$, $2.96 \pm 0.34\%$, $4.66 \pm 0.14\%$, $5.05 \pm 1.07\%$, $1.23 \pm 0.57\%$ for DPA I, DPA II, DPA III, PPA I, PPA II and PPA III respectively.

Once the nanoplex get internalised through endocytic pathway, then its release from the endosomes is one of the major hurdles that should be faced by the polymeric vectors for efficient gene delivery. Maturation of endosomes causes their fusion with lysosomes that contain digestive enzymes which degrade the nucleic acids. So escape from this endosomal compartment before its fusion with lysosomes is an inevitable step for an ideal gene delivery vector. Proton sponge mechanism is the widely accepted postulate that explains the release of cationic polymers from the endosomal compartments. According to this hypothesis, cationic polymers act as a proton sponge that absorbs excess protons prevailing within this acidic compartment. This in turn results in the osmotic swelling and rupturing of these vesicles and the subsequent release of polyplexes to the cytoplasm. Hence, polymeric vectors intended for gene delivery should possess buffering capacity over the pH, 7-5 in order to buffer the acidic environment that prevailing within the endosomal compartment and also for their release into cytosol.

Buffering capacity of AOETMAC derivatives was analysed over the pH range 10 – 4 by acid - base titration method (figure 25). Irrespective of the reduction in amino groups caused by the grafting of AOETMAC molecules, these polymer derivatives exhibit higher buffering capacities, especially over the pH range 7-10 as compared to that of parent chains (i.e. DP and PP). However, at the acidic pH (i.e.7-5), the buffering capacities of these polymer derivatives were almost similar to that of the parent chains. One possible reason for this observation was that the introduction of zwitter ionic molecules (AOETMAC) into the CPs may causes swelling of these polymer derivatives in a pH dependent manner. During its swelling, more amino

groups get exposed onto the surface and that resist the change in the pH by the addition 0.01N HCl. In a study conducted by Lee *et al*, (2011), found that chitosan undergoes pH dependent swelling while grafted with AOETMAC. This chitosan derivative swells both at higher and lower pH. They hypothesised that swelling of the polymer occurs at the result of electrostatic repulsion between quaternary ammonium group in AOETMAC molecules and protonated amine cations in the chitosan. The strength of electrostatic repulsion depends on the type and concentration of counter anion in the surrounding medium (Lee *et al*, 2011).

Nanoplex size and zeta potential are another two major parameters that determines cellular uptake, blood circulation time and toxicity. Nanoplexes were prepared with ctDNA at six different weight ratios (0.5:1, 1:1, 2:1, 3:1, 4:1 & 5:1). Net surface charge and binding affinity of carrier towards DNA are the two important factors that determine the size of the nanoplexes (Tang *et al*, 2014b). Net surface charge on the polyplexes prevents aggregation by electrostatic repulsion.

Polyplexes formed with AOETMAC derivatives found to decrease with increase in the polymer to DNA weight ratio (figure 26.A). This observation was in accordance with previous reports (Tang *et al*, 2012, 2013). Particle size at lower weight ratios may be attributed by the uncomplexed AOETMAC derivatives or ctDNA molecules. Nanoplexes of these polymer derivatives tend to aggregate during the transition of negative to positive surface charge due to the weaker repulsion forces. Hence, larger sized nanoplexes formed at the weight ratio, 4:1 for all these AOETMAC derivatives except PPA III and DPA I. However, at the weight ratio 5:1, these polymer derivatives condense ctDNA and form nanoplexes around 150 nm. Although, the

polyplexes of these AOETMAC derivatives (except PPA III) exhibit negative zeta potential; at the weight ratio 5:1, they turn to be zero or slightly positive (figure 26.B). This could be attributed to the shielding of amino groups that is present in the parent chains (DP and PP) by the grafting of AOETMAC molecules. However, PPA III derivatives due to the lower grafting density of this vinyl monomer, they form positively charged nanoplexes even at the weight ratio 2:1.

Nanoplex stability of the AOETMAC derivatives was analysed by performing agarose gel electrophoresis. Nanoplexes were prepared from these polymer derivatives through electrostatic interactions with ctDNA. Strong interactions between polymer and DNA, retard the mobility of the later under an external electric field. Gel retardation assay reveals that whether the gene was shielded completely by the cationic polymer or just it exposed on the surface of the polyplex (Jana *et al*, 2016). As expected, all these AOETMAC derivatives except PPA III failed to retard the mobility of ctDNA even at the 5:1 weight ratio (figure 27). Negative zeta potential of the polyplexes contributes for the poor DNA condensation capability of AOETMAC derivative. However, PPA III owing to their positive zeta potential retards the mobility of the ctDNA from the polyplexes prepared at higher weight ratios (i.e from 2:1 ratio onwards). Nanoplex stability also analysed in the presence of plasma proteins and these results were also similar to that of the nanoplexes alone (figure 28).

Plasma protein interactions with cationic polymers determine the fate of these vectors in systemic circulation. Some of these interactions cause rapid removal or degradation of these polymeric vectors (Gottfried & Dean, 2013). So in order to

improve the transfection efficiency under *in vivo* conditions, polymeric vectors should be designed in such a way to minimize interactions with plasma proteins. Grafting of AOETMAC molecules to the CPs greatly improved their compatibility with plasma proteins as these molecules have antifouling properties (Krishnamoorthy *et al*, 2014). Native PAGE analysis revealed that AOETMAC derivatives show no interactions with plasma proteins and the protein bands were similar to that of the negative control, saline (figure 29). However, PEI, the positive control shows strong interactions with plasma proteins as most of the protein bands are missing in this lane.

Inherent toxicity is one of the major drawbacks faced by the cationic polymers as a gene delivery vector. Various factors like molecular weight, charge density, type of cationic centre, structure and conformational flexibility contribute for this toxicity of the cationic polymer (Sgouras & Duncan, 1990; Fischer *et al*, 2003b; Morgan *et al*, 1988). Higher cationic charge density is a boon and a curse to the cationic polymeric systems. As it is inevitable for their cellular internalisation for these polymer derivatives and at the same time it also causes cytotoxicity through unfavourable interactions with anionic plasma membrane (Moghimi *et al*, 2005; Kafil & Omid, 2011; Xiong *et al*, 2007). In this study, cationic charge densities of all these polymeric derivatives except PPA III were largely shielded by AOETMAC grafting and it was evidenced from the zeta potential measurements. These polymer derivative exhibits above 75% and 80% cell viabilities in C6 and HeLa cells respectively (figure 30). However, in C6 cells, PPA III derivatives were found to be toxic at higher polymer concentration and this may be attributed by the higher

cationic charge density of this polymer derivative. Cytocompatibility was also estimated in L929 cells using PPA I and DPA I as the representative polymers. Both these polymer derivatives exhibit above 80% cell viability even at higher polymer concentration. Cytocompatibility of the nanoplexes of these polymer derivatives was also evaluated in all the three cell lines (C6, HeLa and L929) by preparing polyplexes with ctDNA at the weight ratio 5:1. Nanoplexes of these polymer derivatives also found to cytocompatible and exhibit above 90% in all the three cell lines tested.

Cellular internalisation is the next important barrier that should overcome by the polymeric vectors for efficient gene delivery. The polymeric vectors without any targeting ligands enter cells via non specific endocytotic mechanism. Cellular internalisation of AOETMAC derivatives studied both in C6 and HeLa cell lines by preparing polyplexes with YOYO I tagged ctDNA prepared at the weight ratio 5:1. Irrespective of their negative zeta potential, the nanoplexes of these polymer derivatives readily get internalised in C6 cells (figure 31). However, in HeLa cells, these polymer derivatives (except PPA III) exhibit poor cellular internalisation (figure 32). The difference in structure and composition of plasma membrane and glycocalyx may contribute for this differential uptake in C6 and HeLa cell lines. Moreover, the first step in the cellular internalisation is the passive adsorption of nanoplexes onto the cell surface. But the antifouling nature of AOETMAC molecules may prevents the interactions with proteins that present on the HeLa cell surface (Krishnamoorthy *et al*, 2014). This may be one of the reasons for reduced uptake AOETMAC derivatives in HeLa cells. However, the cellular uptake of nanoplexes of

PPA III in HeLa cells suggests that magnitude of the cationic charge also contributes for the cellular uptake in these cells.

Transfection efficiency of AOETMAC derivatives studied using p53 plasmid whose expression causes apoptosis in cancer cells while brought reversible cell cycle arrest in normal cells. Irrespective of good cellular internalisation, the polyplexes of this polymer derivatives exhibit poor transfection efficiency in C6 cells as most of the cells remain alive in the culture plate transfected with the polyplexes of AOETMAC derivatives (figure 33). One possible explanation for this observation is that the cellular uptake studies were carried out using genomic DNA (ctDNA) which is in methylated form while transfection efficiency studied with unmethylated p53 plasmid. Moreover, the loose complexation of AOETMAC derivatives with DNA molecules makes it susceptible to the degradation by the digestive enzymes. Owing to their larger size and methylated nature, genomic DNA (ctDNA) resists the degradation caused by these digestive enzymes. On the other hand, unmethylated, smaller sized plasmid DNA (p53) was highly susceptible to this degradation (Singal & Ginder, 1999; Cheng, 1995). Moreover, AOETMAC derivatives exhibit good buffering capacity over the pH range 10 to 7 and not in the acidic pH which is essential for endosomal escape. The poor buffering capacity exhibited by these polymer derivatives causes their entrapment in the endosomal compartment once these nanoplexes get internalised. Hence, irrespective of good cellular internalisation observed in C6 cells, AOETMAC derivatives exhibit poor transfection efficiency. To summarize, AOETMAC modification improves the cytocompatibility of CPs, and reduces the interactions with plasma proteins. However, the poor complexation with

DNA, owing to their negligible cationic charge affects the transfection efficiency of these polymer derivatives.

5.4 Vinyl imidazole (VI) grafted cationised polysaccharides for gene delivery

Vinyl imidazole was grafted to the cationised polysaccharides in order to help in their endosomal escape by membrane destabilisation and also to improve their cytocompatibility. The imidazole ring possesses a pKa around 6 which helps these moieties to behave in a pH sensitive manner. At acidic pH, they exist in fully protonated form and that will improve the buffering capacity of the cationised polysaccharides (CPs) in the endosomal compartment. However at the physiological pH, these moieties are in the unprotonated state possessing negligible charge and this will cause the release of plasmid DNA once the nanoplex get released into the cytosol (Asayama *et al*, 2010b). This modification will also help to improve the cytocompatibility of the polymer. Vinyl imidazole grafted cationised polysaccharides (PPI and DPI) were synthesized at three different weight ratios through free radical addition reaction using CAN as the initiator. Chemical structure of these grafted polymers was then analysed by FTIR and NMR spectroscopy. In FTIR spectra, the characteristic bands around 1640 cm^{-1} and 1570 cm^{-1} corresponding to the C=O stretching and N-H bending of carbamate bond that present in the CPs gets reduced to the single band by the VI grafting (figure 34). These results infer that nucleophilic addition of VI moieties also occurs at the secondary amino groups that present in the carbamate linkage in addition to the primary amino groups present in the CPs. Moreover, the appearance of additional bands over the region, 668 cm^{-1} and 822 cm^{-1}

corroborated the presence of imidazole ring in these grafted polymers. These bands are corresponding to the puckering and out of plane bending vibrations of imidazole ring respectively (Talu *et al*, 2015; Lippert *et al*, 1985). ¹H NMR spectra (Fig.1) further confirms the grafting of VI to the CPs (figure 35). In these spectra, the appearance of shifts around 6-8 ppm corresponds to the imadazole ring while that around 2.5-2.8ppm are associated with the resonance of protons in the methylene group of PEI (-CH₂-CH₂-N-).The shifts around the region 3.4-4.0 ppm and 4.8-5.4 ppm are from the protons of anomeric carbons, C₂ to C₆and C₁ of hexose units respectively (Jiang & Salem, 2012b; Asayama *et al*, 2010b).

Nanoplex which get internalised via endocytic pathway experiences an acidic environment in the endosomal compartment. Once the endocytic vesicles get matures, they fuse with lysosomes containing degradative enzymes. So the nanoplex have to escape from this endosomal compartment before its fusion with lysosomes. For this, polymeric gene delivery vector should possess buffering capacity over the pH range 7-5 in order to resist the pH drop experienced in the endosomal compartment and also for their release into the cytosol. Imidazole and PEI moieties present in the VI derivatives buffers the acidic pH prevailing within the endosomal compartment and helps in the release of polyplexes into the cytosol by destabilising the membrane (Swami *et al*, 2007; Chen *et al*, 2002; Fischer *et al*, 2003a). However, the buffering capacity of the VI derivatives (figure 36) was found to be lower when compared to that of CPs (PP and DP). This lowered buffering capacity of VI derivatives might have resulted from the reduction in the protonable amino groups present in the parent chain by the VI modification. These results suggest that the VI

modification does not compensate fully for the reduction in primary and secondary amino groups present in the PEI by their grafting. Even though VI possesses pKa around 6.9, the amino groups present in the PEI exhibit stronger buffering capacity over the endosomal pH range as compared to that of the former. Among VI derivatives, DPI derivatives exhibit higher buffering capacity compared to that of the PPI derivatives. It can be explained based on the published reports in which the pKa value of PEI get reduced while modifying with bulky groups like cyclodextrin, lauryl groups due to their steric hindrance effect (Suh *et al*, 1997; Tseng *et al*, 2005). Likewise, steric hindrance caused by the pullulan owing to their higher molecular weight reduces the protonation of PEI and hence the buffering capacity as compared to that of dextran derivatives.

Physiochemical properties of the polymeric gene delivery systems are very critical as they determine the fate of the polyplexes. Of these, size plays a major role in the determination of half life of these polyplexes in the systemic circulation and also their cellular entry. It was reported in the literature that the smaller particles having a size less than 10 nm will be rapidly filtered by kidney cells while that having larger size will be cleared off by RES. Particle size less than 200 nm found to be optimum for gene delivery purpose although controversies are also reported (Choi *et al*, 2010a, 2010b; Soo Choi *et al*, 2007; Dufort *et al*, 2012; Shang *et al*, 2014). Both PPI and DPI derivatives condense DNA into a more compact structure (figure 37.A), with average size in the range of 70-150nm and polydispersity index (PDI) between 0.1 to 0.3 for the nanoplexes prepared at a higher polymer to DNA weight ratios (i.e., from 3:1 to 5:1). Low polydispersity index indicates the formation of a more homogenous

population especially at 5:1 ratio. At this weight ratio, DPI derivatives form smaller sized polyplexes compared to that of PPI derivatives. The nanoplexes formed by the DPI derivatives were in the range of 80 to 90nm while for PPI derivatives it was around 90 to 150nm at the weight ratio 5:1. These results infer that DPI derivatives form tight complexes with ctDNA as compared with that of PPI derivatives and this may be due to the difference in molecular weight of these polysaccharides. Owing to the higher molecular weight, the cationic charge density of PEI gets masked by pullulan to a greater extent when compared to that of dextran. As a result, free amino groups available for DNA condensation get reduced in PPI derivatives and this leads to the formation of large sized polyplexes as compared to that of DPI derivatives.

Another important factor that determines the physiological stability of these polyplexes and also their cellular interactions is the surface charge. Cellular entry of these polyplexes occurs via non specific adsorptive endocytosis mechanism in which interaction between positively charged groups of polymer with anionic proteoglycans present on the cell membrane is essential for the internalization of the nanoplex(Fröhlich, 2012; Alexis *et al*, 2008; Dash *et al*, 1999). Higher charge density also contributes to the formation of smaller sized nanoplexes by preventing aggregation via electrostatic repulsion (Tang *et al*, 2014b). Grafting density of VI found to influence the zeta potential of these polymer derivatives. Initial increase in the zeta potential observed for these derivatives with the increase in the VI grafting density (figure 37.B). This can be explained based on the study conducted by Carner *et al* in which they found out the solubility of chitosan in water gets increased by VI grafting. They gave two possible explanations for this increase in solubility of

chitosan. One is the water soluble nature of VI and another one is the reduced intramolecular hydrogen bonding in chitosan by VI grafting (Caner *et al*, 2007). Similarly, in this study, the increase in zeta potential owing to higher VI grafting density may be attributed by the disruption of intermolecular hydrogen bonding that prevails within the structure of these polymer derivatives. This, in turn, exposes more amino groups to their surface imparting a higher positive charge to the nanoplexes formed by these polymer derivatives. However, irrespective of their higher grafting densities, PPI III and DPI III exhibited lower zeta potential as compared to that of other VI derivatives. Extensive VI grafting causes a significant reduction in amine density and this in turn results in the decreased zeta potential for these VI derivatives. By considering size, PDI and zeta potential, 5:1 weight ratio was optimised for further cell studies for all these derivatives. Since at this weight ratio, these polymer derivatives form more homogenous, smaller sized nanoplexes possessing higher positive zeta potential with ctDNA.

Ability to form stable complexes with the gene of interest is one of the prerequisites of polymeric vectors for successful gene delivery. Nanoplex formation protects the DNA from the degradation caused by enzymes and also helps in their cellular internalisation and subsequent cytoplasmic trafficking. The major driving force that leads to the formation of nanoplex is the electrostatic interaction between polymers and DNA owing to their positive and negative charges respectively. The strength of this association depends on the degree of complexation and also the polymer to DNA weight ratio. The strong association between cationic polymer and ctDNA retards the mobility of the latter under an external electric field. In gel retardation assay, the

loosely bound complexes fail to retard the mobility of DNA under the electric field while that of tight complexes retains in the well. Depending on the binding strength, access of EtBr to intercalate with DNA gets restricted. Hence, in a tightly packed complex, DNA will not be visible even in the wells. Gel retardation assay reveals that VI derivatives form tight complexes with ctDNA such that these derivatives prevent the free mobility of ctDNA even at the 1:1 weight ratio (figure 38). Moreover, polyplexes of these derivatives were also stable even in the presence of plasma protein (figure 39). Nanoplex stability of VI derivatives was also evaluated in the presence of DNase enzyme. From the results (figure 40 & 41), it was clear that nanoplexes formed by the VI derivatives were quite stable even in the presence of this digestive enzyme. Figure 42 also reveals that VI derivatives are compatible with human plasma as most of the protein bands were remained intact as that of the negative control, saline.

Inherent toxicity of cationic polymers owing to their unfavourable interactions with anionic membranes and proteins is one of the major limitations of polymeric gene delivery vectors (Layek & Singh, 2013). In the present study, cytocompatibility of VI derivatives was assessed in C6 and HeLa cells at four different polymer concentrations by carrying out MTT assay. Grafting of VI greatly improves the cytocompatibility of the polymer, both in C6 and HeLa cells, even at a higher polymer concentration (figure 43). Improved cytocompatibility may be attributed to the hydrophilic nature of VI and the presence of polysaccharides. On comparing Cell viability, all the PPI derivatives except PPI III shows above 90% cell viability even at higher polymer concentration in both C6 and HeLa cell lines which is slightly

higher than DPI derivatives which shows only above 80% cell viability. MTT assay also reveals that cytocompatibility of DPI derivatives was slightly higher for HeLa cells when compared to that of C6 cells (figure 41). Cellular response to the toxic effect of materials differs based on the anatomical source from which cells are isolated and also based on the cellular physiology like endocytosis, exocytosis, the antioxidant levels, repair mechanisms etc (Zhou *et al*, 2015; Park *et al*, 2009). Moreover, there are reports suggesting that doubling time of the cells and also their metabolic activities found to influence the sensitivity of these cells towards various materials. In a study conducted by Williams *et al* found that rapidly dividing cells are found to be highly sensitive to the toxic materials when compared to that of the cells having longer doubling time. They examined the responses of various cell lines towards the same concentration of photoinitiator (Williams *et al*, 2005b). Similarly, in this study, among HeLa and C6 cell lines, the doubling time of the former is higher and it is almost twice as compared to that of the latter. Hence, HeLa cells are found to be less sensitive to the cationic polymer when compared to that of C6 cells. Cytocompatibility of selected VI derivatives (PPI II and DPI II) were also analysed in L929 cells and they exhibit above 95% cell viability in this cell line. Nanoplexes of these derivatives prepared with ctDNA at their optimised weight ratio ie, 5:1 also found to be cytocompatible in all these three cell lines tested.

The efficiency of gene delivery vector relies on how readily it get internalised into the cells and deliver the gene of interest into the target site of action. The amino groups present in the VI derivatives neutralize negative charge of DNA and also helps in their cellular entry by interacting with anionic proteoglycans of the plasma

membrane. Nanoplexes of both DPI and PPI derivatives prepared with YOYO I tagged ctDNA exhibit similar uptake in C6 and HeLa cells. However, the cell morphology gets disrupted slightly for those transfected with DPI derivatives while it was unaffected with PPI derivatives (figure 44 & 45). This variation in the cell behaviour towards these derivatives may be attributed to the difference in the nature of polysaccharides. Higher molecular flexibility of pullulan mask the cationic charge density of PPI derivatives to greater extent and prevents the unwanted interactions with the cell membrane (Rekha & Sharma, 2009a). On the other hand, owing to their rigid nature, dextran fails to mask the cationic density of PEI beyond a certain limit. As a result, these derivatives exhibit higher charge density which was evidenced by the zeta potential measurements of these nanoplexes which in turn causes membrane destabilisation. Moreover, DPI derivatives exhibit higher buffering capacity when compared to that of PPI derivatives. In a study conducted by Tseng *et al*, found that the high relative buffering capacity exhibited by the polymer is a boon and a curse. Although it improves the transfection efficiency, it also induces toxicity by creating an imbalance in the intracellular proton thereby causing the disruption of intracellular organelles (Tseng *et al*, 2005).

Cellular entry of nanoplexes was studied in the presence of inhibitors to elucidate the endocytic pathway by which the nanoplexes of VI derivatives get internalised. For this study, nanoplexes of PPI II prepared with YOYO I tagged ctDNA at the optimised weight ratio (5:1). Cellular uptake of these nanoplexes was studied in the presence of endocytic inhibitors like amiloride, chlorpromazine and filipin that inhibit macropinocytosis, clathrin and caveolae mediated pathways respectively.

These inhibitors were selected because it is reported in the literature, the prominent way of polyplexes entry into the cell is either through caveolae or clathrin mediated pathway (Morille *et al*, 2008; Rejman *et al*, 2005 b). However, the cellular uptake of these nanoplexes does not get affected even in the presence of these inhibitors (table 3). These results indicate that nanoplexes of this derivative does not depend on any single pathway but it gets into the cell using multiple pathways.

Ihm *et al*, reported the use of polyvinyl imidazole (PVI) as a gene delivery vector and also discussed their merits over PEI (Ihm *et al*, 2003). Asayama *et al*, synthesised amino modified PVI and studied its applications towards gene delivery purpose. This modification greatly increases the gene transfection efficiency and also acts in a pH sensitive manner (Asayama *et al*, 2007). In this study, VI modification improves the transfection efficiency of CPs and at the same time the cytocompatibility of the polymer does not get compromised. Among PPI and DPI derivatives, the transfection efficiency was higher for the former when compared to that of later (figure 46 & 47). As evidenced from size, zeta potential and agarose gel electrophoresis, DPI derivatives form tight complexes with plasmid DNA. This makes vector unpacking and subsequent release of therapeutic gene difficult. Hence DPI derivatives exhibit lower transfection efficiency compared to that of PPI derivatives. Comparison of transfection efficiency among the PPI derivatives shows that PPI II and PPI III exhibit almost similar transfection efficiency and it was slightly higher when compared to that of PPI I (figure 48). These results suggest that transfection efficiency of VI derivatives initially found to increase with an increase in the grafting density of this vinyl monomer. After a certain limit, further addition of

VI does not bring much change in transfection efficiency. Among PPI II and PPI III, the former was found to be a better gene delivery agent as they possess good cytocompatibility and transfection efficiency. However, these polymer derivatives cannot be stored for longer time periods since their property get changed during this storage period.

5.5 Diethyl amino ethyl methacrylate (DEAEM) grafted cationised polysaccharide for gene delivery

The pH and thermo responsive behaviour together with the water soluble nature of diethyl aminoethyl methacrylate (DEAEM) make it of great interest in the field of biomedical science (Nagasaki *et al*, 1997; Dai *et al*, 2008; A *et al*, 2015). The polymeric form of this vinyl monomer is used as a gene delivery vector to transfect a wide variety of cell types. They possess the ability to condense DNA, helps in the cellular entry by transiently disrupting lipid bilayer and also buffer the acidic pH that prevails within the endosomes (van de Wetering *et al*, 1998; Takeda *et al*, 2004; Moselhy *et al*, 2007). Hence, in this study, diethyl amino ethyl methacrylate was grafted to the cationised polysaccharides in order to improve their buffering capacity and also to assist in their cellular entry. Cationised polysaccharides (DP and PP) were modified with this vinyl monomer at two different weight ratios via Michael addition reaction and synthesised four different polymer derivatives viz DPD I, DPD II, PPD I and PPD II. Grafting percentage of this vinyl monomer to these polymer derivatives was determined by copper sulphate assay as its grafting results in the reduction of the amino groups in the parent chain (PP and DP). It was found to be $6.5 \pm 0.36\%$, $2.4 \pm 0.01\%$, $3.89 \pm 0.17\%$ and $2.06 \pm 0.5\%$ for DPD I, DPD II, PPD I and

PPD II respectively.

Chemical structure of these polymer derivatives was then analysed by FTIR and NMR spectra. In the FTIR spectra (figure 49), the characteristic bands of carbamate linkage occur over the region 1640cm^{-1} and 1566cm^{-1} corresponding to the $-\text{C}=\text{O}$ stretching and $-\text{N}-\text{H}$ bending vibrations respectively. No other bands specific to this vinyl monomer observed in the FTIR spectra. This may be due to the overlapping of the vibrations of the ester group that is present in this vinyl monomer with that of the carbonyl group that is present in the carbamate linkage of the parent polymer. Similar observations were reported in the literature where the vibrations of ester group which is likely to occur around 1740cm^{-1} shifted to lower wavelength and overlap with that of the carbonyl group in the carbamate linkage due to the formation of hydrogen bonds (Coleman *et al*, 1994; Wang *et al*, 2017). However, the grafting of this vinyl monomer to these CPs was confirmed by NMR spectra. In these spectra (figure 50), besides the characteristic peaks of parent chains, the appearance of an additional shift around 1ppm corresponds to the resonance of protons in the methyl group of DEAEM molecule.

Cellular processing of polyplexes once they get internalised into the cell determine the fate of these polymeric gene delivery systems. Cationic polyplexes adhere to the cell membrane through electrostatic interactions with the anionic plasma membrane and subsequently get engulfed by the cell via the endocytotic pathway. Once these endocytotic vesicles mature, they fuse with lysosomes containing digestive enzymes. So, escape from this endosomal compartment before its fusion with lysosomes is critical for any polymeric gene delivery systems (Wattiaux *et al.*, 2000).

Cationic polymeric gene delivery systems postulated to escape from this endosomal compartment via proton sponge mechanism as discussed in earlier sections. In this study, DEAEM modification found to reduce the buffering capacity of the cationised polysaccharides. This may due to the reduction in the amino groups caused by their grafting. Still, these derivatives exhibit moderate buffering capacity over the acidic pH. Buffering capacity found to reduce with the increase in the DEAEM grafting density. Hence PPD I and DPD I derivatives were found to exhibit higher buffering compared to that of PPD II and DPD II derivatives. Comparison between pullulan and dextran derivatives (ie PPD and DPD) shows no significant difference in the buffering capacity (figure 51).

Self assembly of cationic DEAEM derivatives with ctDNA leads to the formation of nanosized complexes called polyplexes. These polyplexes are compact inter polyelectrolyte complexes (IPEC) formed by the association of anionic phosphate groups of DNA with cationic amino groups that present in the polymer through electrostatic interactions (Slita et al., 2007). This IPEC greatly improves the resistance of DNA to the degradation caused by the nucleases and also enhances the cellular uptake of this genetic material by masking their anionic charge density (De Smedt et al., 2000).

Size and Zeta potential of the polyplexes formed by the DEAEM polymer derivatives with ctDNA were analysed by dynamic light scattering experiments. Sizes of the nanoplexes formed with PPD I and DPD II derivatives were found to decrease with the increase in the polymer to DNA weight ratio (figure 52.A). However, PPD II and DPD I derivatives form smaller sized particles at both weight ratios that exhibiting

higher positive and negative zeta potential. Zeta potential of all these DEAEM derivatives were found to be negative at the lower weight ratios i.e. upto 1:1 ratio and after this, the zeta potential turns either positive or nearer to zero for DPD and PPD derivatives respectively (figure 52.B). From weight ratio 3:1 onwards, all these derivatives exhibit positive zeta potential. Among dextran and pullulan derivatives, the former exhibit higher zeta potential than the later. This can be explained based on the molecular weight of the polysaccharides. Pullulan, owing to their higher molecular weight, mask the amino groups of PEI more effectively when compared to that of dextran. Hence, the former exhibits lower zeta potential in comparison with that of the later. The weight ratio at which these polymer derivatives form homogenous, smaller sized nanoplexes with positive zeta potential was chosen for further studies. DEAEM derivatives form smaller sized nanoplexes around 120 nm with positive zeta potential that ranges between 3 to 9 mV and narrow PDI (0.1-0.3) at the weight ratio 5:1. Hence this weight ratio was used for further cell studies.

DEAEM derivatives ability to condense and form stable complexes with DNA was analysed by agarose gel electrophoresis. Stability of the nanoplexes was analysed based on the polymeric vectors capability to retard the motion of DNA under an external electric field. DEAEM derivatives form stable complexes with ctDNA and it was evident from the gel (figure 53). DNA was not even visualized in the wells that are loaded with nanoplexes, prepared at the higher weight ratios ie from 2:1 onwards. This result suggests that the interactions between the DEAEM derivatives and ctDNA were so tight such that the former impedes the access of EtBr to intercalate with the later. However, slight DNA leach out was observed in the lower ratios (till

1:1 ratio). The stability of these nanoplexes was also determined in the presence of plasma proteins. As these proteins are anionic in nature, there is a possibility to compete with DNA and replaces them from these nanoplexes. However, the nanoplexes are quite stable even in the presence of plasma proteins. The experiment was also repeated in the presence of DNase to evaluate the ability of DEAEM derivatives to protect the DNA against the action of this digestive enzyme (figure 54). The stable complex formed by DEAEM derivatives with ctDNA shields the later to the degradation caused by the digestive enzyme. On the other hand, naked DNA treated with DNase show degradation and it was evidenced by the appearance of DNA as a band rather than a smear, the characteristic appearance of genomic DNA. The results were counter checked by treating the nanoplexes with heparin. This glycosaminoglycan owing to their high anionic nature causes the dissociation of DNA from these nanoplexes. The appearance of DNA as a smear in the lanes loaded with nanoplexes reveals the intactness of ctDNA that got displaced from these nanoplexes through the interaction with heparin. This experiment further confirms the stability of nanoplexes formed by the DEAEM derivatives with ctDNA in the presence of the digestive enzyme, DNase.

Plasma kinetics of polymeric gene delivery vector is very important as it determines the half life in the systemic circulation. Cationic polymeric vectors owing to their positive charge interact with anionic plasma membranes of the blood components and also with plasma proteins which leads to their rapid clearance from the blood circulation. So, one of the prerequisites for effective systemic gene delivery, the cationic polymer should not aggregate when it exposed to the blood cells and

proteins (Read *et al*, 2005; Ward *et al*, 2001). Plasma protein interactions of DEAEM derivatives were studied by performing polyacrylamide gel electrophoresis (Native PAGE). DEAEM derivatives show no interactions with plasma proteins and the bands were similar to that of negative control, saline (figure 55). As expected, positive control, PEI owing to their higher charge density show strong interactions with plasma proteins and most of the protein bands were absent in this lane.

One of the major drawbacks faced by cationic polymeric systems is their intrinsic cytotoxicity. The higher charge density of these vectors leads to the unfavourable interactions with the plasma membrane, anionic proteins and other cellular components (Kafil & Omid, 2011b; Xiong *et al*, 2007; Moghimi *et al*, 2005b). Hence, the cytocompatibility of DEAEM derivatives with cells was analysed in three different cell lines viz C6, HeLa and L929 via MTT assay. DEAEM derivatives show excellent compatibility with all these cell lines tested and exhibit above 80 % cell viability (figure 56). Comparison of cytocompatibility between the DEAEM derivatives reveals that percentage cell viability slightly decreases with increase in the grafting percentage. PPD II and DPD II derivatives exhibit above 85% cell viability when compared to that of PPD I and DPD I which shows only above 80% viability and the order is DPDI > PPD II > DPD I = PPD I in all the three cell lines tested. The cytotoxicity of the polymer depends on various factors like type of amino group, flexibility of the polymer, cationic charge density - its number and also its arrangement in three dimensional matrix (Fischer *et al*, 2003b). According to Ryser, to elicit a biological response on the cell membrane, three- point attachment is necessary. Increase in the space between reactive amino groups decreases the activity

of the polymer (Ryser, 1967; Fischer *et al*, 2003b). Hence, in this study, by the grafting of this vinyl monomer, space between the reactive amino groups increased in the DEAEM derivatives compared to that of parent chains (PP and DP). So these derivatives were more cytocompatible when compared to that of parent chains.

Semipermeable nature of plasma membrane act as a barrier that separating the external environment from the cell's interior. Polymeric gene delivery vector without any targeting ligands enter into the cells via a non specific endocytotic pathway. Polyplex size and zeta potential play an important role in this type of cellular internalisation. Cationic charge of the polymeric vectors helps to adhere to the anionic cellular membrane while polyplex size determines the route of cellular internalisation. Particles having a size greater than 1 μ m size enter the cells via macropinocytosis while that having size \leq 120nm and \leq 90nm get internalised via clathrin-mediated and caveolin-mediated endocytotic pathways respectively (Conner & Schmid, 2003; Doherty & McMahon, 2009; Rejman *et al*, 2005b; Evans *et al*, 2011).

Cellular uptake of DEAEM derivatives was studied in three different cell lines C6, HeLa and L929 cells. Nanoplexes were prepared by complexing with YOYO Iodide tagged ctDNA at the optimised weight ratio ie, 5:1. DEAEM derivatives exhibit good cellular uptake in C6 and HeLa cells and ctDNA readily entered into the nucleus which was evidenced by the appearance of green fluorescence in the nuclear region (figure 57). Moreover, their internalisation did not cause any disruption in cellular morphology of these cells which reinforces the cytocompatibility of these polymer derivatives. On the other hand, DEAEM derivatives exhibit poor cellular uptake in

L929 cells. Similar results were obtained in the study conducted by Natalie *et al.*, in which Maghemite–rhodium citrate (MRC) nanoparticles were used as an antitumor agent in breast cancer cell lines. They observed that these iron oxide nanoparticles rapidly get internalised in cancer cells when compared to that of the normal cell line. They explained this difference in cellular uptake brought about the difference in cell membrane composition and metabolic activity of these cells (Chaves *et al.*, 2017; Kettler *et al.*, 2014). Moreover, it was also reported in the literature that cancer cells exhibit the different amount of various receptors over the cell surface as compared to that of normal cells. Hence they readily bind with the nanoparticles and get internalised (Brunner *et al.*, 2006; Kettler *et al.*, 2014). Cellular uptake of nanoplexes of DEAEM derivatives was also quantified in C6 and HeLa cells by flow cytometric analysis and it was above 95% in both these cell lines tested (figure 58).

Cells exhibit distinct endocytic pathways like macropinocytosis, clathrin-mediated, caveolin-mediated pathways for the uptake of these polymer/DNA complexes. Selection of these pathways depends on the cell type and nature of the polyplexes (ie size, surface charge etc) (Evans *et al.*, 2011; Doherty & McMahon, 2009; Mayor & Pagano, 2007). Hence, to elucidate the endocytotic pathway by which DEAEM derivatives shuttle into the cells, cellular uptake experiments were repeated in the presence of specific endocytotic inhibitors. Amiloride, chlorpromazine and filipin were the specific pharmacological inhibitors chosen for this study to specifically obstruct macropinocytosis, clathrin and caveolin mediated pathways respectively. These specific inhibitors were chosen based on the previous literature. Cellular uptake of polyplexes of DEAEM derivatives not get affected even in the presence of

these inhibitors. These results suggest that nanoplexes of these vinyl monomer derivatives not simply rely on any specific pathway rather it get into cells through multiple pathways (table 5).

Cellular uptake studies revealed that the ctDNA enter into the nucleus of both C6 and HeLa cells. In order to elucidate whether ctDNA alone gets into the nucleus or as a nanoplex, ctDNA and polymer both tagged with different fluorescent dyes and cellular uptake experiments were once again repeated. The polymer was tagged with TRITC that emit red fluorescence while ctDNA tagged with YOYO I that emit green fluorescence. Cells nuclei were stained with Hoechst that emit blue fluorescence. Confocal microscopic images revealed that ctDNA alone get into the nucleus while polymer remains in the cytoplasm. These results suggest that vector unpacking of DEAEM derivatives occurs in the cytoplasm (figure 59).

Transfection efficiency of DEAEM derivatives was analysed in C6, HeLa and L929 cells using the therapeutic gene, p53 whose expression leads to apoptosis in cancer cells. Live cells were distinguished from dead cells by using differential staining technique. Membrane integrity gets disrupted in dead cells and hence they allow the ethidium bromide to get inside and stained red. On the other hand, live cells were stained green by the action of intracellular esterase which cleaves acetoxymethyl group of Calcein AM and produces the fluorescence. DEAEM derivatives exhibit good transfection efficiency in both cancer cell lines- C6 and HeLa as most of the cells were stained red as the indication of cell death (figure 60 & 61). However, poor transfection efficiency was observed in L929 cells. There are two possible reasons for the difference in transfection efficiency observed in cancer and L929 cells. The

first reason is the difference in morphology and anatomy of cancer and L929 cells. Cancer cells exhibit more receptors for the uptake of nanoplexes when compared to that of L929 cells which were evident from the cellular uptake data. Secondly, the p53 gene induces apoptosis only in cancer cells while causing reversible cell cycle arrest in the normal cells. AnnexinV staining also confirms the cell death that occurs in the transfected cells was through the induction of apoptosis (figure 64).

It is reported in the literature that PEI based gene delivery systems due to their higher cationic charge density induce cell death (Fischer *et al*, 1999; Florea *et al*, 2002). Molecular mechanisms behind the PEI mediated toxicity was studied by Moghimi *et al* and postulated two step mechanism – the immediate necrotic like changes (30 min post transfection) and delayed apoptotic response (24 h post transfection) (Moghimi *et al*, 2005b). So, in order to confirm the cell death that observed in transfected cells was through the expression of p53 gene and not by the toxicity induced by the polymer, experiments are repeated treating C6 cells with DEAEM derivatives. As expected, no cell deaths observed in these cells (figure 62). However, immunostaining experiments carried out in the C6 cells transfected with polyplexes prepared with p53 plasmid reveals the expression of p53 protein (figure 65).

Biodistribution of DEAEM derivatives was studied in BALB/c mice. DPD II and PPD II were selected as representative polymers of the DEAEM derivatives since they exhibit better cytocompatibility when compared to that of DPD I and PPD II derivatives. Fluorescently tagged polymer solution was intravenously administered to BALB/c mice via tail vein. These animals were then sacrificed using CO₂ chamber at four different time periods namely 15 minutes, 3h, 6h and 24h. Organs like brain,

heart, lungs, liver, kidney and spleen were collected from these deceased animals and photographed using IVIS *in vivo* image analyser at the Ex/Em 745/820 nm.

Fifteen minutes after intravenous administration, these two polymer derivatives found to be concentrated more on kidney cells while trivial fluorescence observed on lungs and liver tissue (figure 66). DPD II takes 3 h to reach the liver tissue while PPD II enters into the liver during the 6th hours. This may due to the difference in the molecular weight of these two polymer derivatives. DPD II owing to smaller molecular weight readily gets into the liver tissue while the higher molecular weight of pullulan increases its blood circulation time. In a study conducted by Yamaoka *et al*(1994), found that poly (ethylene glycol) (PEG) having high molecular weight retained in the blood circulation for a longer period than that of the low molecular weight PEGs. Translocation of smaller molecular weight PEG from the systemic circulation into the extravascular tissues occurs rapidly via diffusion as compared to that of high molecular weight PEGs. Hence, the vascular permeability determines the time of tissue accumulation of these polymers (Yamaoka *et al*, 1994).

Good renal clearance was also observed for both PPD II and DPD II derivatives which were evidenced by the appearance of fluorescence in the kidney cells by 6th h post administration. At the 24th hour, some of the fluorescence found to be retained on the liver tissue while that gets reduced in the kidney cells. To summarize, both PPD and DPD get rapidly cleared off from the body of these animals within the time period of 24h while certain amounts of these polymers get retained in the liver tissue. Both of these derivatives were not found to accumulate in any other tissues other than liver. This specific targeting of liver cells may be due to the presence of

asialoglycoprotein receptors in these cells that play an important role in the sugar uptake.

6. Summary and Conclusion

Knowledge gathered over the last few decades on the progress and proliferation of cancer cells opened the way for the development of novel therapeutic approaches in this disease management. Gene therapy is one such approach which has the potential to revolutionize the field of medicine. In this approach, manipulations are done at the genetic level to treat, prevent or alleviate disease. However, the growth of this approach was impeded by the lack of an ideal gene delivery vector. Naked nucleic acids are highly susceptible to the degradation caused by digestive enzymes. So, in order to protect these nucleic acids from the degradation caused by the nucleases and also to assist in their intake by target cells, there is a need for delivery systems. Viral vectors proved to be efficient in gene delivery. However, immunogenicity associated with these vectors and also their cost of production limits their application in gene delivery. So, nowadays, greater attention paid towards the development of non viral vectors especially polymeric systems, as they are cost effective, the simple procedure involved in their production and comparatively much safer than viral counter parts.

The success of polymeric gene delivery systems depends on how efficiently it protects the gene of interest and delivers them towards the target site of action. However, these polymeric systems have to face numerous hurdles during this journey under *in vivo* conditions. Some of these obstacles include stability in systemic circulation, cellular uptake, endosomal escape, vector unpacking and release of the gene of interest for its expression. Hence, careful and rational designing of polymeric vectors is needed for the successful clinical translation of this therapeutic approach. In this study, polymeric vectors were designed using natural,

biocompatible polysaccharides – pullulan and dextran as vector backbones and modified with PEI to impart cationic groups and further modified with selected vinyl monomers to impart specific functions. The gene transfection efficiency of these vectors was then evaluated in the cancer cell lines using therapeutic gene, p53.

The larger size and anionic nature of DNA prevents their passage across the cellular membrane. Moreover, they are highly susceptible to the degradation caused by nucleases. So, in order to protect and condense these DNA molecules, the polymeric vectors should possess enough cationic charge density. The cationicity is also required for efficient cellular uptake. So, in order to provide cationicity, pullulan and dextran were modified with PEI using CDI chemistry. Chemical structure analysis of these cationised polysaccharides (CPs) using FTIR and ¹H NMR spectroscopic techniques confirms the grafting of PEI to these polysaccharides. Buffering capacity of CPs was found to be lower than that of the PEI but still, they exhibit an appreciable level of buffering capacity over the endosomal pH range i.e. 7-5. At their optimised weight ratio (i.e. 2:1 for PEI and 5:1 for CPs) both PEI and CPs form polyplexes with ctDNA having a size below 90nm and zeta potential ranges between +13 to +30 mV. Gel retardation assay reveals that CPs form tight complexes with ctDNA even at the lower weight ratios i.e. 1:1. Strong plasma proteins interactions and cytotoxicity of PEI get reduced by polysaccharide modifications. Still, these CPs exhibit some interactions with plasma proteins and also become toxic at higher polymer concentrations in C6 and L929 cells. Irrespective of these demerits, CPs exhibit good cellular internalisation and transfection efficiency in both C6 and HeLa cell lines.

The balance between cytotoxicity and transfection efficiency is essential for cationic polymers for efficient gene delivery. Increase in the transfection efficiency of cationic polymers is usually associated with an increase in the toxicity. For example, PEI of high molecular weight, that is 25 K, found to transfect cells more effectively when compared to that of low molecular weight PEI i.e. 2000 Da. However, the former exhibit higher toxicity than that of the later. Cytotoxicity of PEI can be reduced without compromising its transfection efficiency via crosslinking low molecular weight PEI into high molecular weight structures using suitable molecules containing bonds that cleavable at physiological conditions. So, once these molecules get released into the cytosol they revert back to the non toxic, low molecular weight PEI by the cleavage of the bond at this reductive environment. Similarly, to reduce the toxicity of pullulan PEI (PP), they are cross linked with ethylene glycol dimethacrylate (EGDMA) containing cleavable ester bond. These derivatives were synthesised by Michael addition reaction using CAN as the catalyst at two different weight ratios (0.01:10 and 0.015:10) and synthesised PPE I and PPE II derivatives. Using a similar mechanism, dextran PEI derivatives were also synthesised but they turn out to be insoluble due to extensive crosslinking. Chemical characterisation of the PPE derivatives was done using FTIR and ¹H NMR spectroscopy and confirmed the crosslinking of EGDMA. These derivatives exhibit excellent buffering capacity over the pH range 7-5 and form tight complexes with ctDNA only at higher polymer concentration. At their optimised weight ratio (i.e. 5:1), these derivatives form nanoplexes having a size around 150nm and the zeta potential ranges between +6 to and 10 mV. Plasma protein interactions of PP got reduced by EGDMA cross linking. These polymer derivatives and their polyplexes were found to be cytocompatible

with C6, HeLa and L929 cell lines. They exhibit good cellular internalisation and transfection efficiency in C6 cells. However, these derivatives failed to transfect HeLa cell lines owing to the poor uptake.

[2- (acryloyloxy) ethyl] trimethyl ammonium chloride (AOETMAC) is an amphoteric molecule, grafted to the CPs in order to avoid unwanted interactions with plasma proteins and extend their half life in the systemic circulation. AOETMAC grafted CPs synthesised at 3 different weight ratios viz 0.01:10, 0.015:10 and 0.0025:10 via Michael addition reaction and synthesised six different derivatives namely DPA I, DPA II, DPA III, PPA I, PPA II and PPA III respectively. These polymer derivatives exhibit excellent buffering capacity in the pH range 10-7 and not in the acidic pH which is required for the endosomal escape. Even though, AOETMAC derivatives form smaller sized nanoplexes of around 150 nm size at the weight ratio 5:1, their zeta potential is either negative or nearer to zero (except PPA III). All these derivatives except PPA III fail to retard the mobility of ctDNA under even higher polymer to DNA weight ratio. As expected, this modification greatly reduced plasma protein interactions. AOETMAC derivatives (except PPA III) are cytocompatible and exhibit above 75% Cell viability in both C6 and HeLa cells. PPA III derivatives owing to their less grafting density, their physiochemical properties are similar to that of parent chain, PP. Irrespective of their good cellular internalisation, AOETMAC derivatives exhibit poor transfection efficiency in C6 cells. However, no cellular internalisation (except PPA III) and transfection efficiency observed for these polymer derivatives in HeLa cells.

Imidazoles are of greater importance in biological systems as they are structural constituents of many biological components like histamine, histidine, purine, biotin etc. Incorporation of imidazole moieties to the gene delivery vectors renders endosomal escape by membrane destabilisation. Imidazole ring also exhibits a pKa around 6 which helps them to buffer in the acidic pH that is prevailing within the endosomes. Moreover, at physiological pH, they remain in the unprotonated state having negligible charge and this property promotes the vector unpacking once the polyplex gets released into the cytosol. Hence, to impart these specific functions, vinyl imidazole moieties were grafted to the CPs via free radical addition reaction using CAN as the initiator. This vinyl monomer grafted with CPs at three different weight ratios (10:0.005, 10:0.01, 10:0.02) and synthesised 6 different polymer derivatives viz DPI I, DPI II, DPI III, PPI I, PPI II and PPI III. Grafting of this vinyl monomer to the CPs was confirmed by the FTIR and ¹H NMR spectroscopic techniques. Buffering capacity of these polymer derivatives found to be lower than that of corresponding parent chains (DP and PP) and this may be due to the reduction in primary amino groups caused by their grafting. However, they exhibit an appreciable level of buffering capacity over the acidic pH i.e. 7-5. VI derivatives form smaller sized nanoplexes of around 150 nm with zeta potential ranging between +10 to +22 mV at the weight ratio, 5:1. Gel retardation assay further reveals that the nanoplexes formed by these polymer derivatives are quite stable as ctDNA leaches out only at lower polymer concentration. These polyplexes are also stable even in the presence of plasma proteins and digestive enzyme, DNase. VI derivatives were quite cytocompatible and exhibit good cellular uptake both in C6 and HeLa cells. However, the morphology of the cells transfected with DPI derivatives slightly gets

disrupted. PPI derivatives exhibit excellent transfection efficiency in both cell lines and their results are consistent as compared to that of DPI derivatives.

The ability to condense DNA together with the buffering capacity over the acidic pH makes the vinyl monomer, 2-diethylaminoethyl methacrylate (DEAEM) attractive in the field of gene delivery. Moreover, these molecules also assist in the cellular entry by transiently disrupting lipid bilayer. Hence, in this study, DEAEM molecules were incorporated into the cationised polysaccharides via Michael addition reaction at two different weight ratios and synthesised four polymer derivatives namely DPD I, DPD II, PPD I and PPD II. Chemical characterisation of these polymer derivatives (FTIR and ¹H NMR spectroscopic techniques) established the grafting of this moiety. These derivatives exhibit excellent buffering capacity over the pH range 7-5 and form nanoplexes of size around 120 nm with the zeta potential between +3 to +9 mV at their optimised weight ratio (i.e. 5:1). Nanoplex stability was assessed by the gel retardation assay and found to be stable even in the presence of plasma proteins and DNase. These derivatives are cytocompatible and exhibit 80% cell viability in all the three cell lines (C6, HeLa and L929) tested. Moreover, these derivatives exhibit excellent cellular internalisation and transfection efficiency in both C6 & HeLa cell lines. Biodistribution studies carried out in BALB/c mice reveal their accumulation in the liver tissue. Good renal clearance was also observed for these derivatives.

To conclude, vinyl monomers grafted cationised polysaccharides were successfully synthesised and evaluated for gene delivery purpose. All these vinyl monomer modifications improved the cytocompatibility and minimize plasma protein interactions of cationised polysaccharides- PP and DP. EGDMA derivatives exhibit

good cellular uptake and moderate transfection efficiency in C6 cells while poor cellular uptake and transfection efficiency observed in HeLa cells. Irrespective of their good cellular uptake, AOETMAC derivatives exhibit poor transfection efficiency in C6 cells while there is no cell uptake and transfection efficiency observed in HeLa cells. VI derivatives exhibit good cellular uptake and transfection efficiency in both C6 and HeLa cells. But the results were not consistent and their properties get changed while stored for long time. DEAEM was found to be better transfection agent as compared to all other derivatives investigated, as it exhibits good transfection efficiency in both C6 and HeLa cells. Moreover, the results were consistent and long term storage also possible for these derivatives.

Addressing potential hurdles and by maintaining a strong focus on improving vectors, gene therapy will surely improve the outcome of a range of diseases. Among pullulan and dextran derivatives, the former found to be better gene transfection agents as they exhibit better cytocompatibility and transfection efficiency. EGDMA and AOETMAC modifications found to minimize the plasma proteins interactions and improve the cytocompatibility of CPs. However, their cellular uptake and hence transfection efficiency get compromised, especially in HeLa cells. Of the 4 derivatives prepared, DEAEM derivatives found to be promising as gene delivery vectors since they exhibit better biological compatibility and gene transfection efficiency. In future, *in vivo* studies should be carried out to assess the efficacy of these DEAEM derivatives to deliver gene in tumour models. It would be beneficial, if these derivatives explored for the combination of drug and gene delivery in future.

References

- Ahl PL, Bhatia SK, Meers P, Roberts P, Stevens R, Dause R, Perkins WR & Janoff AS (1997) Enhancement of the in vivo circulation lifetime of 1- α -distearoylphosphatidylcholine liposomes: importance of liposomal aggregation versus complement opsonization. *Biochim. Biophys. Acta BBA - Biomembr.* **1329**: 370–382
- Ahn C-H, Chae SY, Bae YH & Kim SW (2002) Biodegradable poly(ethylenimine) for plasmid DNA delivery. *J. Controlled Release* **80**: 273–282
- Akinc A, Thomas M, Klibanov AM & Langer R (2005) Exploring polyethylenimine-mediated DNA transfection and the proton sponge hypothesis. *J. Gene Med.* **7**: 657–663
- Akiyoshi K, Kobayashi S, Shichibe S, Mix D, Baudys M, Wan Kim S & Sunamoto J (1998) Self-assembled hydrogel nanoparticle of cholesterol-bearing pullulan as a carrier of protein drugs: Complexation and stabilization of insulin. *J. Controlled Release* **54**: 313–320
- Al-Dosari MS & Gao X (2009) Nonviral Gene Delivery: Principle, Limitations, and Recent Progress. *AAPS J.* **11**: Available at: <http://www.ncbi.nlm.nih.gov/pmc/articles/PMC2782077/> [Accessed December 15, 2016]
- Alexis F, Pridgen E, Molnar LK & Farokhzad OC (2008) Factors Affecting the Clearance and Biodistribution of Polymeric Nanoparticles. *Mol. Pharm.* **5**: 505–515
- Aoki K, Furuhata S, Hatanaka K, Maeda M, Remy JS, Behr J-P, Terada M & Yoshida T (2001) Polyethylenimine-mediated gene transfer into pancreatic tumor dissemination in the murine peritoneal cavity. *Gene Ther.* **8**: 508
- Asayama S, Hakamatani T & Kawakami H (2010a) Synthesis and Characterization of Alkylated Poly(1-vinylimidazole) to Control the Stability of its DNA Polyion Complexes for Gene Delivery. *Bioconjug. Chem.* **21**: 646–652
- Asayama S, Hakamatani T & Kawakami H (2010b) Synthesis and Characterization of Alkylated Poly(1-vinylimidazole) to Control the Stability of its DNA Polyion Complexes for Gene Delivery. *Bioconjug. Chem.* **21**: 646–652
- Asayama S, Sekine T, Kawakami H & Nagaoka S (2007) Design of Aminated Poly(1-vinylimidazole) for a New pH-Sensitive Polycation To Enhance Cell-Specific Gene Delivery. *Bioconjug. Chem.* **18**: 1662–1667
- Badding MA, Vaughan EE & Dean DA (2012) Transcription Factor- Plasmid Binding Modulates Microtubule Interactions and Intracellular Trafficking During Gene Transfer. *Gene Ther.* **19**: 338–346

- Bai H, Lester GMS, Petishnok LC & Dean DA (2017) Cytoplasmic transport and nuclear import of plasmid DNA. *Biosci. Rep.* **37**: Available at: <https://www.ncbi.nlm.nih.gov/pmc/articles/PMC5705778/> [Accessed May 8, 2019]
- Bando T & Sugiyama H (2006) Synthesis and Biological Properties of Sequence-Specific DNA-Alkylating Pyrrole–Imidazole Polyamides. *Acc. Chem. Res.* **39**: 935–944
- Baptiste N, Friedlander P, Chen X & Prives C (2002) The proline-rich domain of p53 is required for cooperation with anti-neoplastic agents to promote apoptosis of tumor cells. *Oncogene* **21**: 9
- Barak Y, Juven T, Haffner R & Oren M (1993) mdm2 expression is induced by wild type p53 activity. *EMBO J.* **12**: 461–468
- Bataille I, Meddahi-Pellé A, Le Visage C, Letourneur D & Chaubet F (2011) Pullulan for Biomedical Uses. In *Polysaccharides in Medicinal and Pharmaceutical Applications*, Popa V (ed) pp 145–182. UK: Smithers Rapra Technology
- Behr J-P (1997) The Proton Sponge: a Trick to Enter Cells the Viruses Did Not Exploit. *Chim. Int. J. Chem.* **51**: 34–36
- Bender H, Lehmann J & Wallenfels K (1959) Pullulan, ein extracelluläres Glucan von *Pullularia pullulans*. *Biochim. Biophys. Acta* **36**: 309–316
- Benjaminson RV, Matthebjerg MA, Henriksen JR, Moghimi SM & Andresen TL (2013) The Possible “Proton Sponge ” Effect of Polyethylenimine (PEI) Does Not Include Change in Lysosomal pH. *Mol. Ther.* **21**: 149–157
- Bennis JM, Mahato RI & Kim SW (2002) Optimization of factors influencing the transfection efficiency of folate–PEG–folate-graft-polyethylenimine. *J. Controlled Release* **79**: 255–269
- Bernier B (1958) The production of polysaccharides by fungi active in the decomposition of wood and forest litter. *Can. J. Microbiol.* **4**: 195–204
- Bottai G, Truffi M, Corsi F & Santarpia L (2017) Progress in nonviral gene therapy for breast cancer and what comes next? *Expert Opin. Biol. Ther.* **17**: 595–611
- Boussif O, Lezoualc’h F, Zanta MA, Mergny MD, Scherman D, Demeneix B & Behr JP (1995a) A versatile vector for gene and oligonucleotide transfer into cells in culture and in vivo: polyethylenimine. *Proc. Natl. Acad. Sci. U. S. A.* **92**: 7297–7301
- Boussif O, Lezoualc’h F, Zanta MA, Mergny MD, Scherman D, Demeneix B & Behr JP (1995b) A versatile vector for gene and oligonucleotide transfer into cells in culture and in vivo: polyethylenimine. *Proc. Natl. Acad. Sci.* **92**: 7297–7301
- Boussif O, Zanta M & P Behr J (1996) Optimized galenics improve in vitro gene transfer with cationic molecules up to 1000-fold. *Gene Ther.* **3**: 1074–80
- Brandén LJ, Mohamed AJ & Smith CIE (1999) A peptide nucleic acid–nuclear localization signal fusion that mediates nuclear transport of DNA. *Nat. Biotechnol.* **17**: 784

- Brown TA, Bouchard T, John TS, Wayner E & Carter WG (1991) Human keratinocytes express a new CD44 core protein (CD44E) as a heparan-sulfate intrinsic membrane proteoglycan with additional exons. *J. Cell Biol.* **113**: 207–221
- Brunner TJ, Wick P, Manser P, Spohn P, Grass RN, Limbach LK, Bruinink A & Stark WJ (2006) In Vitro Cytotoxicity of Oxide Nanoparticles: Comparison to Asbestos, Silica, and the Effect of Particle Solubility. *Environ. Sci. Technol.* **40**: 4374–4381
- Caner H, Yilmaz E & Yilmaz O (2007) Synthesis, characterization and antibacterial activity of poly(N-vinylimidazole) grafted chitosan. *Carbohydr. Polym.* **69**: 318–325
- Carlisle RC, Etrych T, Briggs SS, Preece JA, Ulbrich K & Seymour LW (2004) Polymer-coated polyethylenimine/DNA complexes designed for triggered activation by intracellular reduction. *J. Gene Med.* **6**: 337–344
- Casé AH, Picola IPD, Zaniquelli MED, Fernandes JC, Taboga SR, Winnik FM & Tiera MJ (2009) Physicochemical characterization of nanoparticles formed between DNA and phosphorylcholine substituted chitosans. *J. Colloid Interface Sci.* **336**: 125–133
- Catley BJ (1971) Utilization of Carbon Sources by *Pullularia pullulans* for the Elaboration of Extracellular Polysaccharides. *Appl Env. Microbiol* **22**: 641–649
- Catley BJ, Ramsay A & Servis C (1986) Observations on the structure of the fungal extracellular polysaccharide, pullulan. *Carbohydr. Res.* **153**: 79–86
- Charles PT, Stubbs VR, Soto CM, Martin BD, White BJ & Taitt CR (2009) Reduction of Non-Specific Protein Adsorption Using Poly(ethylene) Glycol (PEG) Modified Polyacrylate Hydrogels In Immunoassays for Staphylococcal Enterotoxin B Detection. *Sensors* **9**: 645–655
- Chaves NL, Estrela-Lopis I, Böttner J, Lopes CA, Guido BC, de Sousa AR & Bão SN (2017) Exploring cellular uptake of iron oxide nanoparticles associated with rhodium citrate in breast cancer cells. *Int. J. Nanomedicine* **12**: 5511–5523
- Chen HH, Ho Y-P, Jiang X, Mao H-Q, Wang T-H & Leong KW (2008) Quantitative Comparison of Intracellular Unpacking Kinetics of Polyplexes by a Model Constructed From Quantum Dot-FRET. *Mol. Ther. J. Am. Soc. Gene Ther.* **16**: 324–332
- Chen PL, Chen YM, Bookstein R & Lee WH (1990) Genetic mechanisms of tumor suppression by the human p53 gene. *Science* **250**: 1576–1580
- Chen Q-R, Zhang L, Luther PW & Mixson AJ (2002) Optimal transfection with the HK polymer depends on its degree of branching and the pH of endocytic vesicles. *Nucleic Acids Res.* **30**: 1338–1345
- Cheng X (1995) Structure and Function of DNA Methyltransferases. *Annu. Rev. Biophys. Biomol. Struct.* **24**: 293–318
- Choi HS, Ashitate Y, Lee JH, Kim SH, Matsui A, Insin N, Bawendi MG, Semmler-Behnke M, Frangioni JV & Tsuda A (2010a) Rapid translocation of nanoparticles from the lung airspaces to the body. *Nat. Biotechnol.* **28**: 1300–1303

- Choi HS, Liu W, Liu F, Nasr K, Misra P, Bawendi MG & Frangioni JV (2010b) Design considerations for tumour-targeted nanoparticles. *Nat. Nanotechnol.* **5**: 42–47
- Cohen RN, van der Aa MAEM, Macaraeg N, Lee AP & Szoka FC (2009) Quantification of plasmid DNA copies in the nucleus after lipoplex and polyplex transfection. *J. Controlled Release* **135**: 166–174
- Coleman MM, Xu Y & Painter PC (1994) Compositional heterogeneities in hydrogen-bonded polymer blends: infrared spectroscopic results. *Macromolecules* **27**: 127–134
- Conner SD & Schmid SL (2003) Regulated portals of entry into the cell. *Nature* **422**: 37–44
- Couchman JR (2003) Syndecans: proteoglycan regulators of cell-surface microdomains? *Nat. Rev. Mol. Cell Biol.* **4**: 926–938
- Dai S, Ravi P & Tam KC (2008) pH-Responsive polymers: synthesis, properties and applications. *Soft Matter* **4**: 435–449
- Dais P, Vlachou S & Taravel FR (2001) ¹³C Nuclear Magnetic Relaxation Study of Segmental Dynamics of the Heteropolysaccharide Pullulan in Dilute Solutions. *Biomacromolecules* **2**: 1137–1147
- Das SK, Menezes ME, Bhatia S, Wang X-Y, Emdad L, Sarkar D & Fisher PB (2015) Gene Therapies for Cancer: Strategies, Challenges and Successes. *J. Cell. Physiol.* **230**: 259–271
- Dash PR, Read ML, Barrett LB, Wolfert MA & Seymour LW (1999) Factors affecting blood clearance and in vivo distribution of polyelectrolyte complexes for gene delivery. *Gene Ther.* **6**: 643–650
- Dean DA (2000) Peptide nucleic acids: versatile tools for gene therapy strategies. *Adv. Drug Deliv. Rev.* **44**: 81–95
- Demeneix B & Behr J (2005) Polyethylenimine (PEI). In *Advances in Genetics* pp 215–230. Academic Press Available at: <http://www.sciencedirect.com/science/article/pii/S0065266005530086>
- Deng J, Liu X, Ma L, Cheng C, Sun S & Zhao C (2016) Switching biological functionalities of biointerfaces via dynamic covalent bonds. *J. Mater. Chem. B* **4**: 694–703
- Dhaneshwar SS, K M, pal, Gairola N & Kadam SS (2006) Dextran: A promising macromolecular drug carrier. *Indian J. Pharm. Sci.* **68**: 705
- Dick CR & Ham GE (1970) Characterization of Polyethylenimine. *J. Macromol. Sci. Part - Chem.* **4**: 1301–1314
- Doh K-O & Yeo Y (2012) Application of polysaccharides for surface modification of nanomedicines. *Ther. Deliv.* **3**: 1447–1456
- Doherty GJ & McMahon HT (2009) Mechanisms of Endocytosis. *Annu. Rev. Biochem.* **78**: 857–902

- Dong W, Li S, Jin G, Sun Q, Ma D & Hua Z (2007a) Efficient Gene Transfection into Mammalian Cells Mediated by Cross-linked Polyethylenimine. *Int. J. Mol. Sci.* **8**: 81–102
- Dong W, Li S, Jin G, Sun Q, Ma D & Hua Z (2007b) Efficient Gene Transfection into Mammalian Cells Mediated by Cross-linked Polyethylenimine. *Int. J. Mol. Sci.* **8**: 81–102
- Douglas JT & Curiel DT (2005) Viral Vectors for Cancer Gene Therapy. In *Cancer Gene Therapy* pp 379–391. Humana Press Available at: https://link.springer.com/chapter/10.1007/978-1-59259-785-7_25 [Accessed November 28, 2017]
- Dow SW, Fradkin LG, Liggitt DH, Willson AP, Heath TD & Potter TA (1999) Lipid-DNA Complexes Induce Potent Activation of Innate Immune Responses and Antitumor Activity When Administered Intravenously. *J. Immunol.* **163**: 1552–1561
- Dufort S, Sancey L & Coll J-L (2012) Physico-chemical parameters that govern nanoparticles fate also dictate rules for their molecular evolution. *Adv. Drug Deliv. Rev.* **64**: 179–189
- El-Deiry WS, Kern SE, Pietenpol JA, Kinzler KW & Vogelstein B (1992) Definition of a consensus binding site for p53. *Nat. Genet.* **1**: 45
- El-Deiry WS, Tokino T, Velculescu VE, Levy DB, Parsons R, Trent JM, Lin D, Mercer WE, Kinzler KW & Vogelstein B (1993) WAF1, a potential mediator of p53 tumor suppression. *Cell* **75**: 817–825
- El-Sayed A & Harashima H (2013) Endocytosis of Gene Delivery Vectors: From Clathrin-dependent to Lipid Raft-mediated Endocytosis. *Mol. Ther.* **21**: 1118–1130
- Escalante J, Carrillo-Morales M & Linzaga I (2008) Michael Additions of Amines to Methyl Acrylates Promoted by Microwave Irradiation. *Molecules* **13**: 340–347
- Evans CW, Fitzgerald M, Clemons TD, House MJ, Padman BS, Shaw JA, Saunders M, Harvey AR, Zdyrko B, Luzinov I, Silva GA, Dunlop SA & Iyer KS (2011) Multimodal Analysis of PEI-Mediated Endocytosis of Nanoparticles in Neural Cells. *ACS Nano* **5**: 8640–8648
- Fabbro M & Henderson BR (2003) Regulation of tumor suppressors by nuclear-cytoplasmic shuttling. *Exp. Cell Res.* **282**: 59–69
- Ferruti P (2013) Poly(amidoamine)s: Past, present, and perspectives. *J. Polym. Sci. Part Polym. Chem.* **51**: 2319–2353
- Fischer D, Bieber T, Li Y, Elsässer H-P & Kissel T (1999) A Novel Non-Viral Vector for DNA Delivery Based on Low Molecular Weight, Branched Polyethylenimine: Effect of Molecular Weight on Transfection Efficiency and Cytotoxicity. *Pharm. Res.* **16**: 1273–1279

- Fischer D, Li Y, Ahlemeyer B, Krieglstein J & Kissel T (2003a) In vitro cytotoxicity testing of polycations: influence of polymer structure on cell viability and hemolysis. *Biomaterials* **24**: 1121–1131
- Fischer D, Li Y, Ahlemeyer B, Krieglstein J & Kissel T (2003b) In vitro cytotoxicity testing of polycations: influence of polymer structure on cell viability and hemolysis. *Biomaterials* **24**: 1121–1131
- Florea BI, Meaney C, Junginger HE & Borchard G (2002) Transfection efficiency and toxicity of polyethylenimine in differentiated Calu-3 and nondifferentiated COS-1 cell cultures. *AAPS PharmSci* **4**: 1–11
- Forrest ML, Koerber JT & Pack DW (2003) A Degradable Polyethylenimine Derivative with Low Toxicity for Highly Efficient Gene Delivery. *Bioconjug. Chem.* **14**: 934–940
- Forrest ML, Meister GE, Koerber JT & Pack DW (2004) Partial Acetylation of Polyethylenimine Enhances In Vitro Gene Delivery. *Pharm. Res.* **21**: 365–371
- Fröhlich E (2012) The role of surface charge in cellular uptake and cytotoxicity of medical nanoparticles. *Int. J. Nanomedicine* **7**: 5577–5591
- Funhoff AM, Nostrum CF van, Janssen APCA, Fens MHAM, Crommelin DJA & Hennink WE (2004) Polymer Side-Chain Degradation as a Tool to Control the Destabilization of Polyplexes. *Pharm. Res.* **21**: 170–176
- Geall AJ & Blagbrough IS (2000) Rapid and sensitive ethidium bromide fluorescence quenching assay of polyamine conjugate–DNA interactions for the analysis of lipoplex formation in gene therapy. *J. Pharm. Biomed. Anal.* **22**: 849–859
- Giacca M (2010) Gene Therapy Springer Science & Business Media
- Gilbert HF (1995) [2] Thiol/disulfide exchange equilibria and disulfidebond stability. In *Methods in Enzymology* pp 8–28. Academic Press Available at: <http://www.sciencedirect.com/science/article/pii/0076687995511075>
- Glover DJ, Leyton DL, Moseley GW & Jans DA (2010) The efficiency of nuclear plasmid DNA delivery is a critical determinant of transgene expression at the single cell level. *J. Gene Med.* **12**: 77–85
- Glover DJ, Lipps HJ & Jans DA (2005) Towards safe, non-viral therapeutic gene expression in humans. *Nat. Rev. Genet.* **6**: 299–310
- Godbey WT, Barry MA, Saggau P, Wu KK & Mikos AG (2000) Poly(ethylenimine)-mediated transfection: A new paradigm for gene delivery. *J. Biomed. Mater. Res.* **51**: 321–328
- Godbey WT, Wu KK & Mikos AG (1999a) Tracking the intracellular path of poly(ethylenimine)/DNA complexes for gene delivery. *Proc. Natl. Acad. Sci.* **96**: 5177–5181
- Godbey WT, Wu KK & Mikos AG (1999b) Poly(ethylenimine) and its role in gene delivery. *J. Controlled Release* **60**: 149–160

- Gottfried LF & Dean DA (2013) Extracellular and Intracellular Barriers to Non-Viral Gene Transfer. Available at: <http://www.intechopen.com/books/novel-gene-therapy-approaches/extracellular-and-intracellular-barriers-to-non-viral-gene-transfer> [Accessed November 24, 2017]
- Grandinetti G, Smith AE & Reineke TM (2012a) Membrane and Nuclear Permeabilization by Polymeric pDNA Vehicles: Efficient Method for Gene Delivery or Mechanism of Cytotoxicity? *Mol. Pharm.* **9**: 523–538
- Grandinetti G, Smith AE & Reineke TM (2012b) Membrane and Nuclear Permeabilization by Polymeric pDNA Vehicles: Efficient Method for Gene Delivery or Mechanism of Cytotoxicity? *Mol. Pharm.* **9**: 523–538
- Guhagarkar SA, Gaikwad RV, Samad A, Malshe VC & Devarajan PV (2010) Polyethylene sebacate-doxorubicin nanoparticles for hepatic targeting. *Int. J. Pharm.* **401**: 113–122
- Gupta M & Gupta AK (2004) Hydrogel pullulan nanoparticles encapsulating pBUDLacZ plasmid as an efficient gene delivery carrier. *J. Controlled Release* **99**: 157–166
- Hanna E, Rémuzat C, Auquier P & Toumi M (2017) Gene therapies development: slow progress and promising prospect. *J. Mark. Access Health Policy* **5**: Available at: <https://www.ncbi.nlm.nih.gov/pmc/articles/PMC5328344/>
- von Harpe A, Petersen H, Li Y & Kissel T (2000) Characterization of commercially available and synthesized polyethylenimines for gene delivery. *J. Controlled Release* **69**: 309–322
- Haupt Y, Maya R, Kazaz A & Oren M (1997) Mdm2 promotes the rapid degradation of p53. *Nature* **387**: 296
- Hermeking H, Lengauer C, Polyak K, He T-C, Zhang L, Thiagalingam S, Kinzler KW & Vogelstein B (1997) 14-3-3 σ Is a p53-Regulated Inhibitor of G2/M Progression. *Mol. Cell* **1**: 3–11
- Herskowitz I (1987) Functional inactivation of genes by dominant negative mutations. *Nature* **329**: 219
- Hollstein M, Sidransky D, Vogelstein B & Harris CC (1991) p53 mutations in human cancers. *Science* **253**: 49–53
- Honda R, Tanaka H & Yasuda H (1997) Oncoprotein MDM2 is a ubiquitin ligase E3 for tumor suppressor p53. *FEBS Lett.* **420**: 25–27
- Hosseinkhani H, Azzam T, Tabata Y & Domb AJ (2004) Dextran–spermine polycation: an efficient nonviral vector for in vitro and in vivo gene transfection. *Gene Ther.* **11**: 194
- Hufnagel H, Hakim P, Lima A & Hollfelder F (2009) Fluid Phase Endocytosis Contributes to Transfection of DNA by PEI-25. *Mol. Ther.* **17**: 1411–1417

- Hyde SC, Pringle IA, Abdullah S, Lawton AE, Davies LA, Varathalingam A, Nunez-Alonso G, Green A-M, Bazzani RP, Sumner-Jones SG, Chan M, Li H, Yew NS, Cheng SH, Christopher Boyd A, Davies JC, Griesenbach U, Porteous DJ, Sheppard DN, Munkonge FM, et al (2008) CpG-free plasmids confer reduced inflammation and sustained pulmonary gene expression. *Nat. Biotechnol.* **26**: 549–551
- Ihm J-E, Han K-O, Han I-K, Ahn K-D, Han D-K & Cho C-S (2003) High Transfection Efficiency of Poly(4-vinylimidazole) as a New Gene Carrier. *Bioconj. Chem.* **14**: 707–708
- Ikada Y & Tsuji H (2000) Biodegradable polyesters for medical and ecological applications. *Macromol. Rapid Commun.* **21**: 117–132
- Ishida T, Ichihara M, Wang X, Yamamoto K, Kimura J, Majima E & Kiwada H (2006) Injection of PEGylated liposomes in rats elicits PEG-specific IgM, which is responsible for rapid elimination of a second dose of PEGylated liposomes. *J. Controlled Release* **112**: 15–25
- Ishida T, Wang X, Shimizu T, Nawata K & Kiwada H (2007) PEGylated liposomes elicit an anti-PEG IgM response in a T cell-independent manner. *J. Controlled Release* **122**: 349–355
- Iwai M, Harada Y, Tanaka S, Muramatsu A, Mori T, Kashima K, Imanishi J & Mazda O (2002) Polyethylenimine-Mediated Suicide Gene Transfer Induces a Therapeutic Effect for Hepatocellular Carcinoma in Vivo by Using an Epstein–Barr Virus-Based Plasmid Vector. *Biochem. Biophys. Res. Commun.* **291**: 48–54
- Jackson M, Marks L, May GHW & Wilson JB (2018) The genetic basis of disease. *Essays Biochem.* **62**: 643–723
- Jana P, Sarkar K, Mitra T, Chatterjee A, Gnanamani A, Chakraborti G & Kundu PP (2016) Synthesis of a carboxymethylated guar gum grafted polyethyleneimine copolymer as an efficient gene delivery vehicle. *RSC Adv.* **6**: 13730–13741
- Jiang D & Salem AK (2012a) Optimized dextran-polyethylenimine conjugates are efficient non-viral vectors with reduced cytotoxicity when used in serum containing environments. *Int. J. Pharm.* **427**: 71–79
- Jiang D & Salem AK (2012b) Optimized dextran–polyethylenimine conjugates are efficient non-viral vectors with reduced cytotoxicity when used in serum containing environments. *Int. J. Pharm.* **427**: 71–79
- Joerger AC & Fersht AR (2007) Structure–function–rescue: the diverse nature of common p53 cancer mutants. *Oncogene* **26**: 2226
- Jones CH, Chen C-K, Jiang M, Fang L, Cheng C & Pfeifer BA (2013a) Synthesis of Cationic Polylactides with Tunable Charge Densities as Nanocarriers for Effective Gene Delivery. *Mol. Pharm.* **10**: 1138–1145
- Jones CH, Chen C-K, Ravikrishnan A, Rane S & Pfeifer BA (2013b) Overcoming Nonviral Gene Delivery Barriers: Perspective and Future. *Mol. Pharm.* **10**: 4082–4098

- Jones GD, Langsjoen A, Neumann Smmc & Zomlefer J (1944) The Polymerization of Ethylenimine. *J. Org. Chem.* **09**: 125–147
- Kafil V & Omidi Y (2011a) Cytotoxic Impacts of Linear and Branched Polyethylenimine Nanostructures in A431 Cells. *BioImpacts BI* **1**: 23–30
- Kafil V & Omidi Y (2011b) Cytotoxic Impacts of Linear and Branched Polyethylenimine Nanostructures in A431 Cells. *BioImpacts BI* **1**: 23–30
- Kanatani I, Ikai T, Okazaki A, Jo J, Yamamoto M, Imamura M, Kanematsu A, Yamamoto S, Ito N, Ogawa O & Tabata Y (2006a) Efficient gene transfer by pullulan–spermine occurs through both clathrin- and raft/caveolae-dependent mechanisms. *J. Controlled Release* **116**: 75–82
- Kanatani I, Ikai T, Okazaki A, Jo J, Yamamoto M, Imamura M, Kanematsu A, Yamamoto S, Ito N, Ogawa O & Tabata Y (2006b) Efficient gene transfer by pullulan–spermine occurs through both clathrin- and raft/caveolae-dependent mechanisms. *J. Controlled Release* **116**: 75–82
- Kettler K, Veltman K, Meent D van de, Wezel A van & Hendriks AJ (2014) Cellular uptake of nanoparticles as determined by particle properties, experimental conditions, and cell type. *Environ. Toxicol. Chem.* **33**: 481–492
- Kichler A (2004a) Gene transfer with modified polyethylenimines. *J. Gene Med.* **6**: S3–S10
- Kichler A (2004b) Gene transfer with modified polyethylenimines. *J. Gene Med.* **6**: S3–S10
- Kimoto T, Shibuya T & Shiobara S (1997) Safety studies of a novel starch, pullulan: Chronic toxicity in rats and bacterial mutagenicity. *Food Chem. Toxicol.* **35**: 323–329
- Kircheis R, Schüller S, Brunner S, Ogris M, Heider K-H, Zauner W & Wagner E (1999) Polycation-based DNA complexes for tumor-targeted gene delivery in vivo. *J. Gene Med.* **1**: 111–120
- Kircheis R, Wightman L, Schreiber A, Robitza B, Rössler V, Kursa M & Wagner E (2001) Polyethylenimine/DNA complexes shielded by transferrin target gene expression to tumors after systemic application. *Gene Ther.* **8**: 28–40
- Kong G, Braun RD & Dewhirst MW (2000) Hyperthermia Enables Tumor-specific Nanoparticle Delivery: Effect of Particle Size. *Cancer Res.* **60**: 4440–4445
- Kopatz I, Remy J-S & Behr J-P (2004) A model for non-viral gene delivery: through syndecan adhesion molecules and powered by actin. *J. Gene Med.* **6**: 769–776
- Koppelhus U & Nielsen PE (2003) Cellular delivery of peptide nucleic acid (PNA). *Adv. Drug Deliv. Rev.* **55**: 267–280
- Krishnamoorthy M, Hakobyan S, Ramstedt M & Gautrot JE (2014) Surface-Initiated Polymer Brushes in the Biomedical Field: Applications in Membrane Science, Biosensing, Cell Culture, Regenerative Medicine and Antibacterial Coatings. *Chem. Rev.* **114**: 10976–11026

- Kubbutat MHG, Jones SN & Vousden KH (1997) Regulation of p53 stability by Mdm2. *Nature* **387**: 299
- Kunath K, von Harpe A, Fischer D, Petersen H, Bickel U, Voigt K & Kissel T (2003) Low-molecular-weight polyethylenimine as a non-viral vector for DNA delivery: comparison of physicochemical properties, transfection efficiency and in vivo distribution with high-molecular-weight polyethylenimine. *J. Controlled Release* **89**: 113–125
- Kursa M, Walker GF, Roessler V, Ogris M, Roedl W, Kircheis R & Wagner E (2003) Novel Shielded Transferrin–Polyethylene Glycol–Polyethylenimine/DNA Complexes for Systemic Tumor-Targeted Gene Transfer. *Bioconjug. Chem.* **14**: 222–231
- Labat-Moleur F, M Steffan A, Brisson C, Perron H, Feugeas O, Furstenberger P, Oberling F, Brambilla E & P Behr J (1996) An electron microscopy study into the mechanism of gene transfer with lipopolyamines. *Gene Ther.* **3**: 1010–7
- Lam AP & Dean DA (2010) Progress and prospects: nuclear import of nonviral vectors. *Gene Ther.* **17**: 439–447
- Lander AD & Selleck SB (2000) The Elusive Functions of Proteoglycans: In Vivo Veritas. *J. Cell Biol.* **148**: 227–232
- Lane DP (1992) p53, guardian of the genome. *Nature* **358**: 15
- Layek B & Singh J (2013) Amino Acid Grafted Chitosan for High Performance Gene Delivery: Comparison of Amino Acid Hydrophobicity on Vector and Polyplex Characteristics. *Biomacromolecules* **14**: 485–494
- Leathers TD (2005) Dextran. In *Biopolymers Online* American Cancer Society Available at: <https://onlinelibrary.wiley.com/doi/abs/10.1002/3527600035.bpol5012>
- Lechardeur D, Sohn K-J, Haardt M, Joshi PB, Monck M, Graham RW, Beatty B, Squire J, O’Brodivich H & Lukacs GL (1999) Metabolic instability of plasmid DNA in the cytosol: a potential barrier to gene transfer. *Gene Ther.* **6**: 482
- Lee H-S, Eckmann DM, Lee D, Hickok NJ & Composto RJ (2011) Symmetric pH-Dependent Swelling and Antibacterial Properties of Chitosan Brushes. *Langmuir ACS J. Surf. Colloids* **27**: 12458–12465
- Levine AJ (1997) p53, the cellular gatekeeper for growth and division. *Cell* **88**: 323–331
- Li J, Liang H, Liu J & Wang Z (2018) Poly (amidoamine) (PAMAM) dendrimer mediated delivery of drug and pDNA/siRNA for cancer therapy. *Int. J. Pharm.* **546**:
- Lin C, Blaauboer C-J, Timoneda MM, Lok MC, van Steenberg M, Hennink WE, Zhong Z, Feijen J & Engbersen JFJ (2008) Bioreducible poly(amido amine)s with oligoamine side chains: Synthesis, characterization, and structural effects on gene delivery. *J. Controlled Release* **126**: 166–174
- Lin C & Engbersen JF (2009) The role of the disulfide group in disulfide-based polymeric gene carriers. *Expert Opin. Drug Deliv.* **6**: 421–439

- Lin C & Engbersen JFJ (2008) Effect of chemical functionalities in poly(amido amine)s for non-viral gene transfection. *J. Controlled Release* **132**: 267–272
- Lippert JL, Robertson JA, Havens JR & Tan JS (1985) Structural studies of poly(N-vinylimidazole) complexes by infrared and Raman spectroscopy. *Macromolecules* **18**: 63–67
- Luca LD (2005) Naturally Occurring and Synthetic Imidazoles: Their Chemistry and Their Biological Activities. *Curr. Med. Chem.* Available at: <http://www.eurekaselect.com/55209/article> [Accessed November 17, 2018]
- Lungwitz U, Breunig M, Blunk T & Göpferich A (2005) Polyethylenimine-based non-viral gene delivery systems. *Eur. J. Pharm. Biopharm.* **60**: 247–266
- Luten J, Akeroyd N, Funhoff A, Lok MC, Talsma H & Hennink WE (2006) Methacrylamide Polymers with Hydrolysis-Sensitive Cationic Side Groups as Degradable Gene Carriers. *Bioconjug. Chem.* **17**: 1077–1084
- M. Laird Forrest, James T. Koerber and Pack* DW (2003) A Degradable Polyethylenimine Derivative with Low Toxicity for Highly Efficient Gene Delivery. Available at: <https://pubs.acs.org/doi/abs/10.1021/bc034014g> [Accessed February 13, 2019]
- Mayor S & Pagano RE (2007) Pathways of clathrin-independent endocytosis. *Nat. Rev. Mol. Cell Biol.* **8**: 603–612
- Meng F, Hennink WE & Zhong Z (2009) Reduction-sensitive polymers and bioconjugates for biomedical applications. *Biomaterials* **30**: 2180–2198
- Mesika A, Kiss V, Brumfeld V, Ghosh G & Reich Z (2005) Enhanced Intracellular Mobility and Nuclear Accumulation of DNA Plasmids Associated with a Karyophilic Protein. *Hum. Gene Ther.* **16**: 200–208
- Mishra B, Vuppu S & Rath K (2011) The role of microbial pullulan, a biopolymer in pharmaceutical approaches: A review. *J. Appl. Pharm. Sci* **1**: 45–50
- Mishra R, Ramasamy K, Ahmad N, Eshak Z & Majeed A (2014) pH dependent poly[2-(methacryloyloxyethyl)trimethylammonium chloride-co-methacrylic acid]hydrogels for enhanced targeted delivery of 5-fluorouracil in colon cancer cells
- Mitha AT & Rekha MR (2014) Multifunctional polymeric nanoplexes for anticancer co-delivery of p53 and mitoxantrone. *J. Mater. Chem. B* **2**: 8005–8016
- Moghimi SM, Symonds P, Murray JC, Hunter AC, Debska G & Szewczyk A (2005a) A two-stage poly(ethylenimine)-mediated cytotoxicity: implications for gene transfer/therapy. *Mol. Ther.* **11**: 990–995
- Moghimi SM, Symonds P, Murray JC, Hunter AC, Debska G & Szewczyk A (2005b) A two-stage poly(ethylenimine)-mediated cytotoxicity: implications for gene transfer/therapy. *Mol. Ther.* **11**: 990–995

- Moon H-H, Joo MK, Mok H, Lee M, Hwang K-C, Kim SW, Jeong JH, Choi D & Kim SH (2014) MSC-based VEGF gene therapy in rat myocardial infarction model using facial amphipathic bile acid-conjugated polyethyleneimine. *Biomaterials* **35**: 1744–1754
- Morgan DM, Clover J & Pearson JD (1988) Effects of synthetic polycations on leucine incorporation, lactate dehydrogenase release, and morphology of human umbilical vein endothelial cells. *J. Cell Sci.* **91**: 231–238
- Morille M, Passirani C, Vonarbourg A, Clavreul A & Benoit J-P (2008) Progress in developing cationic vectors for non-viral systemic gene therapy against cancer. *Biomaterials* **29**: 3477–3496
- Moselhy J, Sarkar S, Chia MC, Mocanu JD, Taulier N, Liu F-F & Wu XY (2007) Evaluation of copolymers of N-isopropylacrylamide and 2-dimethyl(aminoethyl)methacrylate in non-viral and adenoviral vectors for gene delivery to nasopharyngeal carcinoma. *Int. J. Nanomedicine* **2**: 461–478
- Na K & Bae YH (2002) Self-assembled hydrogel nanoparticles responsive to tumor extracellular pH from pullulan derivative/sulfonamide conjugate: characterization, aggregation, and adriamycin release in vitro. *Pharm. Res.* **19**: 681–688
- Nagane K, Kitada M, Wakao S, Dezawa M & Tabata Y (2009) Practical Induction System for Dopamine-Producing Cells from Bone Marrow Stromal Cells Using Spermine-Pullulan-Mediated Reverse Transfection Method. *Tissue Eng. Part A* **15**: 1655–1665
- Nagasaki Y, Sato Y & Kato M (1997) A novel synthesis of semitelechelic functional poly(methacrylate)s through an alcoholate initiated polymerization. Synthesis of poly[2-(N,N-diethylaminoethyl) methacrylate] macromonomer. *Macromol. Rapid Commun.* **18**: 827–835
- Nagpal M, Singh S, Singh P, Chauhan P & Zaidi MA (2016) Tumor markers: A diagnostic tool. *Natl. J. Maxillofac. Surg.* **7**: 17–20
- Namvar A, Bolhassani A, Khairkhan N & Motevalli F (2015) Physicochemical properties of polymers: An important system to overcome the cell barriers in gene transfection. *Biopolymers* **103**: 363–375
- Nguyen H-K, Lemieux P, Vinogradov SV, Gebhart CL, Guérin N, Paradis G, Bronich TK, Alakhov VY & Kabanov AV (2000) Evaluation of polyether-polyethyleneimine graft copolymers as gene transfer agents. *Gene Ther.* **7**: 126–138
- Nigro JM, Baker SJ, Preisinger AC, Jessup JM, Hosteller R, Cleary K, Signer SH, Davidson N, Baylin S, Devilee P, Glover T, Collins FS, Weslon A, Modali R, Harris CC & Vogelstein B (1989) Mutations in the p53 gene occur in diverse human tumour types. *Nature* **342**: 705
- Nikonenko NA, Buslov DK, Sushko NI & Zhabankov RG (2000) Investigation of stretching vibrations of glycosidic linkages in disaccharides and polysaccharides with use of IR spectra deconvolution. *Biopolymers* **57**: 257–262

- Nouri F, Sadeghpour H, Heidari R & Dehshahri A (2017) Preparation, characterization, and transfection efficiency of low molecular weight polyethylenimine-based nanoparticles for delivery of the plasmid encoding CD200 gene. *Int. J. Nanomedicine* **12**: 5557–5569
- Ochietti B, Lemieux P, Kabanov AV, Vinogradov S, St-Pierre Y & Alakhov V (2002) Inducing neutrophil recruitment in the liver of ICAM-1-deficient mice using polyethyleneimine grafted with Pluronic P123 as an organ-specific carrier for transgenic ICAM-1. *Gene Ther.* **9**: 939–945
- Ogris M, Brunner S, Schüller S, Kircheis R & Wagner E (1999) PEGylated DNA/transferrin-PEI complexes: reduced interaction with blood components, extended circulation in blood and potential for systemic gene delivery. *Gene Ther.* **6**: 595–605
- Ogris M, Steinlein P, Kursa M, Mechtler K, Kircheis R & Wagner E (1998) The size of DNA/transferrin-PEI complexes is an important factor for gene expression in cultured cells. *Gene Ther.* **5**: 1425–1433
- Ogris M, Walker G, Blessing T, Kircheis R, Wolschek M & Wagner E (2003) Tumor-targeted gene therapy: strategies for the preparation of ligand-polyethylene glycol-polyethylenimine/DNA complexes. *J. Controlled Release* **91**: 173–181
- Ohki R, Nemoto J, Murasawa H, Oda E, Inazawa J, Tanaka N & Taniguchi T (2000) Reprimo, a New Candidate Mediator of the p53-mediated Cell Cycle Arrest at the G2 Phase. *J. Biol. Chem.* **275**: 22627–22630
- Okuda T, Niidome T & Aoyagi H (2004) Cytosolic soluble proteins induce DNA release from DNA-gene carrier complexes. *J. Controlled Release* **98**: 325–332
- Onishi Y, Eshita Y, Murashita A, Mizuno M & Yoshida J (2007) Characteristics of DEAE-dextran-MMA graft copolymer as a nonviral gene carrier. *Nanomedicine Nanotechnol. Biol. Med.* **3**: 184–191
- Oupicky D, Ogris M, Howard KA, Dash PR, Ulbrich K & Seymour LW (2002) Importance of Lateral and Steric Stabilization of Polyelectrolyte Gene Delivery Vectors for Extended Systemic Circulation. *Mol. Ther.* **5**: 463–472
- Ozaki T & Nakagawara A (2011) Role of p53 in Cell Death and Human Cancers. *Cancers* **3**: 994–1013
- Pack DW, Hoffman AS, Pun S & Stayton PS (2005) Design and development of polymers for gene delivery. *Nat. Rev. Drug Discov.* **4**: 581–593
- Pagano JS & Vaheri A (1965) Enhancement of infectivity of poliovirus RNA with diethylaminoethyl-dextran (DEAE-D). *Arch. Für Gesamte Virusforsch.* **17**: 456–464
- Paris S, Burlacu A & Durocher Y (2008) Opposing Roles of Syndecan-1 and Syndecan-2 in Polyethyleneimine-mediated Gene Delivery. *J. Biol. Chem.* **283**: 7697–7704

- Park JS, Park J-K, Nam J-P, Kim W-S, Choi C, Kim M-Y, Jang M-K & Nah J-W (2012) Preparation of pullulan-g-poly(L-lysine) and its evaluation as a gene carrier. *Macromol. Res.* **20**: 667–672
- Park MV, Lankveld DP, van Loveren H & de Jong WH (2009) The status of in vitro toxicity studies in the risk assessment of nanomaterials. *Nanomed.* **4**: 669–685
- Passirani C, Barratt G, Devissaguet J-P & Labarre D (1998) Interactions of nanoparticles bearing heparin or dextran covalently bound to poly(methyl methacrylate) with the complement system. *Life Sci.* **62**: 775–785
- Patnaik S, Arif M, Pathak A, Kurupati R, Singh Y & Gupta KC (2010) Cross-linked polyethylenimine-hexametaphosphate nanoparticles to deliver nucleic acids therapeutics. *Nanomedicine Nanotechnol. Biol. Med.* **6**: 344–354
- Perrimon N & Bernfield M (2000) Specificities of heparan sulphate proteoglycans in developmental processes. *Nature* **404**: 725–728
- Petersen H, Fechner PM, Fischer D & Kissel T (2002a) Synthesis, Characterization, and Biocompatibility of Polyethylenimine-graft-poly(ethylene glycol) Block Copolymers. *Macromolecules* **35**: 6867–6874
- Petersen H, Fechner PM, Martin AL, Kunath K, Stolnik S, Roberts CJ, Fischer D, Davies MC & Kissel T (2002b) Polyethylenimine-graft-Poly(ethylene glycol) Copolymers: Influence of Copolymer Block Structure on DNA Complexation and Biological Activities as Gene Delivery System. *Bioconjug. Chem.* **13**: 845–854
- Pichon C, Billiet L & Midoux P (2010) Chemical vectors for gene delivery: uptake and intracellular trafficking. *Curr. Opin. Biotechnol.* **21**: 640–645
- Pietenpol JA, Tokino T, Thiagalingam S, el-Deiry WS, Kinzler KW & Vogelstein B (1994) Sequence-specific transcriptional activation is essential for growth suppression by p53. *Proc. Natl. Acad. Sci.* **91**: 1998–2002
- Plank C, Mechtler K, Szoka FC & Wagner E (1996) Activation of the Complement System by Synthetic DNA Complexes: A Potential Barrier for Intravenous Gene Delivery. *Hum. Gene Ther.* **7**: 1437–1446
- Poon GMK (2007) Enhancement of oligomeric stability by covalent linkage and its application to the human p53tet domain: thermodynamics and biological implications. *Biochem. Soc. Trans.* **35**: 1574–1578
- Poon GMK & Gariépy J (2007) Cell-surface proteoglycans as molecular portals for cationic peptide and polymer entry into cells. *Biochem. Soc. Trans.* **35**: 788–793
- Poulain L, Ziller C, Muller CD, Erbacher P, Bettinger T, Rodier J-F & Behr J-P (2000) Ovarian carcinoma cells are effectively transfected by polyethylenimine (PEI) derivatives. *Cancer Gene Ther.* **7**: 644
- Prabha S, Zhou W-Z, Panyam J & Labhasetwar V (2002) Size-dependency of nanoparticle-mediated gene transfection: studies with fractionated nanoparticles. *Int. J. Pharm.* **244**: 105–115

- Prevette LE, Mullen DG & Banaszak Holl MM (2010) Polycation-induced Cell Membrane Permeability Does Not Enhance Cellular Uptake or Expression Efficiency of Delivered DNA. *Mol. Pharm.* **7**: 870–883
- Prives C & Hall PA (1999) The p53 pathway. *J. Pathol.* **187**: 112–126
- Priya SS, Rekha MR & Sharma CP (2014) Pullulan–protamine as efficient haemocompatible gene delivery vector: Synthesis and in vitro characterization. *Carbohydr. Polym.* **102**: 207–215
- Purama RK, Goswami P, Khan AT & Goyal A (2009) Structural analysis and properties of dextran produced by *Leuconostoc mesenteroides* NRRL B-640. *Carbohydr. Polym.* **76**: 30–35
- Raina S & Missiakas D (1997) Making and Breaking Disulfide Bonds. *Annu. Rev. Microbiol.* **51**: 179–202
- Ramamoorth M & Narvekar A (2015) Non Viral Vectors in Gene Therapy- An Overview. *J. Clin. Diagn. Res. JCDR* **9**: GE01–GE06
- Regnström K, Ragnarsson EGE, Köping-Höggård M, Torstensson E, Nyblom H & Artursson P (2003) PEI – a potent, but not harmless, mucosal immuno-stimulator of mixed T-helper cell response and FasL-mediated cell death in mice. *Gene Ther.* **10**: 1575
- Rehman Z ur, Zuhorn IS & Hoekstra D (2013) How cationic lipids transfer nucleic acids into cells and across cellular membranes: Recent advances. *J. Controlled Release* **166**: 46–56
- Rejman J, Bragonzi A & Conese M (2005a) Role of clathrin- and caveolae-mediated endocytosis in gene transfer mediated by lipo- and polyplexes. *Mol. Ther.* **12**: 468–474
- Rejman J, Bragonzi A & Conese M (2005b) Role of clathrin- and caveolae-mediated endocytosis in gene transfer mediated by lipo- and polyplexes. *Mol. Ther.* **12**: 468–474
- Rekha MR & Sharma CP (2009a) Blood compatibility and in vitro transfection studies on cationically modified pullulan for liver cell targeted gene delivery. *Biomaterials* **30**: 6655–6664
- Rekha MR & Sharma CP (2009b) Blood compatibility and in vitro transfection studies on cationically modified pullulan for liver cell targeted gene delivery. *Biomaterials* **30**: 6655–6664
- Rekha MR & Sharma CP (2011a) Hemocompatible pullulan–polyethyleneimine conjugates for liver cell gene delivery: In vitro evaluation of cellular uptake, intracellular trafficking and transfection efficiency. *Acta Biomater.* **7**: 370–379
- Rekha MR & Sharma CP (2011b) Hemocompatible pullulan–polyethyleneimine conjugates for liver cell gene delivery: In vitro evaluation of cellular uptake, intracellular trafficking and transfection efficiency. *Acta Biomater.* **7**: 370–379

- Rekha MR & Sharma CP (2011c) Intracellular Trafficking Mechanism and Cytosolic Protein Interactions of a Non Viral Gene Delivery Vector: Studies Based on Transferrin Conjugated Pullulan-PEI. *Curr. Nanosci.* Available at: <http://www.eurekaselect.com/75687/article> [Accessed November 17, 2018]
- Rhaese S, von Briesen H, Rübsamen-Waigmann H, Kreuter J & Langer K (2003) Human serum albumin–polyethylenimine nanoparticles for gene delivery. *J. Controlled Release* **92**: 199–208
- Ross PD & Subramanian S (1981) Thermodynamics of protein association reactions: forces contributing to stability. *Biochemistry* **20**: 3096–3102
- Ryser HJ-P (1967) A Membrane Effect of Basic Polymers dependent on Molecular Size. *Nature* **215**: 934
- Salman H, Abu-Arish A, Oliel S, Loyter A, Klafater J, Granek R & Elbaum M (2005) Nuclear Localization Signal Peptides Induce Molecular Delivery along Microtubules. *Biophys. J.* **89**: 2134–2145
- Sarmiento B & Neves J das (2012) Chitosan-Based Systems for Biopharmaceuticals: Delivery, Targeting and Polymer Therapeutics John Wiley & Sons
- Semple SC, Chonn A & Cullis PR (1998) Interactions of liposomes and lipid-based carrier systems with blood proteins: Relation to clearance behaviour in vivo. *Adv. Drug Deliv. Rev.* **32**: 3–17
- Sgouras D & Duncan R (1990) Methods for the evaluation of biocompatibility of soluble synthetic polymers which have potential for biomedical use: 1 — Use of the tetrazolium-based colorimetric assay (MTT) as a preliminary screen for evaluation of in vitro cytotoxicity. *J. Mater. Sci. Mater. Med.* **1**: 61–68
- Shang L, Nienhaus K & Nienhaus GU (2014) Engineered nanoparticles interacting with cells: size matters. *J. Nanobiotechnology* **12**: 5
- Shingel KI (2002) Determination of structural peculiarities of dexran, pullulan and γ -irradiated pullulan by Fourier-transform IR spectroscopy. *Carbohydr. Res.* **337**: 1445–1451
- Shingel KI (2004) Current knowledge on biosynthesis, biological activity, and chemical modification of the exopolysaccharide, pullulan. *Carbohydr. Res.* **339**: 447–460
- Sidebotham RL (1974) Dextrans. In *Advances in Carbohydrate Chemistry and Biochemistry*, Tipson RS & Horton D (eds) pp 371–444. Academic Press Available at: <http://www.sciencedirect.com/science/article/pii/S0065231808602681>
- Singal R & Ginder GD (1999) DNA Methylation. *Blood* **93**: 4059–4070
- Singh RS, Kaur N & Kennedy JF (2015) Pullulan and pullulan derivatives as promising biomolecules for drug and gene targeting. *Carbohydr. Polym.* **123**: 190–207
- Sionov RV & Haupt Y (1999) The cellular response to p53: the decision between life and death. *Oncogene* **18**: 6145

- Son S, Namgung R, Kim J, Singha K & Kim WJ (2011) Bioreducible Polymers for Gene Silencing and Delivery. Available at: <https://pubs.acs.org/doi/abs/10.1021/ar200248u> [Accessed May 4, 2019]
- Sonawane ND, Szoka FC & Verkman AS (2003) Chloride Accumulation and Swelling in Endosomes Enhances DNA Transfer by Polyamine-DNA Polyplexes. *J. Biol. Chem.* **278**: 44826–44831
- Song Y, Lou B, Zhao P & Lin C (2014) Multifunctional Disulfide-Based Cationic Dextran Conjugates for Intravenous Gene Delivery Targeting Ovarian Cancer Cells. *Mol. Pharm.* **11**: 2250–2261
- Soo Choi H, Liu W, Misra P, Tanaka E, Zimmer JP, Itty Ipe B, Bawendi MG & Frangioni JV (2007) Renal clearance of quantum dots. *Nat. Biotechnol.* **25**: 1165–1170
- Sotiriou C, Lothaire P, Dequanter D, Cardoso F & Awada A (2004) Molecular profiling of head and neck tumors. *Curr. Opin. Oncol.* **16**: 211–214
- Sou SN, Polizzi KM & Kontoravdi C (2013) Evaluation of transfection methods for transient gene expression in Chinese hamster ovary cells. *Adv. Biosci. Biotechnol.* **2013**: Available at: <http://www.scirp.org/journal/PaperInformation.aspx?PaperID=41051> [Accessed November 14, 2018]
- Srinivasachari S, Liu Y, Prevette LE & Reineke TM (2007) Effects of trehalose click polymer length on pDNA complex stability and delivery efficacy. *Biomaterials* **28**: 2885–2898
- Stommel JM, Marchenko ND, Jimenez GS, Moll UM, Hope TJ & Wahl GM (1999) A leucine-rich nuclear export signal in the p53 tetramerization domain: regulation of subcellular localization and p53 activity by NES masking. *EMBO J.* **18**: 1660–1672
- Strand SP, Danielsen S, Christensen BE & Vårum KM (2005) Influence of Chitosan Structure on the Formation and Stability of DNA–Chitosan Polyelectrolyte Complexes. *Biomacromolecules* **6**: 3357–3366
- Suh J, Lee SH, Kim SM & Hah SS (1997) Conformational Flexibility of Poly(ethylenimine) and Its Derivatives. *Bioorganic Chem.* **4**: 221–231
- Sun J, Zeng F, Jian H & Wu S (2013) Grafting zwitterionic polymer chains onto PEI as a convenient strategy to enhance gene delivery performance. *Polym. Chem.* **4**: 5810–5818
- Sun Y-X, Lin B-L, Wang Q-R, Zhang X-Z & Zhuo R-X (2015) Preparation of Poly (2-aminoethyl methacrylate-co-2-(diethylamino) ethyl methacrylate) by Atom Transfer Radical Polymerization for Gene Delivery. *Acta Polym. Sin.*: 113–119
- Sverdlov ED (2011) Genetic Surgery - A Right Strategy to Attack Cancer. *Curr. Gene Ther.* **11**: 501–531
- Sverdlov ED (2016) Multidimensional complexity of cancer. Simple solutions are needed. *Biochem. Mosc.* **81**: 731–738

- Swami A, Aggarwal A, Pathak A, Patnaik S, Kumar P, Singh Y & Gupta KC (2007) Imidazolyl-PEI modified nanoparticles for enhanced gene delivery. *Int. J. Pharm.* **335**: 180–192
- Synnytsya A & Novak M (2014) Structural analysis of glucans. *Ann. Transl. Med.* **2**: Available at: <https://www.ncbi.nlm.nih.gov/pmc/articles/PMC4202478/>
- Takeda N, Nakamura E, Yokoyama M & Okano T (2004) Temperature-responsive polymeric carriers incorporating hydrophobic monomers for effective transfection in small doses. *J. Controlled Release* **95**: 343–355
- Talu M, Demiroğlu EU, Yurdakul Ş & Badoğlu S (2015) FTIR, Raman and NMR spectroscopic and DFT theoretical studies on poly(N-vinylimidazole). *Spectrochim. Acta. A. Mol. Biomol. Spectrosc.* **134**: 267–275
- Tanaka H, Arakawa H, Yamaguchi T, Shiraishi K, Fukuda S, Matsui K, Takei Y & Nakamura Y (2000) A ribonucleotide reductase gene involved in a p53-dependent cell-cycle checkpoint for DNA damage. *Nature* **404**: 42
- Tang GP, Zeng JM, Gao SJ, Ma YX, Shi L, Li Y, Too H-P & Wang S (2003) Polyethylene glycol modified polyethylenimine for improved CNS gene transfer: effects of PEGylation extent. *Biomaterials* **24**: 2351–2362
- Tang Q, Cao B, Lei X, Sun B, Zhang Y & Cheng G (2014a) Dextran–Peptide Hybrid for Efficient Gene Delivery. *Langmuir* **30**: 5202–5208
- Tang Q, Cao B, Lei X, Sun B, Zhang Y & Cheng G (2014b) Dextran–Peptide Hybrid for Efficient Gene Delivery. *Langmuir* **30**: 5202–5208
- Tang Q, Cao B, Wu H & Cheng G (2012) Selective Gene Delivery to Cancer Cells Using an Integrated Cationic Amphiphilic Peptide. *Langmuir* **28**: 16126–16132
- Tang Q, Cao B, Wu H & Cheng G (2013) Cholesterol-Peptide Hybrids to Form Liposome-Like Vesicles for Gene Delivery. *PLOS ONE* **8**: e54460
- Thomas JJ, Rekha MR & Sharma CP (2010) Dextran-protamine polycation: An efficient nonviral and haemocompatible gene delivery system. *Colloids Surf. B Biointerfaces* **81**: 195–205
- Thomas JJ, Rekha MR & Sharma CP (2012) Unraveling the Intracellular Efficacy of Dextran-Histidine Polycation as an Efficient Nonviral Gene Delivery System. *Mol. Pharm.* **9**: 121–134
- Thomsen LB, Lichota J, Kim KS & Moos T (2011) Gene delivery by pullulan derivatives in brain capillary endothelial cells for protein secretion. *J. Controlled Release* **151**: 45–50
- Tiyaboonchai W, Woiszwilllo J & Middaugh CR (2003) Formulation and characterization of DNA–polyethylenimine–dextran sulfate nanoparticles. *Eur. J. Pharm. Sci.* **19**: 191–202

- Tseng W-C, Fang T-Y, Su L-Y & Tang C-H (2005) Dependence of transgene expression and the relative buffering capacity of dextran-grafted polyethylenimine. *Mol. Pharm.* **2**: 224–232
- Tseng W-C & Jong C-M (2003) Improved Stability of Polycationic Vector by Dextran-Grafted Branched Polyethylenimine. *Biomacromolecules* **4**: 1277–1284
- V Crawford L, Pim D & Lamb P (1984) The cellular protein p53 in human tumours. *Mol. Biol. Med.* **2**: 261–72
- Vader P, van der Aa LJ, Engbersen JFJ, Storm G & Schiffelers RM (2012) Physicochemical and Biological Evaluation of siRNA Polyplexes Based on PEGylated Poly(amido amine)s. *Pharm. Res.* **29**: 352–361
- Varala R, Sreelatha N & Adapa SR (2006) Ceric Ammonium Nitrate Catalyzed aza-Michael Addition of Aliphatic Amines to α,β -Unsaturated Carbonyl Compounds and Nitriles in Water. *Synlett* **2006**: 1549–1553
- Varkouhi AK, Scholte M, Storm G & Haisma HJ (2011) Endosomal escape pathways for delivery of biologicals. *J. Controlled Release* **151**: 220–228
- Varshosaz J (2012) Dextran conjugates in drug delivery. *Expert Opin. Drug Deliv.* **9**: 509–523
- Vaughan EE & Dean DA (2006) Intracellular trafficking of plasmids during transfection is mediated by microtubules. *Mol. Ther. J. Am. Soc. Gene Ther.* **13**: 422–428
- Vaughan EE, DeGiulio JV & Dean DA (2006) Intracellular Trafficking of Plasmids for Gene Therapy: Mechanisms of Cytoplasmic Movement and Nuclear Import. *Curr. Gene Ther.* **6**: 671–681
- Vaughan EE, Geiger RC, Miller AM, Loh-Marley PL, Suzuki T, Miyata N & Dean DA (2008) Microtubule Acetylation Through HDAC6 Inhibition Results in Increased Transfection Efficiency. *Mol. Ther.* **16**: 1841–1847
- Vernejoul F, Faure P, Benali N, Calise D, Tiraby G, Pradayrol L, Susini C & Buscail L (2002) Antitumor Effect of in Vivo Somatostatin Receptor Subtype 2 Gene Transfer in Primary and Metastatic Pancreatic Cancer Models. *Cancer Res.* **62**: 6124–6131
- Vert M, Li SM, Spenlehauer G & Guerin P (1992) Bioresorbability and biocompatibility of aliphatic polyesters. *J. Mater. Sci. Mater. Med.* **3**: 432–446
- Vijayanathan V, Lyall J, Thomas T, Shirahata A & Thomas TJ (2005) Ionic, Structural, and Temperature Effects on DNA Nanoparticles Formed by Natural and Synthetic Polyamines. *Biomacromolecules* **6**: 1097–1103
- Vinogradov SV, Bronich TK & Kabanov AV (1998) Self-Assembly of Polyamine–Poly(ethylene glycol) Copolymers with Phosphorothioate Oligonucleotides. *Bioconjug. Chem.* **9**: 805–812
- Vogelstein B (1990) A deadly inheritance. *Nature* **348**: 681

- Vogelstein B, Lane D & Levine AJ (2000) Surfing the p53 network. *Nature* **408**: 307
- Vousden KH & Lu X (2002) Live or let die: the cell's response to p53. *Nat. Rev. Cancer* **2**: 594
- Walker KK & Levine AJ (1996) Identification of a novel p53 functional domain that is necessary for efficient growth suppression. *Proc. Natl. Acad. Sci.* **93**: 15335–15340
- Wang F, Liu P, Nie T, Wei H & Cui Z (2012) Characterization of a Polyamine Microsphere and Its Adsorption for Protein. *Int. J. Mol. Sci.* **14**: 17–29
- Wang W, Naolou T, Ma N, Deng Z, Xu X, Mansfeld U, Wischke C, Gossen M, Neffe AT & Lendlein A (2017) Polydepsipeptide Block-Stabilized Polyplexes for Efficient Transfection of Primary Human Cells. *Biomacromolecules* **18**: 3819–3833
- Wang X, Ishida T & Kiwada H (2007) Anti-PEG IgM elicited by injection of liposomes is involved in the enhanced blood clearance of a subsequent dose of PEGylated liposomes. *J. Controlled Release* **119**: 236–244
- van de Wetering P, Cherng J-Y, Talsma H, Crommelin DJA & Hennink WE (1998) 2-(dimethylamino)ethyl methacrylate based (co)polymers as gene transfer agents. *J. Controlled Release* **53**: 145–153
- Williams CG, Malik AN, Kim TK, Manson PN & Elisseeff JH (2005a) Variable cytocompatibility of six cell lines with photoinitiators used for polymerizing hydrogels and cell encapsulation. *Biomaterials* **26**: 1211–1218
- Williams CG, Malik AN, Kim TK, Manson PN & Elisseeff JH (2005b) Variable cytocompatibility of six cell lines with photoinitiators used for polymerizing hydrogels and cell encapsulation. *Biomaterials* **26**: 1211–1218
- Xi K, Tabata Y, Uno K, Yoshimoto M, Kishida T, Sokawa Y & Ikada Y (1996) Liver Targeting of Interferon Through Pullulan Conjugation. *Pharm. Res.* **13**: 1846–1850
- Xiong MP, Laird Forrest M, Ton G, Zhao A, Davies NM & Kwon GS (2007) Poly(aspartate-g-PEI800), a polyethylenimine analogue of low toxicity and high transfection efficiency for gene delivery. *Biomaterials* **28**: 4889–4900
- Xiong Y, Hannon GJ, Zhang H, Casso D, Kobayashi R & Beach D (1993) p21 is a universal inhibitor of cyclin kinases. *Nature* **366**: 701
- Xu FJ, Li HZ, Li J, Teo YHE, Zhu CX, Kang ET & Neoh KG (2008) Spatially well-defined binary brushes of poly(ethylene glycol)s for micropatterning of active proteins on anti-fouling surfaces. *Biosens. Bioelectron.* **24**: 773–780
- Yamaoka T, Tabata Y & Ikada Y (1994) Distribution and tissue uptake of poly(ethylene glycol) with different molecular weights after intravenous administration to mice. *J. Pharm. Sci.* **83**: 601–606
- Yang H-Y, Wen Y-Y, Chen C-H, Lozano G & Lee M-H (2003) 14-3-3 σ Positively Regulates p53 and Suppresses Tumor Growth. *Mol. Cell. Biol.* **23**: 7096–7107

- Yang X-C, Niu Y-L, Zhao N-N, Mao C & Xu F-J (2014) A biocleavable pullulan-based vector via ATRP for liver cell-targeting gene delivery. *Biomaterials* **35**: 3873–3884
- Yasuda K, Ogawa Y, Yamane I, Nishikawa M & Takakura Y (2005) Macrophage activation by a DNA/cationic liposome complex requires endosomal acidification and TLR9-dependent and -independent pathways. *J. Leukoc. Biol.* **77**: 71–79
- Yin H, Kanasty RL, Eltoukhy AA, Vegas AJ, Dorkin JR & Anderson DG (2014) Non-viral vectors for gene-based therapy. *Nat. Rev. Genet.* **15**: 541–555
- Zanta MA, Belguise-Valladier P & Behr J-P (1999) Gene delivery: A single nuclear localization signal peptide is sufficient to carry DNA to the cell nucleus. *Proc. Natl. Acad. Sci.* **96**: 91–96
- Zauner W, Ogris M & Wagner E (1998) Polylysine-based transfection systems utilizing receptor-mediated delivery. *Adv. Drug Deliv. Rev.* **30**: 97–113
- Zelikin AN, Putnam D, Shastri P, Langer R & Izumrudov VA (2002) Aliphatic Ionenenes as Gene Delivery Agents: Elucidation of Structure–Function Relationship through Modification of Charge Density and Polymer Length. *Bioconjug. Chem.* **13**: 548–553
- Zelphati O, Liang X, Hobart P & Felgner PL (1999) Gene Chemistry: Functionally and Conformationally Intact Fluorescent Plasmid DNA. *Hum. Gene Ther.* **10**: 15–24
- Zelphati O, Liang X, Nguyen C, Barlow S, Sheng S, Shao Z & Felgner P I. (2000) PNA-Dependent Gene Chemistry: Stable Coupling of Peptides and Oligonucleotides to Plasmid DNA. *BioTechniques* **28**: 304–316
- Zhang L & Esko JD (1994) Amino acid determinants that drive heparan sulfate assembly in a proteoglycan. *J. Biol. Chem.* **269**: 19295–19299
- Zhang R, Qin X, Kong F, Chen P & Pan G (2019) Improving cellular uptake of therapeutic entities through interaction with components of cell membrane. *Drug Deliv.* **26**: 328–342
- Zhang X, Yang X, Ji J, Liu A & Zhai G (2016) Tumor targeting strategies for chitosan-based nanoparticles. *Colloids Surf. B Biointerfaces* **148**: 460–473
- Zhao H, Hemmi H, Akira S, Cheng SH, Scheule RK & Yew NS (2004) Contribution of Toll-like Receptor 9 Signaling to the Acute Inflammatory Response to Nonviral Vectors. *Mol. Ther.* **9**: 241–248
- Zhao X, Cui H, Chen W, Wang Y, Cui B, Sun C, Meng Z & Liu G (2014) Morphology, Structure and Function Characterization of PEI Modified Magnetic Nanoparticles Gene Delivery System. *PLOS ONE* **9**: e98919
- Zhong D, Jiao Y, Zhang Y, Zhang W, Li N, Zuo Q, Wang Q, Xue W & Liu Z (2013) Effects of the gene carrier polyethyleneimines on structure and function of blood components. *Biomaterials* **34**: 294–305

- Zhou H, Ma X, Liu Y, Dong L, Luo Y, Zhu G, Qian X, Chen J, Lu L, Wang J & Gao X (2015) Linear polyethylenimine-plasmid DNA nanoparticles are ototoxic to the cultured sensory epithelium of neonatal mice. *Mol. Med. Rep.* **11**: 4381–4388
- Ziller C, Lincet H, Muller CD, Staedel C, Behr J-P & Poulain L (2004) The cyclin-dependent kinase inhibitor p21cip1/waf1 enhances the cytotoxicity of ganciclovir in HSV-tk transfected ovarian carcinoma cells. *Cancer Lett.* **212**: 43–52

LIST OF PUBLICATIONS & CONFERENCES ATTENDED

Diana, Sherly M. Caroline, and M. R. Rekha (2017) "Efficacy of vinyl imidazole grafted cationized pullulan and dextran as gene delivery vectors: A comparative study" *Int J Biol Macromol.* **105**: 947-955.

Diana, Sherly M. Caroline, and M. R. Rekha "Cationized polysaccharide modified with diethyl amino ethyl methacrylate grafted for gene delivery in cancer cells" (Submitted to carbohydrate polymers).

Caroline Diana Sherly. M and Rekha M.R. (2017) "Vinyl monomers grafted PEI for efficient and safe gene delivery" (Oral presentation, in International Conference, Asian Biomaterials conference 6 (ABMC6) held at Trivandrum)

Caroline Diana Sherly. M and Rekha M.R. (2015). "Imidazole Grafted Cationised Pullulan For Invitro Gene Delivery" (Oral presentation in International Conference, Indo Australian Conference On Biomaterials, Tissue Engineering, Drug Delivery And Regenerative Medicine (BiTERM) held at Chennai).

Caroline Diana Sherly. M and Rekha M.R. (2015). "Comparison of efficacy of cationised polysaccharides, pullulan and dextran as gene delivery vectors" (Poster presentation in the International Symposium on Photonics Applications and Nanomaterials (ISPAN) held at Trivandrum).

